



University  
of Glasgow

Allan, Jon (2018) *Modelling the effects of serotonin on the hippocampal CA1 region during navigation*. PhD thesis.

<https://theses.gla.ac.uk/9090/>

Copyright and moral rights for this work are retained by the author

A copy can be downloaded for personal non-commercial research or study, without prior permission or charge

This work cannot be reproduced or quoted extensively from without first obtaining permission in writing from the author

The content must not be changed in any way or sold commercially in any format or medium without the formal permission of the author

When referring to this work, full bibliographic details including the author, title, awarding institution and date of the thesis must be given

# **Modelling the Effects of Serotonin on the Hippocampal CA1 region during Navigation**

Jon Allan  
MB BS BE(Hon) MSc

Submitted in fulfilment of the requirements for  
the degree of PhD

School of Engineering  
College of Science and Engineering  
University of Glasgow

March 2018



# **Abstract**

The mammalian hippocampus is vitally involved in the formation of both episodic memory and semantic memory, and in learning and recognition. These functions are actively involved during spatial navigation through an environment. The rodent hippocampus in particular has been greatly studied, providing a wealth of experimental data; however collation of this data into universally accepted theories of hippocampal function is far from complete. The present study concentrates on events occurring in the rodent hippocampus during such navigation. There is particular emphasis on the hippocampal theta rhythm which is manifested during navigation; on the existence and characteristics of place fields and associated place cells; and on the phenomenon of phase precession. The study has been limited to the CA1 region. Testable assertions are made about these phenomena. These assertions have been incorporated into models which are described in the later chapters of the thesis. The model has been further extended to demonstrate features of serotonergic activity in the CA1 region.

# List of Figures

1.1	Location of hippocampus . . . . .	4
1.2	Cross-section of hippocampus . . . . .	4
1.3	Layers of cornu ammonis . . . . .	5
1.4	CCKBC receptors . . . . .	9
1.5	Pathways through the hippocampus . . . . .	15
2.1	Glutamatergic release at synapse . . . . .	21
2.2	Short-term plasticity - response to an impulse train . . . . .	26
2.3	Integration window . . . . .	28
2.4	Paired-pulse plasticity - Schaffer stimulation . . . . .	29
2.5	LFP recording, mouse . . . . .	31
2.6	Distribution of theta oscillations . . . . .	33
2.7	Theta phase variation with depth . . . . .	36
2.8	Coordinated firing during theta rhythm . . . . .	37
2.9	Place cell firing during a single pass . . . . .	42
2.10	Phase precession - four CA1 pyramidal cells . . . . .	42
2.11	Theta rhythm by superposition of oscillations . . . . .	48
2.12	Events during transit of place field . . . . .	51
3.1	Synaptic gain v. applied frequency . . . . .	60
4.1	Simulating the generation of CA1 theta LFP . . . . .	72
4.2	CA1 theta LFP with differing place cell population sizes . . . . .	72
4.3	Simulating phase precession . . . . .	73
4.4	Phase precession with varying Schaffer stimulation . . . . .	75
4.5	Phase precession with varying total phase range . . . . .	76
4.6	Phase precession with variation in earliest phase lag . . . . .	77
5.1	Combined CA1 postsynaptic potential from Schaffer stimulation . . . . .	79
5.2	Sequence of postsynaptic potentials arising from Schaffer stimulation . . . . .	79
5.3	Convolutions of SR-IN impulse response with OLM firing . . . . .	81
5.4	CA1 pyramidal PSP related to CA3 firing frequency . . . . .	82
5.5	CA1 pyramidal PSP under different input conditions . . . . .	83
5.6	Schematic for phase precession model . . . . .	85

5.7	Factors contributing to phase precession . . . . .	88
6.1	Cells and inputs modelled in CA1 . . . . .	95
6.2	Specifications for pyramidal cell impulse response. . . . .	97
6.3	Pyramidal bursts - model output and experimental examples . . . . .	98
7.1	Model - constant speed transit of place field . . . . .	109
7.2	Modelled effects of CCKBC activity . . . . .	111
7.3	Model - phase precession across the place field . . . . .	112
7.4	Model - further phase precession relationships . . . . .	113
7.5	Model - phase precession with pause during place field crossing . . . . .	114
7.6	Sketch of depolarization ramp . . . . .	116
7.7	Ramp height changes with successive place field transits . . . . .	118
7.8	LTP for mapping field, LTD for object . . . . .	119
7.9	Phasic signal from MRN . . . . .	120
7.10	Raised serotonin in ECF reduces place cell firing . . . . .	122
7.11	Effects of varying activity of the 5HTR4 receptor . . . . .	123
7.12	Models of SSRI-induced states . . . . .	126
8.1	Phase precession and a possible downstream shift register . . . . .	130
9.1	Code . . . . .	134

(Where colours have been used, the high prevalence of dichromacy in the community has been kept in mind, to avoid ambiguity where colour is highly significant.)

## **Declaration**

I declare that the work presented in this thesis is entirely my own work, with the exception of certain figures which are either open source or are reproduced in conformity with their Creative Commons licence. In such cases each source is acknowledged in the legend of the figure.

Signature.....

(Jon Allan)

# Abbreviations

<b>AA</b>	Axo-axonic (interneurons)
<b>AMPA</b>	$\alpha$ -amino-3-hydroxy-5-methyl-4-isoxazole-propionate
<b>ANN</b>	Artificial neural network
<b>AP</b>	Action potential
<b>CA</b>	Cornu ammonis
<b>CCK</b>	Cholecystokinin
<b>CCKBC</b>	Basket cells expressing cholecystokinin
<b>DBB</b>	Diagonal band of Broca
<b>DG</b>	Dentate gyrus
<b>EC</b>	Entorhinal cortex
<b>ECF</b>	Extracellular fluid
<b>EPSC</b>	Excitatory postsynaptic current
<b>EPSP</b>	Excitatory postsynaptic potential
<b>FIR</b>	Finite impulse response (signal filter)
<b>HC</b>	Hippocampus
<b>LFP</b>	Local field potential
<b>LTD</b>	Long-term depression
<b>LTP</b>	Long-term potentiation
<b>MRN</b>	Medial raphe nucleus
<b>MSDB</b>	Medial septum and Diagonal Band of Broca
<b>NMDA</b>	N-methyl-D-aspartate glutamatergic receptor
<b>OLM</b>	Oriens lacunosum-moleculare (cells)
<b>PPR</b>	Paired-pulse ratio
<b>PSP</b>	Postsynaptic potential
<b>PTP</b>	Post-tetanic potentiation
<b>PVBC</b>	Parvalbumin-expressing basket cells
<b>REM</b>	Rapid eye movement (sleep)
<b>SERT</b>	Serotonin transporter

<b>SL-M</b>	.....	Stratum lacunosum-moleculare
<b>SO</b>	.....	Stratum oriens
<b>SPW</b>	.....	Sharp wave
<b>SR</b>	.....	Stratum radiatum
<b>SR-IN</b>	.....	Stratum radiatum interneurons associated with Schaffer collaterals
<b>SSRI</b>	.....	Selective serotonin reuptake inhibitor
<b>STDP</b>	.....	Spike-timing-dependent plasticity
<b>SWR</b>	.....	Sharp wave ripple
<b>VGLUT1,2</b>	...	Vesicular glutamate transporter, types 1 and 2

# Contents

Abstract . . . . .	i
List of figures . . . . .	ii
Declaration of originality . . . . .	iv
Abbreviations . . . . .	v
<b>I Background Information</b>	<b>1</b>
<b>1 Introduction</b>	<b>2</b>
1.1 Hippocampal structure . . . . .	3
1.2 Hippocampal CA1 neurons . . . . .	5
1.2.1 Pyramidal cells . . . . .	5
1.2.2 Interneurons . . . . .	6
1.3 Principal neuromodulators in the HC . . . . .	12
1.3.1 Acetylcholine . . . . .	12
1.3.2 Dopamine . . . . .	13
1.3.3 Other neuroactive substances . . . . .	13
1.4 The sensory information highway . . . . .	14
1.4.1 Pattern formation and recognition . . . . .	16
<b>2 Navigation and its rhythms</b>	<b>18</b>
2.1 Synaptic plasticity . . . . .	18
2.1.1 Long-term plasticity in CA1 pyramidal cells . . . . .	19
2.1.2 Short-term plasticity in CA1 pyramidal cells . . . . .	20
2.1.3 Integration window and excitation window . . . . .	26
2.1.4 Window width and dual Schaffer stimulation . . . . .	27
2.2 Rhythms and navigation . . . . .	30
2.2.1 Local field potential . . . . .	30
2.2.2 Theta rhythm . . . . .	31
2.2.3 Place fields and place cells . . . . .	39
2.2.4 Phase precession . . . . .	41
2.3 Intracellular events during place field transit . . . . .	43
2.3.1 Events in the apical dendrites . . . . .	43
2.3.2 Events leading to LTP . . . . .	44

2.3.3	Ramp of depolarization . . . . .	44
2.3.4	Intracellular theta rhythm . . . . .	45
2.3.5	Modelling phase precession . . . . .	46
2.3.6	Other rhythms . . . . .	50
<b>3</b>	<b>Serotonin and the hippocampus</b>	<b>55</b>
3.1	Nature and general functions . . . . .	55
3.2	The raphe nuclei . . . . .	56
3.2.1	MRN interaction with the hippocampal CA1 region . . . . .	58
3.3	Serotonergic receptor types . . . . .	58
3.4	Theta rhythm activity - (a) phasic regulation . . . . .	62
3.4.1	Theta rhythm activity - (b) tonic regulation . . . . .	63
3.5	Equilibrium, Disequilibrium . . . . .	64
3.5.1	Clinical depression . . . . .	64
<b>II</b>	<b>Models of Hippocampal Phenomena</b>	<b>67</b>
<b>4</b>	<b>Modelling Theta LFP Generation</b>	<b>69</b>
4.1	Purpose of the model . . . . .	69
4.2	Overview of the model . . . . .	70
4.3	Experimental results . . . . .	72
4.3.1	Effects of varying parameters . . . . .	73
<b>5</b>	<b>Modelling Phase Precession</b>	<b>78</b>
5.1	Form of postsynaptic potentials induced in CA1 pyramidal cells by Schaffer collateral stimulation . . . . .	78
5.2	SR-IN behaviour during a theta cycle . . . . .	80
5.3	Schaffer-stimulated place cell firing during place field transit . . . . .	82
5.4	Phase precession simulation . . . . .	85
<b>6</b>	<b>Model of navigational activity</b>	<b>89</b>
6.1	Scope of the model . . . . .	90
6.2	Choice of model type . . . . .	90
6.3	Model subsystems: Constituent neurons and receptors . . . . .	92
6.3.1	Included elements . . . . .	93
6.3.2	Pyramidal cells . . . . .	94
6.3.3	OLM interneurons . . . . .	97
6.3.4	Interneurons acting perisomatically - general points . . . . .	99
6.3.5	PVBC interneurons . . . . .	99
6.3.6	CCKBC interneurons . . . . .	100
6.3.7	Axo-axonic interneurons . . . . .	100
6.3.8	Stratum radiatum interneurons . . . . .	101

6.3.9	Excluded interneurons . . . . .	101
6.3.10	Input to the system . . . . .	102
6.3.11	Deployment of place fields . . . . .	103
6.3.12	Organizing the trajectory . . . . .	104
6.3.13	Serotonergic effects in the model . . . . .	105
6.3.14	Other points . . . . .	106
<b>III</b>	<b>Experimentation and Discussion</b>	<b>107</b>
<b>7</b>	<b>Experimentation</b>	<b>108</b>
7.1	Basic features of hippocampal microassembly action . . . . .	108
7.1.1	Transit of a single place field at constant speed . . . . .	108
7.1.2	Features of phase precession at different speeds . . . . .	110
7.2	Implementation of long-term plasticity . . . . .	114
7.3	Modelling serotonergic effects in CA1 . . . . .	120
7.3.1	MRN phasic signal to CCKBC and MSDB . . . . .	120
7.3.2	Increased tonic action of serotonin . . . . .	121
7.3.3	Effects of 5HTR4 stimulation and inhibition . . . . .	121
7.3.4	Effects on phase precession . . . . .	123
7.3.5	Clinical depression and SSRIs . . . . .	124
<b>8</b>	<b>Discussion</b>	<b>127</b>
8.1	A behavioural model? . . . . .	127
8.2	Modelling theta rhythm . . . . .	128
8.3	Modelling phase precession . . . . .	129
8.4	The final model, and serotonin . . . . .	129
<b>IV</b>	<b>Appendices</b>	<b>132</b>
<b>Appendix A - Access to model source code</b>		<b>133</b>
<b>9</b>	<b>Appendix A</b>	
<b>Source code of the model</b>		<b>133</b>
<b>Appendix A - Access to model source code</b>		<b>133</b>
<b>10</b>	<b>Appendix B</b>	
<b>Parameters for the model</b>		<b>135</b>
<b>Bibliography</b>		<b>137</b>

# **Part I**

## **Background Information**

# Chapter 1

## Introduction

“Every day is alone in itself, whatever enjoyment I’ve had, and whatever sorrow I’ve had”. Such were the words of one Henry Gustav Molaison, to whom we owe a huge 20th century explosion of knowledge about the hippocampus. As a young man in the 1950’s, suffering from severe epilepsy since a childhood accident, he was selected for trial of a new surgical approach to epilepsy treatment. This involved the excision of both medial temporal lobes, including both hippocampi and amygdalae (which at that time were not regarded as having any indispensable function). He was conscious and talking during the operation, and indeed his epileptic condition was greatly improved; but from that moment on, and for the remaining fifty years of his life, he was completely unable to form any new memories. As a result of this disastrous outcome the hippocampus earned a profound new respect in the medical world. He became the subject of a large number of studies, and other epileptic patients were saved from a similar fate.

In the intervening years it has become generally accepted that the human hippocampus plays a major role in the formation of both episodic memory (memory of sequences of associated events) and semantic memory (memory of facts and concepts) (Burgess et al., 2002, Eichenbaum, 2004, Scoville and Milner, 1957, Squire, 1992). Experimentation with rodents has also shed light on the vital role of the hippocampus during spatial navigation through the environment (Hafting et al., 2005, O’Keefe and Dostrovsky, 1971, Wilson and McNaughton, 1993). Local field potential rhythms have been identified and found relevant to such navigation (Buzsáki, 2005, McFarland et al., 1975, Mölle et al., 2006). The present study explores certain aspects of rodent hippocampal function during navigation which remain unclear. A new approach to understanding the generation of certain rhythm phenomena has been formulated, and their proposed operation has been demonstrated using a computer model.

Hippocampal operation during navigation is subject to modulation by projections from other brain regions, mediated by different neuromodulators. One important neuromodulator is the monoamine serotonin, associated with the tracking of expectations of reward or punishment, and involved in eliciting changes in the performance of reward-

seeking actions (Cohen et al., 2015). Serotonergic projections to the hippocampus terminate in at least ten different functionally distinct receptor types (Tanaka et al., 2012). Four major receptor types have been included in the present study, all of which have been found to actively modulate rodent navigational activity. Proposals as to how this modulation is coordinated are presented, and have been demonstrated in the model.

The thesis is divided into three parts.

The **first part**, comprising **chapters 1 to 3**, provides a brief summary of hippocampal anatomy and function, majoring on the features of the CA1 region of the hippocampus. The major cell types of the hippocampus are detailed. Major neurotransmitters and neuromodulators that affect these cells are introduced, with particular attention given to the neuromodulator serotonin.

The **second part - chapters 4 to 6** - describes the models developed for the thesis.

The **final part - chapters 7 and 8** - presents the results of experimentation, and the discussion section.

## 1.1 Hippocampal structure

The mammalian hippocampus (HC) is a paired organ, comprising a longitudinally folded portion of the medial cortex of each temporal lobe (figure 1.1). It is fundamentally important to the functions of information processing and memory consolidation (Eichenbaum, 2004, Langston and Wood, 2010, Squire, 1992). Raw sensory information from different modes of sensation is processed by cortical sensory areas; this processed information then proceeds to the perirhinal cortex and from there to the entorhinal cortex, both structures being adjacent to the HC. These structures integrate information from different sensory origins and to some extent identify objects and their contextual relationships, together with autocentric information, such as head position. In terms of the flow of sensory information, the HC is downstream of the entorhinal cortex, and carries out both pattern recognition and pattern completion with the data supplied. This allows for informed navigation through the environment, and also enables rapid first response patterns of behaviour, for example in the face of sudden danger. It also allows the formation of memory “traces”, believed on strong evidential grounds to be a major function of the HC; such traces are then stored locally and more diffusely through the cortex, available for later retrieval. The HC is of particular importance in the laying down of episodic memory, that is, the memory of a sequence of significant events (Griffin and Hallock, 2013, Smith and Mizumori, 2006, Winocur and Moscovitch, 2011).

Throughout its length, transverse sections demonstrate its division into four main

anatomically and functionally distinctive regions (figure 1.2). Information from the entorhinal cortex (EC) passes first to the hippocampal Dentate Gyrus (DG), appearing as the smaller of two interlocking C-shaped structures on transverse section. Downstream of the DG is the Cornu Ammonis (CA), the larger C-shaped structure. The CA is further divided into the CA3 (receiving input from the DG), a small intermediate CA2 region, and a large CA1 region (with which this thesis is principally concerned). Finally data which has been processed throughout the CA is transmitted to the Subiculum, passing thence to deeper layers of the EC (thus completing a circuit), from which it is widely distributed to cortical and subcortical structures.

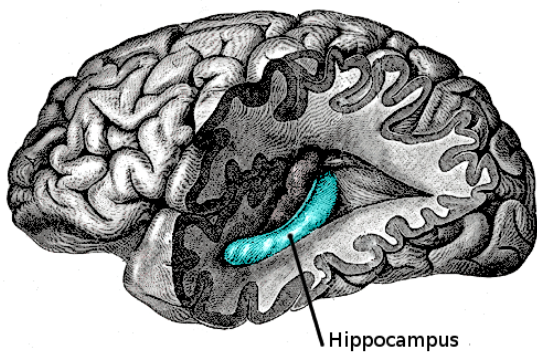


**Figure 1.1:** Hippocampus (blue) - location in human brain. (Anterior to left). (Source: Anatomy of the Human Body, Henry Gray, 1918 edn.).

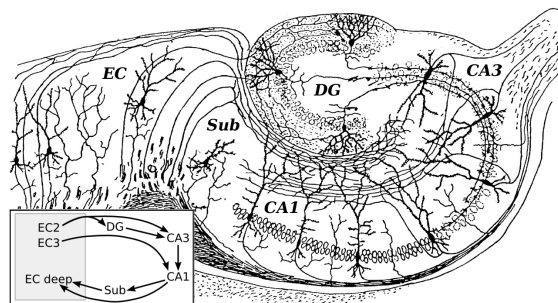


**Figure 1.2:** Cross-section of human hippocampus; inset is connection diagram. (Source: Histologie du Système nerveux de l'Homme et des Vertébrés, Cajal, 1911.)

Almost all of the neurons of the HC fall into two basic groups: those which express glutamate at synapses, and those which express GABA. Approximately 80% of all the neurons of the HC are glutamatergic; throughout all the regions of the hippocampus their cell bodies are confined to a thin central layer. In the DG they are called granule cells; in the CA the corresponding neurons are called pyramidal cells because of their body shape. The two cell types are often grouped together by the term “principal cells”. A large number of models have been constructed demonstrating how these principal cells may perform pattern recognition and pattern completion, operating on input data supplied via the EC. Such pattern phenomena are discussed further in section 1.4.1.

The remaining 20% of hippocampal neurons, are nearly all GABAergic, and therefore inhibitory in function; they are collectively termed interneurons, and are highly diverse in structure, chemistry and function. They mostly inhibit the action of principal cells, though some are specialized to inhibit other interneurons. Some of these interneurons are discussed in more detail below.

Throughout the HC there are broadly three layers. A central layer consists chiefly of the principal cell bodies. One outer layer (more superficial in the DG, deeper in the rest of the HC) carries most inputs to the principal cells, the other outer layer (which

is deeper in the DG, more superficial in the rest of the HC) holds most axons from these principal cells bound for other regions. Within the CA in particular, the central layer, holding the cell bodies of the pyramidal cells, is called the stratum pyramidale (figure 1.3). Most of the dendrites of these cells are found in the deeper layer, which is divided into stratum radiatum (SR) - in which the main dendrites ‘radiate’ out from the apex of the pyramidal cell) - and the thinner stratum lacunosum-moleculare (SL-M), containing most of the terminal tufts of these dendrites. Axons of the pyramidal cells pass through a more superficial layer, the stratum oriens (SO), to join those from earlier hippocampal regions passing through to the subiculum, and from thence to the deeper layers of the entorhinal cortex; the most superficial layer, the alveus, holds these fibres. Interneurons are present in every layer.

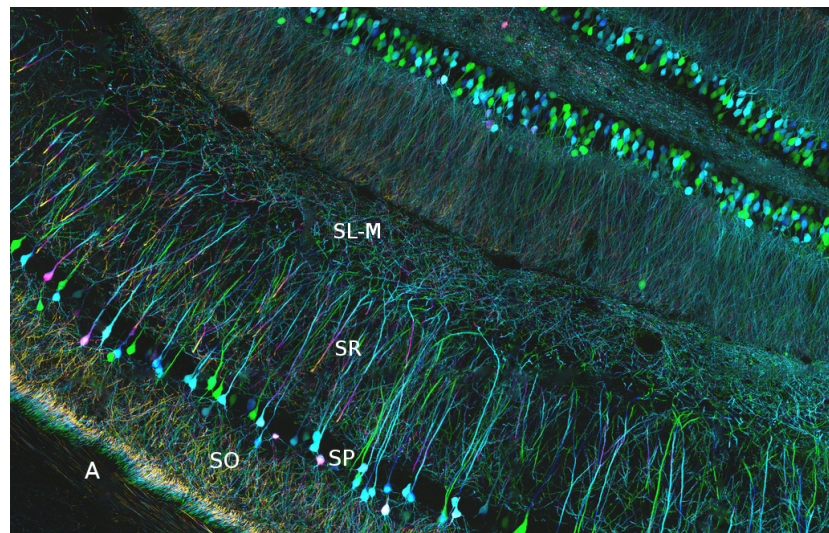


**Figure 1.3:** Layers of the cornu ammonis (mouse, CA1 region). **SL-M:** stratum lacunosum-moleculare; **SR:** stratum radiatum; **SP:** stratum pyramidale; **SO:** stratum oriens; **A:** alveus. Estimated thickness: 0.6 mm. (Source: Yi Zuo, Molecular, Cell and Developmental Biology (MCDB) Department, University of California Santa Cruz; using mice genetically labelled with green fluorescing protein. Notation added.)

## 1.2 Hippocampal CA1 neurons

### 1.2.1 Pyramidal cells

Pyramidal cells are the major excitatory neurons of the brain and spinal cord. In the HC the cell bodies are embedded in the narrow stratum pyramidale, while their dendritic trees extend in parallel into the stratum radiatum, and their axons in parallel to stratum oriens (fig.1.3). The soma (cell body) is approximately triangular in stained sections, hence the name. From the base of this triangle protrudes a single axon, which is of the order of tens of millimetres in length (Cutsuridis et al., 2010b, p. 22). From the apex of the triangle a small number of primary dendrites arise, which branch profusely

with increasing distance from the apex. In the adult rat hippocampus the dendritic tree has a length of the order of a centimetre, and the axons up to several centimetres. In the CA1 (the region of major interest for this thesis), each dendritic tree receives of the order of 30,000 synaptic inputs, the great majority of which are glutamatergic, from the CA3 region and from the EC. A smaller number of inhibitory inputs are present (approximately 3% of the total), mostly from interneurons of the CA1 (Megias et al., 2001).

The dendritic tree in CA1 (as elsewhere) has two functionally differing regions: long radial branches occupying the stratum radiatum (SR) and their highly branching fine terminal tufts in the stratum lacunosum-moleculare (SL-M) layer. (There are also basal dendrites, extending instead into the stratum oriens.) The EC input from the perforant pathway synapses onto the dendritic tufts in SL-M, while the input from CA3 - via the Schaffer collaterals - is directed to the radial branches in SR. The EC input is required for long-term spatial memory consolidation and maintenance, whereas the CA3 input is required for rapid new learning, pattern-completion-based memory recall (Sun et al., 2016). The dendritic tufts are suited for maintenance of signal input as integrators, by virtue of the relatively high output impedance of their connections to main dendrites; while the radial branches respond more rapidly to input and so function better as coincidence detectors (Branco and Häusser, 2011).

### 1.2.2 Interneurons

Interneurons are GABAergic neurons which can be found in all layers of all parts of the HC. Although they represent only about 20% of the total neuron load of the HC, they are hugely diverse; at least 22 types of GABAergic interneurons had been defined by 2012 (Keimpema et al., 2012); there are ongoing attempts to develop a robust classification based on morphological, molecular and physiological criteria (Ascoli, 2008). The great majority of their GABAergic projections are to pyramidal cells, though a few specifically inhibit other interneurons. Their many functions are still largely unknown, but include the avoidance of reverberative excitation by supplying balancing inhibition, and various roles in synchronizing the activity of the pyramidal cells (Rudy et al., 2011). Those interneurons which target the pyramidal cell dendritic tree are able to attenuate the incoming glutamatergic excitation, while those targeting the somatic region and the pyramidal axon control the direct output of the neuron (Woodruff et al., 2010).

Several interneuron types within the CA1 region are known to be particularly important to hippocampal navigation, and so are described here.

## **Parvalbumin-expressing basket cells**

PVBCs are called “basket cells” because of the basket-like distribution of their prolific dendrites. They lie close to the pyramidal cell somas. As they synapse only onto the pyramidal soma, they are well able to inhibit firing. They are driven by glutamatergic input, mostly from CA3 via the Schaffer collaterals, but also to a large extent by positive feedback from local pyramidal cells. They react very rapidly to this input - within a very few ms - by producing dense bursts of action potentials; the rapidity is due in part to their fast membrane time constant (approximately 10 ms) and partly because of active processes speeding transmission down the dendrite, so that even from distal dendrites signals rapidly reach the soma. Parvalbumin itself is a fast Ca<sup>2+</sup> buffer suitable for maintaining high frequency trains of action potentials of up to 100 Hz. PVBCs receive very little neuromodulation, unlike CCKBCs (discussed below). (Ali et al., 1998, Armstrong and Soltesz, 2012, Cea-del Rio et al., 2012, Glickfeld and Scanziani, 2006, Smart, 2010).

## **CCK-expressing interneurons**

Interneurons that express cholecystokinin are found throughout all layers of the CA1 region. The great majority fall into one of two groups: stratum radiatum CCK cells, which synapse onto most of the pyramidal cell dendritic tree; and CCK basket cells (CCKBC), which instead target the pyramidal cell soma and the most proximal portion of the main dendritic branches. Both groups are driven by glutamatergic Schaffer collateral fibres from CA3, and both groups inhibit local pyramidal cells via GABAergic synapses. Of the two sets the CCKBCs have been studied in much more detail, and are known to be intimately involved with hippocampal rhythms (Armstrong and Soltesz, 2012, Freund and Katona, 2007).

CCKBC cell bodies lie close to the pyramidal cells onto which they synapse. Like PVBCs, they directly inhibit pyramidal cell firing by virtue of the perisomatic location of their synapses onto the pyramidal cells. By comparison with PVBCs, CCKBCs respond much more slowly to input; the time constant is three times longer (approximately 30 ms), and dendritic conduction is slower. The neuron therefore acts more as an integrator of applied charge, as calcium transients summate in the dendrites (Armstrong and Soltesz, 2012, Cea-del Rio et al., 2012, Glickfeld and Scanziani, 2006). The operating frequency rarely exceeds 50 Hz (Keimpema et al., 2012).

CCKBCs are susceptible to a range of modulators, including serotonin, acetylcholine (to a greater degree than PVBCs), endocannabinoids, oestrogen and humoral CCK (Armstrong and Soltesz, 2012, Cea-del Rio et al., 2012). Much of this modulation is by fibres from subcortical areas that are slow to conduct and have signals liable to considerable jitter. The integrative function just described acts as a low-pass filter to

smooth this input (Freund and Katona, 2007).

Serotonin action in CCKBCs is mediated by two different receptor types (Fig. 1.4):

#### *The 5HTR3A receptor*

This is the only serotonin receptor which acts as a ligand-gated ion channel; it is selectively permeable to Na<sup>+</sup>, K<sup>+</sup> and Ca<sup>2+</sup> ions. The receptor acts relatively rapidly, having a latency to serotonergic stimulation of approximately 2 ms; the resulting EPSC has a rise time (10% to 90%) of 0.3 ms (Férezou et al., 2002). The receptor is located throughout the CCKBC, from distal dendrites through to axons. Those receptors which are presynaptic to the pyramidal cell are able to rapidly discharge the CCKBC; it has been shown that even a single stimulation of 1 ms duration will frequently evoke an action potential (Varga et al., 2009). On the other hand, receptors within the dendrites are able to increase the integrative load to the CCKBC, and so maintain an increase in its firing rate. The result of 5HTR3A stimulation is therefore both rapid onset and steady maintenance of GABAergic inhibition of the pyramidal cell soma.

#### *The 5HTR1B receptor*

CCKBCs receive glutamatergic feedback from local CA1 pyramidal cells; the CCKBCs as a result increase their inhibition of the same pyramidal cells. This disynaptic negative feedback loop is modulated by serotonin via G protein-coupled 5HTR1B receptors. These receptors are placed in the axon branch from pyramidal cell to CCKBC, presynaptically at its termination. When activated, they inhibit the glutametergic feedback, tending to decouple the CCKBC from CA1 pyramidal cell feedback (Winterer et al., 2011).

### **Axo-axonic cells**

These are also called chandelier cells because of their histological appearance in HC cross-sections. They exclusively target the initial segment of the pyramidal cell axon. They are much less abundant than basket cells. Each axo-axonic cell synapses onto the axon of more than 1000 neighbouring pyramidal cells, and each pyramidal cell axon is estimated to receive connections from 4 to 10 axo-axonic cells (Freund and Buzsáki, 1996). Their main dendritic tree is within stratum radiatum and stratum oriens. There are also basal dendrites, lying in the lower stratum oriens. As pyramidal recurrent collaterals form a plexus here, it has been suggested that this could be a route for CA1 pyramidal cell feedback; on the other hand these dendrites could be principally associated with that part of the Schaffer collaterals which lies in this layer. CA1 feedback has been demonstrated in the case of a subset of axo-axonic cells which only have dendrites in stratum oriens (Buhl et al., 1994, Ganter et al., 2004).

The timing of firing during theta rhythm activity has been assigned differently by different authors. In rats it has been variously assigned to coincide with the peak

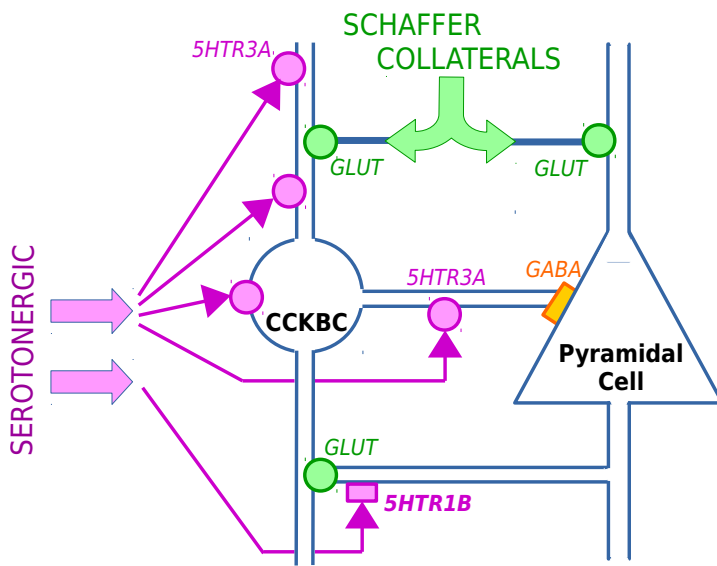


**Figure 1.4: Major receptors of the CCKBC.** Excitatory receptors are indicated by circles, inhibitory receptors by rectangles. The primary action of CCKBCs is to inhibit the pyramidal cells at GABA receptors. The Schaffer collaterals stimulate both pyramidal cells and CCKBCs at glutamatergic junctions ('Glut'). The other glutamatergic input to the CCKBC is from the axons of local pyramidal cells. Serotonergic projections synapse onto the CCKBC via excitatory 5HTR3A receptors, throughout the extent of the cell. Separately there is serotonergic stimulation of the inhibitory 5HTR1B receptor, placed presynaptically in fibres from the pyramidal axon.

amplitude of the theta rhythm (Klausberger et al., 2003, Viney et al., 2013) or to just before the trough, and so shortly before the pace-setting OLM cells fire (Forro et al., 2015). All agree that axo-axonic firing follows all pyramidal cell firing, which is reasonable as axo-axonic firing specifically inhibits pyramidal cell firing.

During sharp-wave-associated ripple activity, in the CA3 they fire immediately before pyramidal neurons are activated (Woodruff et al., 2010), presumably ensuring that no earlier sporadic pyramidal excitation interferes; however they are quiet at this time in the CA1 (Viney et al., 2013).

A paper by Szabadics et al in 2006 demonstrated that it is physiologically possible for the axo-axonic cell to excite, rather than to inhibit, the pyramidal cell (Szabadics et al., 2006). Such an effect has not been demonstrated for live rodents in the hippocampus, and there are questions as to whether it occurs significantly there or in other brain regions (Glickfeld et al., 2008, Woodruff et al., 2010).

Our knowledge of driving inputs to the axo-axonic cell is very incomplete. As late as 2008, Klausberger could write: "Since the discovery of axo-axonic cells in 1983, only one

glutamatergic input from CA1 pyramidal cells has been published; all other excitatory and inhibitory inputs remain inferential predictions” (Klausberger and Somogyi, 2008). There is strong anatomical evidence for the input from Schaffer collaterals and from the EC, as mentioned above; but other input must be involved in the timing of events, as axo-axonic cells consistently fire out of phase with Schaffer stimulation during the theta cycle.

### **Stratum radiatum interneurons**

The term stratum radiatum interneurons (SR-INs) refers throughout this thesis to interneurons in that stratum which are driven by glutamatergic input from Schaffer collaterals. They have also been termed “Schaffer collateral-associated interneurons” (Elfant et al., 2008). Their cell bodies, dendrites and axons are mostly confined to the stratum radiatum. Axons branch densely, ending in GABAergic synapses onto the main dendrite trunks of nearby pyramidal cells (Alkondon et al., 2003).

Unless inhibited, they fire constantly, driven tonically by ambient glutamate (acting on extrasynaptic AMPA and NMDA receptors) and also by ambient acetylcholine (acting on nicotinic receptors of type  $\alpha 3\beta 4\beta 2$ ). In addition there are synaptic AMPA and NMDA receptors, driven by Schaffer collateral input, and synaptic  $\alpha 7$  nicotinic receptors, thought to be driven by cholinergic input from the medial septum. In the rat CA1 a typical steady-state frequency is 40 Hz, but this can be driven to over 100 Hz (Alkondon et al., 2011), (Fuhrmann et al., 2015, supplement, table S1). Despite the presence of NMDA receptors, long-term potentiation does not appear to occur significantly (Alkondon et al., 2003).

This steady-state firing is firmly suppressed by GABAergic input from interneurons of stratum oriens and alveus, putatively OLM cells (which are dealt with below). SRIs thus cease to inhibit pyramidal cells, which as a result are more responsive to both CA3 input and EC input (Fuhrmann et al., 2015).

### **Oriens lacunosum-moleculare cells**

Oriens lacunosum-moleculare cells (OLM) are so called because their cell bodies and dendrites are located mainly in the stratum oriens, yet their axons travel through several layers to the stratum lacunosum-moleculare. In that layer they branch heavily, the branches synapsing onto the tufts of pyramidal cell dendrites. This is the region where glutamatergic input from the EC (via the perforant path) also synapses onto these dendrites; as a result, OLM cells are well able to inhibit EC input to the pyramidal cell (Klausberger, 2009, Maccaferri, 2005). Some branches also occur within the stratum radiatum, where they target other interneurons, particularly the SR-INs just described. By inhibiting SR-INs they indirectly allow stronger excitation of the pyramidal cells

by Schaffer fibres from CA3 (Leao et al., 2012). This dual action of suppressing EC input while enhancing CA3 input to pyramidal cells is discussed later when describing pattern formation and theta rhythm (section 2.2.2).

The OLM cells are subject to glutamatergic, GABAergic and cholinergic control. Most glutamatergic input comes from local pyramidal cells (Klausberger, 2009), but there is strong evidence that glutamatergic input also derives from the medial septum and diagonal band of Broca (MSDB) (Fuhrmann et al., 2015). Less is known about GABAergic stimulation of OLMs, which is mainly from a poorly understood class of interneurons called interneuron specific type III cells (IS-III). OLM cells also express  $\alpha$ 2 nicotinic receptors; it is believed that these are also responsive to MSDB cholinergic stimulation (Leao et al., 2012).

### Bistratified cells

The cell bodies of these interneurons lie in stratum pyramidale. Their axons make inhibitory synapses onto pyramidal main dendrites specifically where Schaffer input also synapses; that is, in stratum radiatum and stratum oriens (Klausberger and Somogyi, 2008). They receive glutamatergic stimulation both from the Schaffer collaterals and as feedback from the CA1 cells which they target. During theta wave activity they fire mainly at the height of CA3 stimulation of CA1 pyramidal cells. They would therefore appear to have an important role in stabilizing pyramidal cell activity and averting the risk of epileptiform behaviour.

There is mutual GABAergic inhibition between bistratified cells and OLM cells. During theta the two cell types fire in phase, though with opposing actions. OLM cells indirectly disinhibit Schaffer input to pyramidal cells, and concurrently inhibit EC input at the terminal tufts of pyramidal cells; bistratified cells on the other hand inhibit the Schaffer input, leaving the EC input active (Baude et al., 2007, Klausberger, 2009, Mäller and Remy, 2014).

### Ivy cells and neurogliaform cells

It is likely that most or all interneurons are involved in stabilizing CA1 pyramidal action, certainly including those mentioned above. But unlike those, most do not yet appear to have a clear function in the generation or modulation of the navigational theta rhythm. The following are briefly mentioned here because they have been well studied and are certainly involved in stabilizing feedback loops.

Ivy cells have cell bodies in the pyramidal layer, and synapse onto proximal pyramidal dendrites at the same locations as Schaffer collateral fibres from CA3. Neurogliaform cells instead are located in stratum lacunosum-moleculare, where they synapse onto

the apical dendritic tufts of pyramidal cells, alongside input from the EC via the perforant pathway. The two cell types are therefore complementary in their distribution. They also appear to be similar in function. To quote Klausberger, “they modulate pre- and postsynaptic excitability at slower time scales and more diffusely than do other interneurons providing homeostasis to the network” (Klausberger and Somogyi, 2008). They also have in common that they release nitric oxide, an important humoral enhancer of long-term potentiation at glutamatergic synapses (Armstrong et al., 2012).

## 1.3 Principal neuromodulators in the HC

The main focus of this thesis is on the neuromodulator serotonin; it is discussed separately in chapter 3. While other neuroactive substances are not specifically involved in the model developed for this thesis, several are important to hippocampal function.

### 1.3.1 Acetylcholine

Outside of the central nervous system, acetylcholine acts as a classical neurotransmitter, chiefly at neuromuscular junctions and in sympathetic nervous system ganglia. Its role is much more as a neuromodulator within the central nervous system, where it acts as a coordinator of responses across many neuronal networks at once. The general theme is to modify the speed and intensity of responses within these networks in accordance with some immediate need for adaptation; it sharpens attention and rapidity of action and speed of learning. Concurrently there may be downgrading of responses to ongoing stimuli which for the moment require little attention. It works by influencing synaptic transmission, by its effects on synaptic plasticity, and by its ability, as a fast-acting agent, to coordinate firing of neuron groups; this is brought about by a precisely timed reinforcement signal disseminated rapidly throughout cortical areas. Acetylcholine receptors are of two types: muscarinic receptors (which are metabotropic) and nicotinic receptors (which are ionotropic). There is no overarching role for either type; they have different deployments within different brain regions. Within the hippocampus and associated cortical regions involved with memory formation, both receptor types are important; the general theme appears to be that the faster nicotinic receptor enhances the effect of afferent inputs to regions, while the muscarinic receptor reduces positive feedback within the same regions (Hangya et al., 2015, Hasselmo, 2006, Picciotto et al., 2012).

Acetylcholine is certainly involved in the HC navigation process. The input comes from the medial septum and diagonal band of Broca (MSDB), along with glutamatergic and GABA input (discussed in section 2.2.2); it is widely disseminated to interneurons throughout the HC. Its effects are too slow to affect the network dynamics within the

theta cycle (Hasselmo et al., 2002b); nevertheless the ablation of this cholinergic input greatly attenuates the magnitude of the theta rhythm (Cea-del Rio et al., 2010).

### 1.3.2 Dopamine

Dopaminic projections to the cortex and diencephalon arise from a midbrain region called the ventral tegmental area (VTA). Dopamine modulatory signals can be divided into two categories, “phasic” (consisting of occasional sudden short-lived bursts) and “tonic” (sustained regular slow firing at a lower amplitude) (Floresco et al., 2003). The phasic signal appears to encode the difference between a reward (or punishment) anticipated and whatever reward (or punishment) is at the current moment being received; as a result, if the reward is as expected there will be no phasic stimulation. The tonic signal is more subject to speculation; a common understanding is that it acts as an integrator of the phasic signal, and so provides a background averaged signal, which might be used for example to increase the vigour with which a current activity is being carried out; if an unexpected reward was phasically signalled, it would be advantageous to move faster in reaping that reward, as it can disappear, or other factors can force the animal to move on (Cools et al., 2010).

The activity just described has been demonstrated within the HC; but a further role of dopamine in the HC has been demonstrated where some novelty has arisen within the environment but as yet there is no reward expected or received. There appears to be a loop involving the HC and the ventral tegmental area (the source of its dopaminic projections). Within the order of 100 ms of confronting a novelty in the environment, such as an unexpected sound, local field potential tracings in the CA1 region of the HC reveal a correlated change in potential, indicating that the novelty has been detected there (Brankačk et al., 1996). A polysynaptic pathway (via nucleus accumbens and ventral pallidum) to the VTA stimulates dopaminic signalling to the HC from VTA. Dopamine released in pyramidal cells increases long-term potentiation (LTP) at glutamatergic (NMDA) synapses; LTP is an important process in the learning of patterns within the HC, so that spatial memory is strongly reinforced by dopamine in this situation (Lisman and Grace, 2005).

### 1.3.3 Other neuroactive substances

A number of other neuromodulators released presynaptically into pyramidal cells and interneurons have been identified. These include oestrogen receptors in CCKBCs, which potentiate synaptic transmission, more particularly in the CA3 region (Kim et al., 2006); and opioid receptors on interneurons, though their precise function is unknown.

In addition there are neuromodulators which diffuse through the extracellular medium over short distances to their site of action. Important examples are:

*Endocannabinoids* induce both short-term and long-term depression in CCKBCs. They are generated within the pyramidal cell in conjunction with increased activity of NMDA glutamatergic receptors. Being lipophilic, they diffuse across GABAergic synapses from CCKBCs onto the same pyramidal cell. At such junctions, on the CCKBC side, there are endocannabinoid receptors which inhibit the release of GABA (Ahumada et al., 2013, Freund and Katona, 2007, Hnasko and Edwards, 2012).

*Nitric oxide* is created by a set of enzymes called nitric oxide synthases, found in pyramidal cells and in particular interneurons, notably ivy cells and neurogliaform cells (Armstrong et al., 2012). It is not stored, and diffuses readily through cell membranes. There are no true nitric oxide receptors; however nitric oxide is important for the synthesis of cyclic guanosine monophosphate (cGMP), an important cell messenger protein. In CA1 it has been found to be important to the development of long-term potentiation at glutamatergic synapses (Cutsuridis et al., 2010b, p.218). It may affect GABA synapses in ways not yet clear (Bartus et al., 2013), and may enhance function at serotonergic synapses (Straub et al., 2007).

*Cholecystokinin* (CCK) is released from interneurons into the extracellular medium. It has different effects on the two major types of basket cells. In CCKBCs it acts on CCK2 receptors that are postsynaptically placed at its GABA terminal on the pyramidal cell; activation of this receptor enhances the release of endocannabinoids, resulting in suppression of GABA activity as mentioned above. In the case of PVBCs, CCK2 receptors in the cell have the opposite effect (due to the activation of a different G-protein system) - they excite PVBCs. The nett effect is at the one time to increase PVBC inhibition while decreasing CCKBC inhibition (Armstrong and Soltesz, 2012).

## 1.4 The sensory information highway

The hippocampus is situated downstream of a chain of complex structures which process sensory information. Visual processing alone involves half of the neocortex in nonhuman primates (DiCarlo et al., 2012), while olfactory processing is of similar prominence in rodents. By the time information reaches the HC - after an interval of just one or two tenths of a second - basic object recognition has occurred (a task involving the nearby inferior temporal cortex), boundaries of the present environment have been identified (involving a region of occipital cortex termed the “occipital place area”), contextual information has been added (perceptual information about the appearance and layout of scenes), and this information has been related to current head position and running dynamics (DiCarlo et al., 2012, Julian et al., 2016). In parallel, the retrosplenial cortex - situated behind and above the corpus callosum - has

been involved in correlating allocentric (objective) and egocentric (subjective) reference frames; this information is available to the reciprocally connected HC, which can then invoke immediate behavioural responses to situations requiring urgent action (Vann et al., 2009).

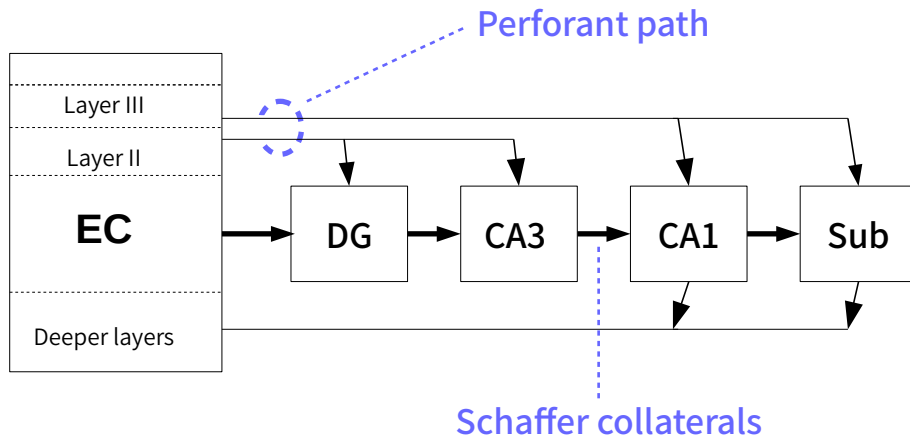


**Figure 1.5: Pathways through the hippocampus.**

Most important for the hippocampal story is the structure immediately preceding it in this information highway, the entorhinal cortex (EC). Many of the glutamatergic neurons in the dorsomedial EC have a strong mapping function, well researched in rodents. Such neurons have been termed “grid cells” (Hafting et al., 2005). If such a grid cell is monitored, it is found to fire each time the rat crosses a vertex of a virtual hexagonal grid which covers the floor of the environment. Adjacent grid cells will have firing grid patterns slightly displaced relative to each other, but the form and size of the grid remains constant. Moreover grid cell firing patterns persist, the same cells firing in the same way each time the animal returns to the same environment. If global remapping is forced - as when a new environment is entered - grid fields of individual cells remap in concert with those of adjacent grid cells, maintaining the same relativity of vertex position and of grid orientation; it seems that the EC generates a metric that can be applied universally across different environments (Buzsaki and Moser, 2013, Fyhn et al., 2007). There are also associated cells which fire according to head direction, others which only fire near boundaries, and some grid cells which have preferred firing along particular grid axes. In general, the EC grid system encodes concurrent location, direction, and movement information (Buzsaki and Moser, 2013, Smith and Mizumori, 2006). Although the details of how this mapping information is accessed within the HC is not yet clear, this upstream fixed mapping resource is vital to the hippocampal function of navigation.

The EC is not only the source of most hippocampal input (via its more superficial

layers), but also represents the major endpoint for hippocampal output (via its deeper layers - see fig.1.5), whence it is widely disseminated to cortical and subcortical structures.

### 1.4.1 Pattern formation and recognition

The entorhinal cortex and hippocampus as a unit have two major identified roles: the guidance of navigation and the formation of declarative memory (Buzsaki and Moser, 2013). Both processes require at any one moment a set of associations which typify the current circumstances in which the subject finds itself. Elements of such a set include information as to the subject's current position within the environment, its relation to objects within this environment, information as to the identity and current significance of such objects, and allocentric information such as the subject's head direction and the dynamics of its current motion. This information is relayed as mentioned in the previous section via the EC, which supplies the HC with both processed sensory input and map grid location. A particular set of such associated information, as stored within the HC, is commonly referred to as a pattern (Rolls and Treves, 1993).

As cerebral processing time and storage space is finite, it is not feasible for every slight change in sensory information to evoke a distinct pattern in the HC. As the environment gradually changes, there are two stages of pattern processing. Where changes from some previous pattern - from the very recent past, or from memory recall - are small and not the focus of close attention, a process of "pattern completion" occurs, by which the new input pattern is conformed to the prior pattern. At some point the differences between the new pattern and the pre-existing pattern become significant, and then the alternative process of "pattern separation" occurs, distinguishing the new pattern as a separate entity (Guzowski et al., 2004).

It is believed, with experimental support, that the recurrent and highly plastic connections in CA3 favour this region for pattern completion, though attempts to relegate pattern separation to particular hippocampal regions have been less successful (Dau-mas et al., 2005, McHugh et al., 2007). More is known, or at least surmised, about pattern separation. The number of glutamatergic principal cells in the DG (called "granule cells") are approximately five times as numerous as the cells of the EC which project to them, at least in the rat (Leutgeb et al., 2007). Of these granule cells, only 1% to 2% are active at any stage throughout a particular sequence of behavioral experiments for a particular animal, despite environmental changes occurring during the sequence; for the rat, this enumerates to the order of 10,000 to 20,000 cells; on the basis of this small number, it is thought that a single principal cell may be involved in many different patterns (Leutgeb et al., 2007, Piatti et al., 2013). As regards the function of these active DG cells, one concept is that each granule cell carries a small and distinct fraction of the total input (Leutgeb et al., 2007). (To this writer this appears doubtful,

given the small number of active cells and the likely complexity of patterns. It may be instead that the DG cells in some sense “bookmark” pattern components (one might call them sub-patterns) which are more completely represented within the much more active CA3 region. Such bookmarking would enable a distinction to be made between what is old and what is new in a particular pattern, This would be useful for both pattern completion and separation, as it would facilitate inclusion and/or rejection of component sub-patterns rather than of individual minutiae of the input.)

By the time information passes from the CA3 region to the CA1 region, pattern completion may be substantially complete (McHugh et al., 2007), and partial separation of completed patterns has occurred (Guzowski et al., 2004). The CA1 pyramidal cells integrate the moment-by-moment sequence of patterns from the CA3 region, with the consequent loss of some detail; Occam’s razor is applied to the bewildering supply of input material, producing summary patterns more representative of the current general state of the milieu, and so more suitable both for the formation of lasting memories and as a basis for determining an immediate behavioural response to an urgent situation (Mizuseki et al., 2012). The role of the EC input is as an ongoing reference to the current coordinates, giving a basis for long-term spatial memory consolidation and for achieving temporal association (Sun et al., 2016).

Certain hippocampal rhythms have been found to be associated with the recruitment of pyramidal cells in pattern storage, and in the maintenance of patterns; what is known of these associations will be examined separately in section 2.3.6.

The HC is not required for object recognition per se; this appears to be principally the function of upstream structures. Nor is it required for egocentric object-place encoding (which is the encoding of where things are, in the environment, relative to oneself), nor for object-context encoding (which is the association of an object with its immediate context: e.g. that object A is “beside” object B). Both of these functions have been carried out before data reaches the HC. On the other hand, the HC is essential for the association of object, place and context as holistic configurations within an environment, and so for the encoding of a holistic comprehension of the environment (Langston and Wood, 2010, Mumby et al., 2002).

# Chapter 2

## Navigation and its rhythms

### 2.1 Synaptic plasticity

The concept behind neuronal synaptic plasticity was first proposed as a “neurophysiological postulate” by Hebb in 1949: “When an axon of cell A is near enough to excite cell B and repeatedly or persistently takes part in firing it, some growth process or metabolic change takes place in one or both cells such that A’s efficiency as one of the cells firing B is increased” (Hebb, 1949, ch.4, p.62). Experimental work also showed an inverse effect, causing Stent in 1973 to propose an extension of the postulate: “When the presynaptic axon of cell A repeatedly and persistently fails to inhibit the postsynaptic cell B while cell B is firing under the influence of other presynaptic axons, metabolic changes take place in one or both cells such that A’s efficiency, as one of the cells inhibiting B, is decreased” (Stent, 1973). Within the HC, the phenomenon of plasticity was demonstrated experimentally in principal cells in 1973 (Bliss and Lømo, 1973).

Plasticity which is highly influenced by the time correlation between presynaptic input spikes and postsynaptic action potential spikes has come to be termed spike-timing-dependent plasticity (STDP). The connection strength at the synapse can either be weakened (“depression”) or strengthened (“potentiation”). Once induced, the change in connection strength may last for hours or days (“long-term”) or only for seconds or minutes (“short-term”), unless modified by intervening factors. A particular and very prevalent form of STDP, described as “Hebbian”, produces either potentiation or depression at a single synapse depending on the interval between presynaptic and subsequent postsynaptic spikes. Where this pre-post spike pair interval is less than approximately 20 ms, long-term potentiation (LTP) occurs; if the interval extends beyond 20 ms to around 100 ms, long-term depression (LTD) results instead (Markram et al., 1997). The effect would not usually be apparent experimentally with just one or a few pre-post spike pairs; typically 60 to 100 pairs are used to induce LTD or LTP,

though even as few as seven pairs delivered over half a second can do so (Volianskis et al., 2013b). Other factors such as firing rate and dendritic depolarization may influence Hebbian STDP (Feldman, 2012).

It should be pointed out that the induction of STDP occurs in response to changes in postsynaptic  $\text{Ca}^{2+}$  levels; in particular, to the rate of increase and the duration of the increase. It is not primarily a phenomenon of glutamatergic synapses, and can be induced by such increases in  $\text{Ca}^{2+}$  concentration arising from other calcium channels, or even from release from binding within the postsynaptic medium (Nishiyama et al., 2000).

### 2.1.1 Long-term plasticity in CA1 pyramidal cells

**Long-term plasticity** that is **Hebbian** under physiological conditions is prominent in glutamatergic synapses onto HC principal cells, where it is regarded as being essential to learning and memory (Bush, 2010, Morris, 2006). LTP and LTD at glutamatergic synapses onto CA1 pyramidal cells has been well studied. Both have been found to relate to postsynaptic calcium ion influx; a brief but high rise in postsynaptic  $\text{Ca}^{2+}$  leads to LTP, while a more sustained but lower rise in  $\text{Ca}^{2+}$  leads to LTD (Chittajallu et al., 1998). The high rise in the case of LTP appears to have two major components:

- *Coincidence detection by NMDA receptors.* The NMDA receptor requires two coincident phenomena in order to fire. First its internal channel must be unblocked, by removal of  $\text{Mg}^{2+}$  ions which obstruct its channel. This occurs when the synaptic membrane is depolarized by back-propagation of the postsynaptic action potential; the less negative potential dislodges the  $\text{Mg}^{2+}$  ions. Secondly, presynaptic release of glutamate must occur, as a result of the presynaptic spike. Because both processes must operate nearly simultaneously to fire the NMDA receptor, together they act as a coincidence detector (Ascher and Nowak, 1987).
- *Increased AMPA expression.* LTP also appears to involve the increased expression of previously silent AMPA glutamatergic receptors in the postsynaptic membrane; this occurs as the result of increased NMDA receptor activity. As some AMPA receptors also transmit  $\text{Ca}^{2+}$  ions, the result is a further increase in postsynaptic  $\text{Ca}^{2+}$  concentration (Feldman, 2012).

The induction of LTD at hippocampal glutamatergic synapses appears to also involve other factors. Specific and prevalent subtypes of NMDA receptors which induce LTD rather than LTP have been identified. There are also several metabotropic glutamate receptors which have been shown to mediate LTD (Collingridge et al., 2010).

The development of LTP passes through different stages involving different molecular mechanisms. The first stage, induced by a short sequence of paired presynaptic

impulses and postsynaptic action potentials, lasts approximately 30 minutes, and in the CA1 at least is dependent on NMDA receptor activity. The synaptic change over the next 2 to 3 hours is maintained instead by metabotropic glutamatergic receptors (mGluRs) and certain proteins (kinases, phosphatases); over the next couple of hours a class of rapid-response genes (IEGs) are activated, preparatory to new protein synthesis; finally, after around 5 hours, these newly synthesized proteins become involved (French et al., 2001, Manahan-Vaughan et al., 2000).

Importantly, LTP is a property of particular synapses onto a neuron, not of the neuron as a whole. Synapses in the same neuron which are not stimulated by paired pre- and postsynaptic events do not share in the LTP of those which are so stimulated (Volianskis et al., 2015).

### 2.1.2 Short-term plasticity in CA1 pyramidal cells

The term “short-term potentiation” is used to describe an earlier phase in the development of NMDA receptor-dependent LTP, which, if not interrupted, transitions into LTP; it is also called “transient LTP”. For rodent CA1 pyramidal cells stimulated with short potential bursts at 200 ms intervals, this component of LTP peaks within three minutes, and then reduces, with a time constant of typically 15 or 30 minutes, to a steady-state level of LTP. (Volianskis et al., 2013b).

There are other forms of short-term plasticity which are independent of NMDA receptors and which act for much shorter periods. Because of their particular importance to our discussion of hippocampal rhythms, they will be examined in more detail. In keeping with the literature, the terms used for these forms will be **synaptic enhancement** and **synaptic depression** (Zucker and Regehr, 2002). While the discussion here is mainly concerned with pyramidal cells of the CA1 hippocampal region, both types of synaptic plasticity have been found in interneurons of CA1 (Sun et al., 2005). It is also worth pointing out that synaptic enhancement has been found to be crucial for the maintenance of working memory in the prefrontal cortex (Mongillo et al., 2008).

Synaptic enhancement and depression are typically quantified using paired-pulse stimulation. Two potential pulses, tens or hundreds of milliseconds apart, are applied presynaptically; the ratio of the postsynaptic response to the second pulse divided by the response to the first pulse is taken as a measure of the synaptic change. This ratio is termed the *paired-pulse ratio* (PPR). Responses are commonly measured in terms of amplitudes of the excitatory postsynaptic potential (EPSP) or current (EPSC) (Dobrunz et al., 1997).

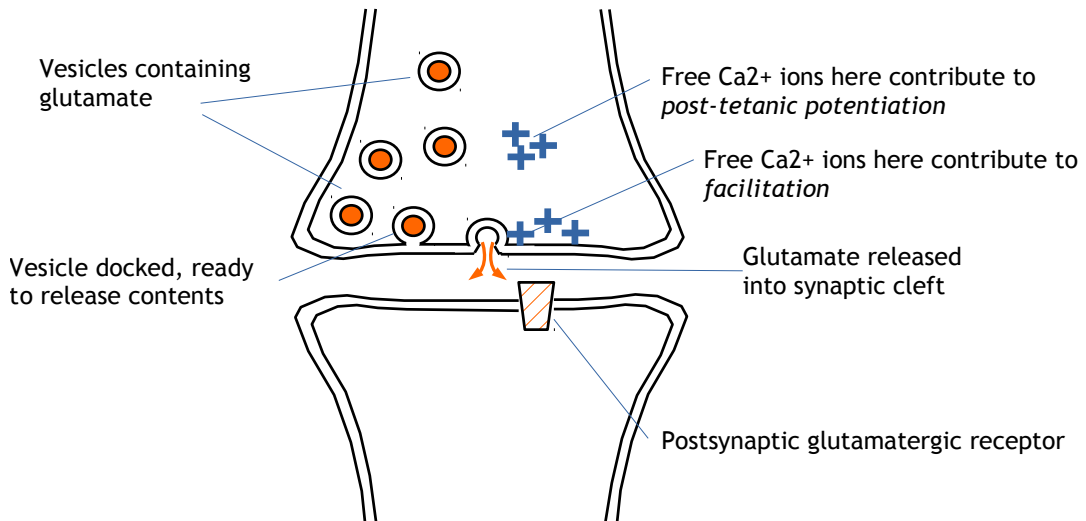


**Figure 2.1:** A presynaptic action potential increases the concentration of free  $\text{Ca}^{2+}$  ions, which causes vesicles containing glutamate (orange) to dock at the presynaptic membrane, and then to release glutamate into the synaptic cleft. From there, glutamate is taken up by receptors in the postsynaptic membrane.

Before discussing forms of short-term synaptic plasticity it is useful to recall the events occurring at a glutamatergic synaptic bouton in response to a presynaptic action potential. The action potential in the presynaptic neuron reaches the synaptic terminal as a wave of increased membrane potential. As a result, voltage-gated calcium channels open. Within the cytoplasm of the terminal are vesicles containing glutamate. The increase in free  $\text{Ca}^{2+}$  concentration in the immediate vicinity of a vesicle triggers it to fuse with the synaptic membrane, to be able to release its contents into the synaptic cleft, ready for uptake by receptors in the membrane of the postsynaptic neuron (fig. 2.1). At this stage an essential step is the tethering of vesicles to calcium channels by RIM proteins; the probability of neurotransmitter release is controlled by these proteins, which in turn are controlled by the expression of RIM genes (Fioravante and Regehr, 2011, Kaeser et al., 2011). Protein binding quickly reduces the concentration of free  $\text{Ca}^{2+}$  ions to a level incapable of stimulating other vesicles to release their contents; however this lower residual level of free  $\text{Ca}^{2+}$  persists for hundreds or thousands of milliseconds (Regehr, 2012, Zucker and Regehr, 2002).

In the case of Schaffer collateral fibres synapsing onto CA1 pyramidal cells, approximately 80% of such fibres have a single synapse site on the CA1 cell; the remaining 20% synapse at 2 to 4 sites (Sorra and Harris, 1993). At any one synapse there are 2 to 20 glutamate-containing vesicles attached ('docked') to the presynaptic membrane. When a presynaptic action potential arrives, several of these will fuse with the membrane and then release their contents; under minimal stimulation, only one such vesicle may fuse

and release (Dobrunz et al., 1997, Oertner et al., 2002, Stevens and Wang, 1995).

Several distinct processes contribute to short-term plasticity, typically occurring concomitantly to form composite effects. They are examined here particularly in the context of glutamatergic synapses onto CA1 pyramidal cells in rodents, though all have been identified widely throughout the CNS and across many animal species (Fioravante and Regehr, 2011, Fisher, 1997). Common to the forms of synaptic enhancement discussed here are the following features: (1) they result from an increased concentration of free  $\text{Ca}^{2+}$  ions in the presynaptic terminal; (2) they are expressed presynaptically; (3) they do not involve the modification of membrane channels; and (4) they are not dependent upon neuromodulators for induction or expression (Fisher, 1997). As a note of caution, however, it is impossible to separate presynaptic plasticity completely from postsynaptic events; for example, the saturation of postsynaptic receptors adds to synaptic depression (Regehr, 2012).

## Facilitation

When a wave of depolarization arrives presynaptically at a glutamatergic synapse onto a CA1 pyramidal cell, the release probability for glutamine by vesicles docked at the synaptic membrane increases dramatically within the first few milliseconds, and remains elevated for several hundred milliseconds afterwards (Stevens and Wang, 1995). This phenomenon is typically studied using paired pulses of presynaptic current; the paired pulse ratio rises within a few milliseconds to approximately 2.5, and subsequently decays with a time constant of several tens of milliseconds (Bartley and Dobrunz, 2015, Dobrunz et al., 1997, Sun et al., 2005). In the case where the first of two pulses is insufficient to cause glutamate release, the second pulse - if able to achieve that release - will still produce an EPSP of the same increased level within 5 ms. On the other hand, where the first pulse does evoke release of glutamate by a vesicle, an inter-pulse interval of up to 20 ms may be required for the second EPSP to reach the same increased level. Mechanisms for this delay of onset have been proposed (Dobrunz et al., 1997). Whether such a delay occurs or not, the same PPR of around 2.5 is always reached by 20 ms, with the same subsequent decay rate. Where the synapse receives bursts of multiple impulses this level of increased PPR does not increase further, but is maintained throughout the bursting period (fig. 2.2) (Fisher, 1997, Sun et al., 2005).

## Post-tetanic potentiation and Augmentation

While facilitation appears to be associated with unbound  $\text{Ca}^{2+}$  acting at or near the site of vesicle fusion with the membrane, the slower processes of post-tetanic potentiation and augmentation are thought to relate to the dynamics of  $\text{Ca}^{2+}$  accumulation within the core of the terminal (Fisher, 1997). These two slower processes are usu-

ally not clearly distinguished (Zucker and Regehr, 2002), and in the CA1 region may conveniently be considered as a single process, referred to simply as post-tetanic potentiation (PTP) (Wang et al., 2016). It is manifested during sustained sequences of pulses; each pulse raises the EPSP amplitude by a few percentage points, leading to a level that at some synapses in the CNS may be several times that induced by the first pulse. Once the pulse train stops, the amplification factor for any later pulse decreases exponentially, but is detectable for many seconds or tens of seconds later (Fioravante and Regehr, 2011, Zucker and Regehr, 2002). In experimentation with the mouse CA1, a recent study indicated that for a 50 Hz input, the increase in EPSP had a time constant of the order of half a second; the amplification of the EPSP tends towards an asymptote of around 2. The subsequent decay of amplitude was of the order of 10 seconds (Wang et al., 2016).

## Depression

Synaptic depression is principally a phenomenon of the depletion of those presynaptic vesicles which are immediately ready to release neurotransmitter, though other processes may have a role, such as desensitization of receptors, and inhibition by currently active GABAergic synapses in the same dendritic region (Dobrunz and Stevens, 1997, Regehr, 2012). At the synapses of Schaffer collaterals to CA1 pyramidal cells the onset of depression has a time constant of 50 ms, and initially decays with a time constant of 500 ms; as vesicular release proceeds there is an increase in residual bound calcium in the region of the synaptic membrane which accelerates recovery of the release rate; the decay time constant of depression becomes less, towards a minimum of about 30 ms (Dittman et al., 2000). Repeated stimulation of the synapse at 1 Hz therefore shows no depression, as the interval between stimuli is sufficient for full recovery. With repeated stimulation in the theta rhythm frequency range the asymptotic drop in the invoked EPSC is of the order of 10% (Dittman et al., 2000, fig. 4C2).

The effect of Schaffer stimulation of the CA1 region is complicated by the dual action of glutamatergic excitation of CA1 pyramidal cells and disynaptic GABAergic inhibition of the same cells, the result of Schaffer stimulation of stratum radiatum interneurons (SR-IN), discussed in the next section. Depression in CA1 pyramidal cells is matched by similar depression in SR-IN cells at an experimental temperature of 33° - 34 ° (Klyachko and Stevens, 2006), which is close to the rat body temperature of approximately 37° (John-Hopkins-University, 2017). For this reason I have not included synaptic depression in the following section.

## Synaptic response to a train of impulses

Combining data from the above-mentioned sources, the following sequence of events typically occurs in the presence of a train of input impulses at Schaffer-to-CA1 synapses (fig. 2.2):

- *Facilitation* will cause a rise in postsynaptic pulse amplitudes over a few milliseconds to a level of the order of 2.5 times the original amplitude; thereafter the component of amplitude due to facilitation will remain steady at this level.
- *Post-tetanic potentiation* will cause a slower rise in output amplitude, with a time constant of around half a second, and an asymptotic value of approximately twice the original amplitude.

As soon as the train of impulses ceases,

- *Facilitation* will decrease exponentially, being undetectable after a few hundred ms.
- *Post-tetanic potentiation* will also decrease exponentially, its effect being undetectable after tens of seconds.

The overall increase in EPSP strength during a train of impulses has been modelled mathematically as a multiple of the individual components. For example, Fisher et al have used the following formula for the duration of the input pulse train (Fisher, 1997):

$$\text{EPSP increase} = (F1 + F2 + 1)^3 \times (AUG + PTP + 1) \quad (2.1)$$

Where F1 and F2 represent faster and slower components of facilitation, AUG represents augmentation and PTP is post-tetanic potentiation. At Schaffer terminals, data from published sources mentioned above do not clearly distinguish between two stages of facilitation, so it is reasonable to replace F1 and F2 with a single exponential function F for modelling facilitation. Also, as mentioned earlier, there is no important distinction between augmentation and PTP at these terminals. A modified formula for the Schaffer terminal might therefore be as follows (replacing “AUG + PTP” with the symbol “P”):

$$\text{EPSP increase} = (F + 1)^3 \times (P + 1) \quad (2.2)$$

The addend “+1” represents the offset of postsynaptic potential from its original level; if there were no facilitation, the function F(t) would equate to 0, so that the facilitation component of the equation would be 1. The power of 3 comes from earlier experimentation, notably by Zenger et al, working with neuromuscular junctions in frogs (Zengel and Magleby, 1982), and so may not be relevant to the hippocampus.

As synaptic depression is thought to be caused by independent factors (including vesicular concentration within the terminal, and postsynaptic events) it is reasonable to include depression as a third multiple in the overall formula that models the effect of a

train of impulses. At the same time, I replace the facilitation power index 3 with 1, as published experimental results (references listed below) confirm that exponential rise and decay functions give a reasonable fit for the data in the CA1 region.

$$\text{EPSP increase} = (F + 1) \times (P + 1) \times (D + 1) \quad (2.3)$$

where function ‘F’ models facilitation, ‘P’ post-tetanic potentiation, and ‘D’ depression.

In section 2.2.3 the concept of “place cells” will be introduced. It will be pointed out that when a rodent is exploring its environment, particular CA1 pyramidal cells called place cells are stimulated to fire. Firing occurs only during a particular segment of the duration of a theta rhythm cycle, and then only when the animal is near or at a particular location (called a “place field”) in its environment. As the animal approaches this location, the place cell will fire once or twice during the first theta cycle in the field. As the animal comes closer, bursts of 2 typically to 4 action potentials will occur, firing being maximal as the animal crosses its centre. Firing reduces as the animal moves on, and finally cease as the animal moves out of range (Epsztein et al., 2011, Harris et al., 2002, O’Keefe and Recce, 1993).

In fig.2.2 a model is shown of how short-term plasticity might occur for a particular place cell during this process. During a burst, APs are of the order of 20 ms apart (Colgin and Moser, 2010). Bursts occur at approximately the frequency of theta rhythm, which is within the typical range of 4 to 12 Hz for rodents (Vanderwolf, 1969, fig.3). The figure shows bursts of 1, 2 and 4 place cell firings (as the animal approaches and reaches the corresponding place field), and then 2 and 1 firings per burst (as the animal moves away).

Formulas used in fig.2.2 are given below. The given time constants and asymptotic values are based on published experimental data applying to Schaffer collateral synapses onto CA1 pyramidal cells (Bartley and Dobrunz, 2015, Dobrunz et al., 1997, Nanou et al., 2016, Papatheodoropoulos, 2015, Sun et al., 2005, Wang et al., 2016).

- *Facilitation:* Given a train of impulses no more than tens of milliseconds apart, starting at time  $T_0$  and finishing at time  $T_1$ , the facilitation function at time  $t$  is dependent only on the start and end times of the impulse train, added to persisting facilitation from any earlier train, and is given by

$$F(t) = F(T_0) + (1.5 - F(T_0)) \times (1 - e^{(T_0-t)/0.006}), \quad T_0 < t \leq T_1; \quad (2.4)$$

$$= F(T_1) \times e^{(T_1-t)/0.1}, \quad t > T_1. \quad (2.5)$$

where times  $T_0$ ,  $T_1$  and  $t$  are in seconds.

- *Post-tetanic potentiation:* For a train of impulses at 50 Hz, starting at time  $T_0$  and continuing till time  $T_1$ , the following equations apply:

$$P(t) = P(T_0) + (1 - P(T_0)) \times (1 - e^{(T_0-t)/0.5}), \quad T_0 < t \leq T_1; \quad (2.6)$$

$$= P(T_1) \times e^{(T_1-t)/3}, \quad t > T_1. \quad (2.7)$$

- *Depression:* No component is modelled in fig.2.2, as explained earlier in this section.

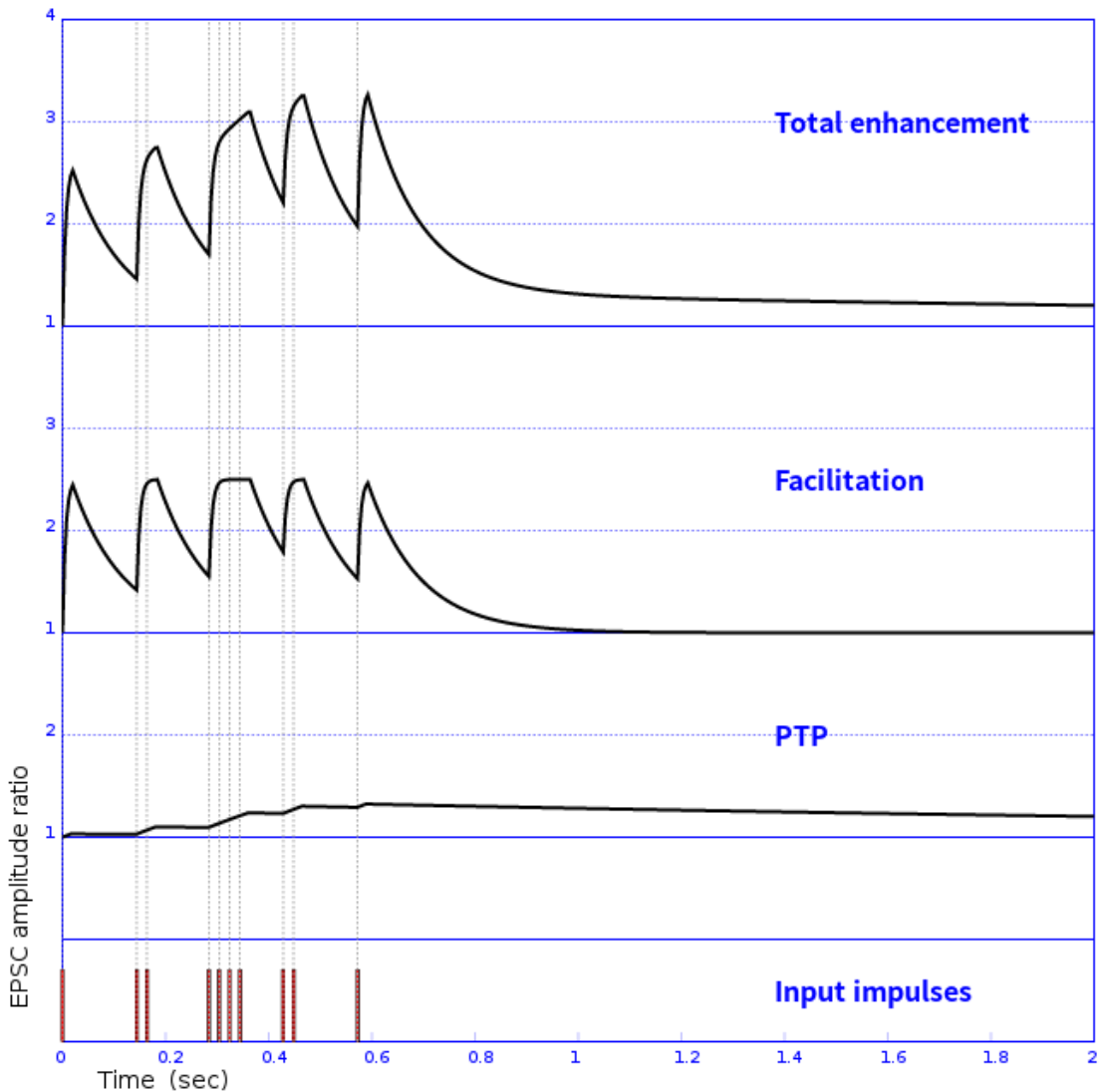


**Figure 2.2:** Short-term plasticity effects expected at a single Schaffer-to-CA1 synapse. All four panels of the figure have the same time scale. The input signal (bottom panel, red bars) consists of single impulses, 20 ms apart, in bursts of 1 to 4 impulses; the burst frequency is 7 Hz. The next two panels show the corresponding increase in EPSP for post-tetanic potentiation and facilitation separately. The top panel shows the combined effect, using eqn.2.3.

### 2.1.3 Integration window and excitation window

In the adult rat the dendritic tree of the CA1 pyramidal cell has a length of the order of a centimetre; over this length it receives around 30,000 synaptic inputs, the great majority of which are glutamatergic (Megias et al., 2001). With such a wide fan-in to the cell it is unlikely that individual synapses could fire the pyramidal cell under normal circumstances; rather, a summation, or “integration”, of positive ion input from many synapses which accumulates until the firing threshold potential of the cell is reached. At the same time leakage of current from the neuronal membrane occurs

(via ion channels and via membrane capacitance); inhibitory input of chloride cations from firing GABAergic interneuron synapses will also act against this summation. As a result of these dissipating processes there will only be a limited time window (termed the “integration window”) during which successive subliminal glutamatergic synaptic inputs can contribute towards a pyramidal action potential.

The integration window is typically demonstrated in hippocampal slices using paired pulse inputs of equal strength applied at separate locations to Schaffer collateral input to a single pyramidal cell. A single impulse would only rarely fire the pyramidal cell; but at the chosen current input the firing probability of the two coincident impulses rises to 30% to 50%. The inputs are then separated by increasing time intervals; repeated firing at each time interval allows the estimation of firing probability for the second impulse. A plot of firing probability against the separation between impulses resembles a peaked Gaussian bell curve (fig.2.3). There is no exact numerical definition of the integral window. The standard deviation of the paired-pulse curve has been used (Pouille, 2001), but may be inappropriate because of the long curve tails containing outlying values (Bartley and Dobrunz, 2015, fig. 5) which disproportionately weight the computation. One could conceivably use the half-width of the curve at a particular firing probability as an estimate.

The width of the integration window determines whether the pyramidal cell is acting predominantly as an integrator or as a coincidence detector. As an integrator it tracks the volume of incoming glutamatergic signal per unit of time, which is important for collating information during navigation. As a coincidence detector it is able to distinguish between strong incoming impulses that are close together in time, and so is better suited for pattern separation and for the discrimination of detail required for learning. The integration window is variable, enabling the same pyramidal cell on different occasions to fulfill each of these functions.

Both intrinsic and extrinsic factors govern this variation in window width. The major intrinsic factor is short-term plasticity (section 2.1.2). In hippocampal slice experimentation where the pyramidal cell has not been recently stimulated, the window of the CA1 pyramidal cell as determined by paired-pulse stimulation of Schaffer collaterals is of the order of 2 or 3 ms (Pouille, 2001; see also the black curves in fig. 2.3). However this stimulation induces short-term potentiation, so that the window widens to the order of 10 ms for a second pair of pulses occurring within hundreds of milliseconds (the red curves in fig. 2.3).

#### 2.1.4 Window width and dual Schaffer stimulation

The extrinsic factor governing window width is the GABAergic input from interneurons that target the dendritic tree of the pyramidal cell, principally the stratum radiatum

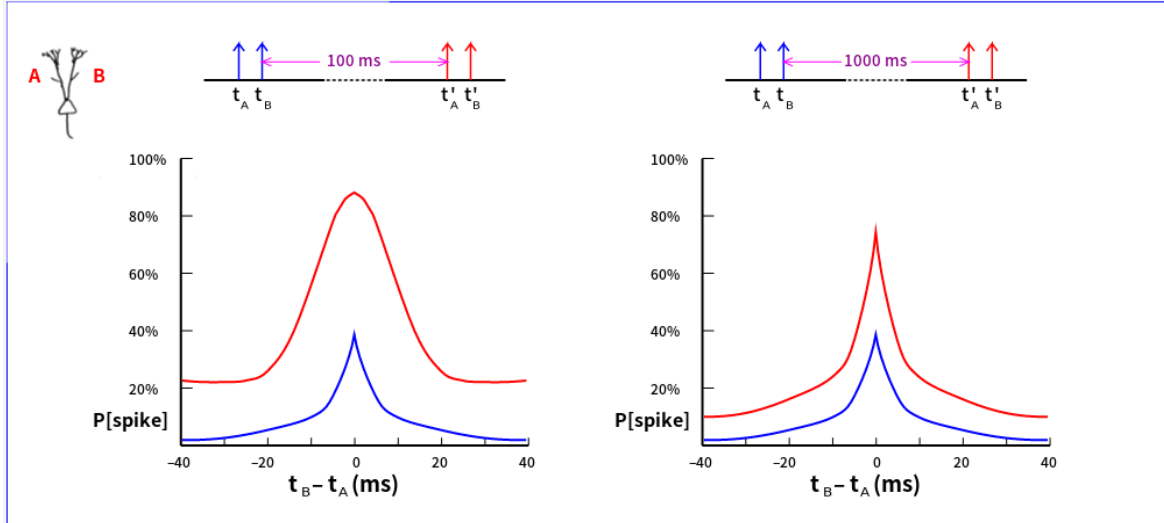


**Figure 2.3:** Idealized experimental demonstration of the integration window for a particular pyramidal cell. The top left inset represents a pyramidal cell. Equal current sources apply stimulation to two independent Schaffer collateral pathways to the cell (A and B); the stimulation level for each is below the threshold for action potential firing. Impulse current is adjusted until coincident impulses at A and B (i.e.  $t_A = t_B$ ) have a 30% to 50% chance of firing the cell. The impulse timing is then altered in small steps; the probability of firing is remeasured for each value of  $t_B - t_A$  (blue arrows of the top inset). The result is a peaked bell curve (blue). After a period of 100 ms (left graph) or 1000 ms (right graph) the procedure is repeated (red arrows in the top inset; red curves). As a result of short-term plasticity after 100 ms, the summation (“integration”) of charge from two subliminal impulses has at least a 50% chance of firing the cell if they occur within a time window of 10 ms. This expanded “integration window” is still demonstrable after 1 second, though the window is narrower. (Based on data from Bartley and Dobrunz 2015, Pouille 2001.)

interneurons (SR-IN; see section 1.2.2). Schaffer collaterals stimulate both CA1 pyramidal cells and SR-INS. The two stimulations are locked together; Schaffer-induced SR-IN activation of GABAergic synapses on the pyramidal cell (“feed-forward inhibition”) is detectable a few ms after glutamatergic activation (Klyachko and Stevens, 2006), and steadily increases as more SR-IN recruitment occurs (Bartley and Dobrunz, 2015). Both types of synapse are subject to short-term plasticity effects, but in opposite senses. At glutamatergic synapses a second impulse is larger than the first by a factor of more than 2, while at GABAergic synapses the factor is around 0.7 (fig. 2.4a).

The complementary action of excitatory and inhibitory synapses produces a total postsynaptic current which undergoes the three stages illustrated in fig. 2.4b, where curves for IPSC, EPSC and total PSC curves are in red, blue and black respectively:

- A few milliseconds of unopposed glutamatergic EPSC.
- Rapid rise of GABAergic IPSC which shortens the excitation phase of the total PSC, causing it to peak early at around 5 ms.
- The total PSC ceases to be excitatory at around 15 ms. By this stage full SR-IN

recruitment has been achieved.

- The total PSC now becomes inhibitory for many milliseconds, as the decay of the EPSC is faster than that of the IPSC from more recently recruited GABAergic input.

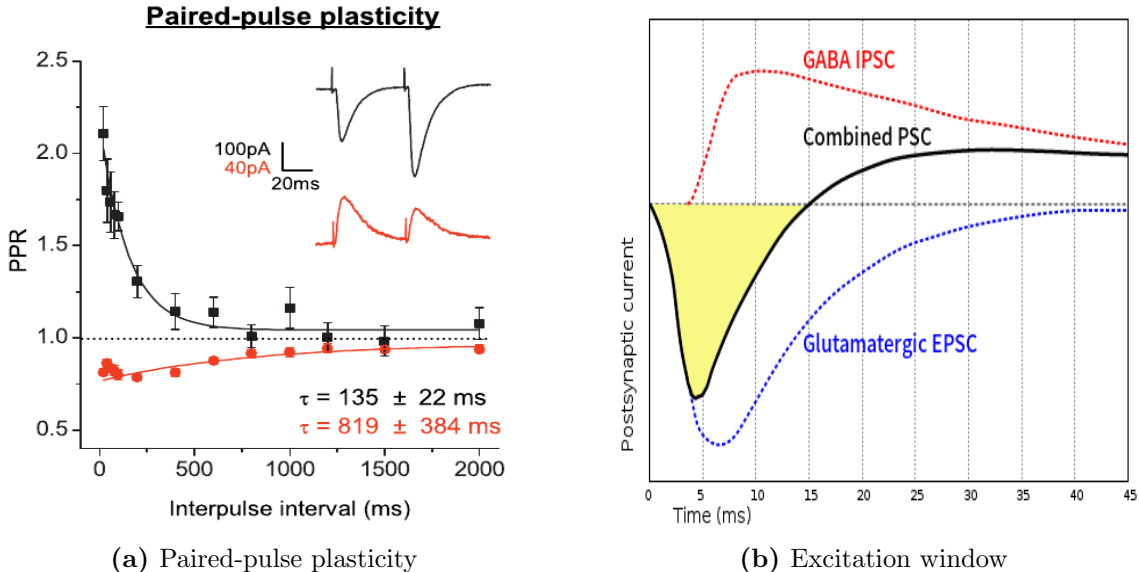


**Figure 2.4:** Fig. 2.4a: Paired-pulse responses (PPR) are plotted against time interval for glutamatergic (black) and GABAergic (red) post-synaptic currents in a CA1 pyramidal cell. Glutamatergic synapses show short-term facilitation, while GABAergic synapses instead show short-term depression. (Source: Klyachko and Stevens 2006, fig. 5C; open-access material.)

Fig 2.4b illustrates the excitation window for a single pyramidal cell. A current impulse is applied to the Schaffer collateral input at time 0. Glutamatergic stimulation commences almost immediately (blue curve); however there is a latent period of a few milliseconds before GABAergic synapses respond (red curve). Thereafter there is a rapid rise of IPSC into the pyramidal cell, reflecting increasing recruitment of SR-INs. Once recruitment is complete, the effect of short-term depression at GABA synapses takes over to reduce IPSC. The resultant postsynaptic current is represented by the black curve. This current is excitatory for only about 15 ms (as indicated by the shaded section). A second Schaffer input would have to occur within this window in order for its EPSC to summate with that of the first impulse. (Sketch based on data in Bartley and Dobrunz 2015.)

The period of time in which the total PSC is excitatory is called the **excitation window**. (It should be noted that “excitation window” refers to an interval during which the total postsynaptic current is depolarizing, whereas “integration window” refers to paired-pulse firing probabilities.) Several EPSCs must sum together in order to fire a pyramidal cell (Bartley and Dobrunz, 2015, Otmakhov et al., 1993); the current width of the excitation window will determine how close they must be in order to fire the pyramidal cell.

The excitation window widens if the SR-IN input is decreased, as would be evident in fig. 2.4b if the red GABAergic curve were flattened. This occurs during the theta cycle, when SR-IN input is considerably reduced by the action of the medial septum

mediated by OLM cells (section 2.2.2). Under such circumstances the pyramidal “place cell” acts effectively as an integrator (Bartley and Dobrunz, 2015).

A feature of the excitation window is that the location of the synapse along the dendritic branch is not materially important. This is counter-intuitive as more distal inputs should take longer to reach the soma, and should attenuate and become broader in the process. Working against this is the deployment of a voltage-gated ionic channel, the “ $I_h$  channel”, a cation-conducting channel which is activated by hyperpolarization and deactivated by depolarization (Pape, 1996). The density of the channels steadily increases from the soma to the apical dendrites by a factor of nearly seven. Depolarization selectively closes these channels, leading to diffusion of cations peripherally, reducing the broadening but not the peak amplitude of distal depolarizing inputs. As a result, sequences of input current impulses at points along the dendrite produce the same peaks of somatic membrane potential as do the same current impulses to the soma itself (Magee, 1999).

A separate form of GABAergic inhibition, not controlled directly by Schaffer stimulation, is the perisomatic inhibition from basket cells. Their input, if not sufficient to completely suppress action potentials, does greatly reduce the firing window to around 2 or 3 ms (Pouille, 2001).

## 2.2 Rhythms and navigation

### 2.2.1 Local field potential

The electric field at any point within the extracellular fluid of cerebral tissue is constantly varying, chiefly as the result of ionic transfers across synaptic membranes and across gated channels. This field is usually referred to as the local field potential (LFP). Synaptic activity tends to be the main contributing factor within the CA1, where approximately 80% of neurons are pyramidal cells. Here, activity at glutamatergic synapses within pyramidal cells is the main source of the low frequency component of the LFP. Excitatory currents within the region of the synapse are associated with an influx of cations from the extracellular medium into the neuron. To compensate, there is a passive flow of ions distributed along the neuron, back into the extracellular medium (Buzsáki et al., 2012).

At many cortical sites network complexity is such that the contributory currents appear to be pseudo-random, so that the resultant LFP superficially resembles noise. The situation is different in the hippocampus, where large numbers of pyramidal cells frequently burst-fire at much the same time, leading to a LFP with amplitudes of the order of a millivolt, and with features such as amplitude and frequency which correlate well with coordinated pyramidal cell firing (Buzsáki et al., 2012, Henze and Buzsáki,

2001). The spatial arrangement of pyramidal cells within the HC also ensures that their electrical signals are aligned in polarity; the cells are arranged with their cell bodies confined to a thin layer, and with their main axons and dendrites lying in an approximately parallel arrangement (fig.1.3).

### 2.2.2 Theta rhythm

Coordinated group-firing of CA1 pyramidal cells occurs particularly as an animal navigates through an environment. In this situation the regular firing results in an approximately periodic low frequency component of the LFP signal, referred to as “theta rhythm” (fig. 2.5). For adult rats the frequency of this component is commonly 7 to 8 Hz, but lies within the range of 4 to 12 Hz (Bland 1998; Vanderwolf 1969, fig. 3). Theta rhythm is characteristically present during locomotion and during rapid eye movement (REM) sleep, and generally absent while the animal is awake but immobile (Buzsáki, 2002). In the case of locomotion, the rhythm commences a few tenths of a second before movement actually begins, and continues throughout locomotion (Fuhrmann et al., 2015). For rodents an approximate linear relationship between running speed and theta frequency has been demonstrated (Bouwman et al., 2005, McFarland et al., 1975, Sławińska and Kasicki, 1998)

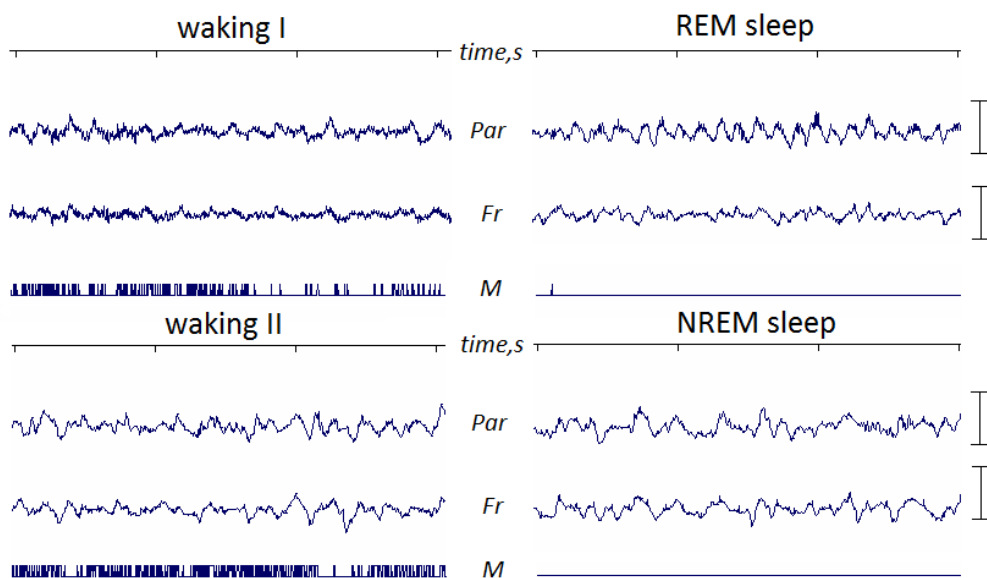


**Figure 2.5:** Local field potentials of a mouse brain, recorded by surface electrodes applied to either the prefrontal region (“Fr”) or over the hippocampal region (“Par”). Tracings are taken over 3 seconds. Peaks labelled “M” indicate movement by the mouse. The vertical scale bars represent 1 mv. “Waking I”: during voluntary movement, while interacting with the environment; “Waking II”: At rest, or with movement unrelated to exploration. “NREM” refers to non-REM sleep. A frequency component of the order of 5 to 7 Hz is apparent in the top two hippocampal traces, and at the right end of the hippocampal trace “Waking II”. (Source: Andrii Cherninskyi, downloaded from [https://commons.wikimedia.org/wiki/File:Normal\\_EEG\\_of\\_mouse.png](https://commons.wikimedia.org/wiki/File:Normal_EEG_of_mouse.png))

## Origin and distribution

Synchronized theta rhythm occurs in all parts of the hippocampus and in associated temporal lobe structures including the entorhinal cortex, perirhinal cortex, cingulate cortex and amygdala (Buzsáki, 2002, Kirk, 1998). Several diencephalic and pontine regions also manifest short bursts of neuronal firing which occur synchronized with theta rhythm frequency. These include the medial septum, the supra-mammary nucleus, the posterior hypothalamic nucleus, and two major pontine regions: the reticularis pontis oralis nucleus and the pediculopontine tegmental nucleus (Bland and Oddie, 2001, Pan and McNaughton, 2004). There is extensive interconnection between these structures (fig. 2.6). No particular region has been unequivocally identified as the generator of the theta oscillation; it is quite likely that generation is distributed throughout the system with its multiple feedback loops (Buzsáki, 2002).

## The role of the medial septum - diagonal band of Broca

The medial septum and the adjacent diagonal band of Broca are together of fundamental importance to the presence of theta rhythm in the hippocampus. As these two regions are intimately interconnected, and appear to work in concert in this context, they are often grouped together using the acronym MS-DBB or MSDB, the latter being chosen for this thesis (Colom, 2006, Dragoi et al., 1999). Destruction or inhibition of the medial septum abolishes theta rhythm in the HC, as does section of fibres from the MSDB to the HC (Andersen et al., 1979, Gray, 1971, Oddie, 1998, Sainsbury and Bland, 1981). Neurons within the medial septum have been identified which burst with the same periodicity as that of theta rhythm within the HC and EC (Stewart and Fox, 1990). Projections from these cells convey the rhythm to all parts of the HC and EC. In all regions receiving these projections the frequency is unaltered, though there are local phase differences which reflect different transmission delays for the various projections (Kirk, 1998).

Projections from the MSDB to the HC are cholinergic, glutamatergic and GABAergic. Projections of all three types terminate almost exclusively on interneurons rather than on principal cells (Colom, 2006, Fuhrmann et al., 2015).

- The *cholinergic fibres* terminate widely on all types of HC interneurons, where they modulate synaptic plasticity; a small proportion terminate on pyramidal cells (Bland and Oddie, 2001). Their stimulation appears to sharpen the animal's attention; this is expressed by a more rapid response to uncertainty and improvement of active learning (Picciotto et al., 2012). Ablation of these fibres greatly attenuates the amplitude of the theta oscillations in the HC (Cea-del Rio et al., 2010). The time constants for onset and decay of cholinergic action are of the order of seconds in the CA1 region (Hasselmo and Fehlau, 2001); conse-

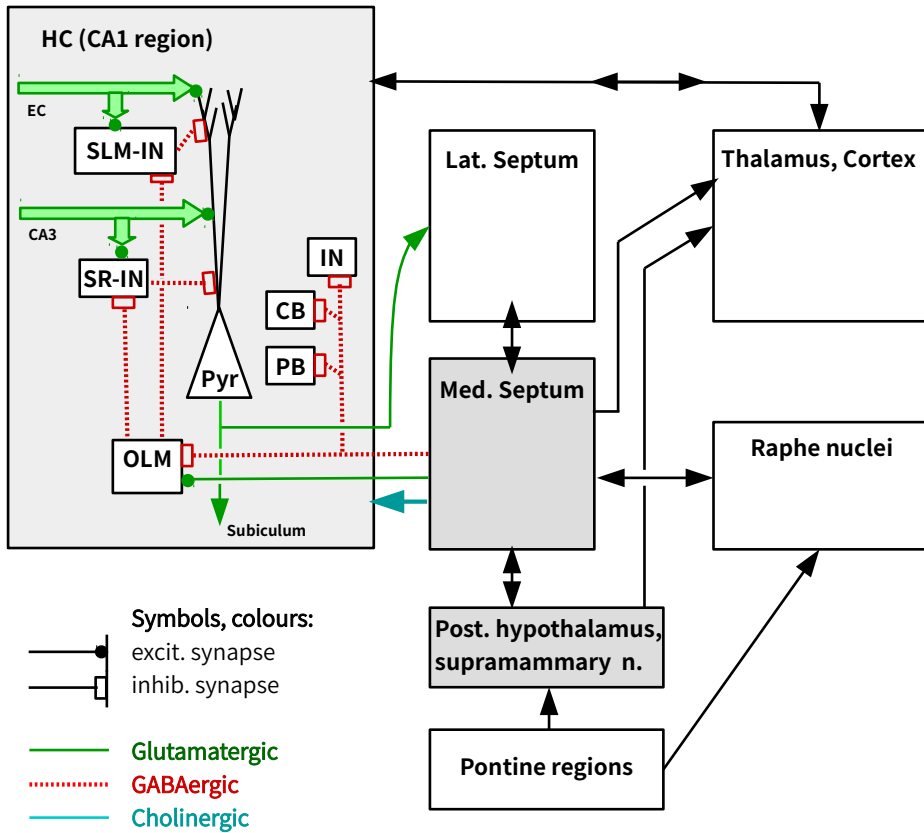


**Figure 2.6:** Major interconnections within the network manifesting and controlling theta oscillations. Neurotransmitter types are only specified for CA1 connections. Boxes with grey backgrounds represent regions where theta oscillations of synchronized frequency can be readily detected.

Abbreviations within the CA1 box: **EC**: Perforant path fibres from EC; **CA3**: Schaffer collaterals from CA3 pyramidal cells; **SLM-IN**: stratum lacunosum-moleculare interneurons; **SR-IN**: stratum radiatum interneurons; **OLM** - stratum oriens lacunosum-moleculare interneurons; **Pyr** - pyramidal cells; **PB** - parvalbumin-expressing basket cells; **CB** - CCK-expressing basket cells; **IN** - other interneuron types, not listed here.

quently the cholinergic input to the HC cannot be involved in events occurring during a single cycle of theta rhythm.

- The *GABAergic fibres* synapse on a wide variety of HC interneurons. They convey phasic bursts which are synchronized with theta rhythm, strongly inhibiting interneuron firing during particular phases of the theta cycle; some interneurons are inhibited during the theta peak, others during the theta trough (Borhegyi et al., 2004, Freund and Buzsáki, 1996). These GABAergic projections also have a role in neuronal recruitment just before locomotion begins, and appear to have a stabilizing role during theta activity (Hangya et al., 2009).
- The *glutamatergic fibres* have only more recently been studied. They constitute about 23% of the total septohippocampal projection; yet until recently neither

their target interneurons nor their function was known (Colom, 2006). More recently the target has been identified as oriens-lacunosum moleculare (OLM) interneurons (Fuhrmann et al., 2015). The target receptor uses glutamate transporter proteins of type VGLUT2 to fill presynaptic vesicles, whereas synapses onto pyramidal cells use the VGLUT1 transporter (Fuhrmann et al., 2015). The significance of this is uncertain, though synapses using VGLUT2 appear to be less suited for the development of long-term potentiation and more for long-term depression (Liguz-Lecznar and Skangiel-Kramska, 2007).

The MSDB also sends glutamatergic axons to layers 2 and 3 of the EC, these layers being the source of the perforant path to all HC regions, and so to the terminal dendritic tufts of CA1 pyramids. These MSDB axons provide speed-related information (Justus et al., 2016).

The major factor for increasing the firing probability of CA1 pyramidal cells at certain stages of the theta oscillation appears to be the glutamatergic input to interneurons in the stratum oriens and alveus layers of the CA1 region, identified as OLM cells (Fuhrmann et al., 2015). Fig.2.6 illustrates the relevant connections. The OLM cells, when so stimulated, provide GABAergic signals to stratum radiatum interneurons (SR-IN) - which were described in section 1.2.2 - and to similar interneurons in stratum lacunosum-moleculare. Both groups of interneurons continuously inhibit pyramidal cells, tonically via cholinergic stimulation and phasically via glutamatergic feedforward input (from Schaffer collaterals, in the case of SR-INs, and from the perforant pathway, in the case of lacunosum-moleculare interneurons). This global inhibition of pyramidal cells is periodically itself inhibited by GABAergic signals from the OLM cells, which in turn are driven by firing bursts at theta oscillation frequency from the glutamatergic fibres from the MSDB. Pyramidal cells are freed from this inhibition as soon as MSDB burst-firing commences, and remain partially free of inhibition for several tenths of a second after the last MSDB burst (Alkondon et al., 2011, Fuhrmann et al., 2015).

The same periodicity is apparent in the GABAergic input from the MSDB. Interneurons which receive this input include CCK-expressing cells (including CCKBCs), PVBCs, axo-axonic cell, bistratified cells, all described in section 1.2.2; and also the OLM cells just mentioned (Somogyi et al., 2014, Somogyi and Klausberger, 2005). As the input is inhibitory to these interneurons, the effect of this GABAergic input is to greatly reduce the inhibition of pyramidal cells at particular stages of the theta cycle.

Our understanding of the role of the rhythmic firing of MSDB GABAergic projections is only partial, and remains one of the challenges for future work (Somogyi et al., 2014, Tukker et al., 2013). Importantly, they richly connect with parvalbumin-expressing basket cells (PVBCs), which have long been regarded as major pace-setters for the pyramidal cells. PVBCs also receive glutamatergic input from CA3 and EC fibres, as well as from local CA1 pyramidal cells (Sun et al., 2016). PVBCs fire just before OLM cells, and their firing comes to an end as the OLM cells start to fire (Forro et al.,

2015). It is likely that MSDB pulsed glutamatergic stimulation of OLM cell firing is synchronous with MSDB pulsed GABA inhibition of PVBCs, causing this sudden end to PVBC firing. Such PVBC firing would have a vital role in stabilizing pyramidal cell action; it would rapidly and completely bring to an end late pyramidal cell firing in the theta cycle, so that there would be no reverberation with the next OLM-gated pyramidal firing. On the other hand, PVBCs would be silenced at the time when pyramidal firing probability increases, that is, the time when OLM inhibition of SR-IN interneurons disinhibits pyramidal cells. If such a sequence of events is confirmed, then the PVBC is to some extent dethroned from its traditional role as a pace-setter for pyramidal cells. On the other hand it would be important as a stabilizing factor, helping to prevent any uncontrolled group firing of pyramidal cells that might arise through spurious positive feedback; it would also ensure that data provided to downstream structures at specific phases of theta rhythm remained discreet, without the added noise of place cell firing beyond such phases. (Axo-axonic cells also fire shortly before OLM cells, and almost certainly share in both of these roles.)

### Timing of firing during theta

Many studies have shown that different groups of neurons fire at different stages of the theta cycle; unfortunately it proves difficult to reconcile individual data sets. One problem is that there is considerable theta phase difference across the width of the CA1 region, as shown in fig.2.7, which is based on work by Bragin et al. 1995. Three successive cycles of theta oscillation were recorded simultaneously at a variety of depths within the rat CA1. The figure shows that there is almost no variation across the layers containing the pyramidal cell body and its axon, namely stratum pyramidale, stratum oriens and the alveus; at these sites the main contributor to the LFP is the action potential of the pyramidal cell, with its rapid transit along the axon. Most of the phase difference occurs across the stratum radialis, which contains the main branches of the pyramidal cell dendritic tree. Here the LFP is dominated by input from CA3 via the Schaffer collaterals and by increasing charge within the dendritic tree prior to the firing of the CA1 pyramidal cell. The phase difference across this layer is of the order of  $90^\circ$ . As the frequency in the original experiment was approximately 8.5 Hz, the theta period is 117 ms, so that a phase difference of  $90^\circ$  corresponds to approximately 30 ms.

Most of the interneurons commonly studied from the point of view of theta coordination have their cell bodies in stratum pyramidale and stratum oriens, throughout which there is no significant theta phase difference. If the depth at which theta were recorded were the only factor causing variation between different authors' data, we might expect that one author's findings might correspond to another author's findings after allowing for an overall phase shift. In fact, as fig.2.8 shows, the differences are not explicable on

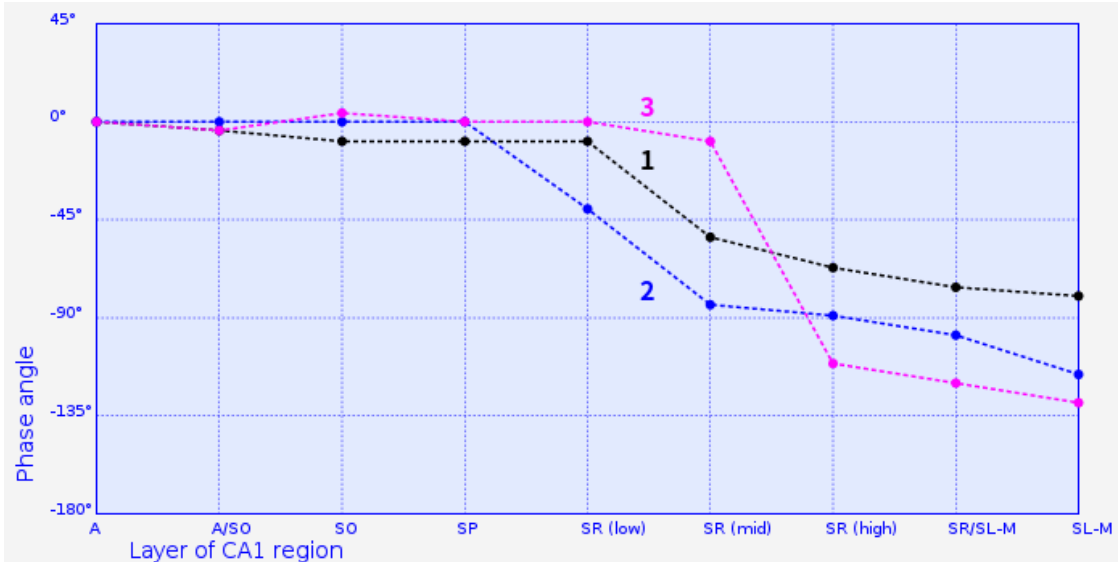


**Figure 2.7:** Variation of theta rhythm phase with depth within the CA1. For each of three successive theta peaks the phase of the peak at different depths was monitored. The reference phase angle ( $0^\circ$ ) is that occurring in the alveus. **A:** alveus; **SO:** stratum oriens; **SP:** stratum pyramidalis; **SR:** stratum radiatum; **SL-M:** stratum lacunosum-moleculare. (Based on data from Bragin et al. 1995, fig.8.)

this basis. I have abstracted data from four papers, as listed in the legend of the figure. Fig.2.8(a) shows an idealized theta wave in the top panel (grey). All four sources have aligned their data with this idealized wave. The various coloured segments in the figure symbolically represent firing probability curves for different neuron types. The left end of each coloured polygon corresponds with the phase angle at which firing probability has risen to half of its maximum value; the right end marks the phase angle where firing probability has fallen to half of the maximal value. The vertical line inside the polygon marks the phase angle of the maximum firing probability. As can be seen, there is approximate agreement across all four sources that OLM firing occurs around the theta trough and ascending limb, while pyramidal cell firing occurs at about the same time or slightly later. Another point of agreement is that AA cells and PVBC cells tend to fire in tandem, the PVBC firing first, and the AA cell firing around  $90^\circ$  later. However there is dramatic variation between sources as to when PVBCs fire relative to the theta trough; the data from Somogyi et al. is exactly  $180^\circ$  out of phase with the data from Forro et al.!

If the primary signal for the firing of the pyramidal cells is the glutamatergic input from the MSDB to OLM cells, as discussed earlier, then this would seem to provide a much more useful reference signal than the theta LFP variation. This data is not available in the literature surveyed; the nearest available reference signal would be OLM firing, as this closely follows the glutamatergic MSDB signal. When one ignores theta phase and instead cross-references firing probability curves in the various sources to their curves for OLM firing, the result is shown in fig.2.8(b). In the top panel, all points of maximal OLM firing have been assigned the phase angle of  $0^\circ$ ; in the lower panels, the coloured

polygons have been moved accordingly, all keeping their phase relationship with OLM firing the same as before. The result for each cell type is a reduction in the variation between sources. In particular, there is now loose clustering of PVBC firing at around 90° before maximal OLM firing.

One other important function of the OLM interneuron is to minimize input from the EC to the pyramidal apical tufts at that stage of the theta cycle when Schaffer input into pyramidal dendritic branches is maximal; it does this via GABAergic synapses to the region (Klausberger, 2009, Maccaferri, 2005). It is believed that the trough of the theta LFP corresponds with an encoding phase of incoming information, for which the mapping information from EC is important; at this stage Schaffer stimulation of CA1 place cells is weak, preventing interference from previously learned associations. The more positive phase of the theta LFP corresponds with frequent pyramidal cell firing, and is believed to be associated with the retrieval of previously learned patterns (Hasselmo et al., 2002a); the inhibition of the apical dendrites by OLM cells at this stage prevents contamination of these patterns with new information.

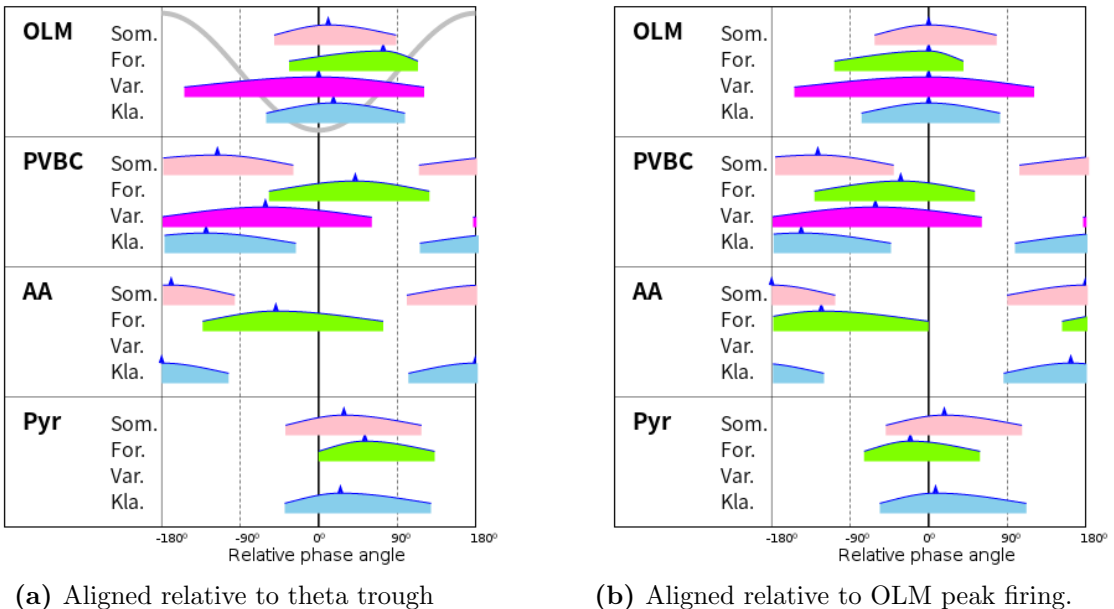


**Figure 2.8:** Data for firing probability for four different CA1 cell types from four different data sources have been combined. The left panel of each plot lists cell types, and for each cell type, the author (Key below). Each shape in the graph symbolizes the probability distribution; the edges occur where the distribution curve amplitude is half the peak amplitude; the central needle in the shape locates the peak amplitude. Colour coding reflects the data source. On the left, firing patterns are aligned in accordance with the theta trough (the idealized theta wave is shown in grey in the top panel). On the right, patterns are aligned by the OLM firing peak.

Key to data sources: *Som.* (Somogyi et al., 2014, fig.1); *For.* (Forro et al., 2015, fig.7 for dCA1); *Var.* (Varga et al., 2012, figs.1,2); *Kla.* (Klausberger and Somogyi, 2008, fig.2).

## Theta rhythm and movement

Occasional papers in the literature have demonstrated a correlation between running speed and theta rhythm frequency. Slawinska and Kasicki in 1998 demonstrated a strong correlation of frequency with stepping rate during movement along a horizontal runway, but unfortunately no information is supplied which correlates stepping rate with running speed (Sławińska and Kasicki, 1998). In 2004, Bouwman et al found a weaker correlation for open-field conditions monitored by video camera. The linear regression data fit for their observations was

$$f = 8.25 + 0.0338 \times v$$

where  $f$  is the frequency (Hz) and  $v$  the running velocity of the rat (cm/sec). Only five rats were involved, and runs could be as short as one second (Bouwman et al., 2005). A more convincing relationship between running speed and theta oscillation - this time measured in the MSDB - is shown by King et all in 1998, for a small number of rats (not stated) (King et al., 1998). The regression fit line for the data was

$$f = 7.87 + 0.0167 \times v \quad (2.8)$$

On the other hand, one study (nine rats, 75 CA1 place cells) showed no significant variation of theta frequency with speed (Huxter et al., 2003).

A clearer picture of the relationship of theta rhythm to movement emerged from recent work by Fuhrmann (Fuhrmann et al., 2015). Optogenetically engineered mice were used. In these mice VGLUT2 glutamatergic neurons contained both the protein GCaMP5 (which fluoresces green in the presence of Ca<sup>2+</sup>, and so allows firing to be visually monitored) and channelrhodopsin-2 (which is expressed in the cell membrane and evokes depolarization when stimulated by light). In this way they could observe the specific activity of MSDB glutamatergic cells under various conditions, and could also study the effects of specifically firing these cells. They further monitored the activity of putative OLM cells in CA1 by injecting an adeno-associated virus expressing the fluorescing protein GCaMP6s into the right dorsal hippocampus; while this infected all cells in the region, an implanted window with microscopic surveillance allowed the specific monitoring of interneurons in stratum oriens and alveus for fluorescence. Their findings include the following:

- Several hundred milliseconds before voluntary motion begins, theta oscillation commences simultaneously with an increase in the activity of MSDB glutamatergic neurons (see also Hangya et al. 2009).
- Once the animal is moving, MSDB glutamatergic activity continues to rise, the rate of its increase at this stage being proportional to the final running speed of the animal.

- If the animal was awake but not moving, optical stimulation at theta frequency of MSDB glutamatergic neurons in most cases induced theta rhythm in CA1 with the same frequency, and after a few seconds induced motion; the final running speed correlated well with the frequency of the optical signal. Fig. 2K in this article indicates a linear relationship:

$$f = 7.87 + 0.0167 \times v \quad (2.9)$$

The role of putative OLM cells was demonstrated, as described in section 2.2.2. MSDB glutamatergic stimulation of OLM cells correlated with sub-threshold depolarization of the pyramidal cell membrane, and consequently with increased pyramidal firing.

The authors are not postulating that the MSDB alone controls locomotion, by means of the glutamatergic projections of the MSDB to CA1. They demonstrated that there are monosynaptic connections to MSDB glutamatergic neurons from the ventral tegmental area, the median raphe nuclei and several hypothalamic nuclei (using immunohistochemical methodology). It is likely that extensive feedback loops from CA1 via the lateral septum are involved in the induction of motion, and that subcortical regions and some hypothalamic nuclei are involved in the matching of theta frequency to changing running speed (Vertes et al., 2004). This is consistent with the finding that there is a gap of several seconds between the onset of optically generated theta stimulation and the commencement of motion.

Although the authors found a strong correlation between theta frequency and final running speed, whether the motion be voluntary or optically induced, they also demonstrated that it does take the mouse a few seconds to accelerate to that final velocity. This was not taken into account in the two earlier papers mentioned above (Bouwman et al. 2005, Sławińska and Kasicki 1998); some of the scatter in their data would be accounted for by not allowing for this settling time.

### 2.2.3 Place fields and place cells

By 1948 it was considered likely that some part of the brain preserved cognitive maps of different environments (Tolman, 1948). During the 1960's the hippocampus became the likely contender for holding such a map (Douglas, 1967). Strong evidence for this came in 1971 with the publication of a paper by O'Keefe and Dostrovsky, demonstrating that in rats navigating a learnt laboratory environment, particular subsets of hippocampal cells would only fire at times when the experimental animal was passing through certain fixed positions in the experimental arena (O'Keefe and Dostrovsky, 1971). Such a cell was termed a “place cell”, and the location at which it consistently fired was described as its “place field”. Many studies since have confirmed the concept and have added considerably to our understanding.

Place cells are a subset of the glutamatergic principal cells of the HC; they have been identified in the dentate gyrus, CA3 and CA1 regions (Rolls et al., 2006). In a given learnt environment, each place cell has its unique place field (typically just one, sometimes more than one) (Wilson and McNaughton, 1993, fig.1). Nevertheless in confined rectangular laboratory environments there is a tendency for place fields to cluster along the perimeter, near corners and midway along the length of walls (O’Keefe and Burgess, 1996). Geometry is not the sole determinant of place field positioning. Other factors include the animal’s current focus of attention, the demands of some task being carried out, and changes in colours and odours (Smith and Mizumori, 2006). Where a linear track is involved, the place cell as determined for one direction does not necessarily fire for movement in the opposite direction (Frank et al., 2004, McNaughton et al., 1983). Place fields are detectable after a single pass through a new environment, becoming stable after minutes of exploration (Frank et al., 2004), and once formed remain stable even if weeks pass between exposures to the same environment (Muller, 1996).

The complexity and detail of this hippocampal map becomes apparent when one considers some statistical parameters. In one experiment using eight tetrodes per rat and an arena of 150 x 140 cm, 322 place fields were identified, this being a lower limit imposed by the resolution of methodology used (Fenton et al., 2008). In another study, 288 putative pyramidal cells in 3 rats were identified, all of which had fired at some time during the ten days of surveillance. Of these, approximately one third showed statistically significant correlation between firing and spatial position during navigation in the experimental environment, while the remaining two-thirds were “virtually silent” at this time (Wilson and McNaughton, 1993). The rat CA1 contains of the order of 300,000 pyramidal cells (Bezaire and Soltesz, 2013). If most or all of these were “functional” in the sense of Wilson’s paper referred to above (that is, they fire at some time during a long experimental period, including rest and sleep), then there would be several tens of thousands of place cells active in one environment in any one rat CA1, each with its own place field deployment. A further figure comes from work by Muller et al. 1987; their work with 17 rats and 40 place cells led them to propose that in CA3 and CA1 “place cells comprise upwards of 60% of complex-spike cells [= putative pyramidal place cells]”. Such large numbers of place fields could conceivably provide a very detailed representation of position, colour, odour, reward content and other environmental factors, which would enable quick detection of differences occurring as the environment undergoes changes.

The development of place fields appears in each region to depend on direct input from the EC (Hafting et al., 2005); in particular, the place fields of CA1 can develop independently of those in the DG and CA3, as shown by experiments inactivating the Schaffer collaterals (Morris, 2006, Rolls et al., 2006). The grid cells within the EC evoke a hexagonal reference grid for the environment, one that can be applied universally across different environments (Buzsaki and Moser, 2013, Fyhn et al., 2007).

A similar metric for land surveyors - the predetermined grid of latitude and longitude lines - enables the assigning of geographical positions to environmental features in the making of land maps.

Place fields are nowhere near as prominent in the primate HC. This may relate to the fact that rodents explore common laboratory environments in more or less a two-dimensional manner, while primates use three-dimensional visual cues far more when navigating, requiring a more complex system of neuronal deployment (Smith and Mizumori, 2006).

#### 2.2.4 Phase precession

During navigational activity, place cells mostly fire during the half-cycle of theta rhythm in which the LFP is rising (fig.2.8). However the timing and amplitude of firing changes as the animal traverses the place field. As the place field is first approached, firing tends to happen just after a theta peak. As the animal traverses the field firing occurs progressively earlier, until towards the end of the transit firing may occur most of a theta cycle earlier, near the preceding theta peak. This change in timing of firing is usually described in terms of a phase angle shift, some point on the theta wave being assigned zero phase; the negative phase shift is termed “phase precession” (O’Keefe and Recce, 1993).

Place cells rarely fire when the subject is moving outside of the corresponding place field. As a result they will have been silent just before the subject reaches the edge of the place field. As the subject enters the place field, the associated place cells begin to fire single APs. In relation to the background theta rhythm, these first APs usually occur just before the theta rhythm potential reaches its maximum amplitude. As the subject moves towards the centre of the place field the place cells fire more than once in each theta cycle. At some point shortly after the centre of the field firing becomes maximal, commonly four times, sometimes up to eight times, per cycle (Harris et al., 2002, Mehta et al., 2002); but the first such AP will now occur earlier in the theta cycle than before. As the subject moves past the centre, towards the periphery of the place field, firing becomes less frequent, but the first AP continues to occur earlier in the theta cycle. Place cell firing finally ceases after the subject has left the place field. (A prolonged tracing illustrating these features may be found in O’Keefe and Recce, 1993, fig. 5 and 6, not reproduced here). The amount of precession is variable, but typically ranges from  $100^\circ$  to  $300^\circ$  (Huxter et al., 2003, O’Keefe and Recce, 1993). Over the last quarter of the place field firing decreases, and the phase relationship with distance becomes increasingly uncoordinated (Mehta et al., 2002).

The process is often illustrated using a pure sine wave to represent theta oscillation, with regularly placed ticks representing the place cell firings; nevertheless for any single

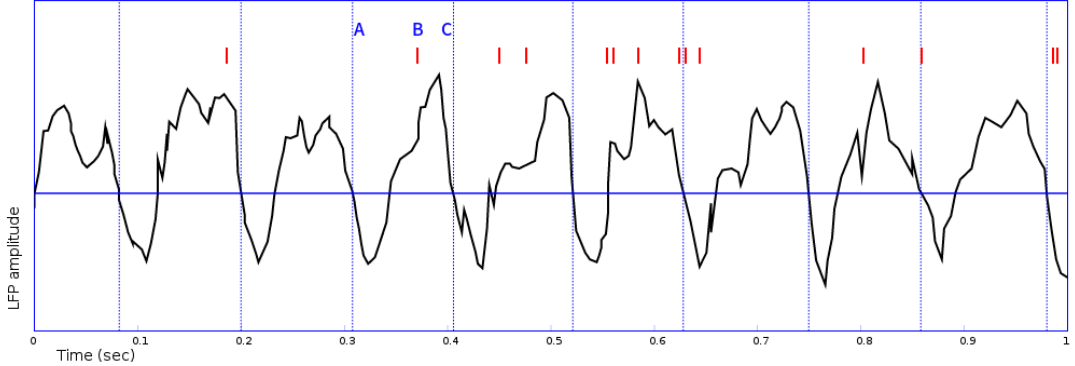


**Figure 2.9:** Representation of a single-pass experimental outcome, where the firing of a particular place cell is monitored simultaneously with the local field potential. The start of a theta cycle may be conveniently taken as the point where the falling LFP reaches the mean potential (points marked with vertical lines). Short red lines represent place cell firing. Phase lead of firing is measured as shown for the firing event labelled B: the next theta cycle start occurs later by time interval BC, and the duration of the particular cycle is AC; hence the phase lead of the event can be measured as  $360 \times BC/AC$ , in this case  $109^\circ$ . The event can equally well be referenced to the earlier theta crossing A, in which case the event would have a phase lag of  $251^\circ$ . (Sketch based on data provided in O'Keefe and Recce 1993.)

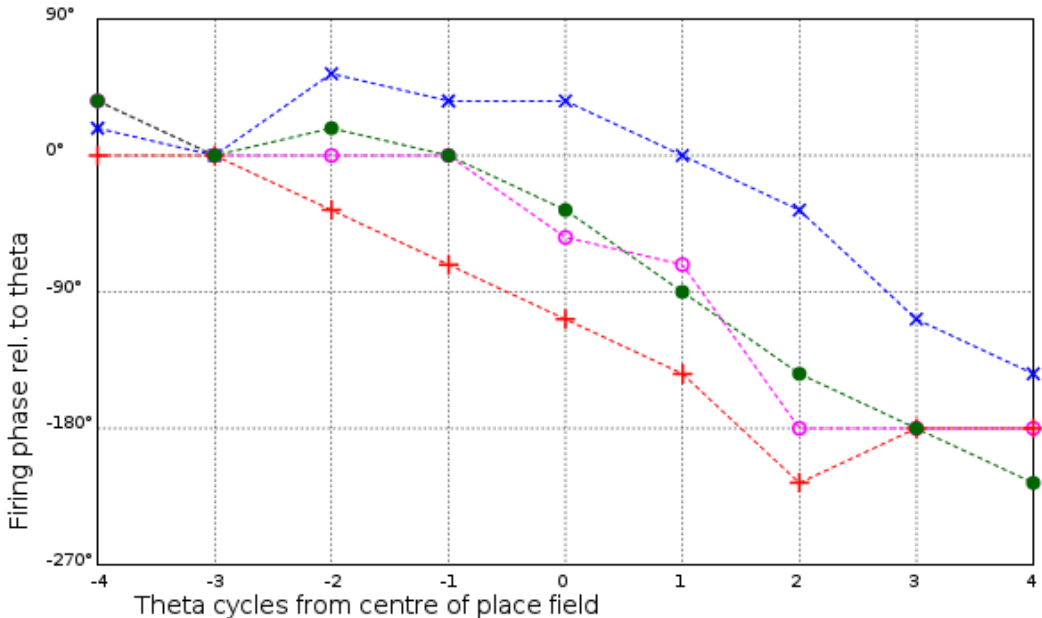


**Figure 2.10:** In one set of experiments reported by Skaggs et al. 1996, the firing phase of four CA1 place cells was related to distance from the centre of the corresponding place field as measured in terms of theta cycles rather than centimetres (horizontal scale of the graph). Data was collected over many passes for each cell, from which the mean firing phase at each theta cycle (vertical scale) could be derived. In the graph above, each cell is represented by a curve of unique colour and point shape. (Figure constructed using data abstracted from Skaggs et al. 1996, fig.6 A-D.)

transit through a place field, recordings of cell activity will be much noisier, as shown in fig.2.9. When firing phase is plotted against the animal's distance from the centre of the field for a large number of transits through the field, the data tends to lie in an ellipse on the graph, and so lends itself to linear regression analysis, in order to produce

a theoretical population linear relationship between phase and distance (O’Keefe and Recce, 1993, fig.3). For individual place cells the phase - position relationship, while still in general linear, is more subject to variation (fig.2.10).

The total phase shift is independent of the speed at which the animal negotiates the place field, as also is the degree of phase shift at any one point within the field; but during faster runs the number of spikes per theta cycle is greater (Huxter et al., 2003).

As experience of the one environment builds up, the curve becomes skewed (Mehta et al., 2000). Place cells begin to fire earlier during the approach, apparently reflecting the development of LTP in the place cells, as the effect can be blocked by an NMDA receptor antagonist (Ekstrom et al., 2001). However the same LTP is unable to prolong firing as the animal exits the field because increased perisomatic inhibition by interneurons at that stage curtails the firing (as discussed in section 2.3.5). Despite this expansion in the spatial extent of the place field with experience, the total phase shift remains the same (Ekstrom et al., 2001). Moreover once the place field is fully learned, the spatial extent of the place field is independent of the animal’s speed, as is the total phase shift (Huxter et al., 2003).

## 2.3 Intracellular events during place field transit

It has been demonstrated that the signal from EC to apical dendrites of CA1 pyramidal cells during theta rhythm is maximal during the troughs of the theta LFP (as measured in the hippocampal fissure), while the signal from CA3 pyramidal cells to CA1 pyramidal cells is maximal at its peaks (Brankack et al., 1993). (The action of OLM cells ensures a degree of separation in the timing of the two signals, as OLM cells inhibit the apical dendrites while disinhibiting the Schaffer input to main branch dendrites.) When a rodent is navigating inside a place field, there are strong signals from EC grid cells to place cells, as well as from corresponding place cells in CA3. The proximity of the two signals has long been believed to be relevant to the development of LTP in place cells (Buzsáki, 2002). It might superficially appear to be that the time gap between the maximal EC signal and Schaffer-induced place cell firing is more than the 20 or 30 ms required for spike-timing-dependent plasticity in pyramidal cells (Bi and Poo, 2001, Nishiyama et al., 2000). A better knowledge of intracellular events gleaned over the last two decades provides more understanding of how potentiation might occur.

### 2.3.1 Events in the apical dendrites

The apical dendrites of CA1 pyramidal cells are the location of synapses from EC projections. When between 10 and 50 neighbouring glutamatergic synapses of this region fire in close timing proximity a plateau of depolarization - called a “dendritic spike” -

develops which lasts typically between 50 and 100 ms, is mediated by NMDA receptors, and has an amplitude of 40 to 50 mV above the rest potential. Local voltage-gated cationic channels become active as a result, and the influx of sodium and calcium ions prolongs the plateau by several hundred ms (Antic et al., 2010).

### 2.3.2 Events leading to LTP

LTP in the hippocampal CA1 (as elsewhere) was long considered as the result of the near-coincidence of synaptic activity and backpropagation from action potentials (Colbert and Levy, 1993). However it was established in 2002 that even in the absence of such back-propagation “locally generated and spatially restricted regenerative potentials (dendritic spikes) contribute to the postsynaptic depolarization and calcium entry necessary to trigger potentiation of distal synapses” (Golding et al., 2002). It has been found that the strongest LTP occurs when apical dendritic spikes are combined with Schaffer-derived glutamatergic input currents that are sufficient to evoke action potentials, even though the back-propagation from the action potential does not contribute significantly to the LTP (Hardie and Spruston, 2009). Such LTP must be occurring even with a single pass of a new place field, as just 40 current spikes at 5 Hz (similar to theta frequency), replicating the same level of EPSP, can induce robust LTP (Hardie and Spruston, 2009).

### 2.3.3 Ramp of depolarization

The concept that the balance of inhibition and excitation determines the amount of depolarizing current input into the pyramidal cell was explored by Mehta et al. 2002 and by Harris et al. 2002; both sources regarded depolarization from this changing balance as central to the idea of phase precession. As place cell firing frequency increases in the early stages of transit of a place field and decreases in the late stages, it is apparent that the changing balance favours increasing depolarization in the early part of the transit, with decreasing depolarization later in the transit. This variation of depolarization can be quantified by measuring the membrane potential between action potentials (Harvey et al., 2009). On a tracing of membrane potential v. time for the subject’s transit at constant speed, the rise of membrane potential appears as a low hill, which has been called the “ramp of depolarization” (Harvey et al., 2009).

Factors that could contribute to the rise of this ramp would include leakage of current from the long-lasting apical dendritic spikes mentioned above; the early stages of LTP, which as mentioned above can occur with just a few input current spikes; and facilitation and posttetanic potentiation (discussed in section 2.1.2).

With regard to LTP, it has been noted that the induction of LTP in the CA1 pyramidal

cell involves several stages. The earliest stage, termed “transient LTP”, is unstable, and declines over approximately half an hour; it is facilitated by NMDA receptors. Later stages involve IEGs (“immediate early genes”, which are activated transiently and rapidly in response to particular stimuli) and after several hours, the synthesis of new proteins (French et al., 2001, Manahan-Vaughan et al., 2000, Volianskis et al., 2013a).

The transient LTP component is volatile. It has the strange property that it persists for hours in the absence of synaptic activity, but rapidly declines after any such activity, such as may be incurred by experimental probing, a feature that has been termed the synaptic version of Heisenberg’s uncertainty principle (Volianskis et al., 2013b). It may well be that ISPCs from perisomatic GABAergic interneurons in the late stages of place field transit are sufficient to greatly reduce or cancel out this transient LTP, without interfering with the development of more gradual LTP forms that follow, and which are not reliant upon the immediate state of glutamatergic receptors.

Whatever is the exact cause of this variation in firing frequency across the place field, it has been incorporated with success into many models of CA1 (Jensen and Lisman, 1996, Mehta et al., 2002, Tsodyks et al., 1996, Wallensteen and Hasselmo, 1997). Experimenting with mice, Harvey et al. 2009 found more support for a depolarization ramp that peaked at around two-thirds of the transit of the place field; my personal experience with the model developed for this thesis has been that this is necessary to avoid reversal of much of the phase precession after the modelled rodent has crossed the middle of the field.

The final decline of the ramp from its peak is at least partly occasioned by increased firing from associated basket cells and axo-axonic cells. Their perisomatic and axonal synapsing sites enable them to suppress depolarization generated within the dendrites that would otherwise have been able to fire the cell. Both PVBC and axo-axonic cells begin to fire late in the theta cycle, some time after pyramidal cell firing has begun (Klausberger and Somogyi, 2008).

### 2.3.4 Intracellular theta rhythm

Ylinen et al. 1995 describe a “theta-related membrane potential oscillation” in hippocampal principal cells, the frequency being independent of membrane potential, and slightly lagging the LFP oscillation in phase. The amplitude of this intracellular oscillation was dependent on potential, as was the phase offset from LFP theta. It has also been found in EC stellate cells, at which site it is believed to contribute to grid cell field spacing and other aspects of space and time encoding (Hasselmo et al., 2007).

A possible mechanism for producing this intracellular oscillation in CA1 pyramids is proposed and illustrated in detail in the Models chapter, in section 5.1. The following

is a brief summary only of points discussed in that section.

It was pointed out in section 2.1.4 that input from the Schaffer collaterals impact the dendritic branches of CA1 pyramidal cells in two ways: monosynaptic excitation via glutamatergic synapses onto the dendrites, and disynaptic inhibition via glutamatergic synapses onto the GABAergic SR-IN interneurons, which in turn synapse onto the same pyramidal dendrites. The two inputs to the dendrite, one excitatory and one inhibitory, are tightly coupled. The SR-IN neurons are themselves subject to inhibition by GABAergic input from OLM cells, responding to MSDB signalling. While the OLM signal is active the SR-IN inhibition of the pyramidal cell is weakened, leading to a period of increasing depolarization in the dendrite. Once the OLM signal ceases, the SR-IN cells partially recover their inhibitory activity, tending to reverse the earlier depolarization. During theta rhythm activity the OLM cells are most likely to fire at around the trough of the theta LFP, or early in the ascending stage, shortly before the time of maximal firing probability for pyramidal cells. Consequently Schaffer input evokes a rise in dendritic membrane potential shortly before maximal pyramidal firing, followed by a subsequent fall in the membrane potential. The result is an oscillation of dendritic membrane potential which is at the same frequency as MSDB stimulation of OLM cells, that is, the frequency of the theta LFP. The peak of this intracellular oscillation will lag the theta LFP peak, which comes at the end of the pyramidal firing period.

### 2.3.5 Modelling phase precession

#### Multiple oscillators

In their 1993 paper on phase precession, O'Keefe and Recce proposed the theory that phase precession was the consequence of superimposing two oscillations, one being the theta rhythm, the other being an unidentified oscillation of slightly higher frequency (O'Keefe and Recce, 1993). Given the right difference between their frequencies the envelope of the resultant curve can be made to have a half-wavelength of similar duration to the time required to cross a place field at a given speed. The idea has immediate appeal, as demonstrated in fig. 2.11. On the left, theta rhythm is shown as a continuous black sinusoidal wave of frequency 7 Hz, while the second oscillation at 8 Hz is shown as a blue dotted curve. Initially they two waves are  $180^\circ$  out of phase. (O'Keefe's suggestion is that both oscillations have the same frequency for most of the time, but being in opposite phase, cancel each other out; but as the animal approaches the place field, the second oscillation rises in frequency.) The magenta curve is the resultant of the two. The red dots on the theta rhythm tracing represent instants at which a maximum occurs in the resultant curve; we could suppose that pyramidal firing might occur close to these peaks in the resultant wave, as the firing threshold of the place

cell is reached. On the right side of the same figure, the theta phase of successive red dots is plotted against time; the relationship between phase and time is approximately linear. (Even the nonlinear dip at the end of the fit curve is consistent with experimental results: Mehta et al. 2002, fig. 1). The yellow bars show the relative amplitudes of the peaks of the resultant oscillation. Again, one could suppose that the greater the amplitude, the more strongly would the place cell fire, leading to maximal firing around the middle of the place field.

To quote an old saying, for this theory “the devil is in the detail”. The mathematical basis provided in O’Keefe’s paper is the space-time equation (for one dimension of space):

$$Y = A(\sin(k_1x - \omega_1t) - \sin(k_2x - \omega_2t))$$

Where  $\omega_1$ ,  $\omega_2$  are the angular frequencies of theta rhythm and the second oscillation respectively, and  $k_1$  and  $k_2$  are hypothesized wave numbers associated with the length dimension. This expands to

$$Y = 2A \cos[(k_1 + k_2)x/2 - (\omega_1 + \omega_2)t/2] \times \sin[(k_1 - k_2)x/2 - (\omega_1 - \omega_2)t/2] \quad (2.10)$$

The sine term in this equation has a much lower frequency than the cosine term; its maxima, if joined together, therefore provide an envelope for the fast oscillation of the cosine term. For the two-oscillator model to explain phase precession, this envelope would be required to span one place field, both in space and in time. A difficulty with this concept is that place field size has been found experimentally to be independent of the speed of the animal as it traverses the field (Huxter et al., 2003). Consider the animal to be traversing the place field at a constant speed of  $V$  cm/sec; then the spatial dimension envelope term of eqn. 2.10 becomes

$$\sin\{0.5 \times [(k_1 - k_2) - (\omega_1 - \omega_2)/V] \times x\}$$

For the half-wavelength of this to be constant with respect to velocity we require either that  $(\omega_1 - \omega_2)$  be proportional to velocity, or that  $(k_1 - k_2)$  also have a strong reciprocal dependency on velocity. In the first case, we know that theta frequency has at most only a small variation with velocity (eqn. 2.8), so the second oscillation would have to vary considerably with velocity in order to keep  $(\omega_1 - \omega_2)/V$  constant. While it may be possible for a pyramidal cell to have a resonant frequency, it is difficult to conceive how that frequency might be so variable; to the best of my knowledge, no such variable resonance has been detected experimentally. The other alternative is for the space wave number difference  $(k_1 - k_2)$  to have a reciprocal relationship with velocity, such that the terms of the sine term of eqn. 2.10 remain constant. One would look for experimental findings which in the first place identified and quantified the wave numbers  $k_1$  and  $k_2$  and then demonstrated this velocity variation of their difference. It would appear that the explanation raises as many problems as it solves, so it is appropriate to look as well at other possible mechanisms.

An interesting interference model has been built which has no less than twelve oscillators with differing frequencies; it is proposed that such oscillators, in the form of ring attractors, occur in the subcortical regions currently associated with theta generation (fig. 2.6), and that signals from grid cells determine which oscillations prevail in a particular spatial location (Blair et al., 2008). This would seem to conflict with other studies in which a single frequency is detected in the medial septum and its projections to the HC (Kirk, 1998, Stewart and Fox, 1990).

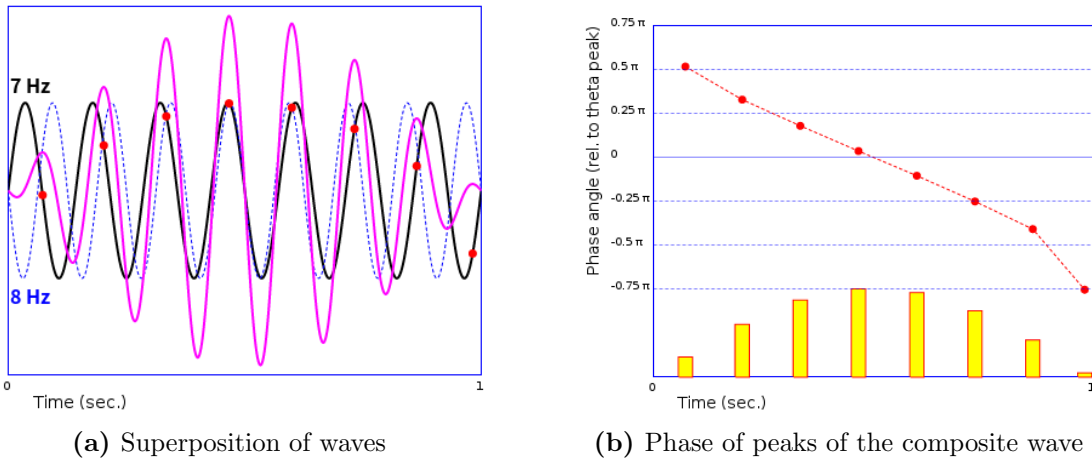


**Figure 2.11:** Effects of superposing two oscillations of similar frequency. In (a) the sine wave of 7 Hz (black) is representative of a typical theta frequency; the negative sine wave of 8 Hz (blue, dotted) represents a theoretical oscillation involving place cells. The magenta curve represents the resultant of these two waves. Red dots along the theta wave correspond to peaks of this resultant wave. In (b) the phase relative to theta peaks of these red dots is plotted. At the bottom of (b) the bars represent the relative amplitude of the peaks of the resultant waves.

## Connectivity and electrophysiology

Models demonstrating phase precession which were based on HC physiology and connectivity began to appear in the later 1990's (Tsodyks et al., 1996, Wallenstein and Hasselmo, 1997). Earlier models involved networks of two cell types, pyramidal cells, and unspecified interneurons which synapsing perisomatically onto the pyramidal cells. Increasing stimulation was applied to the pyramidal dendrites, while inhibition was applied to the soma at the same stage of the theta cycle; the dendritic stimulation became stronger at each theta cycle, so that the somatic inhibition was overcome earlier each cycle, leading to phase advancement (Magee, 2001). As more became known about the firing characteristics of various interneuron types (Freund and Buzsáki, 1996, Klausberger et al., 2003), more sophisticated models appeared. One outstanding example involves basket cells (of unspecified type), axo-axonic cells, bistratified cells and oriens lacunosum-moleculare cells in addition to pyramidal cells (Cutsuridis et al., 2010a, Cutsuridis and Hasselmo, 2010, p.230). This model has a much greater scope than the demonstration of phase precession; its primary purpose is to demonstrate the encoding

and replay of behavioural place sequences during theta rhythm and sharp wave ripple activity (SWR - discussed in section 2.3.6). Regarding phase precession, the effect is attributed to two postulated different phases of the theta wave: an encoding phase (around the theta trough in stratum radiatum) and a retrieval phase (around the theta peak) (Hasselmo et al., 2002a). The encoding phase is associated with strong EC input to the terminal dendritic tufts of the pyramidal cells, but weak input from CA3 to their branching dendrites; during the retrieval phase the CA3 input is much stronger and the EC input much weaker. In the model, the firing characteristics of the pyramidal cells are strongly influenced by the activity of two sets of interneurons; one set of interneurons fires at the theta peak, the other at the theta trough. Phase precession is a consequence of STDP (which is described as “linked with NMDA receptors and Ca<sup>2+</sup> dynamics” but not further specified); as a result, pyramidal cells fire earlier in successive theta cycles. In this model (as not in some oscillator interference models) there is no requirement for place fields to overlap, as the process does not depend on linkage between place cell microassemblies. A small limitation of this otherwise successful model is that phase precession cannot exceed 180° (Cutsuridis and Hasselmo, 2010, p.238), whereas in rats precession typically ranges from 100° to 300° (O’Keefe and Recce, 1993; Huxter et al., 2003).

## Connectivity and firing probabilities

Such an electrophysiological model, while clearly valid and useful, has some limitations. a large number of parameters are used, each with its own range of error, and prone to variation in the living cell; one hopes that the system as a whole has attractor properties such that errors individually do not radically perturb behaviour. A further problem with an idealized single-cell model is its distance from the behaviour of real cells. In live animal studies individual pyramidal cells react differently on different runs; it is only over many repeats of the same situation that strong trends develop (Fenton and Muller, 1998). A further problem is that a single virtual interneuron in the model must often represent a population of cells of the particular type which converge upon any one actual place cell.

Another approach might be to model behaviour of constituent cells using experimentally determined statistic firing characteristics and probabilities, as has been done in models to be presented later in this thesis. Description of such models is left to Part 3 of the thesis; however a concept diagram is presented in fig. 2.12, where events occurring during the journey of a rodent across a place field are represented in three stages, in columns labelled A to C. At the top of each column is the image of a rat, indicating its location in the place field. Below this are curves representing the dynamics of neuronal activity during a single theta cycle at that particular stage of the transit. The figure has four numbered layers:

*Layer 1* shows one cycle of an idealized theta rhythm LFP.

*Layer 2* shows the firing probability of OLM cells throughout the cycle; this firing is maximal in the trough of the theta cycle (as shown in fig. 2.8).

*Layer 3* represents the summation of two inputs to the pyramidal cell dendritic branches: (a) direct Schaffer collateral glutamatergic excitation; and (b) disynaptic Schaffer-driven GABAergic inhibition by SR-IN cells. More correctly, the displayed curve represents the upper envelope of their combined action. The form of the curve is described more fully in chapter 5. While OLM firing is high, SR-IN firing is suppressed, allowing the dendritic potential to rise. As OLM firing subsides, SR-IN firing to a large extent resumes; the consequent inhibition causes the pyramidal cell potential to fall again. The result is a saw-tooth appearance of the potential curve across the place field. The height of the curve grows during the transit, partly from increased Schaffer stimulation (section 2.2.3) and partly from the rising “ramp” of depolarization described in section 2.3.3.

*Layer 4* shows curves of firing probability for two perisomatic inhibitors, PVBC cells (blue curve) and AA cells (red curve). The AA firing probability curve is represented as having a constant shape across the place field, while the PVBC firing probability curve is shown as growing as the subject advances through the place field, as a result of feedback from targetted pyramids. AA cells mostly fire at a time when pyramidal cells never fire under normal conditions. They appear to have the important role of preventing continuous runs of pyramidal APs across theta cycles (an event hypothetically shown in fig. 5.7b, where perisomatic inhibition is represented as not present). PVBC firing on the other hand has an important role in shaping the bursts of pyramidal cell firing; it limits the length of such bursts at the middle and later parts of the place field transit. Inhibition from this source is responsible for the increased downward slope of the ends of layer 3 curves in columns B and C.

CCKBC cells are omitted from this representation, as these perform as modulators of the degree of place cell firing rather than as contributors to the timing of events (Foldy et al., 2010, Klausberger and Somogyi, 2008).

### 2.3.6 Other rhythms

The most prominent and well-studied other LFP rhythms of the hippocampus are sharp waves and associated ripples, and a class of oscillations collectively termed gamma rhythm.

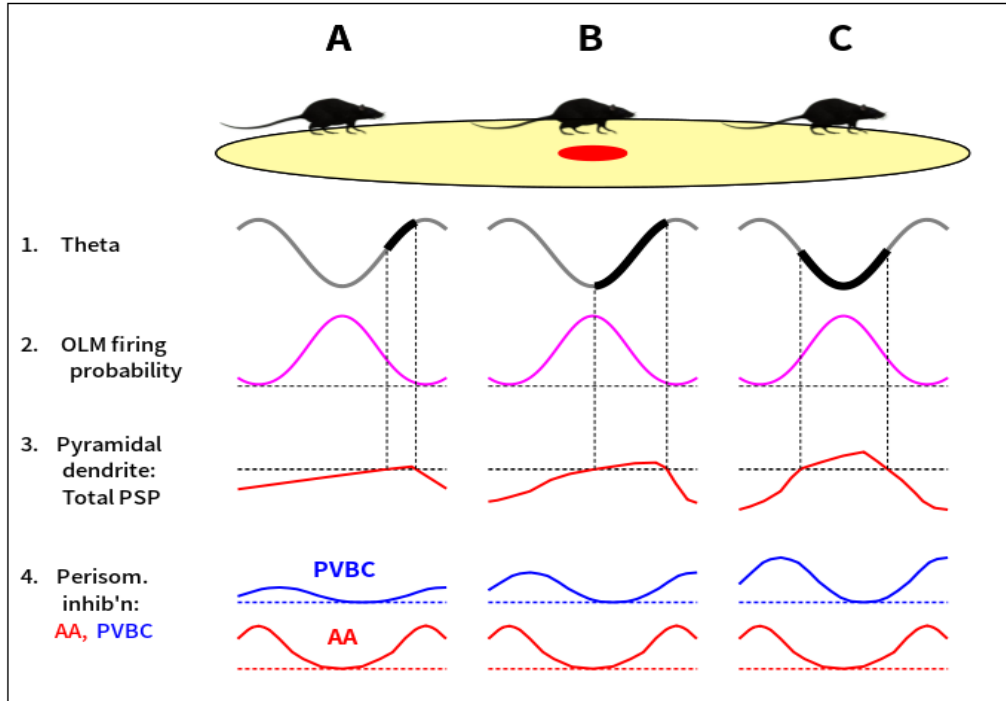


**Figure 2.12:** Diagrammatic representation of place cell firing occurring as a subject crosses the corresponding place field. The place field is represented by the oval at the top (centre marked in red). Three representative stages of the crossing are labelled A to C. Below each letter is a column of curves representing behaviour within a single theta rhythm cycle of that stage. In each column the top curve (grey) represents the local field potential. Below this is a curve (magenta) representing the firing probability of OLM cells. The next curve down (red) represents the summation of potentials within the place cell dendritic branch resulting from direct Schaffer glutamatergic excitation and Schaffer-driven SR-IN inhibition. (The curve actually represents the upper envelope of potential variation; fig. 5.7c demonstrates the shape more completely.) At the bottom of each column are curves representing somatic inhibition by PVBC cells and axonic inhibition by AA cells.

### Sharp waves and Sharp wave ripples

A “sharp wave” (SPW) is a large-amplitude wave of depolarization, starting from apical dendrites in CA3 pyramidal cells, evoking firing which is amplified by the strongly recurrent CA3 collateral system. The wave flows over into the CA1 region to depolarize pyramidal cells there. These CA1 pyramidal cells, upon firing, stimulate local interneurons with which they have excitatory synapses. The interaction between pyramidal cells and their inhibitory interneurons - notably basket cells and bistratified cells (but not axo-axonic cells) - produces a damped oscillation of 140 to 220 Hz that lasts for 50 to 150 ms, and which is termed a “sharp wave ripple” (SWR). (Buzsáki and Silva, 2012, Klausberger and Somogyi, 2008, Somogyi et al., 2014). The time scale of the repeated stimulation of pyramidal cells is well suited for NMDA receptor-dependent plasticity to occur, thus allowing temporary enhancement of connections between particular assemblies of CA3 and CA1 pyramidal cells (Sadowski et al., 2011). In this way they appear to have an important role in the consolidation of memories. Studies

involving place cells have shown a tendency for a SWR event to briefly stimulate the same place cells, firing 1 to 4 or more times each, firing either in the order in which their place fields are deployed or in the reverse order (Buzsáki and Silva, 2012, Girardeau and Zugaro, 2011). The firing sequence is compressed into a much shorter time than the firing sequence of the same cells during the run. Forward-ordered firing often occurs just before a run through the place fields, analogous to an anticipatory rehearsal of the trajectory; reverse-ordered firing may occur upon resting, after such a run. This may occur even when the animal is resting in a different environment, where there is a different deployment of place fields not involving the same cells. Forward-ordered SWR firing also occurs in deep sleep. It would appear that SWRs are important for memory consolidation during rest, and later, in deep sleep (Buzsáki and Silva, 2012, Girardeau and Zugaro, 2011).

Using fMRI (functional magnetic resonance imaging) studies on monkeys, Logothetis et al. noted that during periods of sleep and calmness, most of the cortex is activated during hippocampal ripples, while most diencephalic, midbrain and brainstem regions are strongly and consistently inhibited. This was taken as evidence that during memory consolidation at such times, a “privileged interaction state between hippocampus and cortex” was established, while subcortical centres that could interfere with the transfer of information were silenced (Logothetis et al., 2012).

Several neuromodulators, including dopamine, acetylcholine, norepinephrine and serotonin, are believed likely to affect the electrophysiological properties of cells involved in SWR-mediated memory consolidation (Sadowski et al., 2011). With regard to serotonin - a subject of this thesis - no clear-cut role has been identified. However the median raphe nucleus (MRN) does appear to have significant influence through non-serotonergic projections; such signals from the MRN completely suppress SWRs. Stimulation of serotonergic MRN neurons, on the other hand, produces only a mild reduction in CA1 ripple activity (Wang et al., 2015).

## **Gamma waves**

More sustained oscillations in the frequency range 25 Hz to 140 Hz are termed gamma waves. They were originally detected and studied in the visual cortex, but subsequently were found to occur in most brain areas (de Almeida et al., 2009). Theta rhythm, with its period of 100 or more ms, is well suited for interconnection between networks across the cortex and striatum where conduction delays are considerable, and also for quantizing the intake of sensory information for information processing. But many operations must occur locally on a much finer time scale; these would include rapid selection of inputs, grouping of pyramidal cells and interneurons into functional assemblies, and retrieving memories needed rapidly for the performing of a previously learned task. The short period of gamma waves provides the appropriate time scale for

such operations (Colgin and Moser, 2010). The main source of gamma waves appears to be rhythmically induced IPSPs in pyramidal cells, rather than from the actual firing of pyramidal cells (Colgin and Moser, 2010).

Gamma oscillations are usually divided into “slow gamma” (or just “gamma”) waves, at frequencies below 90 Hz, and “fast gamma” (or “epsilon”) waves at higher frequencies (Buzsáki and Silva, 2012). In this section I will refer to them as slow and fast gamma respectively, and consider their properties only within the hippocampus.

**Fast gamma rhythm** (90 to 140 Hz) in the CA1 region correlates with the same rhythm in layer III of the medial EC. This layer projects directly to CA1, to synapses on the apical dendrites of pyramidal cells. These projections convey information about the animal’s current location; this would suggest that the gamma rhythm is involved with the transmission of this information (Colgin and Moser, 2010).

**Slow gamma rhythm** (25 to 90 Hz) in the CA1 region appear to derive from similar oscillations in CA3, to which many CA1 neurons are phase-locked.

### **Gamma rhythm, theta rhythm and CA1 place cells**

During most theta cycles some form of gamma rhythm is detectable as a field potential within CA1 (Csicsvari et al., 2003). In the great majority of such cycles either slow or fast gamma is present, but rarely both. Cycles with fast gamma are nearly twice as common as those with slow gamma. Cycles of the one gamma type tend to cluster in their timing (Colgin et al., 2009).

**Fast gamma sequences** in CA1 correlate closely with fast gamma activity in the medial EC; the two gamma rhythms are largely phase-locked. About one third of place cells also fire phase-locked to fast gamma oscillations. Fast gamma activity (as measured by signal power) peaks about 20 ms before maximal place cell firing (Colgin et al., 2009, suppl.). Such a small average interval between input and pyramidal cell firing would be consistent with the induction of spike-timing-dependent potentiation at individual synapses, thus reinforcing the connection between the individual place cell and the geographical location input from the EC.

**Slow gamma sequences** in CA1 correlate with slow gamma activity in CA3. About one third of place cells are phase-locked with slow gamma rhythm. As the peak of slow gamma activity is at a time when place cells are mostly silent (on the descending part of the theta wave), it is thought that slow gamma may be largely inhibitory, only those place cells with stronger synaptic connections with CA3 overcoming the inhibition; these are presumably the ones which fire phase-locked to the slow gamma (Colgin et al., 2009, Senior et al., 2008).

## **Gamma rhythm and the recruiting of new place cells during navigation**

. Intracellular recording of CA1 pyramidal cells before exploration of a new environment shows that future place cells can be distinguished on the bases of intracellular characteristics; they tend to have a lower firing threshold, a larger peak-threshold potential difference when they do fire, and different bursting profiles. It is believed that these features are transient, so that cells currently not eligible on the basis of intracellular characteristics at the moment of first exploration may well become so at a later exploration of another environment (Epsztein et al., 2011). Short bursts of gamma rhythm are believed to be able to select such cells, inducing them to fire; a mathematical model for how this might occur has been devised (de Almeida et al., 2009).

# Chapter 3

## Serotonin and the hippocampus

### 3.1 Nature and general functions

Serotonin, which is also known as 5-hydroxytryptamine (with the commonly used acronym 5-HT), is a monoamine derived from the amino acid tryptophan. It is found both inside the nervous system and outside (as in the digestive system). Within the central nervous system it is a neuromodulator, along with other monoamines such as dopamine, adrenaline and noradrenaline. Its modulatory effects are involved in a large range of cognitive functions, including behavioural coping and control, decision-making, learning and memory, emotional regulation, processing of reward and punishment, and delay discounting (Fischer et al., 2015, Nakamura, 2013).

To discuss “the effects of serotonin” in such a general way is like describing a football match in terms of the ball, ignoring the skills of the players. The team captains in this case are two midbrain nuclei, the dorsal raphe nucleus (DRN) and the median raphe nucleus (MRN), which together control almost all serotonin modulation within the cortex and diencephalon. These two nuclei integrate inputs from a wide range of brain centres that supply motivational information (Pollak Dorocic et al., 2014, Vertes and Linley, 2008).

While serotonin modulation operates across a range of cortical and subcortical functions, there is a common theme to its effects. It is known that the DRN keeps track of the reward value associated with a task; it is believed that the DRN provides to relevant regions a continuous level of motivation throughout the performance of the task, which will be combined with other salient information to evoke appropriate behaviour (Nakamura, 2013). This value tracking persists for minutes. It has been shown in rats that serotonin neurons increase their steady (“tonic”) firing while the rat waits for an expected but delayed reward; if the reward is delayed too long, this steady firing ceases, and does so just before the animal starts to move away (Miyazaki et al., 2011). The overall effect of this persisting value signal is that impulsive behaviour becomes

less likely. It has been demonstrated that forebrain serotonin depletion leads to premature actions and reduces the ability to maintain reward-motivated behaviour when the reward is delayed (Cardinal, 2006).

The serotonin modulation system is often compared with the dopamine modulation system, an equally important system which is mostly coextensive with it. Both systems receive their inputs from the same brain regions associated with processing appetitive and aversive information, and supply motivational information to their recipients. But the information differs. Dopamine neurons encode the difference between the reward that was expected and whatever reward is being received (or not). Hence if a reward is expected and received, there is no signal. The serotonin system, on the other hand, signals a valuation, namely the value of the reward or punishment currently anticipated or being experienced. This valuation represents a trade-off of the costs and benefits of such activity as waiting for a reward, or holding back to avoid punishment (Cools et al., 2010, Nakamura, 2013, Nakamura et al., 2008).

## 3.2 The raphe nuclei

As mentioned, the DRN and MRN mediate almost all of the serotonergic action within the diencephalon and cortex. The DRN is larger than the MRN, but the two are similar in structure. Together they integrate a huge amount of input from the brainstem and limbic forebrain in particular, but more generally from all parts of the CNS. The most obvious difference between the two centres lies in their output distributions; the DRN supplies the neocortex and some limbic structures, while the MRN almost exclusively supplies the hippocampus, the medial septum and the amygdala. Of the two, the DRN has been much more studied, though it is likely that the internal characteristics of the MRN are broadly similar (Nakamura, 2013, Pollak Dorocic et al., 2014, Vertes and Linley, 2008, p. 69.7).

While the raphe nuclei are the source of almost all serotonergic projections above the brainstem, in fact only around 20% of neurons in the MRN are serotonergic in rodents. Other cells express other neurotransmitters including GABA, glutamine, dopamine, noradrenaline and acetylcholine. The interaction of the various cell types is as yet poorly understood. Nevertheless there is growing understanding of the performance and diversity of those neurons which do express serotonin (Dougalis et al., 2012, Nakamura et al., 2008, Pollak Dorocic et al., 2014).

The raphe nuclei modulate responses across many systems in the face of challenges to behaviour, mediated by a variety of receptor types with differing properties. Both the DRN and the MRN have been found to facilitate the resolution of conflict anxiety, while the DRN, but not the MRN, acts to inhibit panic-like fight-or-flight responses, giving cognitive areas of the cortex time to develop more appropriate responses (Andrade

et al., 2013, Paul and Lowry, 2013).

Within the raphe nuclei two subpopulations of serotonergic neurons have been identified, denoted by some authors as “slow-firing” and “fast-firing” neurons (Allers and Sharp, 2003, Kocsis et al., 2006). “Slow-firing” neurons are more numerous. They fire with single wide action potentials (approximately 4 ms in duration, inclusive of a long afterhyperpolarization potential); they do so at a frequency typically of 1 or 2 Hz, in bursts of 10 to 20 action potentials followed by a period of inactivity. They are further distinguished by the presence of inhibitory autoreceptors of type 5HTR1A on the cell body and dendrites, which could act to smooth input patterns and limit firing rate and amplitude swings (Kiyasova et al., 2013, Kocsis et al., 2006, Riad et al., 2000). The tonic signal from such neurons would be well able to signal a continuous level of motivation and hedonic experience throughout the performance of a task. Such a signal may provide a “reward context” signal to the targets of DRN projections, where the signal may be used differently depending on the type of 5-HT receptor present (Nakamura, 2013). The smaller subpopulation of “fast-firing” serotonergic raphe neurons lack the autoreceptor, and so fire at a faster rate (Kiyasova et al., 2013), some synchronizing with hippocampal theta LFP rhythm when that is present (Kocsis et al., 2006). Such neurons would be well equipped to relay information to end organs reflecting sudden changes in reward value.

A division of serotonergic neurons into separate groups of slow- and fast-firing cells may not be as clear cut as was formerly believed. A study of 29 DRN serotonergic neurons in mice showed that the same serotonergic neurons may on occasions have both slow-firing and fast-firing characteristics. Serotonergic neurons tended to fire at rates of 1 to 4 Hz during and in between trials, episodes of firing lasting for minutes. Such firing may well comprise a tonic value signal relating to recent and anticipated experiences. At other times the same neurons developed bursts of faster firing (up to 16 Hz), lasting for a few hundred milliseconds, when the mice were confronted with reward-predicting or punishment-predicting condition stimuli (Cohen et al., 2015).

The occurrence of slower tonic and faster phasic firing within the raphe nuclei is paralleled by responses in regions receiving the serotonergic projections. In most situations serotonin-related effects occur slowly, over hundreds of milliseconds or longer, mediated by metabotropic receptors. Such a time scale is suitable for the rate at which cortical processing occurs. But there are also effects which occur over a few milliseconds, mediated by a fast ionic receptor, where sudden changes of behaviour are to occur (Varga et al., 2009). As these occur almost exclusively in particular cortical interneurons which inhibit principal glutamatergic cells, they would appear to function as a sudden check on some ongoing pattern of behaviour.

A further distinction amongst DRN neurons has been made between those which fire strongly in relation to large rewards (whether expected or received) and those which

fire strongly in relation to small rewards (Nakamura, 2013).

Much less data is available regarding serotonergic neuron performance and diversity in the MRN. The general similarity of the two nuclei (pointed out in section 3.2) justifies a provisional hypothesis that we might expect similar performance and diversity of neurons within the MRN.

### 3.2.1 MRN interaction with the hippocampal CA1 region

The effects of MRN serotonergic stimulation on the HC are mediated both by direct projections to the HC and via strong connections to the medial septum and diagonal band of Broca (MSDB). The MSDB and HC act in a coordinated manner, as discussed in section 2.2.2, where it was pointed out that the MSDB output is involved not only in the generation of CA1 theta rhythm but also in initiating navigation. Their close coordination is consistent with the finding that approximately 10% of MRN neurons individually project to both the HC and the MS (Vertes and Linley, 2008, p.78).

Most of the MRN fibres projected to the HC express serotonin; they form a dense plexus in two layers, one in the stratum oriens and alveus, and one at the border between stratum radiatum and stratum lacunosum-moleculare (Varga et al., 2009). 80% of these neurons co-express serotonin and glutamate receptors (Fischer et al., 2015); and as the only such co-expressed glutamate receptors so far identified occur in CCK-expressing interneurons (El Mestikawy et al., 2011), it appears that most of the MRN input is destined for these cells. Nevertheless there is some input into pyramidal cells, acting on other receptors, to produce much slower reactions.

## 3.3 Serotonergic receptor types

Fourteen different serotonergic receptor types are found in the mammalian CNS, arranged in seven families, designated as 5HT<sub>R1</sub> through 5HT<sub>R7</sub>. All but one of the families are comprised of G protein-coupled receptors; the exception is the 5HT<sub>R3</sub> family, members of which contain ionic channels permeable to Na<sup>+</sup>, K<sup>+</sup>, Ca<sup>2+</sup> and other cations (Roth, 2006, p. 277 ff). Here I discuss only those which are of particular importance to the hippocampal CA1 region.

### Receptors mainly responsive to ambient serotonin - 5HT<sub>R1A</sub>, 5HT<sub>R1B</sub>:

5HT<sub>R1</sub> receptors, when activated, hyperpolarize their host neurons. They occur throughout the CNS, mostly away from synaptic junctions, responding to serotonin present in the extracellular fluid (ECF) or diffused within the host neuron. Their relatively high affinity for serotonin enables them to respond to low, tonic levels of serotonin in the ECF. When levels of serotonin are high, this affinity acts as a buffer

to appreciably lower the serotonin concentration locally in the ECF (Malagié et al., 2002, Riad et al., 2000, Samuels et al., 2014).

The *5HTR1A receptor* is important to our study at two locations:

- In the **raphe nuclei** they occur as autoreceptors in most serotonergic cells, as well as in some non-serotonergic cells. Here they respond to raised levels of intracellular and extracellular serotonin by inhibiting the host cell, and hence the cell's action at terminals in target organs. They also inhibit the release of serotonin within the cell (Barnes and Sharp, 1999, Hannon and Hoyer, 2008, Kiyasova et al., 2013).
- In the **hippocampus** they are distributed throughout the somata and dendritic branches of pyramidal cells, though sparse in their apical branches (Riad et al., 2000). Some are present in dendritic spines, others away from synapses, suggesting a mix of auto- and heteroreceptor action. In this way they can react both to direct connections from the MRN and to free serotonin released by blind axons - "varicosities" - which lie close to the pyramidal dendrites (Suwa et al., 2014).

The receptor has a long latency (interval between stimulation and response), of the order of hundreds of milliseconds (Roychowdhury et al., 1994). Excessive serotonin in the ECF eventually invokes desensitization of the receptor, though the process requires 3 to 6 weeks to occur (Bockaert et al., 2008).

The *5HTR1B receptor* occurs in axon branches from hippocampal pyramidal cells to CCKBC cells. These branches constitute a disynaptic negative feedback mechanism for pyramidal firing. The 5HTR1B receptors are close by the terminal glutamatergic synapses of this feedback loop; there they inhibit glutamatergic action when stimulated by ambient serotonin (Winterer et al., 2011). Like the 5HTR1A receptor, it is particularly sensitive to extrasynaptic serotonin; both are thus thought to be activated and regulated by low ambient ("tonic") concentrations of serotonin, and also, by virtue of their uptake, to be important as a means of buffering the concentration of serotonin within the hippocampus (Riad et al., 2000, Roth, 2006, p.396).

### **Receptors at MRN projection terminals: (1) 5HTR4**

The 5HTR4 receptor is found somatodendritically in hippocampal pyramidal cells, where it is largely coextensive with 5HTR1A receptors. Its primary action is to depolarize its host cell. It also increases AP spike height and reduces the afterhyperpolarization period, thus reducing spike frequency adaptation (Mlinar et al., 2006); the result would be a more conformed and unambiguous signal downstream to the subiculum and ultimately to the cortex. A further effect of stimulation of the receptor is to modulate the release of other neuromodulators, including GABA, ACh and dopamine (Hagena and Manahan-Vaughan, 2017).

The 5HTR4 receptor is vitally concerned with hippocampus-dependent learning and

memory. In rodent experiments, activation of 5HT<sub>4</sub> receptors immediately prior to exploration result in improved place and object recognition; and knockout mice lacking the receptor take much longer to learn such details, as evidenced by a longer exploration period (Mlinar et al., 2006). Activation of these receptors after exploration, in the consolidation phase, results in improved future object recognition. In studies with humans, 5HT<sub>4</sub> expression has been positively correlated with both cognitive processing and memory performance (Hagena and Manahan-Vaughan, 2017).

A key feature of the receptor, unique within hippocampal pyramidal cells, is its effect on adjacent glutamatergic synapses. Under different circumstances it may invoke either potentiation or depression at these synapses. Since the demonstration of LTP in hippocampal principal cells in 1973, LTP has been considered important for the process of memory formation (Artola and Singer, 1993, Bliss and Lømo, 1973). More recently LTD has been found to play a role, specifically in reducing the salience of objects within an environment while preserving the salience of space mapping features. Consequently, during exploration of a new environment there is an interplay between these two receptor gain states (Kemp and Manahan-Vaughan, 2004). The ability of the 5HT<sub>4</sub> receptor to facilitate either synaptic potentiation or depression under differing circumstances appears to underlie its effects on memory acquisition and object recognition (Hagena and Manahan-Vaughan, 2017).

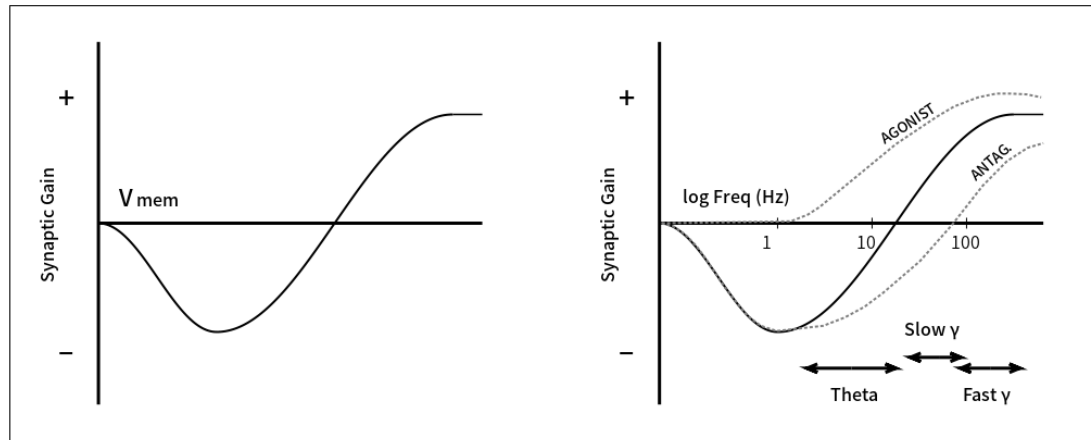


**Figure 3.1:** The **left graph** illustrates the “ABS rule”. At low membrane potentials (associated with slow intracellular Ca<sup>2+</sup> current), depression occurs at the synapse; higher potentials (associated with a surge in [Ca<sup>2+</sup>]) invoke potentiation. The **right graph** (solid curve) illustrates a similar effect when the synapse is subjected to oscillatory potentials; increasingly rapid membrane potential changes result in faster Ca<sup>2+</sup> currents. The effect of 5HT<sub>4</sub> receptor action is indicated by the dotted grey curves. Full activation by a receptor agonist raises the synaptic gain curve to lie wholly in the positive gain region, while inactivation of the receptor by an antagonist results in depression at all but fast gamma frequencies.

The left graph is based on data supplied by Artola et al. 1990; the right graph is based on data from Hagena and Manahan-Vaughan 2017.

A demonstration of how the receptor may influence synaptic gain is given in fig.3.1.

The graph on the left illustrates the “ABS rule” (developed by authors Artola, Bröcher and Singer, 1990), according to which the gain at a glutamatergic receptor subject to long-term plasticity depends on the membrane voltage. If postsynaptic depolarization exceeds a basic level but remains below the threshold necessary to activate NMDA receptors, LTD is induced; once that threshold is exceeded, LTP is induced. In terms of intracellular Ca<sup>2+</sup> currents, a slow current with lower [Ca<sup>2+</sup>] favours LTD, while a surge of current with the development of a higher [Ca<sup>2+</sup>] favours LTP (Artola et al., 1990, Artola and Singer, 1993). A similar curve is shown on the right; but here the horizontal axis is scaled by applied signal frequency. (The connecting factor between the two graphs may be that rapidly changing potentials associated with oscillation invoke surges of Ca<sup>2+</sup> current.) Under normal conditions, a frequency in the theta rhythm range evokes depression lasting beyond 24 hours at Schaffer-to-CA1 pyramidal synapses at lower frequencies, and more transient and less persistent depression at higher theta frequencies. Beyond the theta frequency range potentiation increasingly occurs, and at an applied frequency of 100 Hz lasts for more than 24 hours. However this variation in synaptic gain is greatly altered by either strong stimulation or inactivation of 5HTR4 receptors. In the CA1 region, strong activation (as by applying a receptor agonist) prevents the development of depression altogether, and leads to potentiation from the mid-theta frequencies upward. Inactivation on the other hand results in the development of depression for all frequencies in the theta and low gamma range, finally inducing potentiation in the high gamma range (Hagena and Manahan-Vaughan, 2017, Kemp and Manahan-Vaughan, 2005).

The 5HTR4 receptor within the CA1 region has been found to be vital for decreasing the salience of objects, familiar or unfamiliar, within a new environment being explored. While LTP occurs as the rat learns the new environment, LTD has been demonstrated to occur instead during interaction with such objects; this LTD does not occur if the receptor is inactivated (Kemp and Manahan-Vaughan, 2004). (The plasticity change would be expected to occur only in those place cells actively firing at the location, so that the LTD or LTP would be induced in those cells specifically, rather than across all pyramidal cells of the region.) It is interesting that the situation is different for the CA3 region, where 5HTR4 activation suppresses both LTD and LTP (Hagena and Manahan-Vaughan, 2017). As discussed in section 1.4, The CA3 region is considered more important for pattern completion and for short-lived working memory, relatively evanescent functions which may not require long-term potentiation to the same degree as the CA1 region, where the focus is on long-term and episodic memory formation. An episodic memory trace cannot be a complete record of everything in the environment at a particular time; it needs mapping pointers, but also should not preserve detail irrelevant to the focus of the memory. Differential synaptic gains across CA1 pyramidal cells induced during the exploration period would be useful for obtaining the right balance between salience and detail.

It is interesting that no state of the 5HTR4 receptor suppresses LTP within the fast gamma frequency range (fig. 3.1). This oscillation appears to be derived from layer III of the medial EC, and is thought to convey mapping information about the animal's current location (Colgin and Moser, 2010). It is also notable that the 5HTR1A receptor - a suppressor of pyramidal cell activity - is sparse in the stratum lacunosum-moleculare of CA1, this being the location of the EC-derived perforant pathway synapses onto pyramidal cells (Riad et al., 2000). It appears that mapping reference input from the EC must be always available and enduring.

### **Receptors at MRN projection terminals: (2) 5HTR3A**

This receptor occurs in CCK basket cells, and was discussed in that context in section 1.2.2. It will therefore not be further described here, save to reiterate that it is the only serotonin receptor which acts as a ligand-gated ion channel, and that it evokes rapid-onset and steady GABAergic inhibition of the pyramidal cell soma by the CCK basket cell.

### **Receptors at MRN projection terminals: (3) 5HTR2A**

The 5HTR4 receptor acts to depolarize host cells. It is found widely in the cortex, inclusive of the HC, both in principal glutamatergic cells and in interneurons. Within pyramidal cells the receptor is located in the apical dendrites. In the case of the CA1 region, the receptor is concentrated in the stratum lacunosum-moleculare (SL-M), a position in which its excitation facilitates direct mapping input from the EC projection onto the apical dendrites (Bombardi and Di Giovanni, 2013, Puig and Gullede, 2011, Wyskiel and Andrade, 2016). (This contrasts with the localization of the 5HTR4 along main dendritic branches and perisomatically, where it may facilitate glutamatergic input from Schaffer fibres.)

## **3.4 Theta rhythm activity - (a) phasic regulation**

Phasic serotonin activity affects pyramidal cell activity during the theta rhythm both directly and indirectly. The principal direct action occurs via MRN projections onto hippocampal CCK basket cells (which are discussed in section 1.2.2) and onto 5HTR4 receptors in pyramidal cells (section 3.3). The indirect action - discussed first - is mediated by the MSDB. Serotonergic signalling from the MRN to the MSDB terminates hippocampal theta rhythm; without such input from the MRN, theta rhythm persists even in the absence of navigational activity (Crooks et al., 2012). This appears to be a switching phenomenon: the theta rhythm is either "on" or "off" according to MRN signalling.

The effect of direct MRN stimulation of hippocampal CCKBCs is more one of modulation. The CCKBC interneuron expresses the 5HTR3A receptor which, being a ligand-gated ion channel, has a much faster onset of action than other serotonergic re-

ceptors. The MRN projections to CCKBCs co-express serotonin and glutamine. Both synapse types evoke a rapid stimulatory response; a glutamate-induced EPSP occurs first, joined shortly after by a serotonin-induced EPSP; their joint action produces CCKBC firing bursts in well under 10 ms (Varga et al., 2009). The 5HTR3A receptor is distributed along the full extent of the CCKBC, from distal dendrites through the somatic region and along axons which synapse onto the pyramidal cell (Dorostkar and Boehm, 2007, Férezou et al., 2002) The perisomatic receptors can rapidly discharge the cell upon MRN phasic stimulation. There is minimal latency; experimentation using optical stimulation of MRN projections to the HC has shown that even a single stimulation of 1 ms duration will reliably evoke an AP in the CCKBC (Varga et al., 2009). The distal dendritic receptors contribute more to ongoing signal integration, so facilitating further firing. The action of CCKBC cells appears to be to modulate the firing rate of pyramidal cell firing rather than to affect precise timing within the theta cycle (Freund and Katona, 2007, Klausberger and Somogyi, 2008). They are well suited to do so, as their synapses onto pyramidal cells are located perisomatically, and as the timing of their maximum firing probability during the theta cycle coincides with that of pyramidal place cell firing.

The 5HTR4 receptor was discussed in some detail in section 3.3. As a consequence of its ability to modulate receptor gain, it is able to favour LTP for mapping features during exploration of a new environment, while facilitating LTD when the exploration path takes the animal in the vicinity of objects not justifying high salience. When strongly activated it not only enhances LTP at theta oscillation frequencies but also sharpens the clarity of place cell AP bursts (by increasing firing amplitude and conformity), thus adding to the contrast between prioritized and less significant environmental detail. As the animal may be moving quite fast, the 5HTR4 must be able to switch quickly between states of activity in response to phasic MRN signalling.

### 3.4.1 Theta rhythm activity - (b) tonic regulation

Tonic regulation by the MRN occurs as a result of continuous signals from mainly slower firing serotonergic cells within the MRN, as pointed out in section 3.2. Within the hippocampus the tonic signal is partly mediated directly at synapses, but partly also by direct release into the hippocampal ECF by blind axons (“varicosities”) (Berumen et al., 2012). This humoral component might act as a smoothed, more persistent echo of the original tonic MRN signal.

It is likely that any serotonergic receptor would respond to high enough concentrations of ambient serotonin; but receptors of the 5HTR1 family are particularly sensitive, hence their responsiveness to tonic release from non-synapsing axon terminals. The consequence, in the case of the 5HTR1A receptor distributed along the pyramidal soma and dendrites, is a uniform inhibitory hyperpolarization. The 5HTR1B receptor

within the disynaptic feedback loop to the CCKBC cell, when so stimulated, acts to decouple this negative feedback, thus enabling the CCKBC to further inhibit pyramidal cell action during the period of maximal pyramidal firing probability within the theta cycle.

While the MRN is capable of completely suppressing theta rhythm by its action on the MSDB, it exercises a more graded tonic control over CA1 place cell activity during navigation by its direct projections to the HC.

## 3.5 Equilibrium, Disequilibrium

While there are many players and sub-themes in the orchestral performance of serotonergic activity, there is one overlying major theme of importance across the cortex, inclusive of the hippocampus: the equilibrium between *depolarizing receptors* in pyramidal cell membranes (5HTR2A and 5HTR4) that respond to phasic signalling, and the *hyperpolarizing receptor 5HTR1A*, also in pyramidal cell membranes, which responds to tonic signalling, particularly as represented by changes in ambient serotonin concentration. A depolarizing receptor and a hyperpolarizing receptor in the same pyramidal cell - what is going on? According to the “bipartite model”, in the face of some stressful situation the hyperpolarizing 5HTR1A receptor mediates coping passively with the stress, tolerating the pain, while the depolarizing receptor mediates more active coping by interaction with the situation (Carhart-Harris and Nutt, 2017, Puglisi-Allegra and Andolina, 2015). In CA1 the 5HTR1A receptor responds to slowly changing tonic signalling, being particularly sensitive to serotonin released into the ECF by blind axons; while the 5HTR4 must respond quickly to phasic signalling, as it is responsible for switching between facilitating LTP and facilitating LTD within the pyramidal place cell as a rodent navigates an environment (both receptors were discussed in section 3.3). This balance is chronically disturbed if either type of receptor is downregulated. If 5HTR1A is downregulated, impulsivity increases, as may be seen in depression with anxiety; if 5HTR4 is downregulated, inaction predominates, as may be seen in depression with psychomotor retardation.

### 3.5.1 Clinical depression

Common features of human clinical depression include a settled state (or mood) of sadness; inability to experience pleasure (anhedonia); insomnia; and psychomotor retardation (slowing down of thinking and reduced movement). Where these are present, neuroimaging abnormalities have been identified in the PFC, amygdala and hippocampus (Akiskal and Akiskal, 2007, Insel and Charney, 2003). Subjective features such as mood change and anhedonia cannot be directly assessed in non-primate animals; in-

stead, animals are typically studied when subjected to situations known to predispose to depression in humans, such as inescapable shock, chronic social defeat, chronic mild stress and social isolation (Andrews et al., 2015).

Half a century ago the concept developed that depression in humans was associated with reduced serotonergic activity within the CNS (Coppen, 1967). This led to the development of a class of therapeutic agents called SSRIs (selective serotonin reuptake inhibitors). These agents inhibit the action of the cell membrane transporter protein SERT (serotonin transporter) which recycles serotonin by transferring it from the extracellular medium back into the synaptic terminal for reuse. This class of drugs is now the most commonly used for managing clinical depression.

The concept that depression is associated with a deficiency of serotonin within the CNS has recently been challenged in reviews of the experimental evidence (Gururajan et al., 2016, Liu et al., 2017, Perkovic et al., 2018). One review goes further, and proposes that instead depressive states are associated with an increase in both production and turnover of serotonin (Andrews et al., 2015). The trend appears to be to move away from theories based simply on the levels of serotonin and other monoamines and to postulate other factors, such as the neurotoxicity of chronic stress and other failures of “neuroplasticity”, a loose term which “usually refers to neurogenesis, synaptogenesis, dendritic length and branching, spine density etc.” (Liu et al., 2017).

Whatever the underlying causes of depression, many research papers have been published to support the effectiveness of SSRIs in its treatment. Their effectiveness has in recent years been called into question. A multicentric metastudy on 43 such papers which had been submitted to the US Food and Drug Administration concluded that “Drug-placebo differences in antidepressant efficacy increase as a function of baseline severity, but are relatively small even for severely depressed patients. The relationship between initial severity and antidepressant efficacy is attributable to decreased responsiveness to placebo among very severely depressed patients, rather than to increased responsiveness to medication” (Kirsch et al., 2008). More recently, a combined review by psychiatrists from Columbia University and pharmacologists from Université Paris-Sud concluded that “only about 33% of patients [treated with SSRIs for depression and anxiety] show remission to first-line treatment” (Samuels et al., 2014) - which is within the limits for the placebo response to treatment for depression (Sonawalla and Rosenbaum, 2002). On the other side, a metastudy just published reviewed 522 trials of antidepressant treatment; the conclusion was that “all antidepressants were more effective than placebo” (Cipriani et al., 2018).

Apart from questions of efficacy, a major problem with the use of SSRIs to treat depression is the delay of typically 3 to 6 weeks before any improvement can be expected in the patient’s condition (Andrews et al., 2015, Blier and de Montigny, 1999, Bockaert et al., 2008). During this “therapeutic delay” period, anxiety often increases; with

adolescents in particular, there is a well recognized increased risk of suicidal behaviour at this stage (Corrado Barbui et al., 2009). Inasmuch as SSRIs are effective in the treatment of depression, it has been suggested that the effect may well be the consequence of three weeks of disruption to the existing equilibrium between mood and emotional tone, allowing for the subsequent development of a new balance between the two (Andrews et al., 2015, Harmer et al., 2009). If this were the case, then SSRI therapy for depression would be more like a slow-acting equivalent of electroconvulsive treatment than a direct mood modifier.

## **Part II**

### **Models of Hippocampal Phenomena**

Three models are presented in this section of the thesis. The first two are of limited scope, but are necessary to demonstrate particular features that are incorporated into the third and final model, which is a more comprehensive demonstration of CA1 function during navigation, with the facility to model different serotonergic effects.

**Chapter 4** describes the simplest of the three models. The purpose is to demonstrate that it is justifiable to use the glutamatergic signal from the MSDB to the OLM cells as a reference timing point for events occurring during navigation, rather than using the theta rhythm component of the hippocampal LFP, as is usually done. As MSDB projections are responsible for the initiation and maintenance of the theta LFP rhythm in CA1 (section 2.2.2), it would appear to be more suitable to use that signal as a reference, rather than the derived noisy low-frequency component of the LFP rhythm. As an added feature, the model demonstrates the production of LFP tracings which visually closely resemble recordings of LFPs that are available in the literature.

**Chapter 5** implements the proposals laid out in section 2.2.4 as to how the phenomenon of phase precession may arise.

**Chapter 6** describes the design and functioning of the complete model, which incorporates features of the preceding two models: the use of the MSDB signal for timing, and the phenomenon of phase precession.

**Appendix A** gives details of the programming language used, and provides online links for accessing both the source code used for the complete model and the code of the programming language used. A skeleton outline of program flow is also provided in this appendix.

# Chapter 4

## Modelling Theta LFP Generation

### 4.1 Purpose of the model

This model has a very limited, but nevertheless very useful, role. Its purpose is to demonstrate that the group firing activity of place cells in CA1 produces a composite signal that closely resembles experimentally measured theta rhythm local field potential (LFP). In this way it demonstrates that it is possible to describe cyclical events during navigation without regarding the theta LFP rhythm as a primary phenomenon. This change in reference for timing is convenient, as the LFP rhythm is very noisy, and varies in phase with location within the CA1 (fig. 2.7).

The model **makes no attempt** to deal with how phase precession might be generated; that issue is addressed by the second model (chapter 5).

The model demonstrates the development of CA1 hippocampal LFP theta rhythm as a consequence of just these phenomena:

- MSDB signals to CA1 interneurons during transit of a place field evoke the firing of place cells (the mechanism is described in section 2.2.2).
- The probability of place cell firing increases as the subject approaches the centre of the field and decreases as the subject approaches the end of the field.
- Rhythmic input from the MSDB to the CA1 during navigation evokes rhythmic firing of place cells.
- As the subject crosses a place field, such rhythmic firing of the associated place cell occurs earlier in successive cycles of the MSDB signal.

Although the last phenomenon is usually referred to as “phase precession”, I have avoided the term in this particular context on semantic grounds: Phase precession is defined in terms of progressively earlier firing within the theta LFP rhythm, whereas here I am relating the theta LFP rhythm itself to a large population of place cells which

fire progressively earlier with respect to the MSDB signal.

The variation in the probability of place cell firing is modelled by a Gaussian function. The function is allowed to have a wide range of widths, so that at extremes of width it can approximately model a very short impulse or a steady state level across the place field (fig. 4.4).

## 4.2 Overview of the model

A virtual rodent runs along a linear track with which it is familiar, so that place fields are already established. As was pointed out in section 2.2.3, in any one environment there are large numbers of place cells which will sooner or later fire, at least hundreds and possibly thousands. The model allows for any number of place cells to be active, and assigns them place fields reasonably evenly along the track (the actual positions are first generated at regular intervals along the track, and then these positions are perturbed using a Gaussian randomizing function).

The **reference input signal** is the sequence of leading edges of the pulses that represent cyclical MSDB firing bursts. The frequency of pulses is constant, as the subject is assumed to be running at a steady speed.

In accordance with the last phenomenon on the list given above, there is a time lag between the rise of the MSDB pulse and the first firing of the place cell. This time lag becomes smaller, in a linear manner, as the animal crosses the place field.

## Parameters

The **number of place cells** active in the run can be freely varied from 10 to 10,000 (or higher, if computing time is not an issue).

The **frequency of the MSDB signal** is not limited, and may vary over the whole range relevant to rodents. The MSDB signal itself is represented as a train of pulses at theta frequency; but the form of the signal does not affect the algorithms used, as only the leading edge of signal pulses is used.

The **width of a place field** can be widely varied. As the animal is travelling at a constant speed, it is convenient to express place field width in terms of **the number of theta cycles per transit of a place field** rather than in length units.

The **variation in place cell firing probability** with distance from the place field centre is modelled by a Gaussian function, the mean being taken as the centre of the place field; the **standard deviation** for the function can be freely varied.

The **duration of the run** is again freely variable.

The **time lags in firing**, mentioned in the overview above, are expressed as **phase**

**angles** relative to the edge of the MSDB pulse, rather than as time units. To allow for a wide range of deployment of such phase angles, two parameters are provided, which can be widely varied: the **phase lag of the first place cell firing** as the rodent enters the place field; and the **total phase change** that has occurred by the end of the place field transit. (Again I point out that this is not “phase precession”, which by definition is referenced to the theta LFP.)

## Operation

For this demonstration the speed is constant, and so for convenience the progress of the animal across the field is measured in time units rather than length units. In particular, place field width is measured in terms of the number of MSDB cycles taken to cross the field. The firing pattern of any particular place cell is computed as follows. As the animal enters the place field, the first AP will occur at the time of the most recent MSDB impulse (leading edge) plus the time equivalent of the phase lag at entry to the field (parameter mentioned above). For successive cycles, the first AP of each new MSDB cycle will occur after a linearly reducing phase lag; by the last MSDB cycle for the place field, the total phase lag will be the original phase lag minus the total phase change for a field (parameter mentioned above).

However there are usually multiple firings of a place cell around the centre of the place field. Using data referred to in sections 2.2.3 and 2.2.4, this increases and decreases in a manner which can be modelled by a Gaussian function of distance, the mean for the function being the place field centre; the standard deviation can be varied at will (parameter mentioned above). In the model the height of this Gaussian function, when rounded, gives the number of action potentials occurring at any particular cycle. Two factors allow for the wide variation seen in actual rodent place cell firing. The first is the perturbing of the output of the Gaussian function before rounding; the second is variation in the peak of the Gaussian function - that is, the maximum number of APs per cycle - by a random coefficient ranging from 1 to 6 (but constant for any one cell); this coefficient represents the activity of the particular cell.

The final point to model is the time interval between successive place cell firings in bursts that occur during an MSDB cycle. Where there are multiple APs in any one cycle, they are spaced at an interval of 10 to 15 milliseconds, each interval being calculated separately as a random number within these limits.

The **local field potential** is produced as follows. The above has produced an array which records the instant of occurrence of every AP produced by every place cell in the whole set. This time range is now segmented into bins, the width of a bin being one eighth of an MSDB cycle; the times of AP firing are binned accordingly. A histogram showing the heights of these bins across the entire time range is taken as a

representation of the local field potential. Before being graphed it is normalized to lie entirely between the range of 0 and 1. This approach to modelling the LFP does not allow for the time lag of current diffusion through the stroma of the HC from place cell locations to the point of measurement.

### 4.3 Experimental results

Fig. 4.1 holds the entire simulated theta output for a run of 30 seconds with 5000 place cells. The general noisy waveform is visually very similar to published theta rhythm strips, such as that of O’Keefe and Recce, fig. 5. As the number of place cells is reduced the waveform gradually deteriorates (fig. 4.2). This is consistent with the hypothesis of section 2.2.3 that there are likely to be thousands of place cells active in the rat CA1 during navigation in any particular environment.

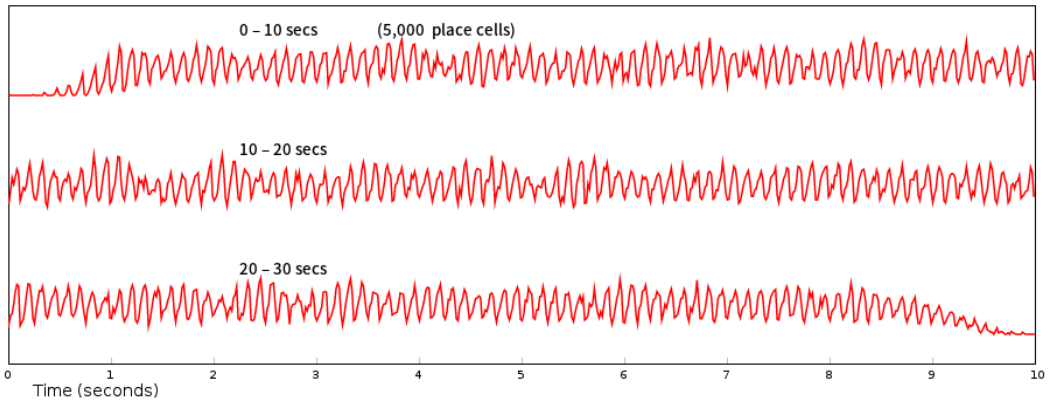


**Figure 4.1:** Simulated theta rhythm strip for an entire run of 30 seconds.

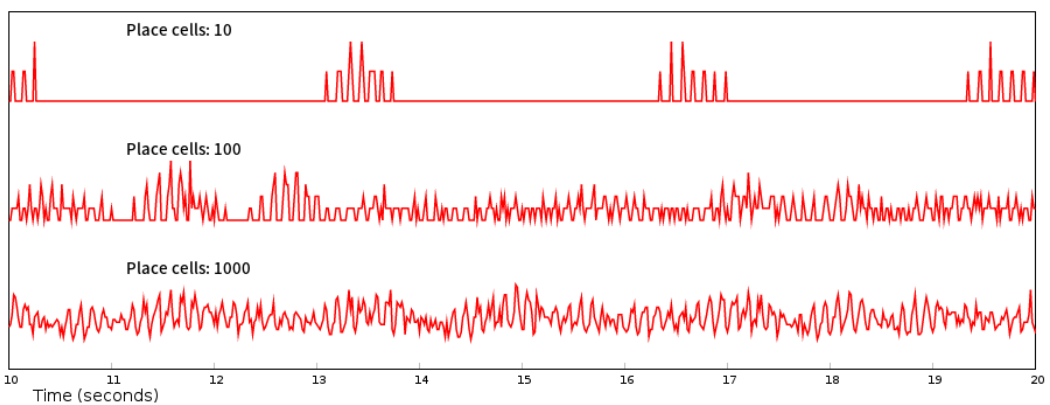


**Figure 4.2:** Ten seconds of simulated theta with place cell populations of different sizes.

In fig. 4.3 the firing of one place cell is shown; the place field centre for this cell is at 5.26 seconds, the total run taking 10 seconds. The lower waveform represents the MSDB signal; the shape is unimportant, as only the leading edge of the ON pulse is used as a timing reference. The place cell fires as indicated with vertical arrows. The first arrow of each burst is numbered, as is the corresponding MSDB impulse. The

arrows project onto the MSDB waveform, being represented there by blue dots. The earliest AP occurs later than the corresponding MSDB impulse by a little less than  $\frac{3}{4}$  of a cycle. The last AP is slightly earlier than the corresponding MSDB impulse.

At the top of the graph of fig. 4.3 the theta LFP is displayed. Again, place cell APs are projected onto this waveform as blue dots. Phase precession is apparent, as the blue dots move through approximately  $270^\circ$  along the waveform to the left. The first AP would appear to occur earlier on the theta LFP than usual; experimentally the first AP occurs nearer the peak of the theta. This reflects the fact that there is no time delay in the building of theta LFP from place cell firings, whereas in live recordings there would be a time delay due to the diffusion time of ionic currents. If a delay of 10 to 15 ms were applied to the calculated theta LFP, the first place cell AP would occur much closer to the theta peak in the model.

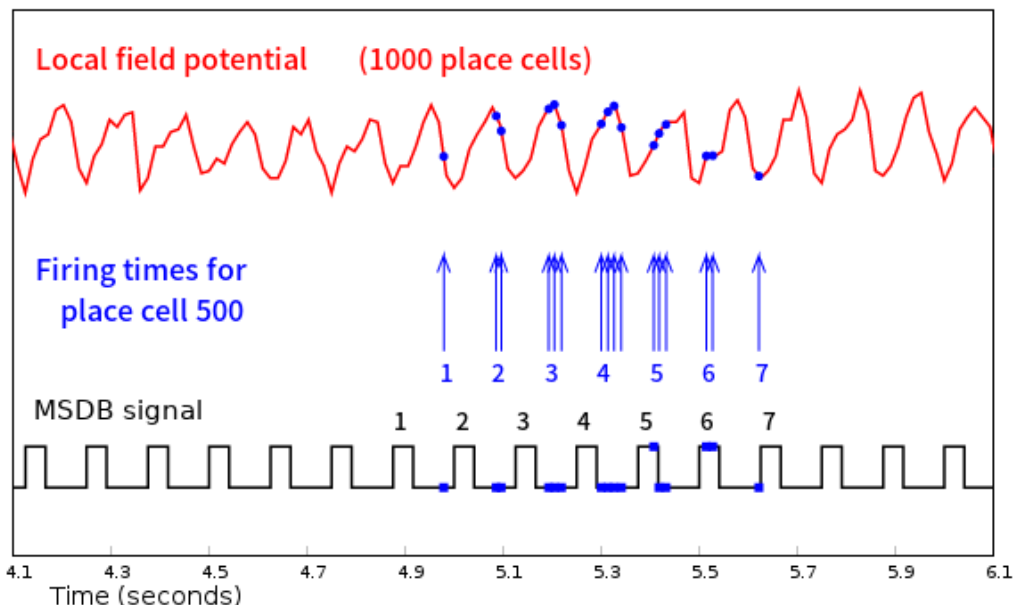


**Figure 4.3:** The rectangular waveform at the bottom represents MSDB signalling at 8 Hz. (The shape is irrelevant, as only the leading edge of the peak is used as a timing reference.) The red curve at the top is the LFP developed as a histogram of all firing times of all 1000 place cells, with 8 bins to an MSDB cycle. In the middle of the graph are arrows representing firing times for a particular place cell, in this case the 500th, out of 1000 cells. The initial APs of each of the seven bursts are numbered in blue. Relevant MSDB impulses are correspondingly numbered in black. The first AP lags the corresponding MSDB impulse by most of a cycle; the last AP has a slight phase lead. Each AP arrow projects onto both the MSDB waveform and the simulated theta LFP waveform as a blue dot. In both cases a phase advance along the waveform is apparent with successive firings.

#### 4.3.1 Effects of varying parameters

**Variation of MSDB frequency** over the range from 4 Hz to 16 Hz was carried out. Throughout this range the form of the LFP remained typical of recorded theta rhythms, though by 16 Hz it had become more corrupted by noise than at lower frequencies.

Table 4.1 shows the effects of this variation on some parameters. The second column records the phase difference between the MSDB impulse (centre) and the previous trough of the theta LFP. This is remarkably steady at around  $60^\circ$  to  $70^\circ$  over a large range of frequencies. This phase lag compares well with values given in the literature (see fig.2.8).

The next two columns show the phase lag of the first place cell AP (column 3) and of the total phase shift through the place field (column 4), these phases being related to the MSDB impulse leading edge. They are understandably constant, apart from some jitter introduced by perturbation, since the model uses a priori values of 270 degrees and 360 degrees respectively for these as starting points for the algorithm.

The last two columns show true phase precession; that is, phase is related to the derived theta LFP, and in particular to the theta peak. As expected, first firing always occurs after a peak. Experimentally the first firing is closer to the peak, but as explained earlier, we have not allowed for delays in LFP transmission, which would move the LFP curve to the right, so that first firing would occur nearer the peak.

The full phase range of phase precession is that commonly found in experimental work (section 2.2.4).

**Table 4.1:** Effects on model parameters from varying MSDB signal frequency

MSDB Freq	MSDB lag relative to $\theta$ trough	Phase lag rel. to MSDB: First AP	Phase lag rel. to MSDB: Total range	Phase lag rel. to $\theta$ peak: First AP	Phase lag rel. to $\theta$ peak: Total range
4 Hz	100°	245°	308°	150°	300°
6 Hz	76°				
8 Hz	65°	249°	309°	100°	300°
10 Hz	63°				
12 Hz	60°	245°	308°	55°	300°
16 Hz	0°	242°	308°	25°	300°

Variation in the **width of the place field**, as expressed in terms of the number of MSDB cycles required for its transit, had no effect on the general appearance of the theta LFP. With the MSDB frequency constant at 8 Hz, an increase in this parameter caused firing to begin later ( $90^\circ$  phase lag from the theta peak, for a field width of 4 cycles;  $100^\circ$  for a field width of 7 cycles; very variable, but around  $135^\circ$  for a field width of 10 cycles). There was very little impact on the full range of phase precession ( $270^\circ$  for field widths of both 4 and 7 cycles, increasing to  $315^\circ$  for a field width of 10 cycles).

Varying the **duration of Schaffer stimulation** of a place cell turned out to be quite important. For the Gaussian curve of stimulation the model normally uses a standard deviation of 0.2 of the width of the place field; the resulting variation of Schaffer stimulation as the rodent crosses a place field is shown as a grey dotted curve

at the bottom of both graphs of fig. 4.4. This figure shows the effect of changing the standard deviation, first to a much smaller value (4.4a) and then to a much larger value giving almost constant Schaffer stimulation during the firing window for this place cell (4.4b). Both theta rhythm and phase precession persist with the very narrow window, indicating that the actual SD used is not very critical. On the other hand the ungraded stimulation of Schaffer input during the firing window leads to the destruction of theta rhythm, and consequently of phase precession; examining the LFP for the whole run (not shown here) sees short bursts of activity at the higher firing rate of place cells (as occurs in the middle part of 4.4b) joined by strips of chaotic variation. (It is proposed that the short regular strips occur where, by dint of perturbation, some place field is relatively isolated from neighbouring fields; this idea was not explored.)

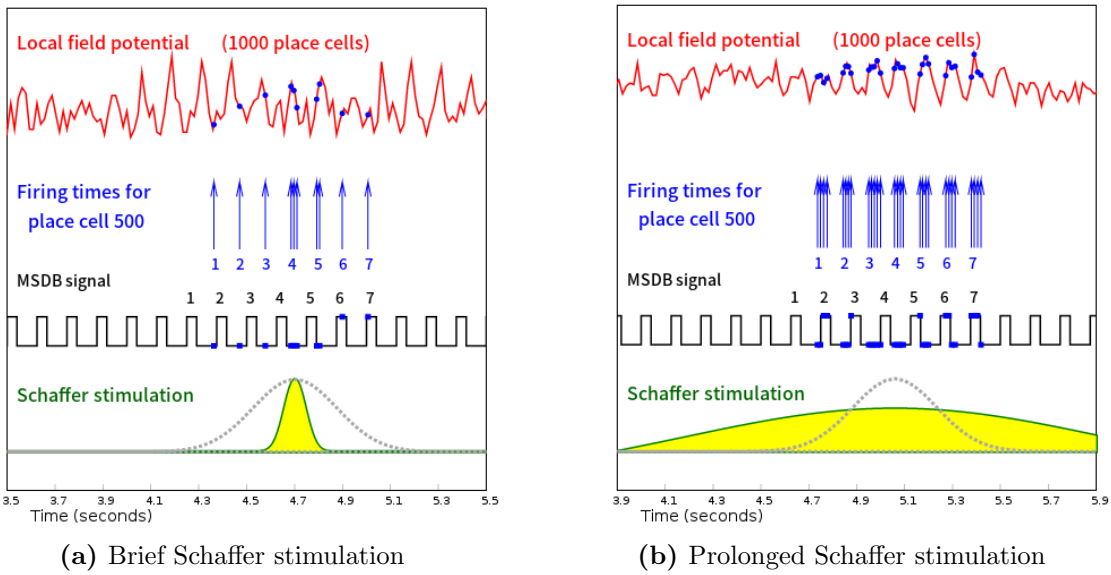


**Figure 4.4:** Effects of varying the width of the Gaussian stimulation of place cells by Schaffer collaterals. The model uses a standard deviation of 1.4 MSDB cycles, so that the width of the Gaussian curve at this level is 2.8 MSDB cycles, which is 0.4 of the width of the place field. In both graphs above, this is represented by a dotted grey curve. In the left figure above, the standard deviation has been reduced to one quarter of this. Theta rhythm is still present, though very noisy. Phase precession occurs over something of the order of 300°, as for the standard model. The figure on the right shows the standard deviation increased to the full width of the place field, so that Schaffer stimulation is almost constant throughout the field. Theta LFP has degraded into a short regular strip with irregular behaviour on either side of it. There is no phase precession, as the heavy firing of place cells at a constant rate has temporarily taken over the LFP rhythm.

Varying the **allowed range of phase lag** for place cell firing, relative to the corresponding MSDB impulse, had no visible effect on the form of the theta LFP, over the range from 180° to the normal model setting of 360°. Phase precession also occurred normally, though its range was necessarily limited to a little below the set allowed range. Examples are shown in fig. 4.5. Note also that the peak of the MSDB signal stays close to the trough of theta LFP in both cases, as for the original model (fig.

4.3).

There would be no point in increasing the allowed phase range beyond  $360^\circ$ , as in the live situation all prior activity is terminated by the action of perisomatic interneurons which occurs after the place cell firing window in every theta cycle.

The final variation is of the **phase lag of earliest firing**. The original setting for this is  $270^\circ$ . Variation of this over the entire range from  $0^\circ$  to  $360^\circ$  had no effect whatever on the theta LFP shape, as was evident when the same random number seed was used for all runs with variation of this parameter, and as is apparent in fig. 4.6. Phase precession was also unaltered, starting and finishing at exactly the same point on the theta LFP. The relationship of the MSDB impulse to the theta LFP trough does change, the amount of change being the same as the change in the phase angle of the earliest firing.

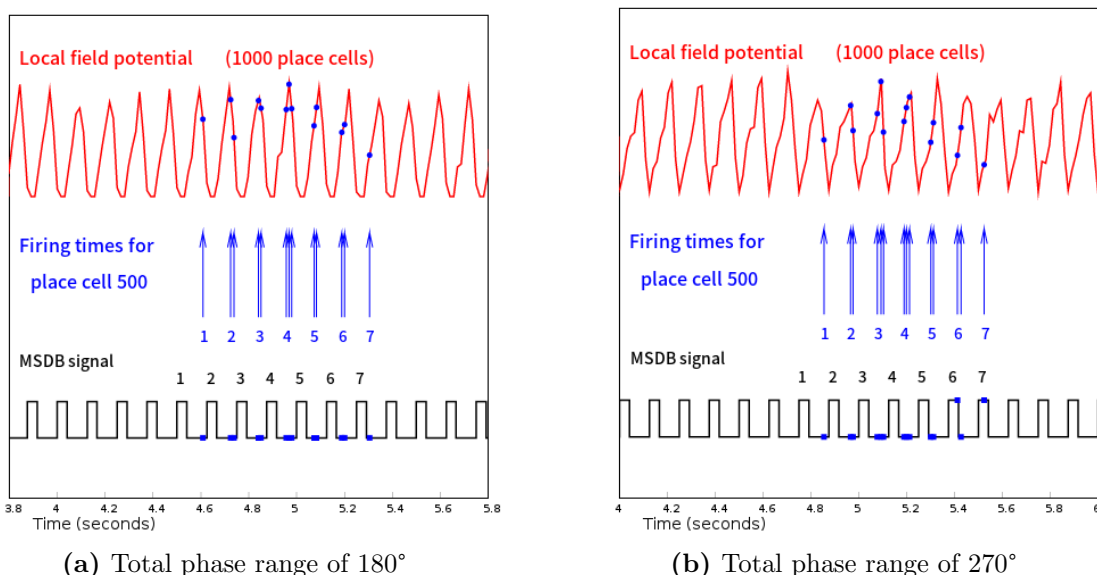


**Figure 4.5:** The total phase range is the allowed variation in phase lag from that of the earliest possible place cell firing to the latest possible firing; the achieved phase range is always a little less. In this case the normal range of  $360^\circ$  has been reduced to  $270^\circ$  (left figure) and  $180^\circ$  (right figure). There is no perceptible effect on the general form of the theta LFP with these changes. Phase precession occurs normally, except that its range is limited to a little less than the set phase range.

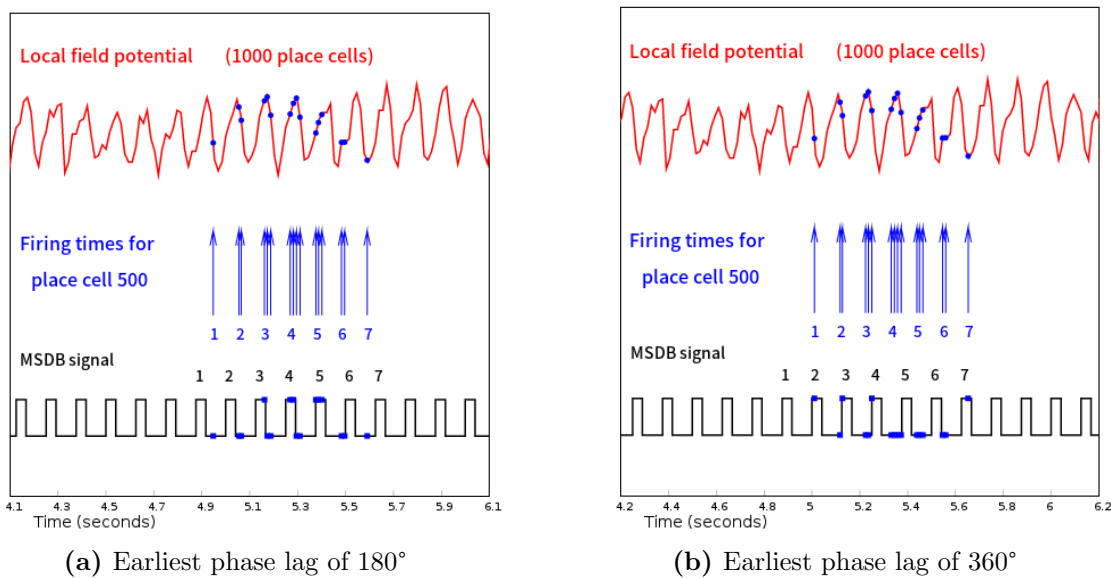


**Figure 4.6:** Variation in the allowed phase lag for the first place cell firing has no effect on the shape of the theta LFP waveform. (The same random seed value was used for both runs.) There is also no effect on the extent of phase precession, nor on the stage of the theta rhythm at which the first place cell occurs (see initial blue dots on the top curves).

# Chapter 5

## Modelling Phase Precession

This chapter starts by examining the form of the postsynaptic potential arising in pyramidal cells from Schaffer collaterals stimulation (section 5.1). This is a dual action, resulting from the combination of direct Schaffer glutamatergic stimulation and indirect inhibition via SR-IN cells. To model this dual action we need to know more about the behaviour of the SR-IN cell; this is the subject of section 5.2. Next, section 5.3 examines the circumstances in which these dual postsynaptic potentials may evoke an action potential in the pyramidal cell, and the relevance of this to phase precession. Finally section 5.4 utilizes these results to simulate phase precession occurring as a rodent transits a place field.

### 5.1 Form of postsynaptic potentials induced in CA1 pyramidal cells by Schaffer collateral stimulation

Schaffer collaterals stimulation has a dual action on the dendritic branches of the CA1 pyramidal cell. On the one hand there is monosynaptic stimulation at glutamatergic synapses distributed along the dendritic branches in stratum radiatum; on the other hand, there is disynaptic GABAergic inhibition at the same branches, resulting from parallel Schaffer stimulation of stratum radiatum interneurons (SR-IN); these in turn inhibit the pyramidal cells at GABAergic synapses onto the same pyramidal dendrites. The two opposing actions are tightly coupled (Csicsvari et al., 1999, Klyachko and Stevens, 2006). As a consequence, a single Schaffer stimulation evokes both an EPSC of glutamatergic origin and an IPSC of GABAergic origin in the CA1 pyramidal dendrite, as was discussed in section 2.1.4. The IPSC starts approximately 5 ms later, is slower to reach a peak, and has a much longer decay period than the EPSC (fig. 5.1). Repeated Schaffer stimulation of the two will, after a few impulses, lead to a stable

mean postsynaptic potential (Klyachko and Stevens, 2006), as indicated in a simulation in fig.5.2. This level will be considerably lower than occurs if the SR-IN-derived IPSC component is disabled, as is also shown in that figure.

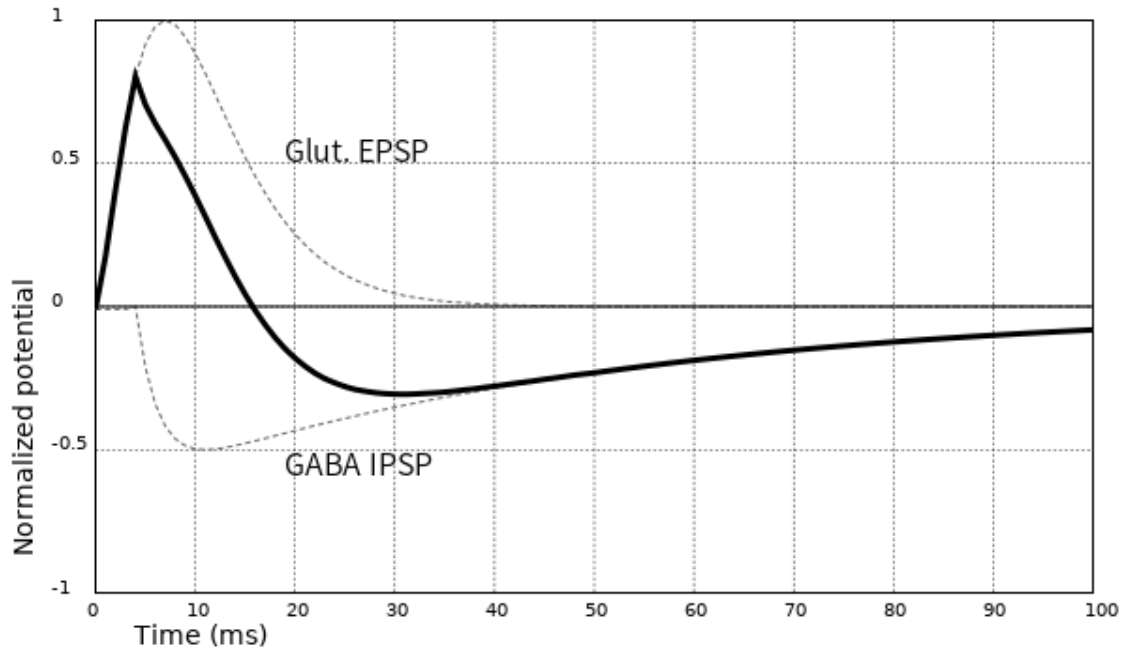


**Figure 5.1:** Schaffer stimulation evokes in a CA1 pyramidal cell both a glutamatergic EPSP (upper dotted curve) and a GABAergic IPSP (lower dotted curve), which, being disynaptic via SR-INs, is delayed by a few milliseconds. The IPSP has a lower peak but a much longer tail than the EPSP. The continuous curve represents the resultant postsynaptic potential. This simulation was prepared for use in generating the next figure. Potentials are normalized to the height of the glutamatergic component.

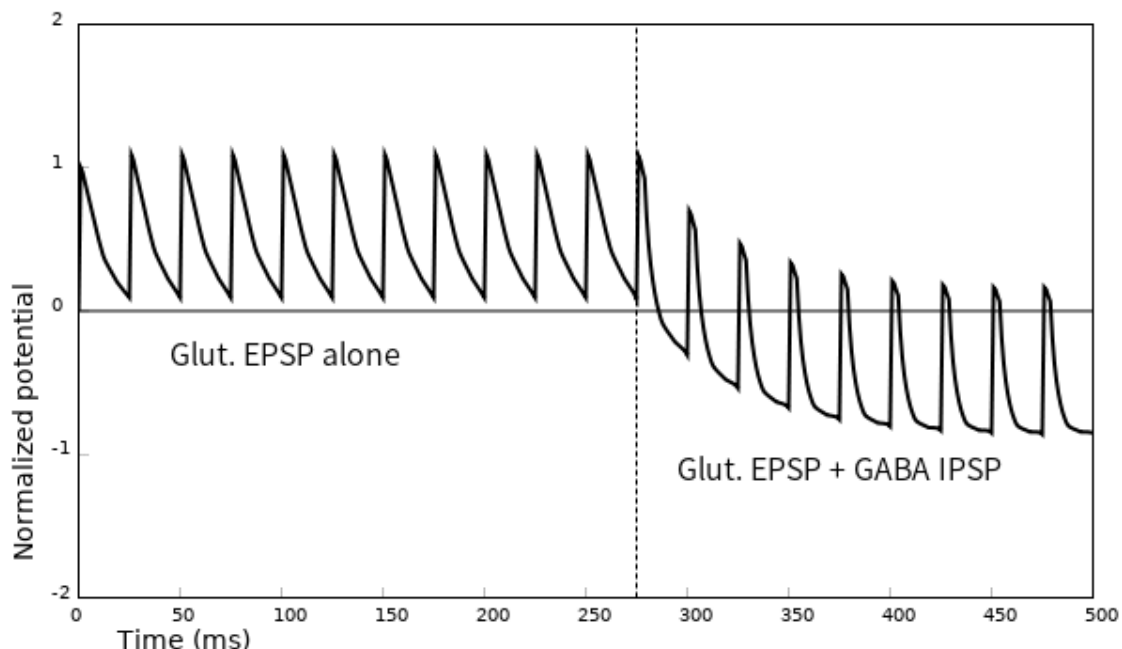


**Figure 5.2:** A run of Schaffer pulses at a frequency of 40 Hz is demonstrated, using the curve generated in fig. 5.1. For the first ten pulses the SR-IN component is switched off. Potentials are normalized to the height of the glutamatergic component.

## 5.2 SR-IN behaviour during a theta cycle

SR-IN interneurons also receive input from OLM cells. This input is GABAergic; the resulting inhibition of SR-IN cells is therefore maximal in that time segment of the theta cycle in which OLM cells are firing most frequently. At such times the inhibition of pyramidal cells by SR-IN interneurons will be at its weakest.

We can estimate the effect of OLM firing on the SR-IN cell membrane potential as follows. First we need to know how this membrane potential varies in response to a single impulse of OLM input. This information is available (Fuhrmann et al., 2015, Leao et al., 2012). The membrane potential drops over a few milliseconds from the resting potential to a hyperpolarization of approximately 3 mv depth; this hyperpolarization then decays with a time constant of approximately 100 milliseconds (fig. 5.3b).

Next we need to model the signal from the OLM to the SR-IN cell. This signal can be represented as a train of impulses, the frequency of which varies in accordance with the normalized firing probability curve for the OLM cell during the theta cycle (fig. 5.3a). As we do not know the mean frequency of OLM inputs to a single SR-IN cell, we can try various different values for this, to see if this parameter is critical. If we choose a trial value for this mean frequency, we can build a stream of OLM impulses that accord with it; the interval between individual firings will reflect the height of the OLM firing probability curve at that stage of the theta cycle. An example is shown in fig. 5.3a, where the vertical red arrows represent actual firing for a chosen mean firing rate of 20 impulses per cycle.

Before going further, it would be helpful to know if there are any statistics that might help us choose a realistic value for the mean frequency of OLM impulses to a single SR-IN cell. Some figures are available in the literature. Studies of single OLM cells have indicated that they typically fire between one and three times per theta cycle (Forro et al., 2015, Somogyi et al., 2014, Varga et al., 2012). A metastudy of the literature on the rat CA1 region carried out by Bezaire and Soltesz 2013 indicates that there is approximately a one-to-one connection rate between OLM cells and SR-INs (called “SCA” - Schaffer-associated interneurons - in their article). If these figures are correct, it would mean that an SR-IN cell receives typically one to three OLM stimulations per theta cycle. As the figures in Bezaire and Soltesz 2013 are based on a large number of assumptions (44 are listed), this may however be an underestimate. In what follows, I shall examine the case for three representative values: 2, 7 and 20 OLM impulses per cycle.

Given the impulse response of the SR-IN membrane potential to a single OLM input impulse, and given a train of OLM impulses occurring over a given time interval, it would be possible to generate the variation in SR-IN membrane potential over that interval by taking the **convolution** of the OLM impulse train with the impulse response

over that interval. (The assumption is made that the SR-IN IPSPs from successive OLM impulses are additive. As we shall see, convolution values rarely exceed  $-4$  mV, so that such an assumption does not result in unrealistic hyperpolarization.)

A demonstration of the results of carrying out this convolution for three different average OLM firing rates is given in fig. 5.3c. A further convolution is carried out between the normalized OLM firing probability curve itself and the SR-IN impulse. Given the considerable uncertainty as to how many OLM neurons impact on a SR-IN neuron, I have elected to use the convolution of the firing probability curve with the SR-IN response curve for the model, as the curve is closely followed by all mean OLM firing rates tried, although for the case of 2 impulses per second the curve is very jittery. Of interest in the convolution is the lag between the peak of OLM firing probability and the consequent trough of SR-IN hyperpolarization, which is of the order of  $90^\circ$  (25 ms).

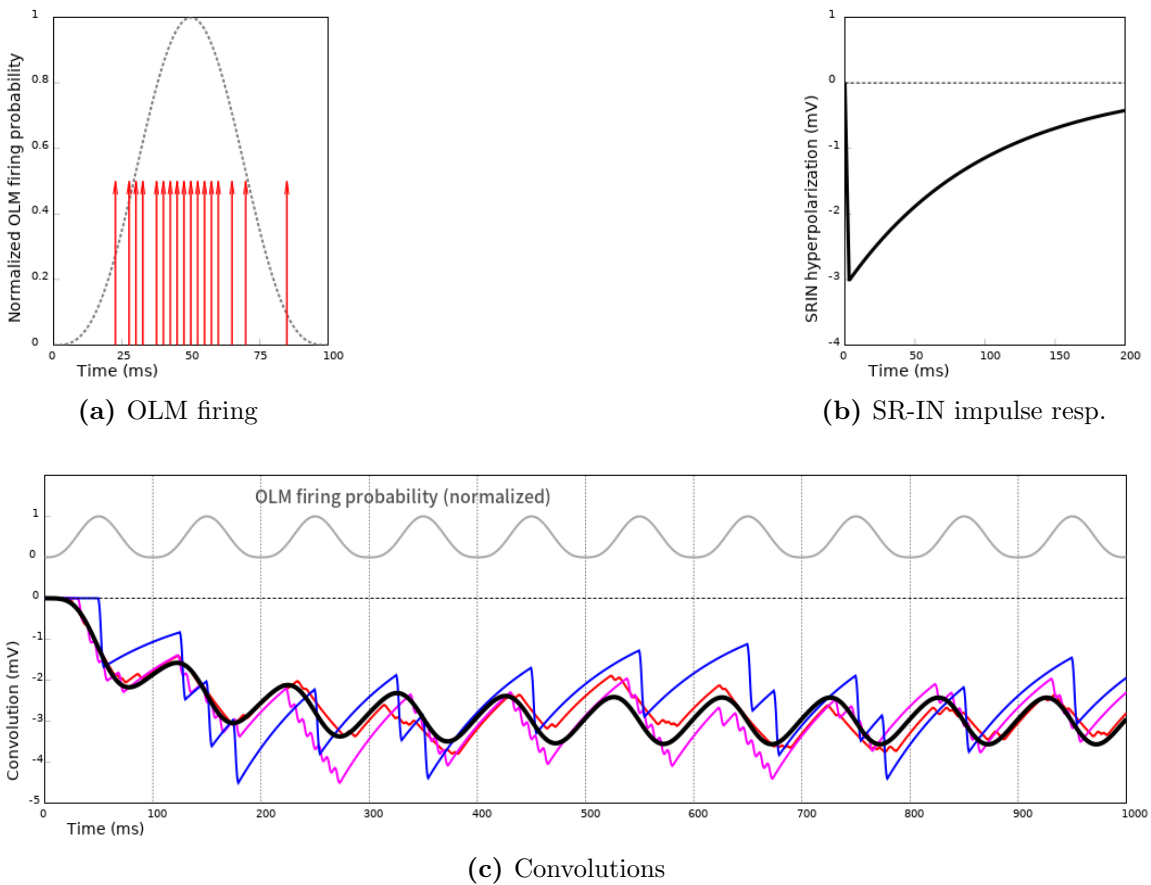


**Figure 5.3:** Fig. 5.3a shows the normalized firing probability of OLM cells during a theta cycle (dotted curve); instants of simulated actual OLM firing in a single cycle are shown as vertical arrows. Fig. 5.3b represents the IPSP induced in an SR-IN cell by a single OLM GABAergic stimulation, referenced to the resting potential of the cell (represented as 0 mv). Fig. 5.3c shows several convolutions. All involve the SR-IN IPSP of fig. 5.3b. The other convolution argument is variously: (a) a sequence of OLM firing (coloured curves), the mean firing rates per theta cycle being 2 (blue curve), 7 (magenta curve) and 20 (red curve); and (b) the normalized firing probability curve of fig. 5.3a (thick black curve). In all cases the convolution is taken over ten cycles of theta rhythm at a frequency of 10 Hz.

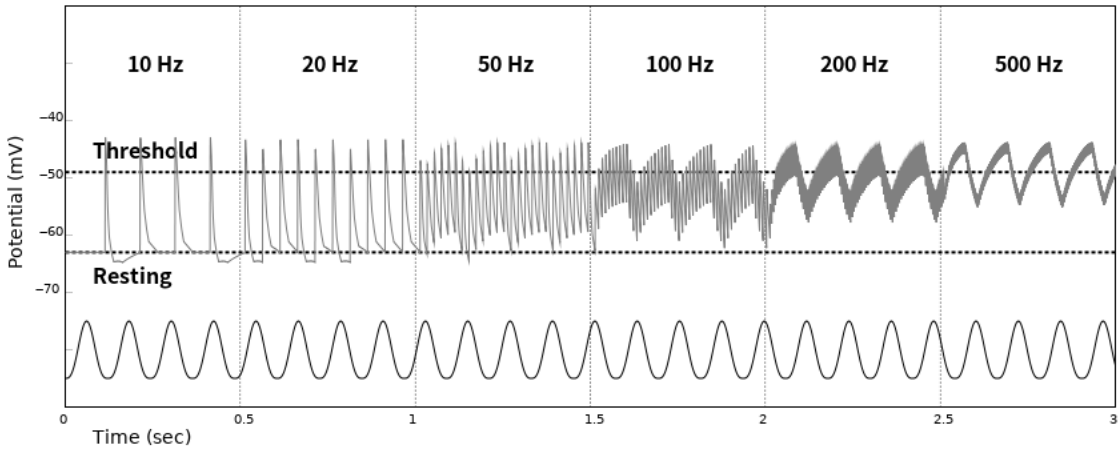


**Figure 5.4:** The **central curve** tracks that component of postsynaptic potential developed in a CA1 pyramidal cell which results from the summation of direct Schaffer glutamatergic stimulation and Schaffer-stimulated SR-IN GABAergic inhibition. Impulses are generated as demonstrated in figs. 5.1 to 5.3. Six sample frequencies of Schaffer stimulation are shown, from 10 Hz to 200 Hz.

The **lower curve** tracks the firing probability of OLM cells during theta rhythm (not drawn to scale). Peaks in OLM activity coincide with maximal SR-IN suppression, during which time the relatively unopposed glutamatergic input to the pyramidal cell raises the mean of the postsynaptic potential. As OLM firing subsides, SR-IN activity becomes more prevalent, and the mean of the postsynaptic potential falls. (Maximal SR-IN suppression lags maximal OLM firing by a fraction of a cycle; this results from the convolution process, as shown in fig. 5.3c).

### 5.3 Schaffer-stimulated place cell firing during place field transit

The concept that the balance of inhibition and excitation determines the amount of depolarizing current input into the pyramidal cell was explored by Mehta et al. 2002 and by Harris et al. 2002; both sources regarded the interaction as central to the idea of phase precession. The variation of pyramidal postsynaptic potential in response to altering balance of inputs is illustrated in fig. 5.4. In this figure the curve at the bottom represents the firing probability of OLM cells during a theta rhythm of slightly above 8 Hz. Independently there is Schaffer stimulation occurring, at six different test frequencies from 50 to 500 Hz. The combined postsynaptic potential (PSP) resulting from direct Schaffer glutamatergic input and disynaptic GABAergic input is represented by the central curve. At all but the lowest frequency the effect of OLM inhibition of the disynaptic component is apparent: As OLM firing probability increases from the previous trough, the amplitudes of the pyramidal PSP gradually increase (though with a phase lag of approximately 90°, due to the convolution described in the previous section); the balance has tipped in favour of the glutamatergic element of the Schaffer stimulation, as OLM input is suppressing SR-IN firing. As OLM firing decreases the SR-IN input is strengthened, so that the amplitudes of the PSP fall.

The “ramp of depolarization” of the place cell that occurs during transit of a place

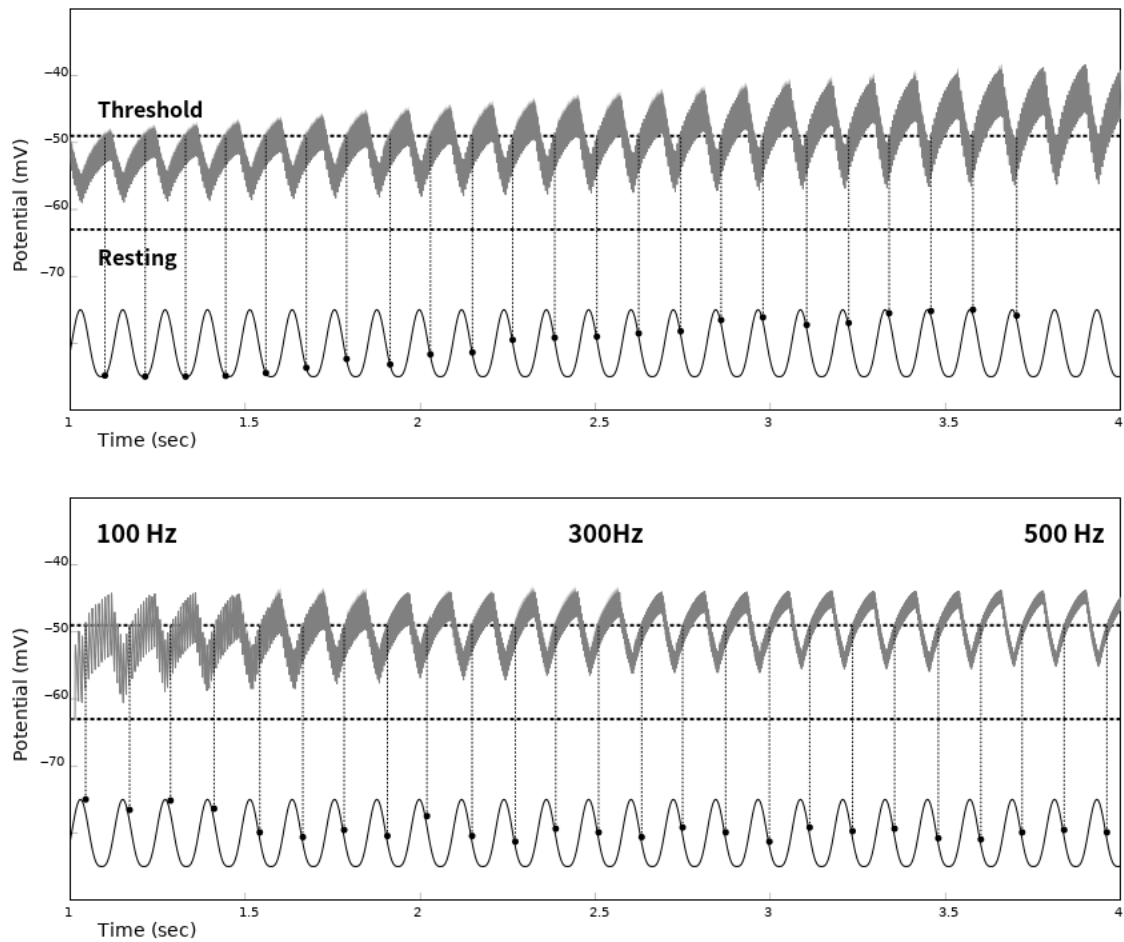


**Figure 5.5:** The **upper graph** shows pyramidal postsynaptic potential variation with increasing activation of glutamatergic receptors, the frequency of CA3 input being held constant at 200 Hz. As activation increases the “saw tooth” segments of the PSP graph rise, so that the pyramidal firing threshold is reached earlier in each cycle (as indicated by the dotted lines projecting onto the OLM firing frequency curve).

The **lower graph** was constructed with a fixed degree of glutamatergic activation but with increasing CA3 input frequency, from 100 Hz (left end) to 500 Hz (right end). The phase at which the threshold is crossed is almost independent of the frequency.

field was described in section 2.3.3.

Of key importance to the development of phase precession is the increase in place cell firing that occurs as the rodent passes through the first half of the place field, and a little beyond (section 2.2.4). It is unlikely that this represents a coupling somehow established between specific place fields of CA3 and CA1, as there is a large degree of dissociation between the two sets of place fields (Lee et al., 2004, Morris, 2006, Rolls et al., 2006). In Buzsáki 2002 it is suggested that “repeated pairing of distal dendritic depolarization by the entorhinal input and the trisynaptically activated CA3 recurrent/Schaffer collaterals to CA3 and CA1 pyramidal cells can result in synaptic modification of the intrahippocampal associational pathways” (p.335). Some contribution to this is undoubtedly from facilitation and posttetanic potentiation, discussed in section 2.1.2 (these have been built into the final model); there may also be other

forms of spike-timing-dependent plasticity operative, reflecting the proximity in time of CA3 and CA1 stimulation. A third contribution may come from the accumulation of charge leaking from the terminal dendritic tufts; CA3 input occurs there shortly before pyramidal firing commences, and the high impedance of the fine tufts causes them to retain charge, acting as integrators (Branco and Häusser, 2011). In this way there would be a trickle of charge into the dendritic branches, raising the background potential there at the stage of the theta cycle when pyramidal firing is favoured. This is supported by data from Harvey et al. 2009, which shows in mice a raised resting level between action potentials of the order of 4 mv (fig. 4C of the article).

Whatever is the exact cause of this variation in firing frequency across the place field, it has been incorporated with success into many models of CA1 (Jensen and Lisman, 1996, Mehta et al., 2002, Tsodyks et al., 1996, Wallenstein and Hasselmo, 1997). This modelling artifice has been described as a “ramp of depolarization” (Harvey et al., 2009), commonly represented as peaking at the centre of the field (as in the above examples). Experimenting with mice, Harvey et al. 2009 found more support for a ramp that peaked at around two-thirds of the transit of the place field; my personal experience with the final model has been that this is necessary to avoid reversal of phase precession after the modelled rodent crosses the middle of the field.

The final decline of the ramp from its peak is at least partly occasioned by increased firing from associated basket cells and axo-axonic cells. Their perisomatic and axonal synapsing sites enable them to suppress depolarization generated within the dendrites that would otherwise have been able to fire the cell. Both PVBC and axo-axonic cells begin to fire late in the theta cycle, some time after pyramidal cell firing has begun (Klausberger and Somogyi, 2008).

The strength of **axo-axonic cell** firing is unlikely to vary during transit of the place field, as AXO cells are relatively few in number, and each connects to approximately 1000 pyramidal cells (Freund and Buzsáki, 1996); this would suggest that they act as a more general stabilizer of the whole pyramidal cell population.

On the other hand, **PVBC cells** have much more focussed interaction with small groups of pyramidal cells within microcircuits (Lee et al., 2014), and receive much feedback from pyramidal cells (discussed in section 1.2.2). As the crossing of the place field proceeds, PVBC inhibition would consequently be expected to increase. But the cumulative effect of PVBC firing has another cause beyond an increase in firing rate. A unique feature of PVBC synapses onto pyramidal somata is their close and specific spatial association with the ClC2 chloride ion gate (Foldy et al., 2010). Unlike other chloride gates of the cell, this gate only operates when pyramidal hyperpolarization reaches a certain degree and when  $\text{Cl}^-$  reaches a high enough concentration; at this point the gate prevents pyramidal cell hyperpolarization exceeding the reversal potential for GABA, that is, the potential at which GABA IPSCs actually become

depolarizing. On the other hand, by not acting till a certain level of hyperpolarization is reached, a steady state level of hyperpolarization and high Cl<sup>-</sup> concentration near the trigger level must be maintained during periods of active PVBC firing. Another factor leading to accumulation of charge is that the speed of decay of IPSCs is slower as the concentration of Cl<sup>-</sup> increases, tending to allow integrative summation of charge when there are frequent PVBCs (Smart, 2010). The nett effect would be a steadily increasing level of hyperpolarization in the pyramidal soma during the transit of the place field, sufficient to have a strong braking effect on pyramidal firing by the later stages of the transit.

So far omitted from the discussion of phase precession have been **CCKBC basket cells**, which also synapse on the perisomatic region of the pyramidal cell. They are omitted because their action appears to be to modulate the strength of the firing rather than to affect its precise timing (Freund and Katona, 2007, Klausberger and Somogyi, 2008). They are well suited for this purpose as they tend to fire at the same time as pyramidal cells.

## 5.4 Phase precession simulation

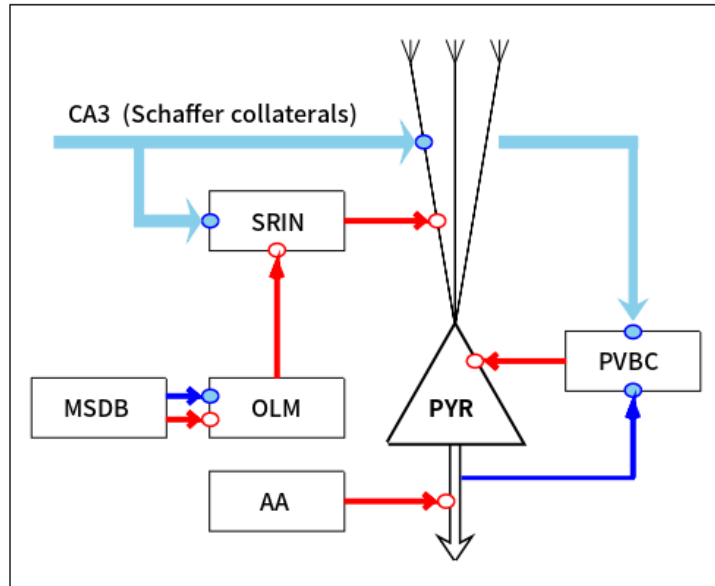


**Figure 5.6:** Components of the phase precession demonstration model. Lines in blue to filled circles represent glutamatergic connections; lines in red to hollow circles represent GABAergic connections.

The simulation was done using the more complete model of chapter 6, but limiting its functionality to what has been presented in this section. The schematic corresponding to this simulation is shown in fig. 5.6. There is a single pyramidal place cell which receives and sums two coincident postsynaptic potentials: an EPSP, representing direct

input from Schaffer fibres, and an IPSP, starting 5 ms later, representing input from SR-IN cells. The summation was demonstrated in figs. 5.1 and 5.2. The weighting of the Schaffer input to the pyramidal cell and to the SR-IN cell are in fixed proportion, and increase during place field transit until two-thirds of the transit is completed (the “ramp of depolarization” described in section 5.3), after which they decrease. The SR-IN component is computed as the convolution of a continuous input signal from the OLM unit with the SR-IN impulse response, as discussed in section 5.2 and illustrated in fig 5.3. The AA unit provides an IPSP to the pyramidal cell which is proportional to the firing probability of AA cells during the theta cycle. As mentioned in the previous section, these are represented as firing at a constant rate during place field transit. The IPSP from the PVBC component is also represented as a signal proportional to the firing probability of PVBC cells during theta rhythm, as also explained in the previous section. This signal increases throughout the transit. I have not found any published data as to the variation the PVBC-induced somatic inhibition during a single place field transit. In the absence of this, I have modelled the inhibition as the sum of two components, one proportional to the Schaffer stimulation and one proportional to the short-term plasticity function developed as discussed in the previous section. Coefficients of proportionality were experimentally derived as values that were sufficient to suppress pyramidal cell firing at the stage where PVBC firing is maximal.

Representative graphs generated by this simulation are shown in fig. 5.7. In each case the simulated rodent is crossing a place field at a constant speed of 15 cm/s. The horizontal axis is marked in seconds; the time extent of the place field crossing is indicated at the top of each graph. OLM action is represented as a firing probability curve at the bottom (not drawn to vertical scale), the frequency of its peaks being slightly greater than 8 Hz. Firing of the pyramidal cell is not instantiated in this simplified model, but is presumed to occur when the intracellular potential rises to the threshold potential of  $-49$  mV. As long as the envelope of the potential curve lies above this level, presumptive firing continues to occur at curve peaks, but not exceeding a maximum firing frequency of 40 Hz. Each place cell firing is indicated by a vertical red arrow. To illustrate phase precession, the time within each OLM cycle of the first crossing of the threshold voltage by the postsynaptic potential curve has been projected onto the OLM firing curve (vertical dotted line), the projection being marked by a red dot on the OLM curve.

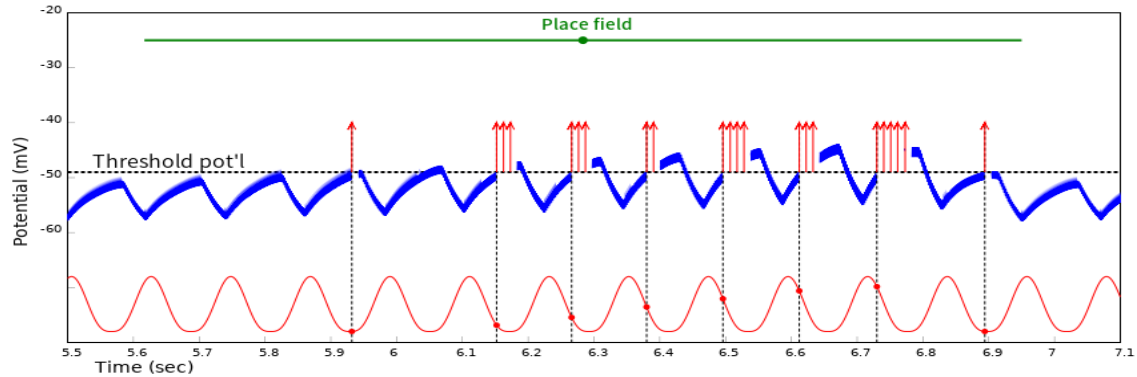
The three graphs of fig. 5.7 represent the separate influences of Schaffer stimulation, place cell plasticity and PVBC inhibition upon phase shifting of place cell firing. All three processes are operational in the final graph.

In **fig. 5.7a** a hypothetical situation is modelled where only Schaffer stimulation is active; that is, there is no plasticity component, and PVBC cells are not active. Red dots on the OLM curve show a precession of phase of approximately  $120^\circ$  by the centre of the place field, but this precession almost completely regresses during the rest of the

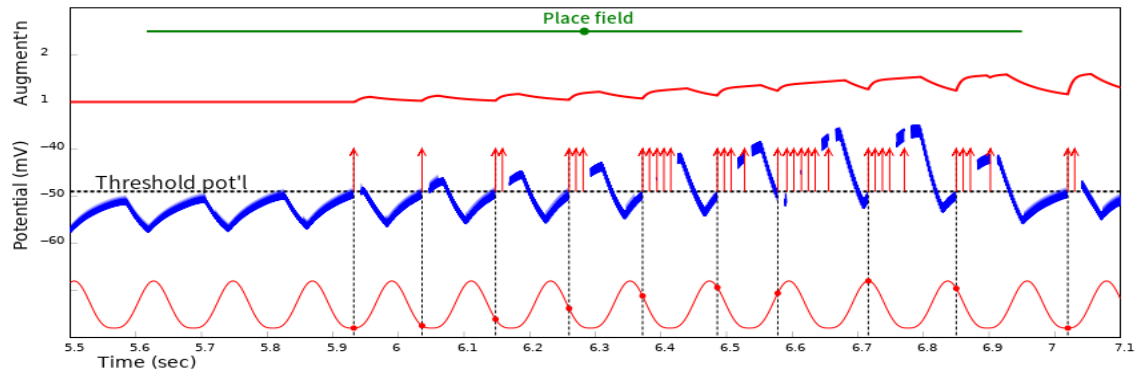
transit.

In **fig. 5.7b** a component of short-term plasticity has been added. The EPSP input to the pyramidal cell has been augmented using the equations and parameters of section 2.1.2. The variation of this augmentation coefficient with time is indicated by the red curve at the top of the figure. Its value before firing commences is 1; by the end of the transit it has reached a maximum value of approximately 2. The red dots on the OLM firing curve now indicate a total phase precession of approximately  $210^\circ$ , which occurs only during the first half of the transit, but does not regress thereafter. However pyramidal cells are now firing continuously across several OLM cycles, a situation which would involve loss of navigational information and would increase the risk of unstable oscillation developing within the CA1.

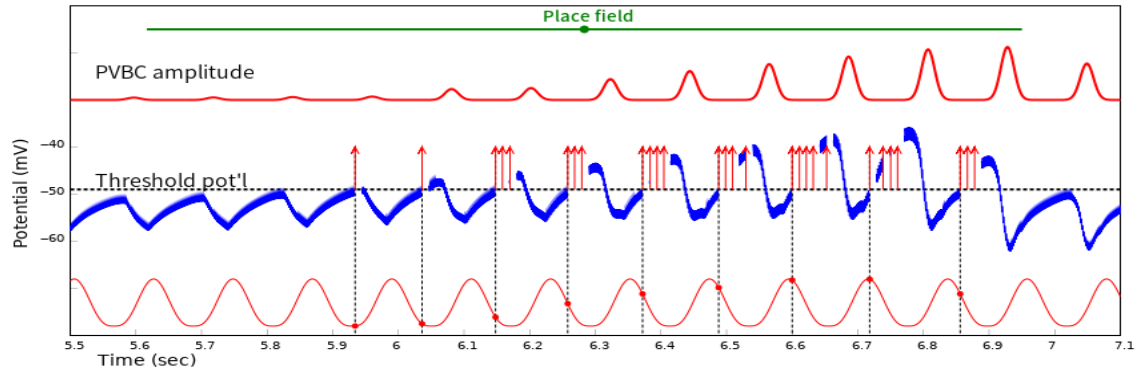
In **fig. 5.7c** PVBC stimulation is added; this has the effect of limiting the duration of place cell firing bursts, confining them to a single OLM cycle. The red curve at the top of the graph represents PVBC inhibition, increasing, as mentioned earlier, towards the end of the transit. The peak of PVBC firing occurs at the stage when OLM inhibition of SR-IN cells has weakened, that is, on the downward slope of each tooth of the ‘saw-tooth’ potential curve. It prevents the tooth from rising further under strong glutamatergic stimulation, thus bringing an end to a particular firing burst; but its effect ends before it could interfere with the rise of the next tooth of the curve. A phase precession of approximately  $240^\circ$  occurs evenly across most of the place field, regressing slightly thereafter.



(a) Schaffer stimulation alone



(b) Schaffer stimulation and short-term plasticity effects



(c) Effect of increasing PVBC inhibition through the place field

**Figure 5.7:** The firing pattern of a pyramidal cell during the subject's transit of a place field at a constant speed of 15 cm/s is represented as largely due to the overlay of three phenomena, artificially isolated in the above diagrams. The model used for the diagram consists of a single pyramidal cell, not compartmentalized, which receives Schaffer-driven glutamatergic input coupled with SR-IN GABAergic input. The resultant intracellular potential is indicated by the blue curves. In each diagram the red curve at the bottom represents OLM firing probability (not scaled), corresponding to a theta rhythm frequency of slightly above 8 Hz. The pyramidal cell's firing threshold is represented by a dotted horizontal line; vertical arrows represent pyramidal cell firing, given a nominal maximum firing rate of 40 Hz. The vertical dotted lines represent the start time of each firing burst; this time is marked as a red dot on the OLM tracing, to indicate phase. Individual graphs are discussed in the text.

# Chapter 6

## Model of navigational activity

The CA1 region of the hippocampus is a complex network of pyramidal cells and GABAergic interneurons. More than 20 types of interneurons have been described (Keimpema et al., 2012). Classification of these interneurons is problematic as they vary in chemistry, cytoarchitecture, genetic origin and interconnections; attempts to draw defining correlations between such features and the perceived functions of these neurons is an incomplete and ongoing task (Ascoli, 2008). Particular neuron types are also not static entities; their dynamic properties include variations in the expression of synaptic receptors and in the expression of genes which modify their postsynaptic neurochemical effects. Cell populations are not necessarily homogeneous. For example, the electrophysiological behaviour of the pyramidal cell varies according to location within the CA1 (Mizuseki et al., 2011), and even within local subgroups at the one location (Grosmark and Buzsaki, 2016). For any one pyramidal cell there is also considerable variation in performance from trial to trial for the same cell during a repetitive task (Fenton and Muller, 1998).

A computer model of regional neuronal activity cannot be complete, given the huge complexity of interconnections and of the internal structure of the neurons involved. The valid purpose of computer modelling is to abstract from the general complexity of the region a small group of interesting behaviour patterns that have been well confirmed, and to model these in relative isolation from the whole. In the process of carrying out this abstraction it is inevitable that simplifications of structure and simplifying assumptions as to function must be made. To ensure that these do not stray too far from reality, the model must first be able to successfully demonstrate certain basic known patterns of behaviour. Beyond that it must justify its existence by making testable predictions as to the outcome of novel patterns of input data.

## 6.1 Scope of the model

The anatomical scope of the present model is the CA1 region of the rodent hippocampus; the functional scope is the behaviour of neurons within this region during navigational activity, at which time theta rhythm is operative, as described in chapter 2. The demonstration of basic known patterns of behaviour will include the phenomenon of phase precession (section 2.2.4) and the generation of a realistic local field potential. With regard to testable predictions, the particular emphasis for the model is to demonstrate the ways in which serotonergic modulation, both synaptic and humoral, may influence CA1 navigational behaviour.

While the model does incorporate synaptic plasticity - a vital part of the process of learning and memory formation - it does not concern itself with the electrophysiology of learning or of the recruiting of new place cells; in particular, there is no representation of sharp waves or of gamma oscillations. It is appreciated that excellent models exist which incorporate such elements, a notable example being that of Cutsuridis et al. 2010a. However the emphasis for the present model is to demonstrate serotonergic effects on CA1 function; serotonin has not so far been demonstrated to play a major role in the generation or operation of sharp waves or gamma oscillations within the CA1 region.

## 6.2 Choice of model type

A complete physiological model of neuronal activity would need to take account of complex metabolic pathways and molecular switches (such as the G-protein family), together with the up- and down-regulation of genes controlling such activity. It would also need to handle the dynamic variation of, for example, individual ion channel impedances, and the continuous variation of properties along the length of the dendrites and axons of cells. This would be a daunting task; I am unaware of any such effort in modelling hippocampal activity.

A much simplified but very successful model of neuronal behaviour was developed by Hodgkin and Huxley 1952. The neuron is modelled using a membrane capacitance, a leakage channel (represented as an EMF in series with a fixed resistance), and sodium and potassium ion channels (each represented as an EMF in series with a resistance that varies, being voltage-dependent); these four elements are represented as parallel arms in an electrical circuit. As only first order differential equations are involved in such a circuit, the model lends itself easily to computation.

The Hodgkin-Huxley model per se does not take account of the dynamics of charge moving along neuronal dendrites and axons. To model transmission line effects a continuous second-order partial differential equation, the “cable equation”, is required;

however the equation does not have general analytical solutions, and the electrical parameters of the neuronal “cable” are not constant along its length. A compromise is typically used by dividing the neuronal unit into smaller lengths or “compartments”, within each of which the potential is approximately constant throughout (Trappenberg, 2010, p.33ff, p.46ff).

Models of CA1 activity which take gamma oscillations into account cannot safely ignore transmission line effects. The stratum radiatum in the adult rat brain is of the order of 0.5 mm thick (Kjonigsen et al., 2015); pyramidal cell conduction velocity is of the order of 0.5 m/s (figure applies for backpropagation in neocortical pyramidal cells: Stuart et al. 1997a). Given these figures, the conduction time for an impulse along the CA1 pyramidal cell dendrite branch would be of the order of 1 ms. Conduction between terminal tufts and the dendritic branches would have a longer delay, as the diameter of the conducting tubes is much narrower; the total conduction time from extreme tufts to soma is likely to be several milliseconds. The oscillation period for fast gamma oscillation is of the order of 10 ms (section 2.3.6). This means that the transmission length of the neuron is of similar order to the wavelength of the oscillation; therefore cable properties cannot be ignored. The division of the pyramidal cell into compartments is therefore essential (though models of gamma oscillation do exist which treat the pyramidal cell as a single compartment, e.g. Kopell et al, Cutsuridis et al. 2010b, p. 423). The situation is different where the highest frequency being modelled is that of theta rhythm, for which the period is in excess of 100 ms (section 2.2.2). Transmission line properties are consequently much less prominent, not per se justifying compartmentalization of the pyramidal neuron.

One difficulty with using a purely electrophysiological approach for a model with the scope defined as above is our current incomplete understanding of the interconnections between key neurons. A dependable state-space analysis of an engineering system requires an accurate description of all significant interconnections within the system. Unfortunately there are still gaps in our understanding of the interconnections between neurons within CA1. For example, the OLM cell is a major component in the generation and maintenance of hippocampal theta rhythm; but the deployment of its glutamatergic and GABAergic inputs and outputs are not yet well understood, with differing hypotheses being put forward by different authors (Fuhrmann et al., 2015, Klausberger, 2009, Leao et al., 2012, MÄller and Remy, 2014).

In place of a deterministic electrophysiological model, the route chosen for the present model has been to construct a **behavioural model** (Willems, 2007). Classical system models have inputs and outputs connected by signal flow diagrams, the signal following a causal pathway through the system. While such analysis can handle feedback and feedforward interconnections, the concept of causality weakens with high interconnectivity, especially when the connections are not fully worked out. In preparing a behavioural model, one first seeks to break the system down into interconnected sub-

systems, if necessary breaking these down into their own constituent subsystems, “until we meet a component whose model follows from first principles, a subsystem whose model has been stored in a database, or where system identification is the appropriate modelling procedure” (Willems, 2007, p.48-49). Such a subsystem may not be suitably described by a transfer function, but rather may be an entity with associated variables, shared with other subsystems, which must bear a particular relationship to one another. Willems gives as an example of such a subsystem the set of Kepler’s laws of planetary motion, which interrelate planetary orbital parameters, but not in such a way as could be represented by an input-output transfer function. In the days before Newton’s more deterministic gravitational theory was developed, this was regularly used as a subsystem within a structure for predicting the future positions of planets.

Once the fundamental subsystems have been teased out, each subsystem must be modelled in terms of the relationships between its constituent parameters. If the subsystem can be accurately modelled in terms of input-output transfer functions, so much the better; otherwise “a subsystem whose model has been stored in a database” may be sufficient to describe behaviour within defined experimental limits.

Finally the interconnections are modelled; this is basically a process of identifying the constraints which must apply to the sharing of variables between subsystems.

The subsystems used in the present model vary according to circumstances, in some cases consisting of typical single-cell action potentials, in others as firing probability of cell types during theta phases, in others as mathematical relationships. The deployment of each will be outlined in the next section, as we deal with particular subsystems.

### 6.3 Model subsystems: Constituent neurons and receptors

The model focusses on what happens at the level of the microassembly comprised by a pyramidal place cell and the interneurons associated with its operation during navigation. While it is not impossible that several pyramidal cells may be associated with one particular place field, experimentally identified place cells have each been found each to have a separate place field (section 2.2.3). The heart of each modelled microassembly is therefore the single pyramidal cell which for the time under consideration is acting as a place cell; interneurons which are known to interact with such a place cell during navigation are included within the representation of each microassembly.

The choice of units and processes incorporated into the model, and the complexity of their interactions, has been made with the following guidelines in mind:

- The model must be able to demonstrate key features of CA1 behaviour during

navigation;

- It must be able to demonstrate known important serotonergic effects applying to the CA1 region during navigation;
- It should not include elements which are not known to contribute significantly to the above.
- Where numerous individual interneurons of the one type fire approximately in unison during theta rhythm activity, a single unit may be used to represent the group.
- Where numerous individual interneurons of the one type fire in a similar manner but at different instants within a segment of a theta rhythm cycle, firing probability should be taken into account in representing the firing of the group.

A list of neurons and receptors which have been included in the model as subsystems is presented below. Descriptions of the implementation of each subsystem then follows. In section 6.3.9 a list of excluded interneurons is provided, together with reasons for excluding them from the model.

### 6.3.1 Included elements

:

- Pyramidal cells
- Interneurons:
  - OLM cells
  - PVBCs
  - CCKBCs
  - Axo-axonic cells
  - Stratum radiatum interneurons associated with Schaffer collaterals
- Inputs
  - from MSDB (glutamatergic + GABAergic)
  - from EC (the perforant path) and from CA3 (Schaffer collaterals)
  - from MRN (serotonergic and glutamatergic)
- Serotonin receptors
  - 5HTR1A and 5HTR4 in pyramidal cells
  - 5HTR3A in CCKBCs

- 5HTR1B in the feedback loop from pyramidal cell to CCKBC.
- Sources outside of the HC
  - MRN
  - MSDB

A diagram representing these features is shown in fig. 6.1, a diagrammatic cross-section through the CA1 region. The five morphologically defined strata of the CA1 are indicated, with their names. The central layer, stratum pyramidale, contains the triangular body of the pyramidal cell. At the top of the diagram the stratum lacunosum-moleculare holds most of its terminal dendritic tufts. Glutamatergic fibres directly from the EC (the perforant path) synapse onto these terminal dendrites. Below this is the stratum radiatum, where the main dendritic branches of the pyramidal cell are found; glutamatergic fibres from CA3 (Schaffer collaterals) synapse onto these, and to a lesser extent onto the basal dendrites shown lower down in the diagram. Five varieties of interneurons are represented by ovals (red): “SR IN” (stratum radiatum interneuron which associate with Schaffer collaterals), “PVBC” (parvalbumin basket cell), “CCKBC” (CCK-expressing basket cell), “AA” (axo-axonic cell) and “OLM” (oriens lacunosum-moleculare cell). Excitatory connections are represented as filled circles, inhibitory connections as empty rectangles. Although the MSDB lies outside the HC, it is for convenience represented at the bottom right of the diagram. The MRN is also shown, with serotonergic projections to the region. The numbering beside the serotonergic arrows indicates the type of receptor involved (for example “1A” for the 5HTR1A receptor).

### 6.3.2 Pyramidal cells

Each pyramidal cell in the model represents a place cell, and is associated with a place field (as described later, in section 6.3.11). A common single-compartment representation of pyramidal cell firing would be the “leaky integrate-and-fire” model, in which summation of input potential occurs but is subject to leakage (the time constant of which is the product of membrane capacitance and the inverse of the average conductance of the parallel set of ion channels). Firing is triggered when a threshold potential is exceeded, producing an output “spike response” which might be a single impulse, or an impulse followed exponential return of potential to the resting level (Trappenberg, 2010, ch. 3). In the present model, the summation of input potential occurs similarly, and does trigger an output when a threshold voltage is reached by the summation. Current leakage is taken into consideration when modelling the combined input to place cell dendritic branches from Schaffer collaterals and Schaffer-stimulated stratum radiatum interneurons (SR-INs), as discussed in section 5, where a curve representing the EPSP at this location displays a time constant of the order of 10 ms.

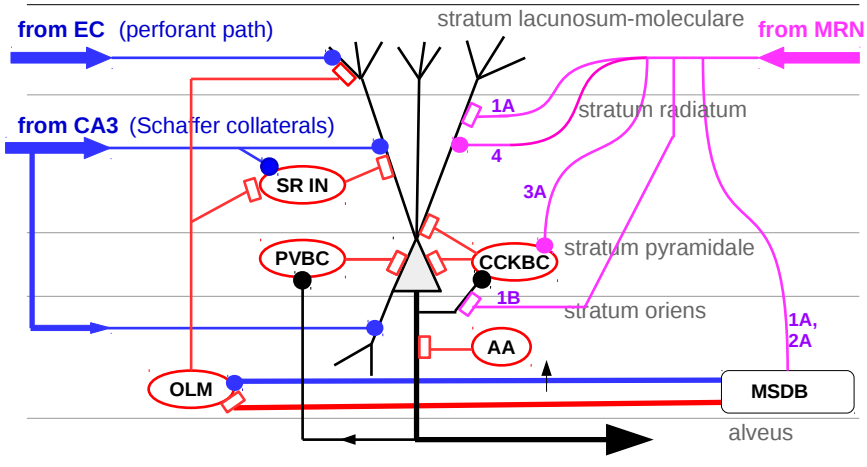


**Figure 6.1:** Diagrammatic cross-section through the CA1 region of the hippocampus, showing features represented in the model, including a pyramidal cell (centre) and related interneurons. Excitatory connections are indicated by terminal filled circles, inhibitory connections by empty rectangles. Numerals beside branches from the MRN refer to the serotonin receptor type.

The present model varies from the typical integrate-and-fire model in that the spike representation has been replaced by a waveform representative of an actual pyramidal cell action potential. In particular, the afterhyperpolarization (AHP) component of the pyramidal action potential has been included in the model, as this enables the modelling of “adaptation”: the reduction of firing frequency and amplitude of a run of APs resulting from constant current stimulation, as shown in fig. 6.3 (Knauer et al., 2013, Tiganj et al., 2015). This is not trivial, as one of the effects of 5HT<sub>4</sub> receptor activation is the reduction of the AHP, and with it a reduction in such adaptation, so that a short firing sequence within the theta rhythm cycle becomes more coherent as a single unit of information, passed first to the subiculum and thence to the EC and to cortical structures (section 3.3). In using a standardized waveform it is understood that there is huge variety in experimentally recorded firing waveforms. The AHP however remains a constant feature (though varying in shape, length and depth); its duration is of the order of 100 times longer than that of the initial impulse. After consulting a number of resources, the final form of the pyramidal firing waveform was set for the model as shown in fig. 6.2 (Graves et al., 2012, Jensen et al., 1994, Mason, 1993, Staff et al., 2000). The length and depth of the AHP component is subject to variation under the action of 5HT<sub>4</sub> stimulation, as described subsequently. (The actual maximum amplitude of the action potential proved to be unimportant, as was found by repeating experiments with a maximum of 0 mv; there was no detectable difference in behaviour.)

It should be pointed out that the adaptation of frequency and amplitude mentioned above applies under the artificial condition of steady-state input to the pyramidal

cell. In the case of stimulation of place cell firing during theta rhythm the level of excitation rises and then falls during that part of the theta period in which place cells fire; consequently maximal firing occurs in the middle of the burst (Skaggs et al. 1996, fig. 6; see also the model output in chapter 7, e.g. fig. 7.5).

## Pyramidal cell compartments?

As pointed out in section 6.2, there is no compelling need to model the pyramidal dendrite in terms of segments for the sake of minimizing transmission line effects, as these are not important at theta frequencies. On the other hand it is reasonable to distinguish between four major regions of the pyramidal neuron on the basis of function: the **terminal dendritic tufts** in stratum lacunosum-moleculare, which receive glutamatergic input primarily from the EC via the perforant pathway; the **dendritic branches** in stratum radiatum, which receive glutamatergic input from CA3 via Schaffer collaterals; the **perisomatic region** (comprised of the soma and the initial portion of the main dendritic branches), which receive GABAergic input from basket cells; and the **axon**, which receives inhibitory input from axo-axonic cells.

The model does not separately model each of these four regions, but incorporates their behaviour into other elements of the model.

- The input to the **terminal dendritic tufts** is implicit in the development of the ramp of depolarization occurring during place field transit (section 5.3), and in changes of this ramp associated with long-term potentiation (section 2.3). Deployment of these in the model is discussed in section 6.3.11.
- The **main dendritic branches** are the site of both direct glutamatergic stimulation and disynaptic GABAergic inhibition, as a consequence of Schaffer collaterals stimulation; the way in which this is modelled was the subject of chapter 5. The features described and illustrated in that chapter are part of the final model.
- The interactions between the **perisomatic region** and inhibitory basket cells are described below when discussing PVBC and CCKBC interneurons.
- The effect of axo-axonic cell inhibition on the **pyramidal axon** is described below when discussing this interneuron.

As was stated at the beginning of section 6.2 in chapter 6, this is a behavioural model after the style of Willems 2007; in such models, the emphasis is on the correct interrelationships of the constituent subsystems, in terms of shared variables, rather than on the component structure of each subsystem. The present model takes pains to ensure that shared variables - usually expressed as membrane potentials - behave between subsystems as expected, in the case of known modelled phenomena, and so have validity in seeking to predict outcomes to novel phenomena.

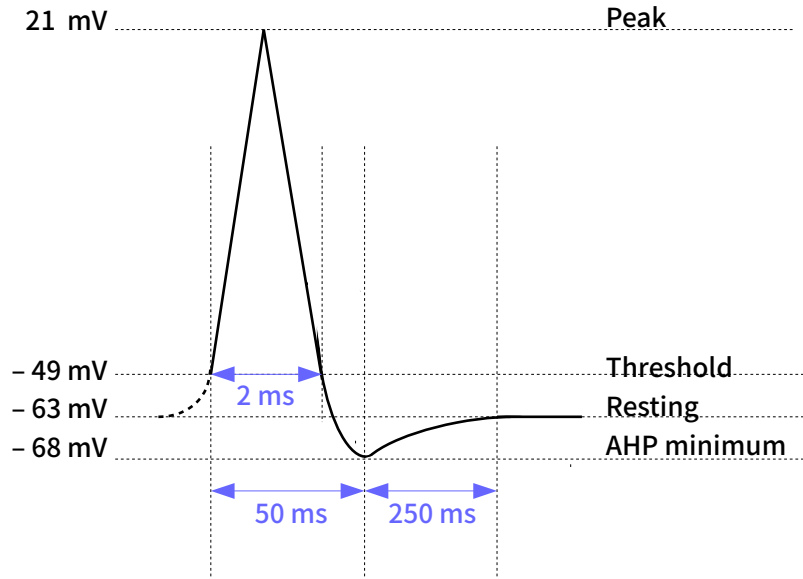


**Figure 6.2:** Specifications used for the pyramidal cell impulse response. Segments are not drawn to scale.

### 6.3.3 OLM interneurons

OLM interneurons receive glutamatergic, GABAergic and cholinergic innervation from the septal area, with some input from pyramidal axons. They project to the terminal dendritic tufts of pyramidal cells; they have also been reported as providing GABAergic output to several interneuron types, most notably SR-IN cells and similar perforant-path-related interneurons; but also to basket cells and to neurogliaform cells.

Of these various connections I have given the highest rating to the glutamatergic input from the medial septum and diagonal band of Broca (MSDB), and to the GABAergic output to SR-IN interneurons. My understanding of the glutamatergic stimulation of OLM cells by the MSDB is based largely on two recent papers. Fuhrmann et al. 2015 reports on extensive research in mice using optogenetic stimulation and fluorometric monitoring with awake running animals, and using retrograde viral tracing to confirm glutamatergic connection between MSDB and OLM cells. Work by Robinson et al. 2016, also using optical activation of septal glutamatergic neurons in mice, provided further information. The implementation of this in the model was outlined in detail in the discussion on modelling phase precession (section 5.2). The trigger for OLM firing is the output of the MSDB subsystem; OLM firing during the theta cycle conforms to this signal; the probability curve itself is used for a convolution with the SR-IN impulse response. The reasons for using the probability curve rather than simulating actual OLM firing are explained in that section.

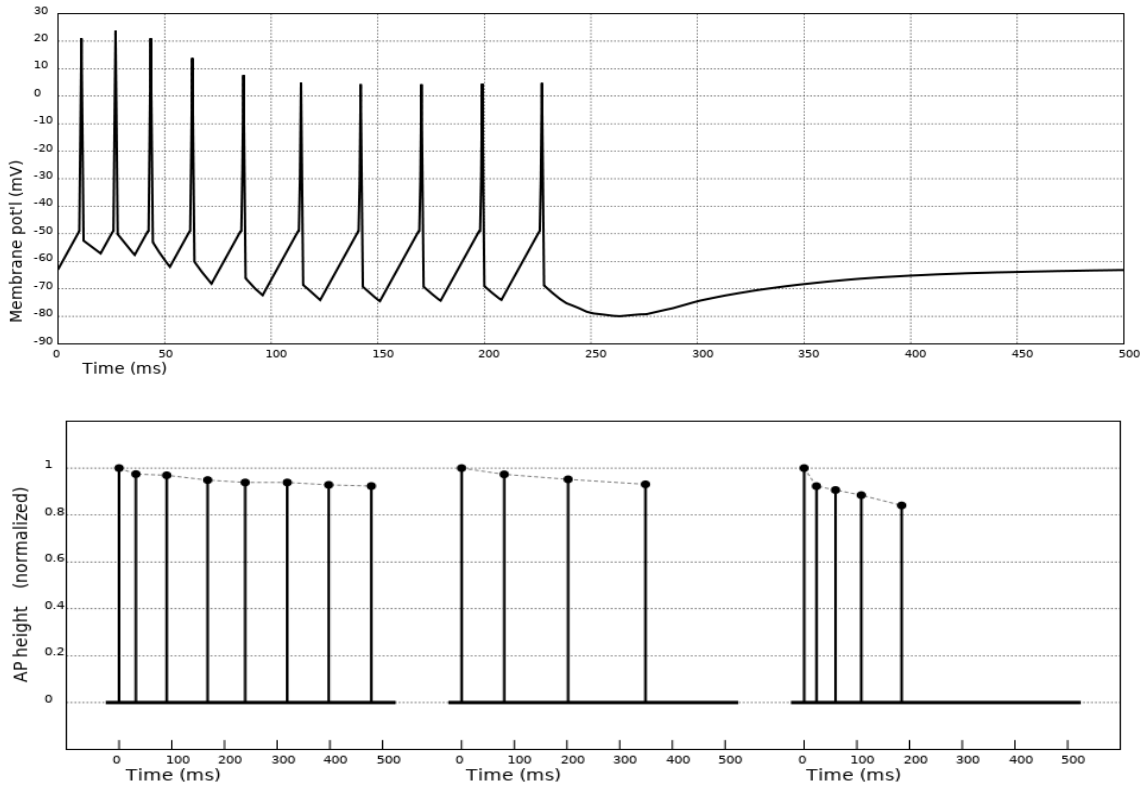


**Figure 6.3:** The **upper graph** simulates pyramidal cell firing resulting from an applied constant current (represented in the graph as a linearly increasing depolarizing potential input). The input is applied until the cell has fired ten times. The burst frequency reduces with time, as does the amplitude. The right half of the graph shows the subsequent decay of the accumulated afterhyperpolarization potential.

The **lower graph**, based on data shown in fig. 2 of Mason 1993, demonstrates similar reduction (or “adaptation”) of frequency and of amplitude shown by actual hippocampal pyramidal cells during constant current stimulation.

The OLM input to the terminal dendritic tufts of pyramidal cells provides a graded inhibitory signal, different to the clear-cut inhibition provided to interneurons (Elfant et al., 2008). The input from the EC is therefore not completely silenced but is muted, allowing the Schaffer input to determine when and for how long place cells fire, thereby providing unequivocal signals downstream of CA1. The EC input to the terminal tufts is not directly modelled; its effect is implicit in the “ramp of depolarization” described in section 2.3.3, an important feature of the model.

As the OLM is activated by glutamatergic input from the MSDB, I have assumed that the parallel GABAergic input has a role in strongly suppressing firing at other times; from the point of view of navigation, this effect would be subsumed in the shape of the OLM firing probability curve. In the same way, in the absence of detailed information on the interconnection between OLM cells and basket cells, the interaction is subsumed into the firing probability curves of these cells. As they also receive direct GABAergic input from MSDB, it would be difficult to tease out how much influence comes from which source; instead I regard the various GABAergic links as reinforcing the general timing imposed by the MSDB, in a manner yet to be fully elucidated.

### 6.3.4 Interneurons acting perisomatically - general points

The next three subsections deal with PVBCs, CCKBCs and axo-axonic cells. In representations of their action, it is considered that:

- They have the *unique ability to prevent action potentials, even when synaptic activation is capable* of producing sufficient depolarization to discharge the pyramidal cell, as action potentials are only generated in the soma (Stuart et al., 1997b).
- Their action is *assumed not to impact on the accumulation of charge within the dendrites*. GABAergic hyperpolarization attenuates with distance from the input site, being very effective near the site of the GABAergic synapse, or at a point where it can block the initiation of an action potential (MÄller and Remy, 2014). The great length of the pyramidal dendrites would therefore be a major barrier to any hyperpolarizing influence of perisomatic GABAergic synapses. Coupled with this is the rich supply of chloride ion gates in the soma (Foldy et al., 2010), reducing the diffusion of these ions back into the dendrites.

The action of perisomatic interneurons will therefore be seen as separate to the dynamics occurring in pyramidal dendrites in the absence of an action potential; their action will be modelled as limiting or preventing the actual occurrence of action potentials which would otherwise result from dendritic depolarization.

### 6.3.5 PVBC interneurons

The principal excitatory input to PVBCs comes from Schaffer stimulation, coupled with feedback from the pyramidal cells with which they are associated (Glickfeld and Scanziani, 2006), both of which inputs would lead to increasing PVBC inhibition of the place cell as the place field is crossed. The modelling of PVBC interneuron firing was discussed in section 5.3. To repeat points made there, **PVBC cells** have focussed interaction with small groups of pyramidal cells within microcircuits (Lee et al., 2014), and receive much feedback from pyramidal cells (discussed in section 1.2.2). (Specifically, the data-mined metastudy by Bezaire and Soltesz 2013 estimates that approximately 17 PVBCs synapse onto a single pyramidal cell.) The feedback is presumed to increase PVBC firing in response to the increased place cell firing during the place field transit. However there is good reason to believe that the impact of this on the pyramidal soma is not of a barrage of discrete and quickly-decaying postsynaptic potentials. A unique feature of PVBC synapses onto pyramidal somata is their close and specific spatial association with the ClC2 chloride ion gate (Foldy et al., 2010). Unlike other chloride gates of the cell, this gate only operates when pyramidal hyperpolarization reaches a certain degree and when Cl<sup>-</sup> reaches a high enough concentration; at this point

the gate prevents pyramidal cell hyperpolarization exceeding the reversal potential for GABA, that is, the potential at which GABA IPSCs actually become depolarizing. On the other hand, by not acting till a certain level of hyperpolarization is reached, a steady state level of hyperpolarization and high Cl<sup>-</sup> concentration near the trigger level must be maintained during periods of active PVBC firing. Another factor leading to accumulation of charge is that the speed of decay of IPSCs is slower as the concentration of Cl<sup>-</sup> increases, tending to allow integrative summation of charge when there are frequent PVBCs (Smart, 2010). From the point of view of the membrane potential at the soma, the overall effect of increased PVBC activity is expected to be a sustained and steadily increasing level of hyperpolarization in the pyramidal soma during the transit of the place field, sufficient to have a strong braking effect on pyramidal firing by the later stages of the transit.

I have represented PVBC output activity as a pyramidal cell hyperpolarization which, during a theta cycle, is proportional to the height of the PVBC firing probability curve. This curve I have modelled on data from various sources (Forro et al., 2015, Somogyi et al., 2014, Varga et al., 2012). As I have not found quantitative detail as to how PVBC input of IPSC to the soma varies during passage through a place field (as the result of positive feedback from the place cell), I have modelled this increase by a linear rise across the field, as shown in the lower graph of fig. 7.1.

### 6.3.6 CCKBC interneurons

In the CA1 region, CCKBCs are only activated during theta rhythm by the dual action of feedforward input (principally from Schaffer collaterals) and feedback from pyramidal cells (Freund and Katona, 2007); as a result they are not recruited until place cell firing has begun (Klausberger and Somogyi, 2008), and their time of their maximum firing probability overlies that of place cell firing. This coincidence of firing period enables them to serve as “modulators that adapt network activity to behavioural states” (Foldy et al., 2010, p.1047), which they do particularly in response to serotonin, but also in response to other neuromodulators (section 1.2.2). They have been modelled as producing a reduction in the probability of firing of a place cell (demonstrated in fig. 7.2).

### 6.3.7 Axo-axonic interneurons

As with PVBCs, the action of axo-axonic cells is represented in the form of reduced firing probability of pyramidal cells, the reduction being determined by the firing probability of axo-axonic cells during the theta cycle. For this I have used data from Somogyi et al. 2014 and Forro et al. 2015. An excluded potential AP would be regarded as coinciding with an axo-axonic firing. The inhibition produced by the axo-axonic firing lasts

for a variable period of up to 40 ms (Ganter et al., 2004, fig. 5); this is reflected in the model by the blockage of further pyramidal firing for 10 ms after a virtual axo-axonic firing event.

Each axo-axonic cell synapses onto the axon of more than 1000 neighbouring pyramidal cells, and each pyramidal cell axon is estimated to receive connections from 4 to 10 axo-axonic cells (Freund and Buzsáki, 1996). Feedback from pyramidal cells has only been demonstrated for a minority population of axo-axonic cells (Ganter et al., 2004). Even if it does occur on a wider scale, it is likely to reflect group pyramidal activity rather than that of a particular pyramidal cell, given these statistics. For this reason the model represents axo-axonic activity as occurring at a fixed amplitude, independent of location within the place field.

### 6.3.8 Stratum radiatum interneurons

The SR-IN cell is represented as producing a postsynaptic hyperpolarizing potential as in fig. 5.1, always matched by a depolarizing potential, shown in the same figure, representing the glutamatergic Schaffer stimulation which is phase-locked to it. The dynamics of this representation was described in considerable detail in chapter 5. The only direct input to the cell is from the Schaffer collaterals; the OLM input is modelled as a variable lowering of the SR-IN membrane potential resulting from the convolution of the OLM input with the SR-IN impulse response to that input, as described in that chapter.

### 6.3.9 Excluded interneurons

In general, interneurons have been included only if they are believed to be positively involved in determining the dynamics of CA1 behaviour during navigation. It is realized that there is a network of GABAergic interconnection between interneurons, partly elucidated, which acts to maintain conformity of action, for example preventing particular interneurons from remaining active beyond their due time in the theta cycle. I have not modelled such connections because - unlike the GABAergic inhibition of SR-IN interneurons by OLM interneurons - they are not actually steering the course of events.

An exhaustive list of exclusions would have to mention every known type of interneuron. The following list is confined to those interneurons which do have known and important functions, yet have been excluded from the model.

*Bistratified cells* were described in section 1.2.2. They synapse onto pyramidal cell dendritic branches alongside Schaffer input; they receive glutamatergic stimulation both from the Schaffer collaterals and from the pyramidal cells which they innervate.

During theta wave activity they fire most frequently at the same time as the Schaffer stimulation of the pyramidal cells. This arrangement would suggest that bistratified cells have an important role in stabilizing pyramidal cell activity and averting the risk of epileptiform behaviour; it does not suggest that bistratified cells are actually determining the sequence of events during theta rhythm. For this reason they are not part of the model, except indirectly in that the weighting of input to modelled pyramidal cells from modelled Schaffer collaterals is adjusted such that the system is stable under normal operating conditions.

*Ivy cells* - which synapse onto pyramidal dendritic branches, alongside Schaffer terminals - and *Neurogliaform cells* - which synapses onto terminal dendritic tufts alongside perforant pathway fibres from EC - are regarded by Klausberger as modulating “pre- and postsynaptic excitability at slower time scales and more diffusely than do other interneurons providing homeostasis to the network” (Klausberger and Somogyi, 2008). They do not appear to be directly involved in determining the sequence of events during theta rhythm activity.

### 6.3.10 Input to the system

#### Schaffer collaterals from CA3

This input drives both the SR-IN interneurons and the glutamatergic synapses onto pyramidal dendrites. These are modelled together, because of the tight coupling between the disynaptic inhibition and the direct excitation of the pyramidal cell, referred to in chapter 5. The unknowns are the number of SR-IN cells and the actual frequency of Schaffer stimulation. As mentioned in section 5.2, there could be as few as just two SR-IN cells per pyramidal cell (Bezaire and Soltesz, 2013); in the light of the number of assumptions made to derive this figure, this may be a significant underestimate. The total stimulation coming from this source would be of the order of the product of the Schaffer input spike frequency and the number of SR-IN cells per pyramidal cell. As I am modelling a single SR-IN cell, I therefore choose what is likely to be an impossibly high frequency for Schaffer stimulation, 500 Hz. Different frequencies were tried; above a certain low frequency the actual frequency does not impact on any aspect of model performance except to increase the amount of jitter (see fig. 5.5, lower graph).

#### Perforant path from EC

This is not directly represented in the model, but is implicit in the deployment of place fields and plasticity effects, discussed below.

## MSDB

The MSDB is represented only in terms of a timing signal which triggers OLM activity, along with the activity of other interneurons represented by probability firing curves, namely PVBCs and axo-axonic cells. The timing signal varies a little with animal speed, as outlined in section 2.2.2.

### 6.3.11 Deployment of place fields

It is appreciated that place fields actually occupy an area, which may be crossed from different directions by free-running rats (Muller et al., 1987). However any one transit through a place field is necessarily linear; and the general properties of place field transits do not appear to be directional. For this reason it is a reasonable simplification to consider the place field as being crossed along a single trajectory.

I have differentiated in some experiments between mapping place fields and “object” fields. In fact, thousands of place fields are evenly distributed across the floor area, at least in the case of a simple cylindrical arena (Muller et al., 1987); this would mean that any object placed in the arena would be trespassing on some pre-existing place field. It has been found that awareness of the animal of a known or newly explored object in a field invokes LTD, facilitated by the serotonin receptor 5HTR4 (Hagena and Manahan-Vaughan, 2017, Kemp and Manahan-Vaughan, 2004). As the only pyramidal cells significantly firing during theta activity are place cells, and as the only place cells strongly firing at the time of object investigation represent adjacent place fields, it is these particular actively firing place cells which must be subject to long-term depression. The fields involved are still “place fields”, but because they are subject to LTD when other fields in the same arena are not, I have distinguished them for the sake of brevity as “object fields”.

The occurrence of place cell firing as a rodent traverses a place field appears to be due to synaptic modification at the place cell dendrites; this appears to be consequent to the repeated pairing of input from CA3 via Schaffer collaterals and of location-dependent input from the EC, via the perforant fibres (Buzsáki, 2002). This augmentation continues throughout the place field transit. After the animal has moved away from the area mapped by the incident perforant fibres from the EC, that input wanes, so that input signals are no longer paired. At the same time, perisomatic inhibition greatly reduces place cell firing in response to ongoing CA3 input. As a result the prior synaptic augmentation is undone until events recur at the next transit.

I have modelled this process using the “ramp of depolarization” described in section 5.3. The weighting of the input to the pyramidal dendrite from SR-IN cells and from Schaffer collaterals is linearly increased until two thirds of the passage through the

place field has occurred, and then reduces to off-field levels by the end of the place field.

While modelling this I came across a dissociation between what could be called a *theoretical place field* and an *experimentally determined place field*. When the animal first reaches the edge of the theoretical place field, there is likely to be a period where weak EC stimulation is occurring at the periphery of the field, but pairing of CA3 and EC input has not yet augmented CA3 stimulation of the pyramidal cell. At some point after this, Schaffer-induced EPSPs are sufficient to induce place cell firing; this point would be the start of the experimentally determined place field. This effect will be apparent in tracings of place cell activity in chapter 7, when discussing experimental results (for example, see fig. 7.2; the first AP occurs about one quarter of the way through the theoretical place field).

The height of the depolarization ramp is variable. I have modelled the ramp as commencing at a very low level when the animal first enters an unexplored field. The existence of a ramp at all at this stage is consistent with the concept that new place cells are assigned as needed by a process of selection, involving short bursts of gamma rhythm, which detect pyramidal cells that momentarily have a lower firing threshold (see section 2.3.6). Long-term potentiation (LTP) is able to raise this ramp, and long-term depression (LTD) to lower it. Such potentiation and depression was described when discussing 5HTR4 serotonin receptors in section 3.3, as this receptor type is crucially important to the development of both LTP and LTD. Experimental examples of modelling such LTP and LTD are given in chapter 7 (section 7.2), where modelled parameters for the ramp are presented and illustrated.

### 6.3.12 Organizing the trajectory

The arena for all runs is a circular strip, along which a variable number of geographical markers and objects are arranged. Geographical markers will become established place fields, initially with low depolarization ramps, the ramp rising quickly with subsequent visits, unless too widely separated (a ‘leak factor’ applies until the ramp height is established at a reasonable level). Objects will be explored and assigned one of five values (from very pleasant, through uninteresting, to very unpleasant). The place fields of uninteresting objects will be prone to LTD. The modelling of the depolarization ramp and of plasticity is discussed in the next chapter, in section 7.2.

The length of the course, number of laps and the deployment of prospective place fields is set before a program run. How the subject will respond to cues is preset as a program within a program. That is, there is a function in the program which is accessed whenever the rodent reaches a landmark (e.g. the location at which an object lying ahead is ‘perceived’). In this function there are various states defined by the user, each

of which involves resetting parameters such as acceleration or deceleration, intended speed, or intended stop; if stopped, intended duration of stop. The states are linked by a flow path, resembling a simple program with conditional branching (“if...”) and unconditional branching (“go to...”) connecting states. Objects are initially tagged as “unknown”, which would usually be set as the occasion for a stop, in the flow path just mentioned. Objects then acquire a value predetermined before the program run, ranging from -2 (noxious) through 0 (uninteresting) to +2 (very pleasant), which will be taken into account next time the subject comes within perception range of this object.

### 6.3.13 Serotonergic effects in the model

The following is a summary of modelled effects. Much fuller details of how these effects have been modelled are supplied in chapter 7, section 7.3.

#### 5HTR1A receptors

The receptor responds to increased ECF concentration of serotonin; as this rises, a proportionate lowering of the resting potential of pyramidal cells occurs, representing hyperpolarization. If the ECF concentration rises beyond a critical level the receptor in effect becomes blocked, and has no effect on the pyramidal cell.

#### 5HTR1B receptors

This receptor also responds to ambient serotonin; as this rises, the probability that the CCKBC cell will suppress pyramidal firing drops proportionately. This receptor also may be blocked by excessive ambient serotonin.

#### 5HTR3A receptors

Stimulation, notionally from the MRN, increases the probability that the CCKBC cell will suppress firing.

#### 5HTR4 receptors

A rule of the “abs” type (section 3.3) is used to influence LTP and LTD, manifested by increase or decrease of the height of the depolarization ramp.

### 6.3.14 Other points

The **discretization of time** throughout the model uses a time quantum of 0.5 ms. This was chosen as being significantly shorter than the duration of modelled action potentials; for example, the pyramidal cell action potential has a width of 2 ms at its base (fig. 6.2). It is also much shorter than the time required for the initiation and conduction of action potentials, estimated to be in the range of 4 to 10 ms per synapse in the rat hippocampus (Bi and Poo, 1999).

# **Part III**

## **Experimentation and Discussion**

# Chapter 7

## Experimentation

Three sets of experiments are detailed here.

**Section 7.1** demonstrates that the model performs well in simulating basic features of place cell behaviour and of phase precession.

**Section 7.2** demonstrates the model's implementation of the effects of synaptic plasticity in modifying place cell behaviour.

**Section 7.3** explores the behaviour of serotonergic receptor activity in CA1.

### 7.1 Basic features of hippocampal microassembly action

As pointed out in the introduction to chapter 6, any model of neuronal microassembly activity must first be able to successfully demonstrate certain basic known patterns of behaviour, before it can be used predictively for novel situations. The experiments of this section demonstrate basic features of behaviour during place field transit by a rodent, including aspects of phase precession.

#### 7.1.1 Transit of a single place field at constant speed

Fig. 7.1 shows some of the features of model behaviour as the virtual rodent crosses a place field at a constant speed of 15 cm/s. The horizontal axis is a time scale. The top graph represents the postsynaptic potential within the place cell dendrite (blue sawtooth curve). The green bar at the top indicates the theoretical place field, that is, the extent across which the ramp of depolarization (section 2.3.3) is active, so that significant EC stimulation of the pyramidal cell is occurring. The direction of motion is indicated by the rat images. Red vertical arrows indicate instants of place cell firing.

The dotted line at  $-49$  mV is the firing threshold voltage for the place cell. Blue ticks at the bottom of the graph represent the start of cyclical MSDB glutamatergic excitation of OLM cells. The lower graph shows several features, occurring concurrently with the upper graph, both having the same horizontal time scale. Place cell firing is shown as red action potentials. Curves representing firing probability are shown (not to scale) for OLM cells, axo-axonic cells (marked AA), and PVBCs. The amplitude of curves for OLM and AA firing probabilities remains constant, while PVBC amplitude grows as the place field is traversed. A simulated theta LFP curve is also shown. This was not computed by the model like all other curves, but was overlaid for the illustration as a sine wave  $180^\circ$  out of phase with the OLM firing probability curve, this phase relationship being an established experimental finding (see section 2.2.2). It is interesting to note that first place cell firing in each cycle occurs at the peak of this idealized theta LFP curve, then travels down the ascending limb of the curve, ending up at the trough (second last firing burst), which is the expected pattern (O'Keefe and Recce, 1993).

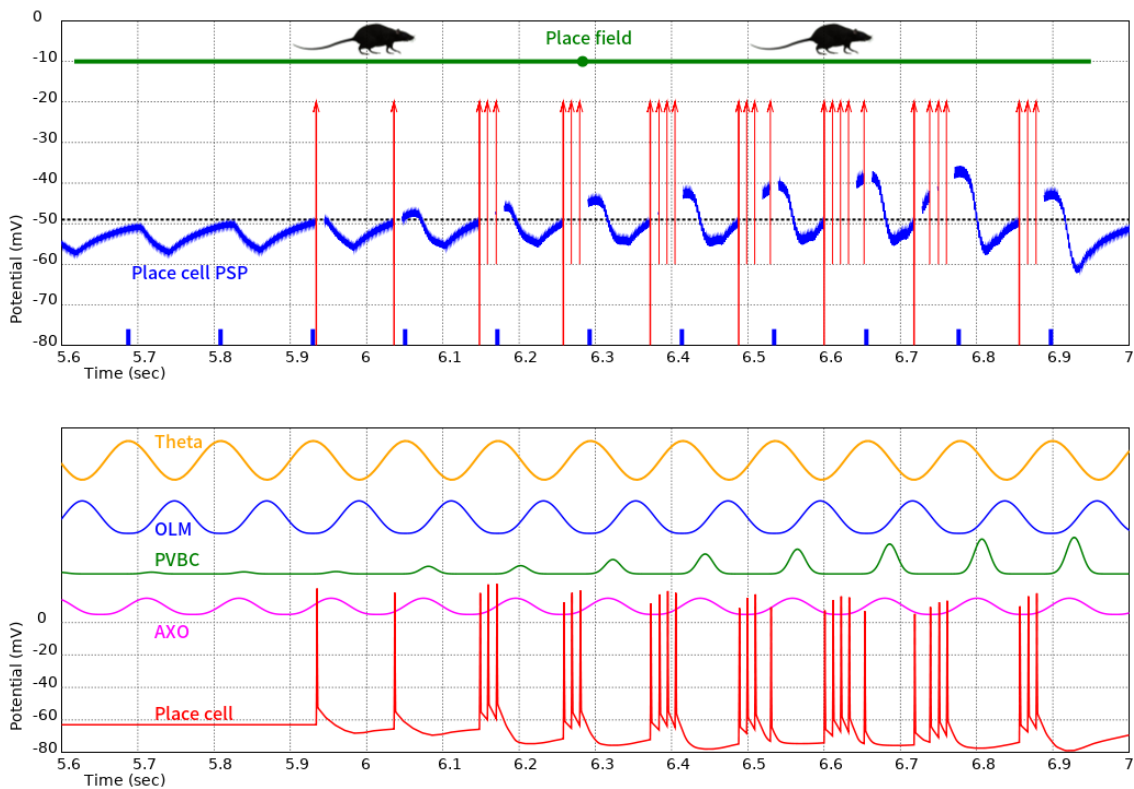


**Figure 7.1:** Graphs generated by the model as a virtual rodent travels across a place field at a constant speed of 15 cm/s. The top graph represents the postsynaptic potential generated in the dendrite by Schaffer collaterals action (direct glutamatergic stimulation along with disynaptic inhibition via SR-IN cells). The lower graph shows place cell output, together with unscaled representations of the firing probabilities of three major interneuron components. Simulated theta is overlaid at the top.

As firing only commences after one quarter of the crossing of the theoretical place field, the experimental place field - as defined by the commencement of firing - is contained within the interval from 5.9 to 6.9 seconds.

The top graph demonstrates phase precession. The vertical arrow representing the first AP of each firing burst is extended to the bottom of the graph, so that its phase relative to the MSDB signal (blue ticks) can be monitored. In this and all subsequent studies, phase is related to the most recent MSDB signal prior to this first AP. This being so, the phase of the first AP of the first burst (at 5.93 sec) is approximately  $+18^\circ$ ; by the eighth burst the first AP (at 6.86 sec) has a phase of  $-173^\circ$ , so that the maximum phase precession in this case is  $191^\circ$ .

The effect of the CCKBC input signal is shown in fig. 7.2. As described in section 6.3.6 the signal is modelled as a reduction in the probability of place cell firing at times when the pyramidal cell is most stimulated. The first CCKBC input cannot occur until a few milliseconds after the pyramidal cell begins to fire (Freund and Katona, 2007). As the membrane time constant of the CCKBC cell is of the order of 25 ms, the effect of the feedback from place cell firing during one theta cycle would be dissipated before the next cycle's firing begins. In fig. 7.2 there are three panels representing the same place field transit as in fig. 7.1, the constant transit speed being the same (15 cm/s). The red line high on each panel shows the probability that the CCKBC signal will suppress any one AP generated by the dendritic input. The central panel has a maximum such probability of 50%, the setting used in most experimental settings and in particular in that used for fig. 7.1. The top panel shows the case where CCKBC influence is absent; bursts are therefore larger. In the bottom panel the CCKBC signal when active completely suppresses firing, resulting in a very large reduction of the size of place cell bursts. The maximum phase shift is the same for all three cases, slightly more than  $180^\circ$ .

### 7.1.2 Features of phase precession at different speeds

Model behaviour was found to be consistent over a wide range of running speeds. To demonstrate this, results have been analysed for transits of a single place field occurring at three different constant running speeds - 5 cm/s, 15 cm/s and 25 cm/s. For each speed the virtual rodent made 100 passes. The location of the place field was perturbed between runs, and a different random seed was used for each run, affecting actual firing where a probability for firing was involved. In the graphs that follow, the experimental place field is used; that is, the place field is viewed as covering the range of actual firing of the place cell, rather than the extent within which the place cell is depolarized above the resting level (“ramp of depolarization”, section 2.3.3). Phase was measured relative to the most recent peak of the OLM firing probability curve, which corresponds approximately to the trough of theta LFP (as indicated in fig. 7.1, lower graph).

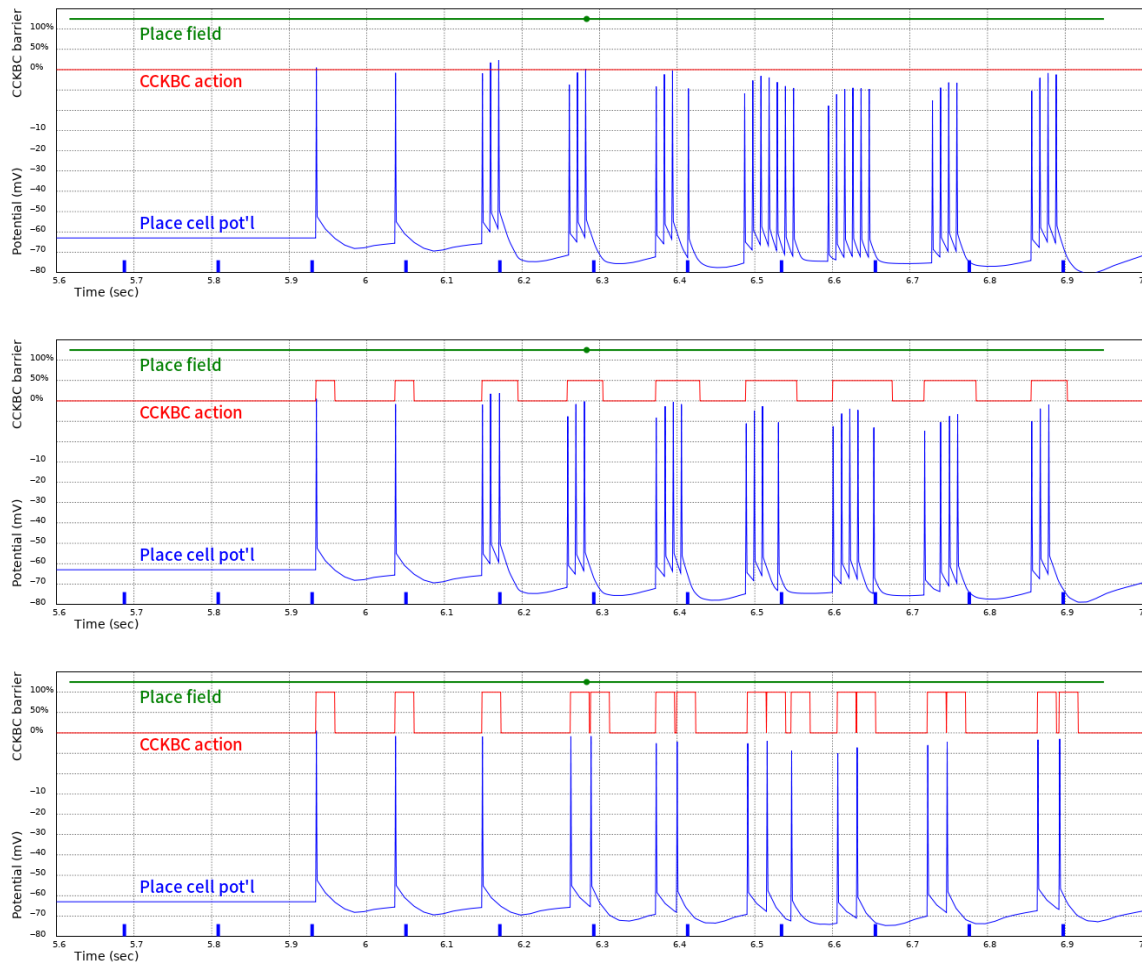


**Figure 7.2:** Demonstration of the effect of modelled CCKBC action on place cell firing. The animal passes through a place field at constant speed 15 cm/s. The upper (red) tracing in each graph represents the probability that the next place cell AP will be prevented. The CCKBC action does not start until the place cell has fired at least once, and ceases soon after the last AP of a burst.

### Rate of phase shift across the place field

Scatter plots of phase v. location within the place field in the consulted literature show a linear trend for phase change until at least the centre of the place field. Subsequently the trend remains linear throughout in plots of Harris et al. 2002 and of Huxter et al. 2003, but in the plots of Mehta et al. 2002 the trend is for a steeper rate of change towards the end of the place field. For all three sources the spread of data around the mean increases towards the end of the place field. The same linear increase of phase precession occurs in the model output (Fig. 7.3), as does the spread of data around the mean in later firing; however the model trends toward a slower rate of phase change towards the end of the place field, deviating from the published data. This suggests that the augmentation of Schaffer collaterals stimulation of the place cell by paired EC-CA3 firing may not increase linearly across the place field (as used for the model), but may instead increase according to a power law - for example, according to a square law - so that the rate of change of augmentation accelerates late in the transit of the

place field.

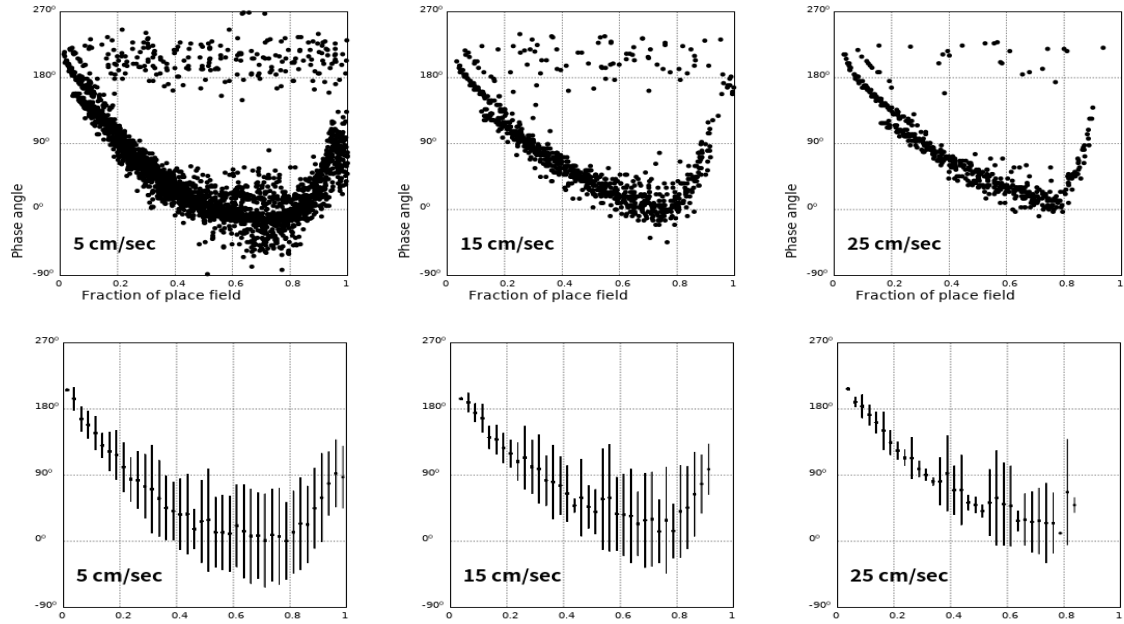


**Figure 7.3:** Plots of the phase of the first AP of a burst v. location within the place field, for different constant speeds. For each speed data was collected from 100 runs across the linear track. Upper graphs are scatter diagrams, lower graphs show the mean phase (large dots) and SD span (vertical lines) for the same data, using a bin width of  $0.025 \times$  place field length.

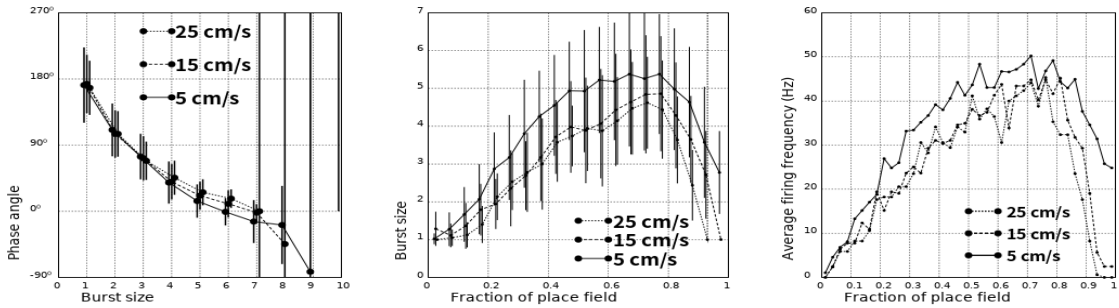
### Average firing frequency across the place field

Fig. 7.4 (Left) correlates increasing size of firing bursts with increasing phase shift, producing a distribution similar to that shown in Harris et al. 2002 (fig. 1d). Fig. 7.4 (Right) indicates a trend for the average firing rate of the place cell to increase as the place field is crossed, until late in the transit. The graph is similar to one published in Mehta et al. 2002 (fig. 3B). Fig. 7.4 (Centre) shows an increase in the number of place cell firings per theta cycle; the shape is similar to that of the above, as would be expected, since the increase in averaging firing rate at some region of the field is a consequence of the increased number of APs that occur in quick succession at that region.

### Established phase precession characteristics demonstrated by the model

The following is a list of published characteristics of phase precession; the results of modelling for each are demonstrated graphically.

- The *total phase precession for a place field transit* ranges between  $100^\circ$  and  $355^\circ$  (O'Keefe and Recce, 1993).
  - Fig. 7.3 illustrates a range consistent with this, across a range of speeds.



**Figure 7.4:** Some features of place cell firing during transit of a place field at three representative constant running speeds. Data was collected from 100 runs for each speed. Vertical lines join points one standard deviation above and below the plotted means. Plots for different speeds are slightly displaced horizontally for the sake of visibility. **Left:** Burst size (the number of action potentials within a single burst) is shown for different degrees of phase precession. **Centre:** Burst size is plotted against relative location in the place field. **Right:** Average firing frequency at particular points in the place field are shown. For each location, a window of  $\pm 0.025$  of the place field width was used for binning action potentials.

- Firing during the place field transit has a *bursting pattern* (O’Keefe and Recce, 1993).
  - Demonstrated in the record of place cell firing in fig. 7.1, and quantified in fig. 7.4.
- Firing as the place field is first entered commences at a *constant phase point* (O’Keefe and Recce, 1993).
  - Demonstrated in the left ends of the scatter plots of fig. 7.3 across different speeds.
- Firing frequency peaks at the centre of the place field (O’Keefe and Recce, 1993) or soon after (Mehta et al., 2002).
  - Demonstrated in fig. 7.4; as in fig. 3b of Mehta et al. 2002, the model shows peaking after the centre of the field.
- Both the phase shift at a particular point and the total phase shift for the place field are independent of speed, even if the animal stops within the place field (Huxter et al., 2003, O’Keefe and Recce, 1993).
  - Confirmed for different speeds for the model in fig. 7.3.
  - Demonstrated for the case where the subject pauses during the place field, in fig. 7.5.

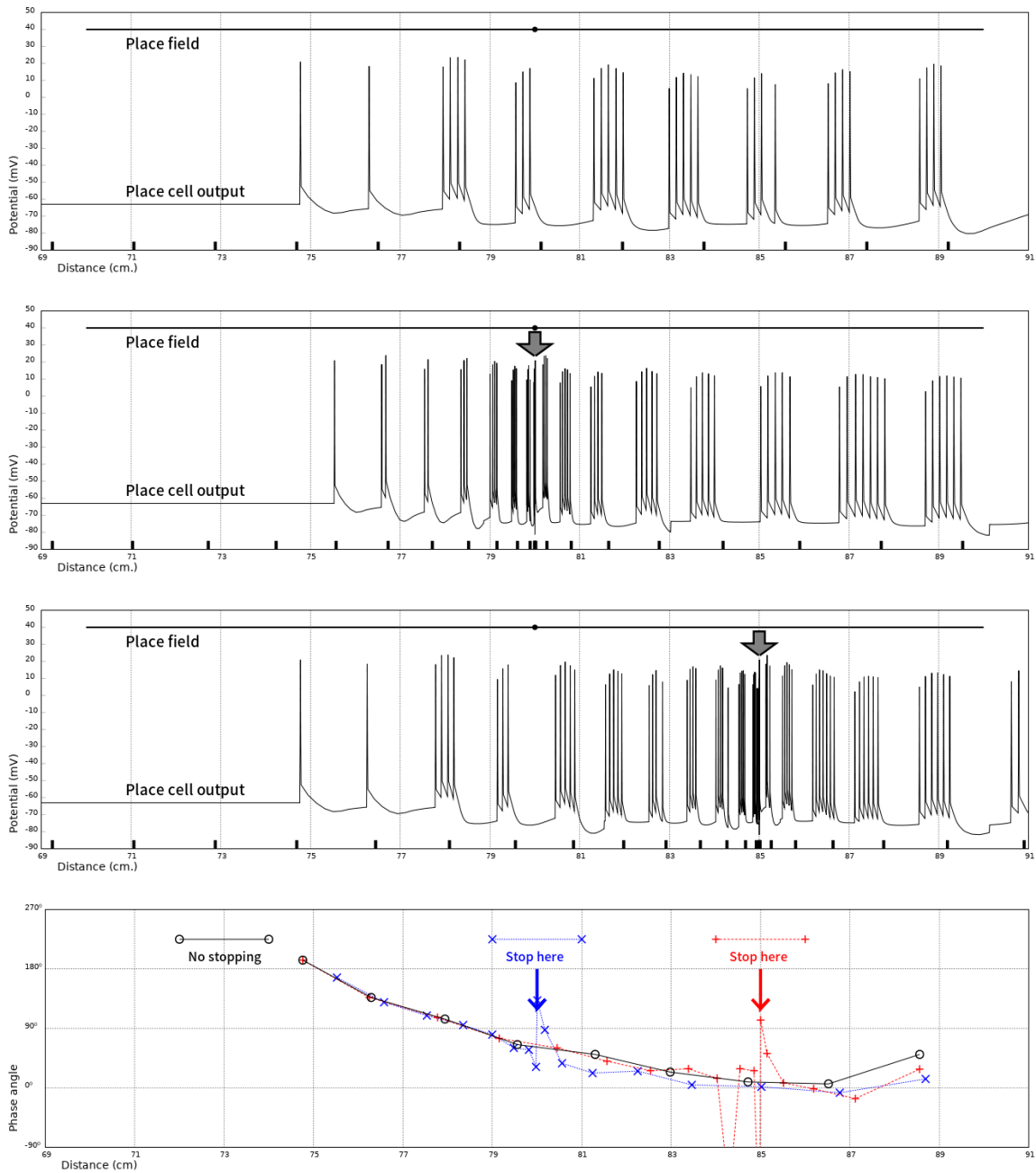


**Figure 7.5:** Graphs of place cell firing v. location, as the subject crosses from left to right. In the top graph, the subject crosses the place field at a constant speed of 15 cm/s; In the second top graph it decelerates from this speed to pause at the point marked by the arrow, halfway through the theoretical place field but early in the experimental place field. In the third graph the pause is later, again as indicated by the arrow. (In both cases the deceleration is approx.  $-11 \text{ cm/s}^2$ ; the pause lasts 1.3 seconds; an acceleration of  $20 \text{ cm/s}^2$  then follows.)

The bottom graph covers the same extent of the runway, and shows the phase of place cell firing bursts for each of the above three cases, coded by colour and point and line shape as indicated. Apart from firing around the actual location of the pause, there is general conformity of phase with position for all three tracings.

## 7.2 Implementation of long-term plasticity

In the absence of a comprehensive mathematical analysis of the processes involved it was necessary to use “trial and error” parameters for the model. These parameters must

produce outcomes which conform to available experimental outcomes. In particular,

- A previously silent cell may become a place cell (as evident by firing at a location) during the first pass through a new place field (Frank et al., 2004, Lee et al., 2012).
- The dependence of place field firing on the depolarization ramp (or “hill” in the quoted article) is indicated by the finding that (a) experimentally depolarizing a silent cell at a location induces a new place field at that location; and (b) experimentally removing the residual depolarization of a place cell eliminates the place field. It was demonstrated that it is the membrane potential, not the experimental current injection, that was responsible (Lee et al., 2012).
- The depolarization at the peak of the ramp ranges up to around 20 mV above the base level for the cell (Bittner et al., 2015, Lee et al., 2012).
- The initial phase of potentiation / depression lasts for about 30 minutes (Volianskis et al., 2013a).
  - This initial potentiation is stable over hours, if the synapse is not disturbed, but resumes its transition to LTP with further synaptic stimulation (Volianskis et al., 2013b).
- Established long-term plasticity is stable after 4 to 6 hours (French et al., 2001, Manahan-Vaughan et al., 2000).
- Stable mapping place field development requires about 5 mins. exposure to a new environment on day 1, and around 10 mins. total exposure (Frank et al., 2004).

These points do not constitute anything like a complete specification for modelling plasticity effects, and therefore a rather heuristic approach must be adopted. I have modelled these effects in the following manner.

The concept of the “ramp of depolarization” was discussed in section 6.3.11 and modelled in its simplest form in the earlier phase precession model (section 5.4). As mentioned there, the height of this ramp is used to calculate an amplifying factor for the combined input to the pyramidal dendrite from direct Schaffer stimulation and disynaptic Schaffer SR-IN inhibition. A distinction is made between place fields which represent geographical markers and place fields representing objects in the environment. In either case, when the subject enters a new environment there is an initial low ramp, just enough to elicit a little firing. In the case of the geographical marker, a single transit of the place field causes a marked rise of the ramp height; subsequent passes raise it to a final level at which it is stable. If, after one or two exposures, the subject is removed from the environment and not able to explore further, the ramp height gradually reduces; a “leakage” factor is built into the model to represent this. Such leakage cannot occur once the ramp height is within a small margin of its final

target level. In the case of objects, the initial ramp height is enough to cause the subject to stop and investigate. Subsequent events depend on the score assigned to the object (from  $-2$  for “very unpleasant”, through  $0$  for “uninteresting”, to  $+2$  for “very pleasant”). If the object is judged uninteresting the peak height lowers - representing long-term depression - to the degree that it is insufficient to evoke a stop as the animal later traverses the region. In the case of a nonzero score, whether positive or negative, the peak height rises, representing long-term potentiation, so that the object will not be ignored at future transits, but will either be the occasion for a stop (if pleasant) or for acceleration past the object (if unpleasant). (The pre-programming or the subject’s behavioural patterns was discussed in section 6.3.12).

The raising or lowering of the peak height (representing putative “learning” or “discounting”) occurs once at each transit, the change in height being proportional to the distance between the present height and the final stable level. There are three such final levels: one for geographical marker place fields, one as a limit for potentiation for “interesting” object fields, and one as a limit for depression for “uninteresting” object fields. (Even in the presence of long-term depression the ramp does not completely disappear, as it must be possible for an uninteresting object to later become “interesting” if it is subsequently found to have changed its value.)

### Implementing the ramp of depolarization

The ramp itself cannot be realized as a simple reduction of the resting membrane potential of the pyramidal cell, as the resting potential is never reached by the membrane potential during place field transit (e.g. fig. 5.1). I have invoked it by varying the weighting of the Schaffer inputs (monosynaptic and disynaptic) to the place cell. This produces a range of depolarization of the order of  $10\text{ mV}$ , consistent with information displayed in sources mentioned in section 2.3.3. It also provides an intracellular theta with an amplitude of the order of  $10\text{ mV}$  (though I note that this is about twice the amplitude reported in Ylinen et al. 1995).

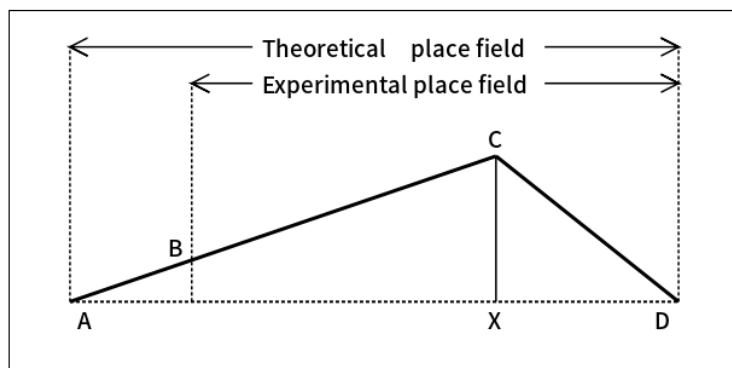


**Figure 7.6:** Sketch of depolarization ramp.

A sketch of the features of the ramp is shown in fig. 7.6. The concepts of theoretical place field and experimental place field were mentioned in section 6.3.11; in the figure,

point A represents the start of the theoretical place field (the start of the ramp, representing early increase of cell membrane potential) and B the start of the experimental place field (the point at which the first place cell firing occurs). The peak occurs at C, most of the way through the place field, and CX is the peak height.

The following is a list of parameters and procedures used to manipulate the depolarization ramp, developed as mentioned on a heuristic basis, to provide a model performance consistent with the bulleted list earlier in this section.

- *Peak heights*: A dynamic array, with one element per place field, stores the current height of each field's ramp.
- *Initial peak*: When the subject first enters an unexplored arena, all ramps in all potential place fields take this value, currently set at 0.2. This value is sufficiently high for the animal to notionally perceive the mapping point or object. (How the animal reacts to that perception is decided by the program function described in section 6.3.12.)
- *Peak level for established mapping place fields*: 0.4. Notional LTP will move a place field's peak height towards this asymptotic value.
- *Peak limits for object place fields*: Minimum height is 0.15; this results from notional LTD, and represents a level which is not perceived by the animal, but remains as a place field marker; in the event of a change in the object's value, it could be subject to LTP and so return to prominence. The maximum height is 0.3.
- *Peak jump factor*: At the end of the transit of a place field, the peak height is incremented by this fraction of the gap between the current peak height and the target peak height. The current value of the peak jump factor is 0.3. For example, if the place field is a newly discovered mapping feature, the peak will increase from the initial value of 0.2 (see above) by an increment equal to 0.3 times the difference ( $0.4 - 0.2$ ); that is, the new peak height will be 0.26.
- *Latches, and Leakage time constant*: The early stages of potentiation and depression are transient and easily reversed (Lee et al., 2012). At around 5 hours, newly activated genes and newly generated intracellular proteins have produced a non-volatile cellular memory. I have modelled the transience by a 'leakage' time constant, which would realistically be set to 1 or 2 hours, but in my experimenting was set to a much shorter value, the flow of experimental time being notionally speeded up. the actual value does not affect modelled outcomes, as long as it is much longer than the duration of a lap of the arena.  
The 'latches' are values set at 0.02 short of the targetted final peak heights. Once peak movements have reached this close to the targetted value they are no longer subject to the 'leakage' just mentioned; the time constant for a real time situa-

tion would be such that, in the case of LTP, this latch level would be reached at around 5 hours.

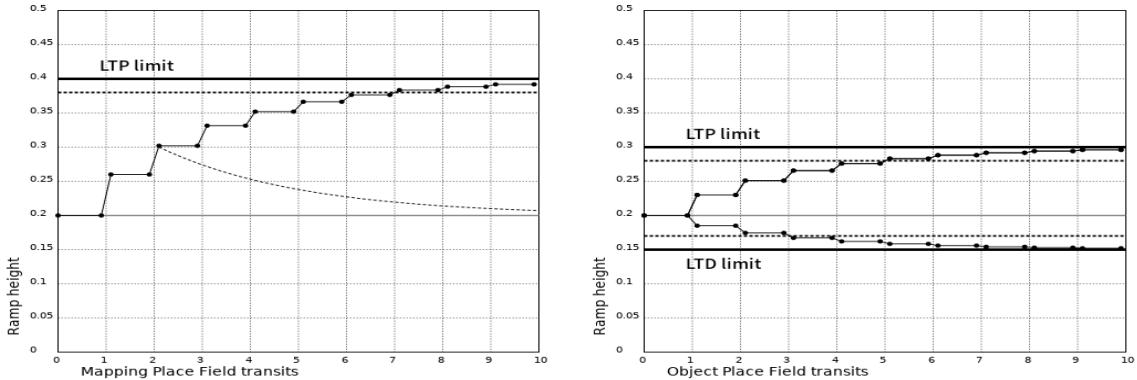


**Figure 7.7:** The **left graph** represents changes to the ramp height as a consequence of successive transits of a mapping place field in an unexplored environment. At each transit the ramp height increases, until close to the asymptotic value for LTP. An alternative situation is indicated by the dotted line; after the second pass the animal leaves the environment; the ramp height decays exponentially till approximately back to the initial value; if re-entering the environment then, the subject would have to explore to re-establish the place field. Leakage cannot happen once the ramp height has risen above the dashed line lying just below the LTP asymptote.

The **right graph** represents similar changes, this time for an object place field. Two paths are shown, one leading to LTP (the object was found to be interesting - whether pleasantly or unpleasantly so) and one to LTD (the object was uninteresting). Exponential decay of ramp height back to the starting level is possible for both LTP and LTD, but is not drawn.

A diagrammatic representation of these processes is shown in fig. 7.7. In fig. 7.8, a situation is portrayed where an animal enters a new arena, explores two locations, one of which is destined to be a mapping place field, the other will be a place field associated with an object at that location. The figure shows place cell output potentials. The animal stops at both locations initially; the object is found to be uninteresting, so LTD operates, discounting the object, as demonstrated by the low firing frequency within the place field by the eighth transit. Meanwhile the mapping place field undergoes potentiation.

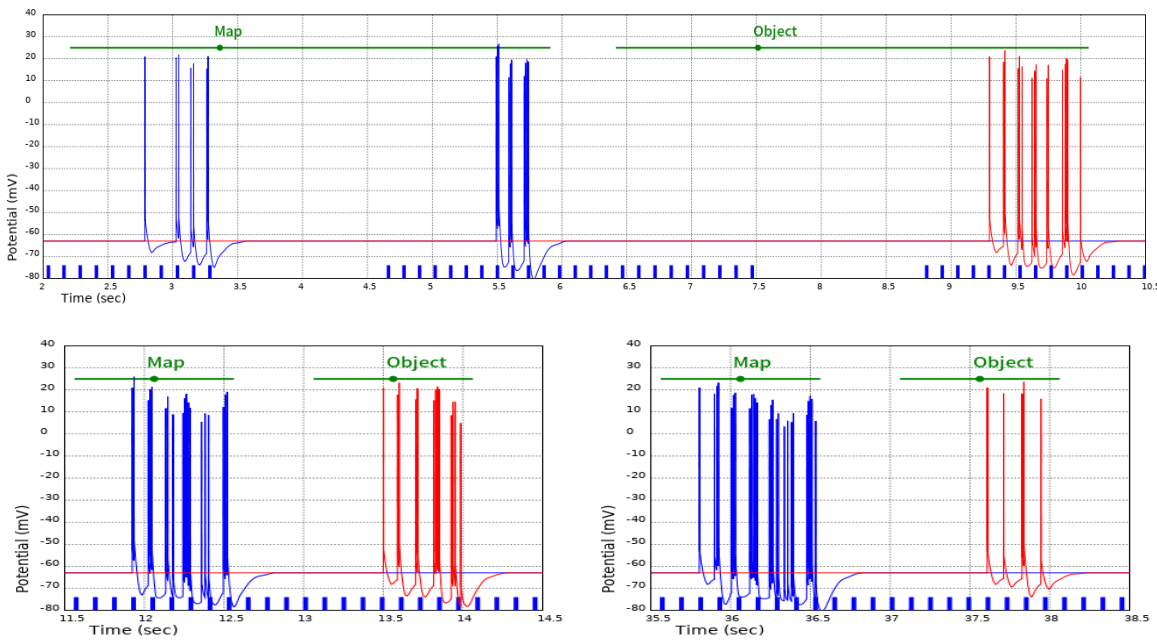


**Figure 7.8:** The **upper graph** shows two place fields, one representing a new geographical feature (marked “Map”) and one representing a new object. As this is the first run, the subject stops to explore each. The horizontal axis is scaled in terms of time, not distance; while the subject is stopped the MSDB theta-stimulating signal (blue ticks at the bottom of the graph) ceases. Some firing occurs in both fields. The **lower left graph** is the second pass through both fields. The subject does not stop at the object because it was found to be uninteresting at the first pass. Both fields still have strong firing. The **lower right graph** is at the eighth pass through the two fields. The mapping place field is fully established in response to long-term potentiation, but firing at the object’s place field is weak as a result of long-term depression.

## 7.3 Modelling serotonergic effects in CA1

The first three experiments demonstrate the modelling of basic features of MSDB and serotonergic action in the CA1 region. Section 7.3.4 seeks to break new ground by eliciting the effects of serotonergic stimulation on phase precession; and section 7.3.5 examines what responses might be expected in the CA1 region from the administration of SSRIs.

### 7.3.1 MRN phasic signal to CCKBC and MSDB

Recently induced context fear memories are retrieved when the animal perceives that it is at a place associated with past painful experience. The retrieval involves many centres, including the hippocampus, retrosplenial cortex, perirhinal cortex, postrhinal cortex and the amygdala, which in particular is able to drive freezing behaviour even in the absence of the hippocampus (Wiltgen and Tanaka, 2013). The freezing response also involves many centres, including the MRN, in which corticotropin-releasing hormone receptors stimulate serotonin release in the hippocampus (Ohmura et al., 2010). The model is able to demonstrate two consequences of sudden phasic stimulation of CA1 by MSDB projections. The immediate reaction, mediated by fast-acting co-expressed glutamatergic and 5HTR3A receptors in CCKBC interneurons, is to suppress place cell firing, while some milliseconds later the transmission of the theta rhythm from MSDB to CA1 ceases. These two actions are demonstrated in fig. 7.9.

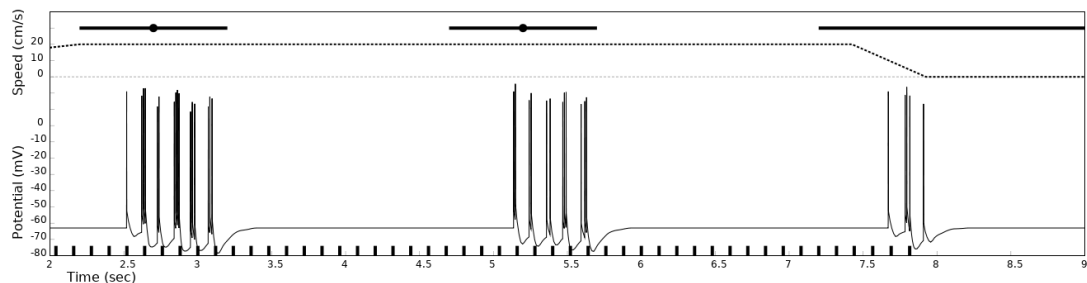


**Figure 7.9:** The animal runs through a known environment with three place fields displayed (indicated by bars at the top of the graph). The dotted lines at the top of the graph show the speed of the animal v. time. The lower curve records the firing of place cells, and the ticks at the bottom of the graph represent the start of MSDB glutamatergic stimulation of OLM cells. As the subject perceives the third place field a fear memory is activated and a “freeze” reaction set in motion. A phasic signal from MRN first activates CCKBC cells, causing a large reduction in pyramidal firing at the edge of the third place field; a few milliseconds later the theta rhythm stops, as indicated by the absence of ticks at the bottom of the graph by the 8 seconds mark.

### 7.3.2 Increased tonic action of serotonin

The 5HT<sub>1</sub> receptors are both highly sensitive to ambient serotonin. In the presence of increased serotonin they function together to ensure a steady reduction of place cell activity. The 5HT<sub>1A</sub> receptor hyperpolarizes the pyramidal cell so that it fires less often during place field transits; activation of the 5HT<sub>1B</sub> receptor inhibits feedback from the pyramidal cell to the CCKBC cell, so that there is less inhibition by the CCKBC of the pyramidal cell. This action counterbalances the 5HT<sub>1A</sub> effect, to give a smoother control of pyramidal firing. This is illustrated in fig. 7.10, where the activation of 5HT<sub>1A</sub> receptors both with and without the concurrent activation of 5HT<sub>1B</sub> receptors is demonstrated.

The effect of 5HT<sub>1A</sub> is modelled as follows. A parameter that represents normalized serotonin concentration is set to 1 for operation under normal circumstances, and can rise to 2 (which it does for fig. 7.10). The increase is multiplied by  $-1.5\text{ mV}$ , and added to the original place cell resting voltage to produce hyperpolarization. These are trial-and-error values in the absence of specific experimental data. The concomitant 5HT<sub>1B</sub> effect is obtained by modifying whatever is the current probability that a potential place cell firing will be blocked, representing CCKBC action. This probability can range from 0% to 100%, as shown in fig. 7.2. This probability is divided by the normalized serotonin concentration, so that the increase of serotonin concentration from 1 to 2 results in halving of the probability that CCKBC will block a place cell firing.

### 7.3.3 Effects of 5HT<sub>4</sub> stimulation and inhibition

The 5HT<sub>4</sub> receptor's unique effects in facilitation both LTP and LTD were described in section 3.3. The receptor is required to respond quickly to phasic stimulation, as it must facilitate LTP when the animal is passing through a place field that needs to be salient, and seconds later be able to facilitate LTD as the animal passes an object that is known and considered uninteresting. The modelling of LTP and LTD has already been described in detail (section 7.2). The 5HT<sub>4</sub> effect on these processes was as follows. Three states only were allowed: (1) Normal receptor activity (no effect). (2) Weak receptor expression (the peak jump described in section 3.3 was reduced from the normal value of 0.3 to 0.2, resulting in smaller steps of potentiation with place field transits). (3) Receptor agonist applied (only LTP occurs, for all objects).

The three possibilities are demonstrated in the three place cell output graphs of fig. 7.11. In each case the animal explores two new objects, one of which it finds to be uninteresting (so to be ignored in future), and one noxious (so to be actively noticed in future, so that it can be avoided by running past as fast as possible). The top graph represents events where the 5HT<sub>4</sub> receptor is normally expressed; the uninteresting

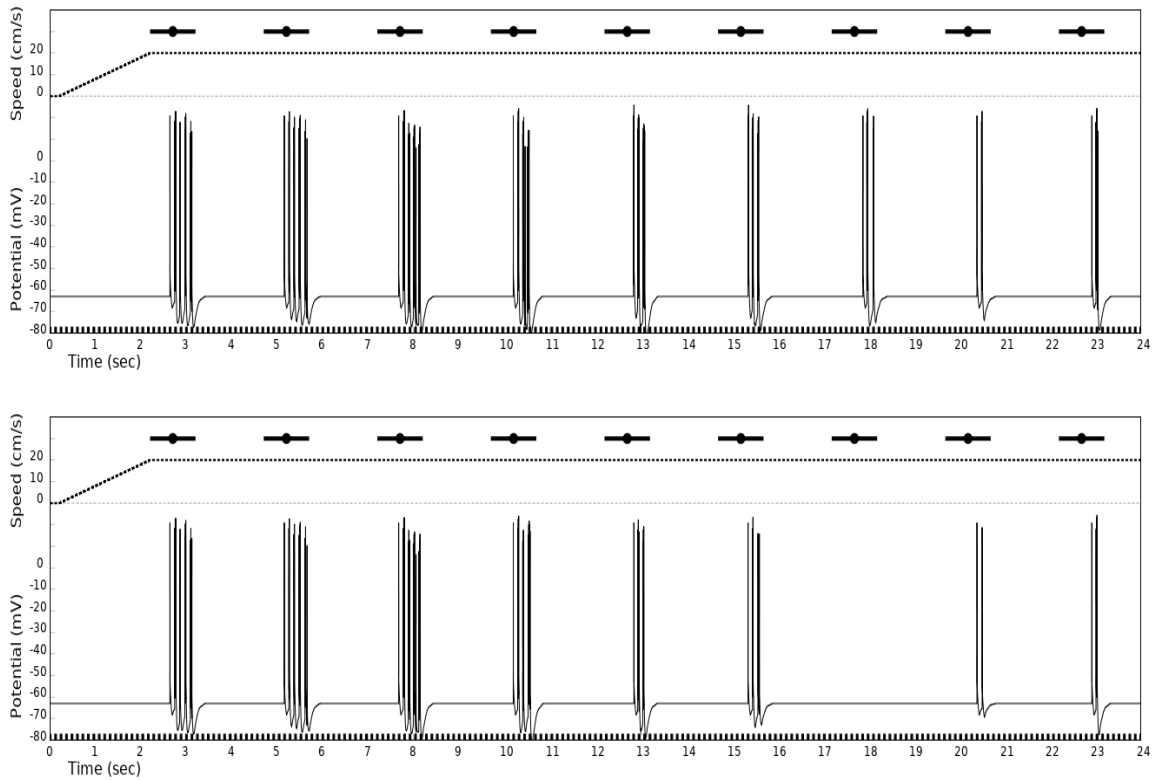


**Figure 7.10:** The subject crosses the same known place field eight times. The serotonin ECF concentration begins to rise at a constant rate after the third transit until a plateau level is reached after the sixth transit. The upper graph is the result of activation of both 5HTR1A and 5HTR1B receptors; in the lower graph only the 5HTR1A is allowed to react to the raised serotonin level. The final level of firing is the same in both cases, but the transition to that level is much smoother when 5HTR1B receptors are active.

object evokes steadily less firing as LTD is induced, while the interesting object evokes stronger firing, as LTP is induced. The middle graph represents the case where 5HTR4 expression is weak; both LTP and LTD still occur as before, but at a reduced rate. The bottom graph represents full-on 5HTR4 expression, as induced experimentally by an agonist; only LTP occurs. As a result, discounting of salience for the uninteresting object is not possible, and the rat will continue to investigate it.

Another action of strong 5HTR4 firing is illustrated in the bottom graph of fig. 7.11. It was mentioned in section 3.3 that the receptor acts to reduce the afterhyperpolarization period of a pyramidal action potential, thus reducing spike frequency adaptation; the result is a more conformed and unambiguous signal downstream to the subiculum and ultimately to the cortex. The more level bursts of place cell firing are more apparent in the bottom graph.

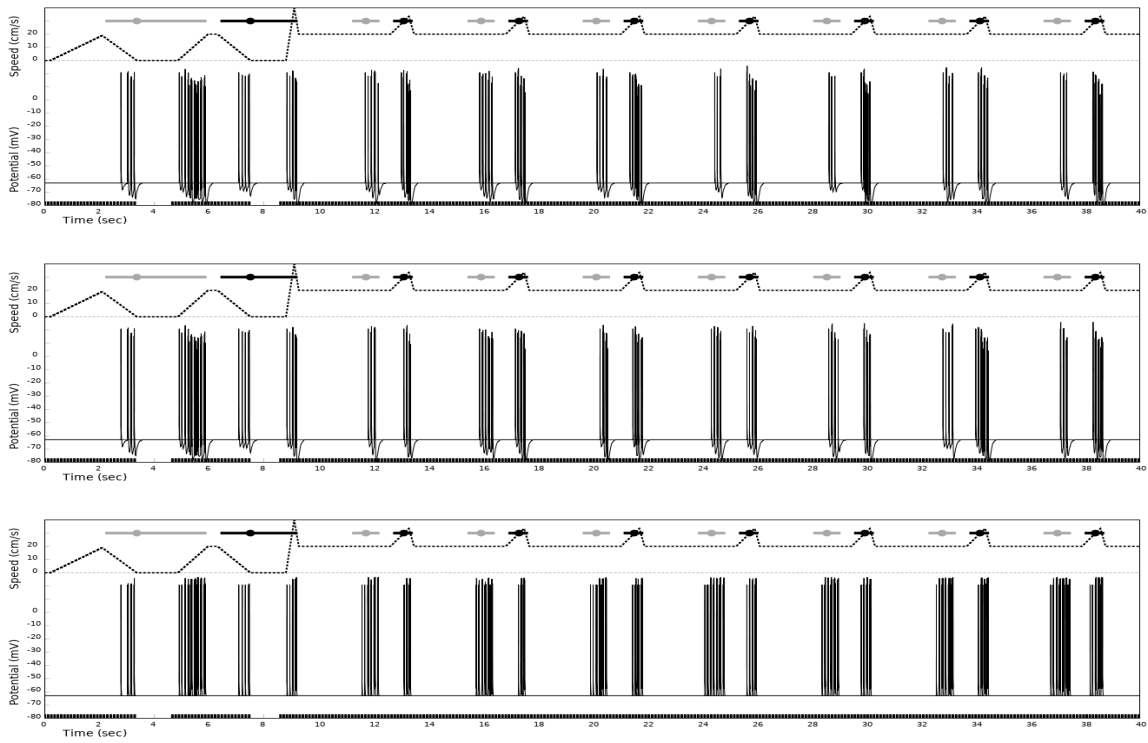


**Figure 7.11:** In each of the three graphs the subject makes eight transits through a circuit which contains two new objects, both explored on the first transit. Their place fields are represented by the top bars - grey for the first object, which proves to be unworthy of attention; black for the second object, which turns out to be noxious. On subsequent transits the subject will ignore the ‘grey object’ but will increase its awareness of the ‘black object’, which must be avoided (represented by an increase in speed, to get out of its reach). Running speed is indicated by the dotted line at the top of the graph. The **upper graph** shows the normative situation: LTP gradually occurs for the unpleasant object, as indicated by increasing place cell firing during place field transits; but LTD occurs for the uninteresting one, as shown by decreased place cell firing. The **middle graph** shows events when 5HTR4 expression is weak; both LTP and LTD proceed slowly. The **lower graph** represents full 5HTR4 activity, as when a receptor agonist is administered. This time only LTP occurs for both objects, and potentiation for both objects occurs faster than for the case of normal receptor expression.

### 7.3.4 Effects on phase precession

The effect of increased ambient serotonin on phase precession was measured for three different situations: (1) normal level of ambient serotonin; (2) doubled level of ambient serotonin, with both 5HTR1A and 5HTR1B responsive; (3) doubled level of ambient serotonin, with 5HTR1B inactivated. In each case the subject traversed a single place field over 100 circuits; code was written to extract the total phase precession for each transit of the place field. The mean and standard deviations were calculated from the three sets of 100 values (table 7.1).

There is only a small decrease in total phase precession in the presence of the higher ambient serotonin, slightly aggravated if 5HTR1B is inactivated. Hence a strong range of phase precession is maintained in the presence of varying serotonin levels.

**Table 7.1:** Effects of ambient serotonin on phase precession

Situation	Mean	SD
Normal serotonin levels	187.5	35.38
High ambient serotonin	172	31.57
High ambient, 5HTR1B inactive	166	33.37

### 7.3.5 Clinical depression and SSRIs

Clinical depression and its treatment by selective serotonin reuptake inhibitors (SSRI) was discussed in section 3.5. The prevailing view has long been that in the depressed state there is reduced serotonergic activity throughout the CNS, and therefore in the HC. SSRIs have been used for two decades to treat clinical depression; a major difficulty with these agents has been that for a small number of weeks there is likely to be no improvement in the depression.

To investigate whether the model can provide any useful information about SSRIs, three scenarios have been modelled. These are:

- *Scenario 1* – The control: Normal responses (normal levels of serotonergic activity, no depression).
- *Scenario 2* – Low serotonergic tonic activity, as is postulated to occur during depression.
- *Scenario 3* – SSRIs have been administered for a short period, not long enough for the antidepressant effect to materialize. Ambient serotonin is high, but MRN projections are inhibited by strong stimulation of 5HTR1A autoreceptors, leading to reduced activity in 5HTR4 receptors. (5HTR3A receptors co-express glutamate, and so remain reactive to glutamatergic input from the MRN.)

The arena for the experiment consists of two place fields, the first being a mapping place field and the second a place field associated with an object. The subject has not explored this arena before. It does five transits of the two place fields. During the first transit of each place field the subject stops to explore. The object proves to be noxious. The subject does not stop again at either field, and in particular accelerates past the object field at each subsequent transit.

Five performance parameters were measured:

- The number of place cell APs per place field transit.
- The number of place cell firing bursts per place field transit.
- The amplitude coherence of bursts (i.e. the degree to which the amplitude varies through a burst of 3 or more APs).
- The degree to which the total APs for a place field transit are grouped into bursts,

rather than occurring haphazardly.

- The height of the ramp of depolarization.

The outcomes of the experiment are displayed in graph form in fig. 7.12. In this figure there are ten graph surfaces; those on the left show performance at the mapping place field, those on the right show performance at the object place field. The five performance parameters are named on the graphs, corresponding from above down with the five items mentioned above. In nearly all graphs there are three curves: a black curve, corresponding to the control scenario; a blue curve, corresponding to scenario 2 above (low serotonergic activity); and a red curve, corresponding to scenario 3 above (early stage of SSRI administration). Each point on each graph is the mean value from five separate runs of the experiment. The larger number of APs shown at transit 1 for all cases is the consequence of the subject stopping at the place field to investigate.

In the case of the mapping place field (left graphs) there is no significant difference between parameters for the control and the “depressed” state (low ambient serotonin), but the early SSRI state results in lower levels of place cell firing and a slow rise of the depolarization peak, both of which would impede formation and recall of memory associated with the physical layout of the arena.

With the object place field (right graphs) there is little difference between the control and the depressed state, except that learning is a little slower in the depressed state (slower rise of the depolarization peak). The early SSRI state on the other hand has much less place cell firing activity, and very slow rise of the depolarization peak; failure to increase salience for the object is likely to lead to accidental rediscovery of its noxious properties.

The coherence parameters in their present form do not appear to be useful; no consistent patterns have emerged from their graphs.

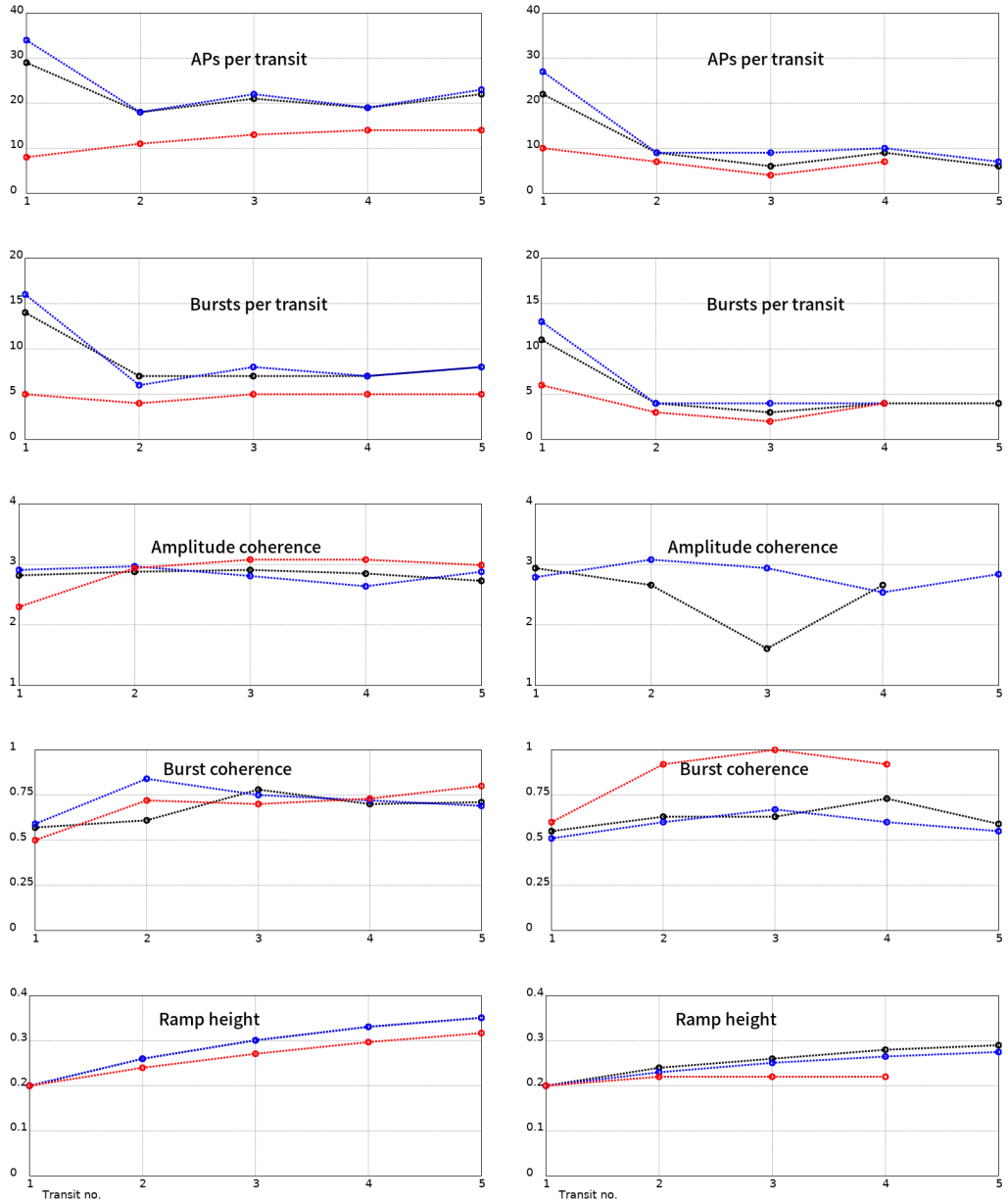


**Figure 7.12:** Measures of performance for three different states associated with SSRI administration. Graphs on the left represent five transits through a mapping place field (horizontal scale: number of the transit). The location is new to the subject. Graphs on the right represent similar transits through a place field that is associated with an object found to be interesting but unpleasant. For all graphs the black curve is the control (no serotonin or SSRI involvement); the blue curve corresponds to a low serotonin state, thought to apply in clinical depression; the red curve corresponds to the acute stage of SSRI administration.

# Chapter 8

## Discussion

The original brief for this project was to design a model of hippocampal function which could be used to demonstrate serotonin-mediated effects. This was intended to be just one component of a much larger model planned by the Department to study serotonergic action throughout the whole limbic system. Unfortunately there was a setback to the time line for that development. In the meantime I have continued with the task in hand. I have limited the scope of the model to the CA1 division of the rodent hippocampus, and in particular to its functioning during rodent navigational activity, as this alone involves complexity enough to match the time and resources available.

### 8.1 A behavioural model?

In a standard electrical connectionist model it is necessary that each component subsystem - usually a neuron, or neuronal compartment - is comprised of the same elements (such as capacitance, conductance, current generators), and that the subsystem's outputs can be calculated accordingly from a knowledge of the parameters and the inputs. It is also necessary to have a full knowledge of the connectivity within the system. This raised major problems for me: (1) there are sizeable gaps in our knowledge of the connectivity between different CA1 interneurons, and between pyramidal cells and interneurons; (2) where we have teased out interconnections there is a paucity of information about the frequency and amplitude of signalling along these interconnections; (3) we often don't have accurate information about the actual numbers of particular cell types associated with, for example, a single pyramidal cell; and (4) some processes cannot be well modelled by direct electrical elements as we lack the necessary knowledge to fit component values to those elements. This is particularly true, for example, of the increase in baseline depolarization of place cells which occurs as a rodent crosses through a place field. We know what happens, but we don't have access to a

mathematically complete model of the processes involved.

In a behavioural model the actual internal structure of the elementary component (or “subsystem”) is not important, as long as the behaviour at its interfacing with other subsystems is valid. This is both liberating and limiting. It is liberating in that one is free to use the best means available to relate values at these interconnections, be it indeed a connectionist model or be it no more than a data-base which can be accessed as a lookup table. On the other hand it is limiting, where for example a data-base is used, in that one cannot drive the subsystem beyond standard operating conditions, because there is no data for unusual circumstances. The intention should be that the behavioural model built on such incomplete information should eventually give way to a more explicit model as knowledge increases.

An analogy from another science is useful to illustrate the point. The astronomer Kepler’s three laws of planetary motion, published in their final form in 1619, were derived from a large data-base of planetary and lunar behaviour. They were empirical laws, with no reference to why the system behaves as it does. Nevertheless as a behavioural model they related observable parameters in ways that enabled better prediction of future positions of planets and moons than did the Copernican system, which had assumed circular orbits. It was not till nearly seventy years later that Isaac Newton demonstrated a firm mathematical basis for planetary motion with his laws of motion and gravity; these laws provided for more accurate astronomical predictions, and so superseded the laws of Kepler for everyday astronomical use.

## 8.2 Modelling theta rhythm

Part three of this thesis begins with a simple demonstration as to how the theta rhythm local field potential (LFP) could develop within the hippocampus as the result of collective place cell firing. Two assumptions were made: (1) that a rhythmical input from the MSDB, by whatever means, evokes the rhythmical firing of CA1 place cells; (2) that phase precession of firing occurs, and can be related to the MSDB input signal. No attempt was made to model mechanisms by which these phenomena occur, this being left to the later models. Many published studies on rodent place cells deal with only a small number of place cells; one could be tempted to think that the total number of place cells operating in any one environment would be tiny. In fact, as explained in section 2.2.3 there are likely to be at least hundreds of place cells active, if not thousands. This model demonstrates that for a population of 1000 place cells the simulated theta LFP is remarkably similar to published traces (fig. 4.2).

The model could not answer the question as to whether the LFP theta itself - as opposed to the MSDB signal - has any independent role in CA1 function. Given its high noise content, its small amplitude (less than half a millivolt), and given the

amount of strong and direct interconnection that otherwise exists between neurons of the region, it is tempting to believe that no such major independent role exists. On the other hand Nature is very opportunistic, and it may be that the LFP does in fact have some role yet to be confirmed. Meanwhile, one could suggest that future studies of events occurring during the theta cycle would be better timed by the MSDB theta signals - both glutamatergic and GABAergic - than by its noisy LFP derivative.

### 8.3 Modelling phase precession

The second model, which was actually a simplified version of the final model, was able to demonstrate the development of phase precession; submitting the model to various different operating conditions provided results consistent with published data from animal experimentation. No interaction between overlapping place fields is necessary for the modelling process, nor any local oscillator to provide a beat frequency. This is not new, as many other models have been successful in this area; but it is important for the final model to be able to reproduce realistic phase precession before being given more complex tasks.

Does phase precession have importance in its own right? The model cannot address this question, but it is highly likely that it is vital as a provider of temporal code to downstream structures. A hypothetical example as to how it could be important is shown in fig. 8.1. The lower part of the figure represents an idealized theta LFP wave, with a set of overlapping place fields overlaid onto it. The arrows at the right end of the diagram indicate a particular moment in time - "Now". At this instant the MSDB glutamatergic signal to the OLM cells has just begun; the MSDB signal is also available in the EC, as elsewhere in subcortical regions. At this instant the burst of APs arriving downstream are from the place field which is just being entered. The remaining place fields have already provided earlier bursts in this theta cycle. Attention is given to this new field for the purpose of memory formation and behaviour modification; then, in my hypothetical example, a shift register effect moves the data along, so that it is still available but removed from immediate salience.

One more point brought out by the modelling of phase precession was that the process generates an intracellular theta rhythm as a by-product; the process would seem to be sufficient in itself for the development of this intracellular theta rhythm.

### 8.4 The final model, and serotonin

The final model involves more components, in particular the perisomatic inhibitors of the CA1 pyramidal cell. A more complete model of phase precession was then possible,

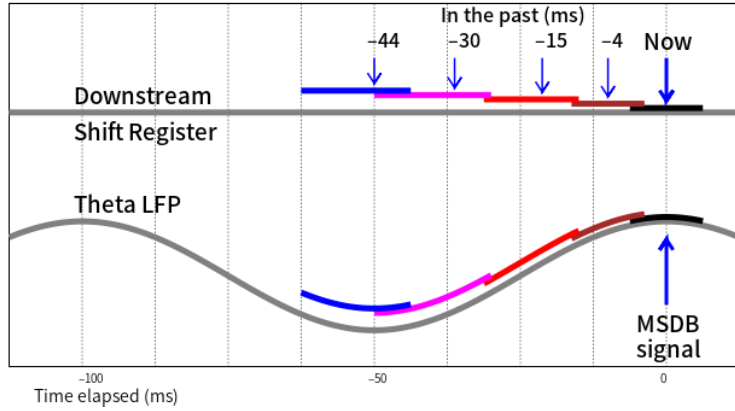


**Figure 8.1:** Representation of how phase precession might function in temporal encoding. The grey sinusoidal curve represents an idealized theta LFP cycle. Coloured extents along the curve correspond to the firing times of successive place fields in this cycle; the rightmost (black) stretch represents a place field just being entered, the leftmost (blue) represents a place field being exited. The present moment is the time labelled “Now”, and corresponds to the time of an MSDB pulse to the HC and EC. At the time of that pulse, a hypothetical shift register, which could be located in the EC, is triggered. The current input at that triggering moment is from the newly entered field, and being current, would require immediate attention. Successive previous inputs have been shifted to the left, still accessible for formation of episodic memory patterns or for behavioural planning.

which was able to demonstrate conformity with a number of published findings. The final model incorporates the effects of plasticity on the ramp of depolarization within place cells, and so is able to model the effects of four major serotonin receptors occurring in the CA1 region.

An interesting finding was made that sheds light on the apparently contradictory actions of the two 5HTR1 receptors. The 5HTR1A receptor inhibits pyramidal cell firing by hyperpolarizing the cell, while the 5HTR1B receptor acts indirectly to increase pyramidal cell firing, by inactivating the positive feed back to its inhibitory CCK basket cell. Both receptors are activated by the same tonic signalling from ambient serotonin. It was demonstrated that this duality actually provides a smooth gradation of pyramidal firing rate in the face of unusually rapid change of tonic signal.

Another pair of opposites is the 5HTR1A inhibitor and the 5HTR4 activator, which are situated in close proximity along the pyramidal dendritic branches. They can be demonstrated in the model to have different and non-interfering roles; the 5HTR1A receptor principally responds to ambient serotonin, much of which comes from blind serotonergic terminals nearby. The 5HTR4 on the other hand must respond rapidly to different situations while navigating, so as to mediate both LTP and LTD in rapid succession during transit of adjacent place fields, acting to strengthen the salience of important features while discounting uninteresting features.

Does serotonin have any effect on phase precession? This was tested under different scenarios corresponding to the involvement of different receptors; the results indicated

no significant effect on the total angle range of phase precession.

Attempts were made to model scenarios associated with clinical depression, and in the early stage of medication with a selective serotonin reuptake inhibitor (SSRI). Some findings were made, as described in section 7.3.5; it appeared that some memory impairment is likely to occur during the acute stage of treatment with an SSRI. However it would be difficult to make strong conclusions from experiments based on the hippocampus alone, as the effects in the hippocampus are greatly overshadowed by actions mediated by the dorsal raphe nucleus (DRN) over a much larger set of subcortical structures. For example, this model cannot demonstrate the anxiety component of the early SSRI treatment stage, as it is the DRN which is associated with panic and fight-or-flight reactions (section 3.2). Even within the realm of median raphe nucleus connectivity, the amygdala cannot be discounted, as it is immensely important in, for example, the induction of freeze reactions. Even within the hippocampus there are different serotonergic effects in other regions, as on neurogenesis in the dentate gyrus. As mentioned earlier, the original and ongoing intention is that a hippocampal model of serotonergic activity will become part of a wider limbic system model under construction.

Several extensions to the model will be needed from this point onwards. First and foremost, it needs to incorporate the activity of SWRs and gamma rhythms, which are vital to the formation of new place fields. This would require further model elaboration to include the CA3 region, dentate gyrus (including neurogenesis) and layers II and III of the entorhinal cortex. As the Department's limbic system develops, it will be necessary to standardize interfacing between models, and transfer of code to a different common language base.

# **Part IV**

## **Appendices**

# Chapter 9

## Appendix A Source code of the model

The model was written in an open source language called “MonoMaths”, originally developed by the author, starting in 2004, during an earlier Masters project requiring special functions; it has been actively maintained and expanded in the intervening years. The underlying computing language is C#, as realized under the Linux operating system using “mono”, which is the open source implementation of Microsoft’s Common Language Infrastructure (.NET). The site for the language is  
<https://github.com/allanjrw/MonoMaths>

The complete code for the model is available online at  
<http://www.samuelallan.info/Thesis/>  
(as file name “HC Model 2.txt”).

A brief summary of program flow is shown in fig. 9.1 below.

## PROGRAM OUTLINE

### Set parameters

Movement (e.g. cruising and maximum speed, max. acceleration)

Arena (e.g. circuit length, no. and locations of place fields, place field width)

Depolarization ramp features (e.g. starting ramp height, location of ramp peak)

Plasticity parameters (factors controlling variation in depolarization ramp height)

Assembly description (no. and type of neurons per assembly; no. assemblies = no. place fields).

Firing unit features (threshold V, peak amplitude, refractory period)

(Certain synapses are also regarded as 'firing units' for ease of processing, the 'firing' resulting in an EPSP / IPSP into the host neuron.)

Timing, wrt MSDB signal, of firing probability curves for most interneurons.

### Set up major data structures

Connection features

(contained in a matrix, "Distributor", which details source and destination, weighting of connection, transmission delay. In the absence of specific information, delays are mostly set at 0.5 ms, except for SR-IN GABAergic synapses onto CA1 pyramidal, where the delay is 4.5 ms.)

Data collection structure (matrix, "Register", which collects all input and output data throughout the run, together with other dynamic parameter values, all saved to disk for later analysis).

### Run loop iterating over intervals of 0.5 ms (experimental time).

Update current location, current speed, location of rat wrt all place fields.

Involves calling a behaviour function, which mimics the rat's responses to stimuli; e.g. the rat slows down to investigate at an unknown object, and according to whether it proves noxious, uninteresting or rewarding, will respond in an appropriate manner. The set of responses can be written for each set of experiments more or less like a simple program, with conditional statements and 'goto' jumps possible.

Update displays (two graphs: rat location v. time, rat speed v. time).

Calculate weightings of SR-IN and Schaffer inputs to place cells, based on current levels of depolarization ramps in all place fields.

Calculate weighting for PVBC EPSPs, increasing with transit through place field.

Update perisomatic interneuron firing probabilities a/c to stage of theta cycle.

Carry out convolution of CA3 and OLM inputs to SR-IN, one theta cycle at a time.

Check input sums for all firing units, and prepare to fire those exceeding threshold. If pyramidal due to fire, apply perisomatic inhibitory probabilities to possibly prevent the firing.

Fire units

Distribute outputs from units that fired, in accordance with matrix "Distributor".

Update "Register" (The Register is saved progressively to disk in blocks in time units of 0.5 secs, as it can be very large; only a portion of it is in working memory at any one time.)

End of run loop

**Display ± store run stats.**

Figure 9.1

# Chapter 10

## Appendix B Parameters for the model

Parameters are listed in approximately the order in which they appear in the program code. Names in bracketted italics are identifiers used in the program code. (*MonoMaths* optionally allows Greek letters in identifiers.) Section references hold details relevant to the choice of parameter value. Only those which are fixed for a particular run are mentioned; dynamic variables are not listed.

**Time quantum** ( $\delta t$ ) - 0.5 ms (section 6.3.14).

**Theta frequency at zero rat speed** ( $MSDBBaseFreq$ ): 8 Hz (section 2.2.2).

**Increment of frequency wrt speed** ( $\delta f_{\delta v}$ ): 1/60 (section 2.2.2).

**Maximum rat speed** ( $MaximumSpeed$ ) = 40 cm/s (based on refs. used in section 2.2.2).

**Maximum rat acceleration** ( $MaximumAccel$ ) = 30 cm/s<sup>2</sup> (no literature source; but exact value does not materially affect program findings).

**Resting potential for pyramidal**s ( $RestingV$ ) = -63 mv (section 6.3.2).

**Threshold potentials for pyramidal**s ( $ThresholdV$ ) = -49 mv (section 6.3.2).

**Width of place field** ( $FieldWidth$ ) – various; I typically used 20 cm. (Figures for rats from literature: approx. 20 to 80 cm, mean around 30 cm - O’Keefe and Recce 1993; approx. 20 to 100 cm - Dragoi and Buzsáki 2017; approx. 15 to 50 cm - Lee et al. 2012).

**Perception range** ( $PerceptionRange$ ) - 2 cm. before the place field. (Taken as the stage at which the rat perceives the next object, in the case of a field associated with an object. Used to determine the rat’s reaction - e.g. to accelerate past, if it is a noxious object; to stop and sample, if it is a new object; to stop and enjoy longer, if it is a known pleasant object. No value obtainable from literature consulted.)

### Weights for interconnections

These were assigned on a trial-and-error basis. No weightings are critical; gradual shifts

in weightings produce gradual changes in model behaviour. (A design principle, kept in mind throughout program construction, and causing the rejection of early approaches, was that no parameter must be so critical that small changes in its value result in major changes in model behaviour.)

*CA3 pyramidal output to CA1 glutamatergic synapse:* weighting = 0.3 (chosen such that a single CA3 AP would evoke an EPSP in the CA1 pyramidal).

*CA3 pyramidal output to SR-IN:* weighting = 0.3 (in parity with the above, with no firm basis other than convenience).

*CA1 Glutamatergic synapse to CA1 dendrite* = 0.19 (Such that a CA3 AP, after multiplication by this and the preceding weightings together, would provide a reasonable level of intracellular theta rhythm amplitude, when combined with the following:)

*SR-IN GABAergic synapse to CA1 dendrite* = -0.095 (i.e. the negative of exactly half of the above weighting, so that the IPSP of the SR-IN has an absolute value of half of the EPSP of the glutamatergic input, as described in section 5.2. The SR-IN IPSP also experiences a 4 ms delay relative to the glutamatergic EPSP - see fig. 5.1.)

# Bibliography

- Ahumada, J., de Sevilla, D. F., Couve, A., Buño, W., and Fuenzalida, M. (2013). Long-term depression of inhibitory synaptic transmission induced by spike-timing dependent plasticity requires coactivation of endocannabinoid and muscarinic receptors. *Hippocampus*, 23(12):1439–1452.
- Akiskal, H. S. and Akiskal, K. K. (2007). A mixed state core for melancholia: an exploration in history, art and clinical science. *Acta Psychiatrica Scandinavica*, 115:44–49.
- Ali, A. B., Deuchars, J., Pawelzik, H., and Thomson, A. M. (1998). Ca1 pyramidal to basket and bistratified cell epsps: dual intracellular recordings in rat hippocampal slices. *The Journal of Physiology*, 507(1):201–217.
- Alkondon, M., Pereira, E. F. R., and Albuquerque, E. X. (2003). Nmda and ampa receptors contribute to the nicotinic cholinergic excitation of ca1 interneurons in the rat hippocampus. *Journal of Neurophysiology*, 90(3):1613–1625.
- Alkondon, M., Pereira, E. F. R., and Albuquerque, E. X. (2011). Endogenous activation of nachrs and nmda receptors contributes to the excitability of ca1 stratum radiatum interneurons in rat hippocampal slices: Effects of kynurenic acid. *Biochemical Pharmacology*, 82(8):842–851.
- Allers, K. A. and Sharp, T. (2003). Neurochemical and anatomical identification of fast- and slow-firing neurones in the rat dorsal raphe nucleus using juxtacellular labelling methods in vivo. *Neuroscience*, 122(1):193–204.
- Andersen, P., Bland, H. B., Myhrer, T., and Schwartzkroin, P. A. (1979). Septo-hippocampal pathway necessary for dentate theta production. *Brain Research*, 165(1):13–22.
- Andrade, T. G. G., Zangrossi, H., and Graeff, F. G. (2013). The median raphe nucleus in anxiety revisited. *Journal of psychopharmacology (Oxford, England)*, 27(12):1107–1115.
- Andrews, P. W., Bharwani, A., Lee, K. R., Fox, M., and Thomson, J. A. (2015). Is serotonin an upper or a downer? the evolution of the serotonergic system and its role in depression and the antidepressant response. *Neuroscience & Biobehavioral Reviews*, 51:164–188.

- Antic, S. D., Zhou, W., Moore, A. R., Short, S. M., and Ikonomu, K. D. (2010). The decade of the dendritic nmda spike. *Journal of Neuroscience Research*, 88:2991–3001.
- Armstrong, C., Krook-Magnuson, E., and Soltesz, I. (2012). Neurogliaform and ivy cells: A major family of nnos expressing gabaergic neurons. *Frontiers in Neural Circuits*, 6.
- Armstrong, C. and Soltesz, I. (2012). Basket cell dichotomy in microcircuit function. *The Journal of Physiology*, 590(4):683–694.
- Artola, A., Bröcher, S., and Singer, W. (1990). Different voltage-dependent thresholds for inducing long-term depression and long-term potentiation in slices of rat visual cortex. *Nature*, 347:69–72.
- Artola, A. and Singer, W. (1993). Long-term depression of excitatory synaptic transmission and its relationship to long-term potentiation. *Trends in Neurosciences*, 16(11):480–487.
- Ascher, P. and Nowak, L. (1987). Electrophysiological studies of nmda receptors. *Trends in Neurosciences*, 10(7):284–288.
- Ascoli, G. A. (2008). Petilla terminology: nomenclature of features of gabaergic interneurons of the cerebral cortex. *Nature Reviews Neuroscience*, 9(7):557–568.
- Barnes, N. M. and Sharp, T. (1999). A review of central 5-HT receptors and their function. *Neuropharmacology*, 38(8):1083–1152.
- Bartley, A. F. and Dobrunz, L. E. (2015). Short-term plasticity regulates the excitation/inhibition ratio and the temporal window for spike integration in ca1 pyramidal cells. *Eur J Neurosci*, 41(11):1402–1415.
- Bartus, K., Pigott, B., and Garthwaite, J. (2013). Cellular targets of nitric oxide in the hippocampus. *PloS one*, 8(2).
- Baude, A., Bleasdale, C., Dalezios, Y., Somogyi, P., and Klausberger, T. (2007). Immunoreactivity for the gabaa receptor alpha1 subunit, somatostatin and connexin36 distinguishes axoaxonic, basket, and bistratified interneurons of the rat hippocampus. *Cerebral cortex (New York, N.Y. : 1991)*, 17(9):2094–2107.
- Berumen, L. C., Rodríguez, A., Miledi, R., and García-Alcocer, G. (2012). Serotonin receptors in hippocampus. *The Scientific World Journal*, 2012:1–15.
- Bezaire, M. J. and Soltesz, I. (2013). Quantitative assessment of ca1 local circuits: Knowledge base for interneuron-pyramidal cell connectivity. *Hippocampus*, 23(9):751–785.
- Bi, G.-q. and Poo, M.-m. (1999). Distributed synaptic modification in neural networks induced by patterned stimulation. *Nature*, 401(6755):792–796.

- Bi, G. Q. and Poo, M. M. (2001). Synaptic modification by correlated activity: Hebb's postulate revisited. *Annual Review of Neuroscience*, 24(1):139–166.
- Bittner, K. C., Grienberger, C., Vaidya, S. P., Milstein, A. D., and Macklin, J. J. (2015). Conjunctive input processing drives feature selectivity in hippocampal ca1 neurons. *Nature Neuroscience*, 18:1133–1142.
- Blair, H. T., Gupta, K., and Zhang, K. (2008). Conversion of a phase- to a rate-coded position signal by a three-stage model of theta cells, grid cells, and place cells. *Hippocampus*, 18(12):1239–1255.
- Bland, B. (1998). Anatomical, electrophysiological and pharmacological studies of ascending brainstem hippocampal synchronizing pathways. *Neuroscience & Behavioral Reviews*, 22(2):259–273.
- Bland, B. H. and Oddie, S. D. (2001). Theta band oscillation and synchrony in the hippocampal formation and associated structures: the case for its role in sensorimotor integration. *Behavioural Brain Research*, 127(1-2):119–136.
- Blier, P. and de Montigny, C. (1999). Serotonin and drug-induced therapeutic responses in major depression, obsessivecompulsive and panic disorders. *Neuropsychopharmacology*, 21:91S–98S.
- Bliss, T. V. P. and Lømo, T. (1973). Long-lasting potentiation of synaptic transmission in the dentate area of the anaesthetized rabbit following stimulation of the perforant path. *The Journal of Physiology*, 232(2):331–356.
- Bockaert, J., Claeysen, S., Compan, V., and Dumuis, A. (2008). 5-HT<sub>4</sub> receptors: History, molecular pharmacology and brain functions. *Neuropharmacology*, 55(6):922–931.
- Bombardi, C. and Di Giovanni, G. (2013). Functional anatomy of 5-HT<sub>2A</sub> receptors in the amygdala and hippocampal complex: relevance to memory functions. *Experimental brain research*, 230(4):427–439.
- Borhegyi, Z., Varga, V., Szilágyi, N., Fabo, D., and Freund, T. F. (2004). Phase segregation of medial septal gabaergic neurons during hippocampal theta activity. *The Journal of neuroscience : the official journal of the Society for Neuroscience*, 24(39):8470–8479.
- Bouwman, B. M., Lier, H. V., Nitert, H. E. J., Dringenburg, W. H. I. M., Coenen, A. M. L., and Rijn, C. M. V. (2005). The relationship between hippocampal EEG theta activity and locomotor behaviour in freely moving rats: effects of vigabatrin. *Brain Research Bulletin*, 64(6):505–509.
- Bragin, A., Jando, G., Nadasdy, Z., Hetke, J., Wise, K., and Buzsaki, G. (1995).

Gamma (40-100 hz) oscillation in the hippocampus of the behaving rat. *Journal of Neuroscience*, 15(1):47–60.

Branco, T. and Häusser, M. (2011). Synaptic integration gradients in single cortical pyramidal cell dendrites. *Neuron*, 69(5):885–892.

Brankačk, J., Seidenbecher, T., and Müller-Gärtner, H.-W. (1996). Task-relevant late positive component in rats: Is it related to hippocampal theta rhythm? *Hippocampus*, 6(5):475–482.

Brankack, J., Stewart, M., and Fox, S. E. (1993). Current source density analysis of the hippocampal theta rhythm: associated sustained potentials and candidate synaptic generators. *Brain Research*, 615(2):310–327.

Buhl, E. H., Han, Z. S., Lorinczi, Z., Stezhka, V. V., Karnup, S. V., and Somogyi, P. (1994). Physiological properties of anatomically identified axo-axonic cells in the rat hippocampus. *Journal of Neurophysiology*, 71(4):1289–1307.

Burgess, N., Maguire, E. A., and O’Keefe, J. (2002). The human hippocampus and spatial and episodic memory. *Neuron*, 35(4):625–641.

Bush, D. (2010). Spike-timing dependent plasticity and the cognitive map. *Frontiers in Computational Neuroscience*, 4.

Buzsáki, G. (2002). Theta oscillations in the hippocampus. *Neuron*, 33(3):325–340.

Buzsáki, G. (2005). Theta rhythm of navigation: Link between path integration and landmark navigation, episodic and semantic memory. *Hippocampus*, 15(7):827–840.

Buzsáki, G., Anastassiou, C. A., and Koch, C. (2012). The origin of extracellular fields and currents — eeg, ecog, lfp and spikes. *Nature Reviews Neuroscience*, 13(6):407–420.

Buzsaki, G. and Moser, E. I. (2013). Memory, navigation and theta rhythm in the hippocampal-entorhinal system. *Nature Neuroscience*, 16(2):130–138.

Buzsáki, G. and Silva, F. L. (2012). High frequency oscillations in the intact brain. *Progress in Neurobiology*, 98(3):241–249.

Cardinal, R. N. (2006). Neural systems implicated in delayed and probabilistic reinforcement. *Neural Networks*, 19(8):1277–1301.

Carhart-Harris, R. L. and Nutt, D. J. (2017). Serotonin and brain function: a tale of two receptors. *Journal of Psychopharmacology*, 31(9):1091–1120.

Cea-del Rio, C. A., Lawrence, J. J., Tricoire, L., Erdelyi, F., Szabo, G., and McBain, C. J. (2010). M3 muscarinic acetylcholine receptor expression confers differential cholinergic modulation to neurochemically distinct hippocampal basket cell subtypes.

*The Journal of neuroscience : the official journal of the Society for Neuroscience*, 30(17):6011–6024.

Cea-del Rio, C. A., McBain, C. J., and Pelkey, K. A. (2012). An update on cholinergic regulation of cholecystokinin-expressing basket cells. *The Journal of Physiology*, 590(4):695–702.

Chittajallu, R., Alford, S., and Collingridge, G. L. (1998). Ca<sup>2+</sup> and synaptic plasticity. *Cell Calcium*, 24(5-6):377–385.

Cipriani, A., Furukawa, T. A., and Salanti, G. (2018). Comparative efficacy and acceptability of 21 antidepressant drugs for the acute treatment of adults with major depressive disorder: a systematic review and network meta-analysis. *The Lancet*, 0:1–10.

Cohen, J. Y., Amoroso, M. W., Uchida, N., and Behrens, T. (2015). Serotonergic neurons signal reward and punishment on multiple timescales. *eLife*, 4:e06346+.

Colbert, C. M. and Levy, W. B. (1993). Long-term potentiation of perforant path synapses in hippocampal ca1 in vitro. *Brain Research*, 606(1):87–91.

Colgin, L. L., Denninger, T., Fyhn, M., Hafting, T., Bonnevie, T., Jensen, O., Moser, M.-B., and Moser, E. I. (2009). Frequency of gamma oscillations routes flow of information in the hippocampus. *Nature*, 462(7271):353–357.

Colgin, L. L. and Moser, E. I. (2010). Gamma oscillations in the hippocampus. *Physiology*, 25(5):319–329.

Collingridge, G. L., Peineau, S., Howland, J. G., and Wang, Y. T. (2010). Long-term depression in the cns. *Nat Rev Neurosci*, 11(7):459–473.

Colom, L. V. (2006). Septal networks: relevance to theta rhythm, epilepsy and alzheimer’s disease. *Journal of Neurochemistry*, 96(3):609–623.

Cools, R., Nakamura, K., and Daw, N. D. (2010). Serotonin and dopamine: Unifying affective, activational, and decision functions. *Neuropsychopharmacology*, 36(1):98–113.

Coppen, A. (1967). The biochemistry of affective disorders. *The British Journal of Psychiatry*, 113(504):1237–1264.

Corrado Barbui, M. D., Eleonora Esposito, M. D., and Andrea Cipriani, M. D. (2009). Selective serotonin reuptake inhibitors and risk of suicide: a systematic review of observational studies. *Canadian Medical Association Journal*, 180(3):291–297.

Crooks, R., Jackson, J., and Bland, B. H. (2012). Dissociable pathways facilitate theta and non-theta states in the median raphe–septohippocampal circuit. *Hippocampus*, 22(7):1567–1576.

- Csicsvari, J., Hirase, H., Czurkó, A., Mamiya, A., and Buzsáki, G. (1999). Oscillatory coupling of hippocampal pyramidal cells and interneurons in the behaving rat. *The Journal of neuroscience : the official journal of the Society for Neuroscience*, 19(1):274–287.
- Csicsvari, J., Jamieson, B., Wise, K. D., and Buzsáki, G. (2003). Mechanisms of gamma oscillations in the hippocampus of the behaving rat. *Neuron*, 37(2):311–322.
- Cutsuridis, V., Cobb, S., and Graham, B. P. (2010a). Encoding and retrieval in a model of the hippocampal ca1 microcircuit. *Hippocampus*, 20(3):423–446.
- Cutsuridis, V., Graham, B., Cobb, S., and Vida, I., editors (2010b). *Hippocampal Microcircuits*. Springer New York, New York, NY.
- Cutsuridis, V. and Hasselmo, M. (2010). *Dynamics and Function of a CA1 Model of the Hippocampus during Theta and Ripples*. Springer Berlin Heidelberg.
- Daumas, S., Halley, H., Francés, B., and Lassalle, J.-M. (2005). Encoding, consolidation, and retrieval of contextual memory: Differential involvement of dorsal ca3 and ca1 hippocampal subregions. *Learning & Memory*, 12(4):375–382.
- de Almeida, L., Idiart, M., and Lisman, J. E. (2009). A second function of gamma frequency oscillations: An e%-max winner-take-all mechanism selects which cells fire. *The Journal of Neuroscience*, 29(23):7497–7503.
- DiCarlo, J. J., Zoccolan, D., and Rust, N. C. (2012). How does the brain solve visual object recognition? *Neuron*, 73(3):415–434.
- Dittman, J. S., Kreitzer, A. C., and Regehr, W. G. (2000). Interplay between facilitation, depression, and residual calcium at three presynaptic terminals. *The Journal of neuroscience : the official journal of the Society for Neuroscience*, 20(4):1374–1385.
- Dobrunz, L. E., Huang, E. P., and Stevens, C. F. (1997). Very short-term plasticity in hippocampal synapses. *Proceedings of the National Academy of Sciences*, 94(26):14843–14847.
- Dobrunz, L. E. and Stevens, F. C. (1997). Heterogeneity of release probability, facilitation, and depletion at central synapses. *Neuron*, 18(6):995–1008.
- Dorostkar, M. M. and Boehm, S. (2007). Opposite effects of presynaptic 5-HT3 receptor activation on spontaneous and action potential-evoked GABA release at hippocampal synapses. *Journal of Neurochemistry*, 100(2):395–405.
- Dougalis, A. G., Matthews, G. A. C., Bishop, M. W., Brischoux, F., Kobayashi, K., and Ungless, M. A. (2012). Functional properties of dopamine neurons and co-expression of vasoactive intestinal polypeptide in the dorsal raphe nucleus and ventro-lateral periaqueductal grey. *European Journal of Neuroscience*, 36(10):3322–3332.

- Douglas, R. J. (1967). The hippocampus and behavior. *Psychological bulletin*, 67(6):416–422.
- Dragoi, G. and Buzsáki, G. (2017). Temporal encoding of place sequences by hippocampal cell assemblies. *Neuron*, 50(1):145–157.
- Dragoi, G., Carpi, D., Recce, M., Csicsvari, J., and Buzsáki, G. (1999). Interactions between hippocampus and medial septum during sharp waves and theta oscillation in the behaving rat. *The Journal of Neuroscience*, 19(14):6191–6199.
- Eichenbaum, H. (2004). Hippocampus. *Neuron*, 44(1):109–120.
- Ekstrom, A. D., Meltzer, J., McNaughton, B. L., and Barnes, C. A. (2001). Nmda receptor antagonism blocks experience-dependent expansion of hippocampal “place fields”. *Neuron*, 31(4):631–638.
- El Mestikawy, S., Wallén-Mackenzie, Å., Fortin, G. M., Descarries, L., and Trudeau, L.-E. (2011). From glutamate co-release to vesicular synergy: vesicular glutamate transporters. *Nature Reviews Neuroscience*, 12(4):204–216.
- Elfant, D., Pál, B. Z., Emptage, N., and Capogna, M. (2008). Specific inhibitory synapses shift the balance from feedforward to feedback inhibition of hippocampal ca1 pyramidal cells. *European Journal of Neuroscience*, 27(1):104–113.
- Epsztein, J., Brecht, M., and Lee, A. K. (2011). Intracellular determinants of hippocampal ca1 place and silent cell activity in a novel environment. *Neuron*, 70(1):109–120.
- Feldman, D. E. (2012). The spike-timing dependence of plasticity. *Neuron*, 75(4):556–571.
- Fenton, A. A., Kao, H.-Y., Neymotin, S. A., Olypher, A., Vayntrub, Y., Lytton, W. W., and Ludvig, N. (2008). Unmasking the ca1 ensemble place code by exposures to small and large environments: More place cells and multiple, irregularly arranged, and expanded place fields in the larger space. *Journal of Neuroscience*, 28(44):11250–11262.
- Fenton, A. A. and Muller, R. U. (1998). Place cell discharge is extremely variable during individual passes of the rat through the firing field. *Proceedings of the National Academy of Sciences*, 95(6):3182–3187.
- Férezou, I., Cauli, B., Hill, E. L., Rossier, J., Hamel, E., and Lambolez, B. (2002). 5-HT<sub>3</sub> receptors mediate serotonergic fast synaptic excitation of neocortical vasoactive intestinal peptide/cholecystokinin interneurons. *The Journal of Neuroscience*, 22(17):7389–7397.
- Fioravante, D. and Regehr, W. G. (2011). Short-term forms of presynaptic plasticity. *Current Opinion in Neurobiology*, 21(2):269–274.

- Fischer, A. G., Jocham, G., and Ullsperger, M. (2015). Dual serotonergic signals: a key to understanding paradoxical effects? *Trends in Cognitive Sciences*, 19(1):21–26.
- Fisher, S. (1997). Multiple overlapping processes underlying short-term synaptic enhancement. *Trends in Neurosciences*, 20(4):170–177.
- Floresco, S. B., West, A. R., Ash, B., Moore, H., and Grace, A. A. (2003). Afferent modulation of dopamine neuron firing differentially regulates tonic and phasic dopamine transmission. *Nature Neuroscience*, 6(9):968–973.
- Foldy, C., Lee, S.-H., Morgan, R. J., and Soltesz, I. (2010). Regulation of fast-spiking basket cell synapses by the chloride channel clc-2. *Nature Neuroscience*, 13(9):1047–1049.
- Forro, T., Valenti, O., Lasztoczi, B., and Klausberger, T. (2015). Temporal organization of gabaergic interneurons in the intermediate ca1 hippocampus during network oscillations. *Cerebral Cortex*, 25(5):1228–1240.
- Frank, L. M., Stanley, G. B., and Brown, E. N. (2004). Hippocampal plasticity across multiple days of exposure to novel environments. *Journal of Neuroscience*, 24(35):7681–7689.
- French, P. J., O'Connor, V., Jones, M. W., Davis, S., Errington, M. L., Voss, K., Truchet, B., Wotjak, C., Stean, T., Doyère, V., Maroun, M., Laroche, S., and Bliss, T. V. P. (2001). Subfield-specific immediate early gene expression associated with hippocampal long-term potentiation in vivo. *European Journal of Neuroscience*, 13(5):968–976.
- Freund, T. F. and Buzsáki, G. (1996). Interneurons of the hippocampus. *Hippocampus*, 6(4):347–470.
- Freund, T. F. and Katona, I. (2007). Perisomatic inhibition. *Neuron*, 56(1):33–42.
- Fuhrmann, F., Justus, D., Sosulina, L., Kaneko, H., Beutel, T., Friedrichs, D., Schoch, S., Schwarz, M. K., Fuhrmann, M., and Remy, S. (2015). Locomotion, theta oscillations, and the speed-correlated firing of hippocampal neurons are controlled by a medial septal glutamatergic circuit. *Neuron*, 86(5):1253–1264.
- Fyhn, M., Hafting, T., Treves, A., Moser, M.-B., and Moser, E. I. (2007). Hippocampal remapping and grid realignment in entorhinal cortex. *Nature*, 446(7132):190–194.
- Ganter, P., Szücs, P., Paulsen, O., and Somogyi, P. (2004). Properties of horizontal axo-axonic cells in stratum oriens of the hippocampal ca1 area of rats in vitro. *Hippocampus*, 14(2):232–243.
- Girardeau, G. and Zugaro, M. (2011). Hippocampal ripples and memory consolidation. *Current Opinion in Neurobiology*, 21(3):452–459.

- Glickfeld, L. L., Roberts, J. D., Somogyi, P., and Scanziani, M. (2008). Interneurons hyperpolarize pyramidal cells along their entire somatodendritic axis. *Nature Neuroscience*, 12(1):21–23.
- Glickfeld, L. L. and Scanziani, M. (2006). Distinct timing in the activity of cannabinoid-sensitive and cannabinoid-insensitive basket cells. *Nature Neuroscience*, 9(6):807–815.
- Golding, N. L., Staff, N. P., and Spruston, N. (2002). Dendritic spikes as a mechanism for cooperative long-term potentiation. *Nature*, 418:326–331.
- Graves, A. R., Moore, S. J., Bloss, E. B., Mensh, B. D., Kath, W. L., and Spruston, N. (2012). Hippocampal pyramidal neurons comprise two distinct cell types that are countermodulated by metabotropic receptors. *Neuron*, 76(4):776–789.
- Gray, J. A. (1971). Medial septal lesions, hippocampal theta rhythm and the control of vibrissal movement in the freely moving rat. *Electroencephalography and Clinical Neurophysiology*, 30(3):189–197.
- Griffin, A. L. and Hallock, H. L. (2013). Hippocampal signatures of episodic memory: evidence from single-unit recording studies. *Frontiers in behavioral neuroscience*, 7.
- Grosmark, A. D. and Buzsaki, G. (2016). Diversity in neural firing dynamics supports both rigid and learned hippocampal sequences. *Science*, 351(6280):1440–1443.
- Gururajan, A., Clarke, G., Dinan, T. G., and Cryan, J. F. (2016). Molecular biomarkers of depression. *Neuroscience and Biobehavioral Reviews*, 64:101–133.
- Guzowski, J. F., Knierim, J. J., and Moser, E. I. (2004). Ensemble dynamics of hippocampal regions ca3 and ca1. *Neuron*, 44(4):581–584.
- Hafting, T., Fyhn, M., Molden, S., Moser, M.-B., and Moser, E. I. (2005). Microstructure of a spatial map in the entorhinal cortex. *Nature*, 436(7052):801–806.
- Hagena, H. and Manahan-Vaughan, D. (2017). The serotonergic 5-HT<sub>4</sub> receptor: A unique modulator of hippocampal synaptic information processing and cognition. *Neurobiology of Learning and Memory*, 138:145–153.
- Hangya, B., Borhegyi, Z., Szilágyi, N., Freund, T. F., and Varga, V. (2009). Gabaergic neurons of the medial septum lead the hippocampal network during theta activity. *The Journal of Neuroscience*, 29(25):8094–8102.
- Hangya, B., Ranade, S. P., Lorenc, M., and Kepcs, A. (2015). Central cholinergic neurons are rapidly recruited by reinforcement feedback. *Cell*, 162(5):1155–1168.
- Hannon, J. and Hoyer, D. (2008). Molecular biology of 5-HT receptors. *Behavioural Brain Research*, 195(1):198–213.
- Hardie, J. and Spruston, N. (2009). Synaptic depolarization is more effective than back-

- propagating action potentials during induction of associative long-term potentiation in hippocampal pyramidal neurons. *Journal of Neuroscience*, 29(10):3233–3241.
- Harmer, C. J., Goodwin, G. M., and Cowen, P. J. (2009). Why do antidepressants take so long to work? a cognitive neuropsychological model of antidepressant drug action. *The British Journal of Psychiatry*, 195(2):102–108.
- Harris, K. D., Henze, D. A., Hirase, H., Leinekugel, X., Dragoi, G., Czurko, A., and Buzsaki, G. (2002). Spike train dynamics predicts theta-related phase precession in hippocampal pyramidal cells. *Nature*, 417(6890):738–741.
- Harvey, C. D., Collman, F., Dombeck, D. A., and Tank, D. W. (2009). Intracellular dynamics of hippocampal place cells during virtual navigation. *Nature*, 461(7266):941–946.
- Hasselmo, M. E. (2006). The role of acetylcholine in learning and memory. *Current opinion in neurobiology*, 16(6):710–715.
- Hasselmo, M. E., Bodelón, C., and Wyble, B. P. (2002a). A proposed function for hippocampal theta rhythm: Separate phases of encoding and retrieval enhance reversal of prior learning. *Neural Computation*, 14(4):793–817.
- Hasselmo, M. E. and Fehlau, B. P. (2001). Differences in time course of ach and gaba modulation of excitatory synaptic potentials in slices of rat hippocampus. *Journal of Neurophysiology*, 86(4):1792–1802.
- Hasselmo, M. E., Giocomo, L. M., and Zilli, E. A. (2007). Grid cell firing may arise from interference of theta frequency membrane potential oscillations in single neurons. *Hippocampus*, 17(12):1252–1271.
- Hasselmo, M. E., Hay, J., Ilyn, M., and Gorchetchnikov, A. (2002b). Neuromodulation, theta rhythm and rat spatial navigation. *Neural Networks*, 15(4-6):689–707.
- Hebb, D. O., editor (1949). *The organization of behavior - a neuropsychological theory*. Wiley, Oxford, England.
- Henze, D. A. and Buzsáki, G. (2001). Action potential threshold of hippocampal pyramidal cells in vivo is increased by recent spiking activity. *Neuroscience*, 105(1):121–130.
- Hnasko, T. S. and Edwards, R. H. (2012). Neurotransmitter corelease: Mechanism and physiological role. *Annual Review of Physiology*, 74(1):225–243.
- Hodgkin, A. L. and Huxley, A. F. (1952). A quantitative description of membrane current and its application to conduction and excitation in nerve. *Journal of Physiology*, 117:500–544.
- Huxter, J., Burgess, N., and O’Keefe, J. (2003). Independent rate and temporal coding in hippocampal pyramidal cells. *Nature*, 425(6960):828–832.

- Insel, T. R. and Charney, D. S. (2003). Research on major depression - strategies and priorities. *JAMA*, 289(23):3167–3168.
- Jensen, M. S., Azouz, R., and Yaari, Y. (1994). Variant firing patterns in rat hippocampal pyramidal cells modulated by extracellular potassium. *Journal of Neurophysiology*, 71(3):831–839.
- Jensen, O. and Lisman, J. E. (1996). Hippocampal ca3 region predicts memory sequences: Accounting for the phase precession of place cells. *Learning & Memory*, 3:279–287.
- John-Hopkins-University (2017). <http://web.jhu.edu/animalcare/procedures/rat.html>.
- Julian, J. B., Ryan, J., Hamilton, R. H., and Epstein, R. A. (2016). The occipital place area is causally involved in representing environmental boundaries during navigation. *Current Biology*.
- Justus, D., Dalugge, D., Bothe, S., Fuhrmann, F., Hannes, C., Kaneko, H., Friedrichs, D., Sosulina, L., Schwarz, I., Elliott, D. A., Schoch, S., Bradke, F., Schwarz, M. K., and Remy, S. (2016). Glutamatergic synaptic integration of locomotion speed via septoentorhinal projections. *Nature Neuroscience*, 20(1):16–19.
- Kaeser, P. S., Deng, L., Wang, Y., Dulubova, I., Liu, X., Rizo, J., and Suedhof, T. C. (2011). Rim proteins tether  $\text{Ca}^{2+}$  channels to presynaptic active zones via a direct pdz-domain interaction. *Cell*, 144(2):282–295.
- Keimpema, E., Straiker, A., Mackie, K., Harkany, T., and Hjerling-Leffler, J. (2012). Sticking out of the crowd: the molecular identity and development of cholecystokinin-containing basket cells. *The Journal of Physiology*, 590(4):703–714.
- Kemp, A. and Manahan-Vaughan, D. (2004). Hippocampal long-term depression and long-term potentiation encode different aspects of novelty acquisition. *Proceedings of the National Academy of Sciences of the United States of America*, 101(21):8192–8197.
- Kemp, A. and Manahan-Vaughan, D. (2005). The 5-hydroxytryptamine4 receptor exhibits frequency-dependent properties in synaptic plasticity and behavioural meta-plasticity in the hippocampal ca1 region in vivo. *Cerebral Cortex*, 15(7):1037–1043.
- Kim, M. T., Soussou, W., Gholmeh, G., Ahuja, A., Tanguay, A., Berger, T. W., and Brinton, R. D. (2006). 17-estradiol potentiates field excitatory postsynaptic potentials within each subfield of the hippocampus with greatest potentiation of the associational/commissural afferents of ca3. *Neuroscience*, 141(1):391–406.
- King, C., Recce, M., and O’Keefe, J. (1998). The rhythmicity of cells of the medial septum/diagonal band of broca in the awake freely moving rat: relationships with

- behaviour and hippocampal theta. *European Journal of Neuroscience*, 10(2):464–477.
- Kirk, I. (1998). Frequency modulation of hippocampal theta by the supramammillary nucleus, and other hypothalamo–hippocampal interactions: Mechanisms and functional implications. *Neuroscience & Biobehavioral Reviews*, 22(2):291–302.
- Kirsch, I., Deacon, B. J., Huedo-Medina, T. B., Scoboria, A., Moore, T. J., and Johnson, B. T. (2008). Initial severity and antidepressant benefits: A meta-analysis of data submitted to the food and drug administration. *PLOS Medicine*, 5(2):1–9.
- Kiyasova, V., Bonnavion, P., Scotto-Lomassese, S., Fabre, V., Sahly, I., Tronche, F., Deneris, E., Gaspar, P., and Fernandez, S. P. (2013). A subpopulation of serotonergic neurons that do not express the 5-HT1A autoreceptor. *ACS chemical neuroscience*, 4(1):89–95.
- Kjonigsen, L. J., Lillehaug, S., Bjaalie, J. G., Witter, M. P., and Leergaard, T. B. (2015). Waxholm space atlas of the rat brain hippocampal region: Three-dimensional delineations based on magnetic resonance and diffusion tensor imaging. *NeuroImage*, 108:441 – 449.
- Klausberger, T. (2009). GABAergic interneurons targeting dendrites of pyramidal cells in the CA1 area of the hippocampus. *European Journal of Neuroscience*, 30(6):947–957.
- Klausberger, T., Magill, P. J., Marton, L. F., Roberts, Cobden, P. M., Buzsaki, G., and Somogyi, P. (2003). Brain-state- and cell-type-specific firing of hippocampal interneurons in vivo. *Nature*, 421(6925):844–848.
- Klausberger, T. and Somogyi, P. (2008). Neuronal diversity and temporal dynamics: the unity of hippocampal circuit operations. *Science (New York, N.Y.)*, 321(5885):53–57.
- Klyachko, V. A. and Stevens, C. F. (2006). Excitatory and feed-forward inhibitory hippocampal synapses work synergistically as an adaptive filter of natural spike trains. *PLOS Biology*, 4(7):e207+.
- Knauer, B., Jochems, A., Valero-Aracama, M. J., and Yoshida, M. (2013). Long-lasting intrinsic persistent firing in rat CA1 pyramidal cells: A possible mechanism for active maintenance of memory. *Hippocampus*, 23(9):820–831.
- Kocsis, B., Varga, V., Dahan, L., and Sik, A. (2006). Serotonergic neuron diversity: identification of raphe neurons with discharges time-locked to the hippocampal theta rhythm. *Proceedings of the National Academy of Sciences of the United States of America*, 103(4):1059–1064.
- Langston, R. F. and Wood, E. R. (2010). Associative recognition and the hippocampus:

Differential effects of hippocampal lesions on object-place, object-context and object-place-context memory. *Hippocampus*, 20(10):1139–1153.

Leao, R. N., Mikulovic, S., Leao, K. E., Munguba, H., Gezelius, H., Enjin, A., Patra, K., Eriksson, A., Loew, L. M., Tort, A. B. L., and Kullander, K. (2012). Olm interneurons differentially modulate ca3 and entorhinal inputs to hippocampal ca1 neurons. *Nat Neurosci*, 15(11):1524–1530.

Lee, D., Lin, B.-J., and Lee, A. K. (2012). Hippocampal place fields emerge upon single-cell manipulation of excitability during behavior. *Science*, 337(6096):849–853.

Lee, I., Rao, G., and Knierim, J. J. (2004). A double dissociation between hippocampal subfields. *Neuron*, 42(5):803–815.

Lee, S.-H., Marchionni, I., Bezaire, M., Varga, C., Danielson, N., Lovett-Barron, M., Losonczy, A., and Soltesz, I. (2014). Parvalbumin-positive basket cells differentiate among hippocampal pyramidal cells. *Neuron*.

Leutgeb, J. K., Leutgeb, S., Moser, M.-B., and Moser, E. I. (2007). Pattern separation in the dentate gyrus and ca3 of the hippocampus. *Science*, 315(5814):961–966.

Liguz-Lecznar, M. and Skangiel-Kramska, J. (2007). Vesicular glutamate transporters (vgluts): the three musketeers of glutamatergic system. *Acta Neurobiologiae Experimentalis*, 67(3):207–218.

Lisman, J. E. and Grace, A. A. (2005). The hippocampal-vta loop: Controlling the entry of information into long-term memory. *Neuron*, 46(5):703–713.

Liu, B., Liu, J., Wang, M., Zhang, Y., and Li, L. (2017). From serotonin to neuroplasticity: Evolvement of theories for major depressive disorder. *Frontiers in Cellular Neuroscience*, 11:1–9.

Logothetis, N. K., Eschenko, O., Murayama, Y., Augath, M., Steudel, T., Evrard, H. C., Besserve, M., and Oeltermann, A. (2012). Hippocampal-cortical interaction during periods of subcortical silence. *Nature*, 491(7425):547–553.

Maccaferri, G. (2005). Stratum oriens horizontal interneurone diversity and hippocampal network dynamics. *The Journal of Physiology*, 562(1):73–80.

Magee, J. C. (1999). Dendritic ih normalizes temporal summation in hippocampal ca1 neurons. *Nature Neuroscience*, 2(6):508–514.

Magee, J. C. (2001). Dendritic mechanisms of phase precession in hippocampal ca1 pyramidal neurons. *Journal of Neurophysiology*, 86(1):528–532.

Malagié, I., David, D. J., Jollet, P., Hen, R., Bourin, M., and Gardier, A. M. (2002). Improved efficacy of fluoxetine in increasing hippocampal 5-hydroxytryptamine outflow in 5-ht1b receptor knock-out mice. *European Journal of Pharmacology*, 443(1-3):99–104.

- Manahan-Vaughan, D., Kulla, A., and Frey, J. U. (2000). Requirement of translation but not transcription for the maintenance of long-term depression in the ca1 region of freely moving rats. *Journal of Neuroscience*, 20(22):8572–8576.
- Markram, H., Lübke, J., Frotscher, M., and Sakmann, B. (1997). Regulation of synaptic efficacy by coincidence of postsynaptic aps and epsps. *Science*, 275(5297):213–215.
- Mason, A. (1993). Electrophysiology and burst-firing of rat subiculum pyramidal neurons in vitro: a comparison with area ca1. *Brain Research*, 600(1):174–178.
- MÄller, C. and Remy, S. (2014). Dendritic inhibition mediated by o-lm and bistratified interneurons in the hippocampus. *Frontiers in Synaptic Neuroscience*, 6.
- McFarland, W. L., Teitelbaum, H., and Hedges, E. K. (1975). Relationship between hippocampal theta activity and running speed in the rat. *Journal of comparative and physiological psychology*, 88(1):324–328.
- McHugh, T. J., Jones, M. W., Quinn, J. J., Balthasar, N., Coppari, R., Elmquist, J. K., Lowell, B. B., Fanselow, M. S., Wilson, M. A., and Tonegawa, S. (2007). Dentate gyrus nmda receptors mediate rapid pattern separation in the hippocampal network. *Science*, 317(5834):94–99.
- McNaughton, B. L., Barnes, C. A., and O’Keefe, J. (1983). The contributions of position, direction, and velocity to single unit activity in the hippocampus of freely-moving rats. *Experimental Brain Research*, 52(1):41–49.
- Megias, M., Emri, Z., Freund, T. F., and Gulyás, A. I. (2001). Total number and distribution of inhibitory and excitatory synapses on hippocampal ca1 pyramidal cells. *Neuroscience*, 102(3):527–540.
- Mehta, M. R., Lee, A. K., and Wilson, M. A. (2002). Role of experience and oscillations in transforming a rate code into a temporal code. *Nature*, 417(6890):741–746.
- Mehta, M. R., Quirk, M. C., and Wilson, M. A. (2000). Experience-dependent asymmetric shape of hippocampal receptive fields. *Neuron*, 25(3):707–715.
- Miyazaki, K., Miyazaki, K. W., and Doya, K. (2011). Activation of dorsal raphe serotonin neurons underlies waiting for delayed rewards. *The Journal of Neuroscience*, 31(2):469–479.
- Mizuseki, K., Diba, K., Pastalkova, E., and Buzsaki, G. (2011). Hippocampal ca1 pyramidal cells form functionally distinct sublayers. *Nature Neuroscience*, 14(9):1174–1181.
- Mizuseki, K., Royer, S., Diba, K., and Buzsáki, G. (2012). Activity dynamics and behavioral correlates of ca3 and ca1 hippocampal pyramidal neurons. *Hippocampus*, 22(8):1659–1680.

- Mlinar, B., Mascalchi, S., Mannaioni, G., Morini, R., and Corradetti, R. (2006). 5-HT<sub>4</sub> receptor activation induces long-lasting EPSP-spike potentiation in CA1 pyramidal neurons. *The European journal of neuroscience*, 24(3):719–731.
- Mölle, M., Yeshenko, O., Marshall, L., Sara, S. J., and Born, J. (2006). Hippocampal sharp wave-ripples linked to slow oscillations in rat slow-wave sleep. *Journal of Neurophysiology*, 96(1):62–70.
- Mongillo, G., Barak, O., and Tsodyks, M. (2008). Synaptic theory of working memory. *Science*, 319(5869):1543–1546.
- Morris, R. G. M. (2006). Elements of a neurobiological theory of hippocampal function: the role of synaptic plasticity, synaptic tagging and schemas. *European Journal of Neuroscience*, 23(11):2829–2846.
- Muller, R. (1996). A quarter of a century of place cells. *Neuron*, 17(5):813–822.
- Muller, R. U., Kubie, J. L., and Ranck, J. B. (1987). Spatial firing patterns of hippocampal complex-spike cells in a fixed environment. *Journal of Neuroscience*, 7(7):1935–1950.
- Mumby, D. G., Gaskin, S., Glenn, M. J., Schramek, T. E., and Lehmann, H. (2002). Hippocampal damage and exploratory preferences in rats: Memory for objects, places, and contexts. *Learning & Memory*, 9(2):49–57.
- Nakamura, K. (2013). The role of the dorsal raphe nucleus in reward-seeking behavior. *Frontiers in Integrative Neuroscience*, 7.
- Nakamura, K., Matsumoto, M., and Hikosaka, O. (2008). Reward-dependent modulation of neuronal activity in the primate dorsal raphe nucleus. *The Journal of Neuroscience : the official journal of the Society for Neuroscience*, 28(20):5331–5343.
- Nanou, E., Sullivan, J. M., Scheuer, T., and Catterall, W. A. (2016). Calcium sensor regulation of the Cav2.1 Ca<sup>2+</sup> channel contributes to short-term synaptic plasticity in hippocampal neurons. *Proceedings of the National Academy of Sciences*, 113(4):1062–1067.
- Nishiyama, M., Hong, K., Mikoshiba, K., Poo, M. M., and Kato, K. (2000). Calcium stores regulate the polarity and input specificity of synaptic modification. *Nature*, 408:584–588.
- Oddie, S. (1998). Hippocampal formation theta activity and movement selection. *Neuroscience & Biobehavioral Reviews*, 22(2):221–231.
- Oertner, T. G., Sabatini, B. L., Nimchinsky, E. A., and Svoboda, K. (2002). Facilitation at single synapses probed with optical quantal analysis. *Nature Neuroscience*, 5(7):657–664.

- Ohmura, Y., Izumi, T., Yamaguchi, T., Tsutsui-Kimura, I., Yoshida, T., and Yoshioka, M. (2010). The serotonergic projection from the median raphe nucleus to the ventral hippocampus is involved in the retrieval of fear memory through the corticotropin-releasing factor type 2 receptor. *Neuropsychopharmacology*, 35(6):1271–1278.
- O’Keefe, J. and Burgess, N. (1996). Geometric determinants of the place fields of hippocampal neurons. *Nature*, 381(6581):425–428.
- O’Keefe, J. and Dostrovsky, J. (1971). The hippocampus as a spatial map. preliminary evidence from unit activity in the freely-moving rat. *Brain Research*, 34(1):171–175.
- O’Keefe, J. and Recce, M. L. (1993). Phase relationship between hippocampal place units and the eeg theta rhythm. *Hippocampus*, 3(3):317–330.
- Otmakhov, N., Shirke, A. M., and Malinow, R. (1993). Measuring the impact of probabilistic transmission on neuronal output. *Neuron*, 10(6):1101–1111.
- Pan, W.-X. and McNaughton, N. (2004). The supramammillary area: its organization, functions and relationship to the hippocampus. *Progress in Neurobiology*, 74(3):127–166.
- Papatheodoropoulos, C. (2015). Striking differences in synaptic facilitation along the dorsoventral axis of the hippocampus. *Neuroscience*, 301:454–470.
- Pape, H. C. (1996). Queer current and pacemaker: The hyperpolarization-activated cation current in neurons. *Annual Reviews*, 58:299–327.
- Paul, E. D. and Lowry, C. A. (2013). Functional topography of serotonergic systems supports the deakin/graeff hypothesis of anxiety and affective disorders. *Journal of psychopharmacology (Oxford, England)*, 27(12):1090–1106.
- Perkovic, M. N., Erjavec, G. N., Strac, D., and Pivac, N. (2018). *Biomarkers of Depression: Potential Diagnostic Tools*, volume 2, pages 35–51. Springer, Singapore.
- Piatti, V. C., Ewell, L. A., and Leutgeb, J. K. (2013). Neurogenesis in the dentate gyrus: carrying the message or dictating the tone. *Frontiers in neuroscience*, 7.
- Picciotto, M. R., Higley, M. J., and Mineur, Y. S. (2012). Acetylcholine as a neuromodulator: Cholinergic signaling shapes nervous system function and behavior. *Neuron*, 76(1):116–129.
- Pollak Dorocic, I., Fürth, D., Xuan, Y., Johansson, Y., Pozzi, L., Silberberg, G., Carlén, M., and Meletis, K. (2014). A whole-brain atlas of inputs to serotonergic neurons of the dorsal and median raphe nuclei. *Neuron*, 83(3):663–678.
- Pouille, F. (2001). Enforcement of temporal fidelity in pyramidal cells by somatic feed-forward inhibition. *Science*, 293(5532):1159–1163.

- Puglisi-Allegra, S. and Andolina, D. (2015). Serotonin and stress coping. *Behavioural Brain Research*, 277:58–67. Special Issue: Serotonin.
- Puig and Gullede, A. (2011). Serotonin and prefrontal cortex function: Neurons, networks, and circuits. *Molecular neurobiology*, 44(3):449–464.
- Regehr, W. G. (2012). Short-term presynaptic plasticity. *Cold Spring Harbor Perspectives in Biology*, 4(7):a005702+.
- Riad, M., Garcia, S., Watkins, K. C., Jodoin, N., Doucet, E., Langlois, X., el Mestikawy, S., Hamon, M., and Descarries, L. (2000). Somatodendritic localization of 5-HT<sub>1A</sub> and preterminal axonal localization of 5-HT<sub>1B</sub> serotonin receptors in adult rat brain. *The Journal of comparative neurology*, 417(2):181–194.
- Robinson, J., Manseau, F., Ducharme, G., Amilhon, B., Vigneault, E., Mestikawy, S. E., and Williams, S. (2016). Optogenetic activation of septal glutamatergic neurons drive hippocampal theta rhythms. *Journal of Neuroscience*, 36(10):3016–3023.
- Rolls, E. T., Stringer, S. M., and Elliot, T. (2006). Entorhinal cortex grid cells can map to hippocampal place cells by competitive learning. *Network: Computation in Neural Systems*, 17(4):447–465.
- Rolls, E. T. and Treves, A. (1993). Neural networks in the brain involved in memory and recall. In *Proceedings of 1993 International Conference on Neural Networks (IJCNN-93-Nagoya, Japan)*, pages 9–14. IEEE.
- Roth, B. L. (2006). *The serotonin receptors from molecular pharmacology to human therapeutics*. Humana Press.
- Roychowdhury, S., Haas, H., and Anderson, E. G. (1994). 5-HT<sub>1A</sub> and 5-HT<sub>4</sub> receptor colocalization on hippocampal pyramidal cells. *Neuropharmacology*, 33(3-4):551–557.
- Rudy, B., Fishell, G., Lee, S., and Hjerling-Leffler, J. (2011). Three groups of interneurons account for nearly 100% of neocortical gabaergic neurons. *Developmental neurobiology*, 71(1):45–61.
- Sadowski, J. H. L. P., Jones, M. W., and Mellor, J. R. (2011). Ripples make waves: Binding structured activity and plasticity in hippocampal networks. *Neural Plasticity*, 2011:1–11.
- Sainsbury, R. S. and Bland, B. H. (1981). The effects of selective septal lesions on theta production in CA1 and the dentate gyrus of the hippocampus. *Physiology & Behavior*, 26(6):1097–1101.
- Samuels, B. A., Mendez-David, I., Faye, C., David, S. A., Pierz, K. A., Gardier, A. M., Hen, R., and David, D. J. (2014). Serotonin 1a and serotonin 4 receptors. *The Neuroscientist*, 22(1):26–45.

- Scoville, W. B. and Milner, B. (1957). Loss of recent memory after bilateral hippocampal lesions. *Journal of neurology, neurosurgery, and psychiatry*, 20(1):11–21.
- Senior, T. J., Huxter, J. R., Allen, K., O'Neill, J., and Csicsvari, J. (2008). Gamma oscillatory firing reveals distinct populations of pyramidal cells in the ca1 region of the hippocampus. *Journal of Neuroscience*, 28(9):2274–2286.
- Skaggs, W. E., McNaughton, B. L., Wilson, M. A., and Barnes, C. A. (1996). Theta phase precession in hippocampal neuronal populations and the compression of temporal sequences. *Hippocampus*, 6(2):149–172.
- Sławińska, U. and Kasicki, S. (1998). The frequency of rat's hippocampal theta rhythm is related to the speed of locomotion. *Brain Research*, 796(1-2):327–331.
- Smart, T. G. (2010). Handling accumulated internal  $\text{Cl}^-$  at inhibitory synapses. *Nat Neurosci*, 13(9):1043–1044.
- Smith, D. M. and Mizumori, S. J. Y. (2006). Hippocampal place cells, context, and episodic memory. *Hippocampus*, 16(9):716–729.
- Somogyi, P., Katona, L., Klausberger, T., Lasztóczki, B., and Viney, T. J. (2014). Temporal redistribution of inhibition over neuronal subcellular domains underlies state-dependent rhythmic change of excitability in the hippocampus. *Phil. Trans. R. Soc. B*, 369(1635):20120518+.
- Somogyi, P. and Klausberger, T. (2005). Defined types of cortical interneurone structure space and spike timing in the hippocampus. *The Journal of Physiology*, 562(1):9–26.
- Sonawalla, S. B. and Rosenbaum, J. F. (2002). Placebo response in depression. *Dialogues in Clinical Neuroscience*, 4(1):105–113.
- Sorra, K. E. and Harris, K. M. (1993). Occurrence and three-dimensional structure of multiple synapses between individual radiatum axons and their target pyramidal cells in hippocampal area ca1. *Journal of Neuroscience*, 13(9):3736–3748.
- Squire, L. R. (1992). Memory and the hippocampus: a synthesis from findings with rats, monkeys, and humans. *Psychological review*, 99(2):195–231.
- Staff, N. P., Jung, H. Y., Thiagarajan, T., Yao, M., and Spruston, N. (2000). Resting and active properties of pyramidal neurons in subiculum and ca1 of rat hippocampus. *Journal of neurophysiology*, 84(5):2398–2408.
- Stent, G. S. (1973). A physiological mechanism for hebb's postulate of learning. *Proceedings of the National Academy of Sciences of the United States of America*, 70(4):997–1001.
- Stevens, C. F. and Wang, Y. (1995). Facilitation and depression at single central synapses. *Neuron*, 14(4):795–802.

- Stewart, M. and Fox, S. E. (1990). Do septal neurons pace the hippocampal theta rhythm? *Trends in Neurosciences*, 13(5):163–169.
- Straub, V. A., Grant, J., O’Shea, M., and Benjamin, P. R. (2007). Modulation of serotonergic neurotransmission by nitric oxide. *Journal of Neurophysiology*, 97(2):1088–1099.
- Stuart, G., Schiller, J., and Sakmann, B. (1997a). Action potential initiation and propagation in rat neocortical pyramidal neurons. *The Journal of Physiology*, 505(3):617–632.
- Stuart, G., Spruston, N., Sakmann, B., and Häusser, M. (1997b). Action potential initiation and backpropagation in neurons of the mammalian cns. *Trends in Neurosciences*, 20(3):125–131.
- Sun, H. Y., Lyons, S. A., and Dobrunz, L. E. (2005). Mechanisms of target-cell specific short-term plasticity at schaffer collateral synapses onto interneurones versus pyramidal cells in juvenile rats. *The Journal of Physiology*, 568(3):815–840.
- Sun, Y., Nguyen, A. Q., Nguyen, J. P., Le, L., Saur, D., Choi, J., Callaway, E. M., and Xu, X. (2016). Cell-type-specific circuit connectivity of hippocampal ca1 revealed through cre-dependent rabies tracing. *Cell Reports*, 7(1):269–280.
- Suwa, B., Bock, N., Preusse, S., Rothenberger, A., and Manzke, T. (2014). Distribution of serotonin 4(a) receptors in the juvenile rat brain and spinal cord. *Journal of Chemical Neuroanatomy*, 55:67–77.
- Szabadics, J., Varga, C., Molnár, G., Oláh, S., Barzó, P., and Tamás, G. (2006). Excitatory effect of gabaergic axo-axonic cells in cortical microcircuits. *Science*, 311(5758):233–235.
- Tanaka, K. F., Samuels, B. A., and Hen, R. (2012). Serotonin receptor expression along the dorsal–ventral axis of mouse hippocampus. *Philosophical Transactions of the Royal Society B: Biological Sciences*, 367(1601):2395–2401.
- Tiganj, Z., Hasselmo, M. E., and Howard, M. W. (2015). A simple biophysically plausible model for long time constants in single neurons. *Hippocampus*, 25(1):27–37.
- Tolman, E. C. (1948). Cognitive maps in rats and men. *Psychological Review*, 55(4):189–208.
- Trappenberg, T. B. (2010). *Fundamentals of Computational Neuroscience*. Oxford University Press, Oxford, England.
- Tsodyks, M. V., Skaggs, W. E., Sejnowski, T. J., and McNaughton, B. L. (1996). Population dynamics and theta rhythm phase precession of hippocampal place cell firing: A spiking neuron model. *Hippocampus*, 6(3):271–280.

- Tukker, J. J., Lasztóczki, B., Katona, L., David, Pissadaki, E. K., Dalezios, Y., Márton, L., Zhang, L., Klausberger, T., and Somogyi, P. (2013). Distinct dendritic arborization and in vivo firing patterns of parvalbumin-expressing basket cells in the hippocampal area ca3. *The Journal of Neuroscience*, 33(16):6809–6825.
- Vanderwolf, C. H. (1969). Hippocampal electrical activity and voluntary movement in the rat. *Electroencephalography and Clinical Neurophysiology*, 26(4):407–418.
- Vann, S. D., Aggleton, J. P., and Maguire, E. A. (2009). What does the retrosplenial cortex do? *Nature reviews. Neuroscience*, 10(11):792–802.
- Varga, C., Golshani, P., and Soltesz, I. (2012). Frequency-invariant temporal ordering of interneuronal discharges during hippocampal oscillations in awake mice. *Proceedings of the National Academy of Sciences of the United States of America*, 109(40):E2726–E2734.
- Varga, V., Losonczy, A., Zemelman, B. V., Borhegyi, Z., Nyiri, G., Domonkos, A., Hangya, B., Holderith, N., Magee, J. C., and Freund, T. F. (2009). Fast synaptic subcortical control of hippocampal circuits. *Science*, 326(5951):449–453.
- Vertes, R. P., Hoover, W. B., and Viana Di Prisco, G. (2004). Theta rhythm of the hippocampus: subcortical control and functional significance. *Behavioral and cognitive neuroscience reviews*, 3(3):173–200.
- Vertes, R. P. and Linley, S. B. (2008). *Efferent and afferent connections of the dorsal and median raphe nuclei in the rat*, chapter 3, pages 69–102. Springer Berkhauser.
- Viney, T. J., Lasztoczi, B., Katona, L., Crump, M. G., Tukker, J. J., Klausberger, T., and Somogyi, P. (2013). Network state-dependent inhibition of identified hippocampal ca3 axo-axonic cells in vivo. *Nat Neurosci*, 16(12):1802–1811.
- Volianskis, A., Bannister, N., Collett, V. J., Irvine, M. W., Monaghan, D. T., Fitzjohn, S. M., Jensen, M. S., Jane, D. E., and Collingridge, G. L. (2013a). Different nmda receptor subtypes mediate induction of long-term potentiation and two forms of short-term potentiation at ca1 synapses in rat hippocampus in vitro. *The Journal of Physiology*, 591(4):955–972.
- Volianskis, A., Collingridge, G. L., and Jensen, M. S. (2013b). The roles of stp and ltp in synaptic encoding. *PeerJ*, 1:e3+.
- Volianskis, A., France, G., Jensen, M. S., Bortolotto, Z. A., Jane, D. E., and Collingridge, G. L. (2015). Long-term potentiation and the role of n-methyl-d-aspartate receptors. *Brain Research*, 1621:5–16.
- Wallenstein, G. V. and Hasselmo, M. E. (1997). Gabaergic modulation of hippocampal population activity: Sequence learning, place field development, and the phase precession effect. *Journal of Neurophysiology*, 78(1):393–408.

- Wang, C.-C., Weyrer, C., Paturu, M., Fioravante, D., and Regehr, W. G. (2016). Calcium-dependent protein kinase c is not required for post-tetanic potentiation at the hippocampal ca3 to ca1 synapse. *Journal of Neuroscience*, 36(24):6393–6402.
- Wang, D. V., Yau, H.-J., Broker, C. J., Tsou, J.-H., Bonci, A., and Ikemoto, S. (2015). Mesopontine median raphe regulates hippocampal ripple oscillation and memory consolidation. *Nat Neurosci*, 18(5):728–735.
- Willems, J. C. (2007). The behavioral approach to open and interconnected systems. *IEEE Control Systems*, 27(6):46–99.
- Wilson, M. A. and McNaughton, B. L. (1993). Dynamics of the hippocampal ensemble code for space. *Science*, 261(5124):1055–1058.
- Wiltgen, B. J. and Tanaka, K. Z. (2013). Systems consolidation and the content of memory. *Neurobiology of Learning and Memory*.
- Winocur, G. and Moscovitch, M. (2011). Memory transformation and systems consolidation. *Journal of the International Neuropsychological Society*, 17:766–780.
- Winterer, J., Stempel, A. V., Dugladze, T., Földy, C., Maziashvili, N., Zivkovic, A. R., Priller, J., Soltesz, I., Gloveli, T., and Schmitz, D. (2011). Cell-type-specific modulation of feedback inhibition by serotonin in the hippocampus. *The Journal of Neuroscience*, 31(23):8464–8475.
- Woodruff, A. R., Anderson, S. A., and Yuste, R. (2010). The enigmatic function of chandelier cells. *Frontiers in neuroscience*, 4.
- Wyskiel, D. R. and Andrade, R. (2016). Serotonin excites hippocampal ca1 gabaergic interneurons at the stratum radiatum-stratum lacunosum moleculare border. *Hippocampus*, 26(9):1107–1114.
- Ylinen, A., Soltesz, I., Bragin, A., Penttonen, M., Sik, A., and Buzsaki, G. (1995). Intracellular correlates of hippocampal theta rhythm in identified pyramidal cells, granule cells, and basket cells. *Hippocampus*, 5(1):78–90.
- Zengel, J. E. and Magleby, K. L. (1982). Augmentation and facilitation of transmitter release. a quantitative description at the frog neuromuscular junction. *The Journal of General Physiology*, 80(4):583–611.
- Zucker, R. S. and Regehr, W. G. (2002). Short-term synaptic plasticity. *Annual Review of Physiology*, 64(1):355–405.